

ЖУРНАЛ
ПРИКЛАДНОЙ ХИМИИ

Volume 32, No. 11

November, 1959

JOURNAL OF

APPLIED CHEMISTRY

OF THE USSR

(ZHURNAL PRIKLADNOI KHIMII)

IN ENGLISH TRANSLATION



CONSULTANTS BUREAU, INC.

RESEARCH BY SOVIET EXPERTS

Translated by Western Scientists

BULLETIN OF THE ACADEMY OF SCIENCES, USSR DIV. OF CHEM. SCI.

In this journal, outstanding Soviet scientists present original papers on new and important theoretical and experimental work in *general, inorganic, physical, and analytical chemistry*. Will be of special interest to chemists, engineers, technicians, and professors.

ANNUAL SUBSCRIPTION: 12 issues, \$45.00. **BACK ISSUES:** 1957-1958, \$45.00; 1956, \$160.00; 1952-55 (6 issues per year), \$80.00 per year.

JOURNAL OF APPLIED CHEMISTRY

Intended for a wide circle of workers in the chemical field, this publication of the Academy of Sciences, USSR, presents original articles on *the applied chemistry of silicates, technology of fuel, production of salts, metallurgy, the basic chemical industry, mineral fertilizers, dyes, paper, plastics, rubber, leather, the flavoring, foods, and fats industries*, and other pertinent fields.

ANNUAL SUBSCRIPTION: 12 issues, \$60.00. **BACK ISSUES:** 1957-1958, \$60.00; 1950-56 (12 issues per year), \$80.00 per year.

JOURNAL OF GENERAL CHEMISTRY

The major chemical publication of the Academy of Sciences, USSR, this important journal publishes original papers on experimental and theoretical work done by outstanding Soviet chemists in *organic and inorganic chemistry*, and on research into the *properties of mineral and organic compounds*.

ANNUAL SUBSCRIPTION: 12 issues, \$90.00. **BACK ISSUES:** 1957-1958, \$90.00; 1956, \$175.00; 1955 (13 issues), \$115.00; 1949-54, \$95.00 per year.

JOURNAL OF ANALYTICAL CHEMISTRY

This publication of the Academy of Sciences, USSR, presents original articles on experimental and theoretical work in *analytical chemistry; on new chemical and physicochemical methods; and on the application of analytical chemistry in different spheres of metallurgy, geochemistry, biochemistry, etc.*

ANNUAL SUBSCRIPTION: 6 issues, \$80.00. **BACK ISSUES:** 1952-1958, \$80.00 per year.

PROCEEDINGS OF THE ACADEMY OF SCIENCES, USSR (Doklady) CHEMISTRY SECTIONS

These sections of Doklady provide concise reports of the most significant advanced research in the fields listed below, as presented by members of the Academy—the foremost scientific body in the Soviet Union.

CHEMICAL TECHNOLOGY

Annual Subscription: 3 double-volume issues, \$25.00.

Back Issues: 1958, \$25.00; 1957, \$15.00; 1956, \$30.00.

CHEMISTRY

Annual Subscription: 6 issues, \$110.00.

Back Issues: 1958, \$110.00; 1956-57, \$95.00 per year.

REDUCED RATE FOR COMBINED SUBSCRIPTIONS: 1959 only, \$120.00

PROCEEDINGS OF THE ACADEMY OF SCIENCES, USSR (Doklady) PHYSICAL CHEMISTRY SECTION

Provides concise information, by the foremost Soviet chemists on the latest Russian advances in *chemical kinetics, interface phenomena, electrochemistry, absorption spectra, etc.*

Annual Subscription: 6 issues, \$160.00.

Back Issues: 1957-58, \$160.00.

Please add \$5.00 for subscriptions outside of the United States.

Payment in sterling may be made to Barclay's Bank in London, England.

CONSULTANTS BUREAU

227 West 17th Street • New York 11, N.Y. • U.S.A.

Volume 32, No. 11

November, 1959

JOURNAL OF
APPLIED CHEMISTRY
OF THE USSR

(ZHURNAL PRIKLADNOI KHIMII)

A publication of the Academy of Sciences of the USSR

IN ENGLISH TRANSLATION

Year and issue of first translation:

Vol. 23, No. 1 January 1950

	<i>U. S. and Canada</i>	<i>Foreign</i>
<i>Annual subscription</i>	<i>\$60.00</i>	<i>\$65.00</i>
<i>Annual subscription for libraries of nonprofit academic institutions</i>	<i>20.00</i>	<i>25.00</i>
<i>Single issue</i>	<i>7.50</i>	<i>7.50</i>

Copyright 1960

CONSULTANTS BUREAU ENTERPRISES, INC.

227 West 17th Street, New York, N. Y.

Editorial Board
(ZHURNAL PRIKLADNOI KHIMII)

P. P. Budnikov, S. I. Vol'fkovich, A. F. Dobrianskii,
O. E. Zviagintsev, N. I. Nikitin (Editor in Chief),
G. V. Pigulevskii, M. E. Pozin, L. K. Simonova
(Secretary), V. V. Skorchelletti, N. P. Fedot'ev

*Note: The sale of photostatic copies of any
portion of this copyright translation is expressly
prohibited by the copyright owners.*

Printed in the United States of America

CONTENTS

	PAGE	RUSS. PAGE
Use of Manganese Dioxide to Remove Hydrogen Sulfide from Gas with Subsequent Extraction of Elementary Sulfur. <u>Ya. Ya. Dodonov, L. D. Borzova, V. S. Kolosova, and V. S. Pokaevskaya.</u>	2437	2373
Rate of Decomposition of Kara-Tau Phosphorites with Phosphoric Acid. <u>M. E. Pozin, B. A. Kopylev, and D. F. Zhil'tsova.</u>	2442	2377
The Decomposition of Aluminate Solutions with Active Seed. <u>S. I. Kuznetsov, A. N. Stolyarov, V. A. Derevyankin, O. V. Serebrennikova, and S. F. Vazhenin.</u>	2449	2384
Physicochemical Properties of Tripotassium Phosphate Solutions. <u>L. S. Bezdel', V. P. Teodorovich, and V. V. Ipat'ev.</u>	2457	2392
Sea System K, Na, Mg Cl, SO ₄ - H ₂ O at 0°. <u>O. K. Yanat'eva and V. T. Orlova</u>	2463	2397
Calculation of Phase Equilibria in Multicomponent Gas Mixtures. <u>I. G. Plit</u>	2471	2405
Effect of Mineral Substances on the Relative Volatility of Components in Liquid Mixtures. <u>V. B. Kogan, S. F. Bulushev, V. M. Safronov, and O. F. Moskovets.</u>	2475	2409
Influence of the Nature of a Binary System on the Efficiency of a Rectification Column. <u>I. N. Bushmakina</u>	2482	2416
Equations and Similarity Criteria of Nonisothermal Diffusion. <u>A. A. Medvedev and P. G. Romankov.</u>	2490	2424
Resistance of the Liquid and Gas Phases in Absorption on Sieve and Bubble-Cap Plates. <u>M. Kh. Kishinevskii and L. A. Mochalova.</u>	2495	2428
Influence of the Operating Conditions of Gas Lifts on Their Hydraulic Resistance. <u>M. L. Varlamov, G. A. Manakin, and Ya. I. Starosel'skii</u>	2504	2436
A Study of the Absorption of Nitrogen Oxides by Soda Solutions in Gas-Lift Equipment. <u>M. L. Varlamov, G. A. Manakin, and Ya. I. Starosel'skii.</u>	2511	2443
Conversion of Organic Sulfur Compounds on Cobalt-Molybdenum Catalyst in Gas Purification. <u>N. I. Brodskaya and V. P. Teodorovich</u>	2516	2448
Use of the Ion-Exchange Method for the Removal of Impurities from Arsenic. <u>G. A. Kataev, A. G. Grigor'eva, and L. N. Rozanova</u>	2520	2452
Chemistry of the Acid Autoclave Leaching of the Monosulfides of Nickel, Cobalt, and Iron. <u>G. N. Dobrokhotoy</u>	2524	2456
Phosphatation of Steels in the Presence of Nitrates of Monovalent Metals. <u>I. I. Khain.</u>	2531	2463
Protection of Steel Against Gaseous Corrosion by Glass-Metal Coatings. <u>E. A. Antonova and A. A. Appen.</u>	2536	2468

CONTENTS (continued)

	PAGE	RUSS. PAGE
Process of Phosphatation of Steel in the Presence of Nitrates of Bivalent Metals. <u>I. I. Khain</u>	2542	2473
Toward the Question of the Determination of Oxygen in Metallic Chromium of High Purity. <u>N. V. Ageev, A. I. Ponomarev, and V. A. Trapeznikov</u>	2548	2479
Influence of Temperature on the Effect of Polarization in the Corrosion Cracking of V-95 Alloy in a 0.1 N Solution of H_2SO_4 + 35 g/liter of NaCl. <u>V. V. Romanov and V. V. Dobrolyubov</u>	2556	2487
Corrosion of Lead in Contact with Graphite. <u>V. V. Titov and E. N. Semkova</u>	2560	2492
The Influence of Current Density and Sulfuric Acid Concentration on the Magni- tude of the Internal Strains in Electrolytic Copper Deposits. <u>N. P. Fedot'ev</u> and <u>A. A. Khonikevich</u>	2566	2497
Cathodic Polarization during Formation of Iron-Cobalt Alloy and the Causes of De- polarization and Over-Polarization. <u>A. L. Rotinyan and E. N. Molotkova</u>	2572	2502
Determination of the Exchange Current of Silver and Cobalt on a Solid Metallic Surface with the Help of Radioactive Indicators. <u>S. E. Vaisburd, N. M. Kozhevnikova, and V. L. Kheifets</u>	2578	2507
Spectrophotometric Method of Determination of the Content of Primary and Secondary Higher Alcohols. <u>Ya. E. Shmulyakovskii</u>	2584	2513
The Ebullioscopic Method of Determination of Reducing Sugars. <u>V. K. Nizovkin</u> and <u>I. Z. Emel'yanova</u>	2588	2516
The Distribution of $C_1 - C_3$ Acids in the System Diisopropyl Ether - Water. <u>V. P. Sumarokov and Z. M. Volodutskaia</u>	2594	2521
Heterogeneous Equilibria in the System Methyl Acetate - Chloroform - Water. <u>N. V. Lutugina and V. M. Kalyuzhnyi</u>	2599	2526
A Chromatographic Study of Arabogalactan and other Water-Extracted Subs- tances of <u>Larix Dahurica</u> . <u>I. P. Tsvetaeva and M. K. Yur'eva</u>	2606	2533
Investigation of the Formation of Catalyst Systems and of Alkylaluminums in Connection with the Polymerization of Ethylene at Atmospheric Pressure. <u>A. Shimon, L. Kovach, D. Dezheni and D. Lekhotski</u>	2614	2541
Biological Aging of Cable Rubber. <u>G. I. Dubrovin</u>	2620	2547
Nitration of Ethylbenzene. <u>O. S. Vladychik, L. L. Bespalova, P. M. Kochergin,</u> <u>V. A. Zasosov, and A. M. Tsyganova</u>	2624	2550
The Bases of Chlorendic Anhydride Technology. <u>L. M. Kogan and N. P. Ignatova</u>	2629	2556
Thermal Isomerization of Rosin. <u>I. I. Bardyshev, A. G. Sokolov and O. T. Tkachenko</u>	2634	2560
Preparation of Divinylbenzene by Catalytic Dehydrogenation of Diethylbenzene. <u>A. A. Balandin, N. I. Shuikin, G. M. Marukyan, I. I. Brusov, R. G. Seimo-</u> <u>vich, T. K. Lavrovskaya, and V. K. Mikhailovskii</u>	2640	2566

BRIEF COMMUNICATIONS

Growth of Germanium Monocrystals from under Melts of Salts and Oxides. <u>V. N. Maslov, Yu. V. Granovskii, and V. D. Samygin</u>	2644	2571
--	------	------

CONTENTS (continued)

	PAGE	RUSS. PAGE
Determination of Copper and Iron Impurities in Arsenic by means of Ion Exchange. <u>L. N. Rozanova and G. A. Kataev</u>	2547	2574
New Method of Preparing Magnesium Sulfate. <u>L. G. Berg, S. G. Ganelina, and É. F. Gubanov</u>	2649	2576
Spectral Absorption of Aluminoborosilicate Glasses Colored with Cobalt Compounds. <u>A. A. Appen and Kan Fu-hsi</u>	2652	2577
Calculation of the Hydrolysis Constants of a Diazo Cation. <u>B. V. Passet and B. A. Porai-Koshits</u>	2655	2580
Liquid - Vapor Phase Equilibria in the System Isopropyl Alcohol - Water - Calcium Chloride. <u>L. L. Dobroserdov</u>	2657	2582
Thermal Stability of the System Urea - Ammonium Nitrate. <u>B. Yu. Rozman and L. I. Borodkina</u>	2660	2585
Change in the Reactivity of Pulverized Cellulose in Different Media. <u>V. I. Sharkov, I. I. Korol'kov, and E. N. Garmanova</u>	2662	2586
Application of Precipitation Chromatography to the Quantitative Determination of Nickel Soaps. <u>V. P. Golendev</u>	2665	2589
Aminophenylimides of 1, 8-Naphthoylene-1', 2'-Benzimidazole-4,5-Dicarboxylic Acids. <u>B. M. Krasovitskii, E. E. Khotinskaya, and V. L. Plakidin</u>	2669	2592
Diazotization and Azo Coupling of Copolymers Based on Acrylonitrile and p-Aminostyrene. <u>G. I. Kudryavtsev, E. A. Vasil'eva-Sokolova, and M. A. Zharkova</u>	2671	2594
Coke Formation During Destructive Catalytic Hydrogenation of Mazut. <u>Ya. R. Katsobashvili, N. P. Volynskii, and T. N. Kuz'mina</u>	2674	2597
Electrosynthesis of Tetra-(β -Cyanoethyl)Stannane. <u>A. P. Tomilov and L. V. Kaabak</u>	2677	2600
Synthesis of Rhodanine. <u>A. P. Grishchuk and S. N. Baranov</u>	2679	2601
Preparative Method for β -(o-Carboxymethylphenyl)Propionic Acid. <u>F. N. Stepanov and M. O. Iodko</u>	2681	2602
Synthesis and Properties of Some Polyesters of Substituted Phosphoric Acids. <u>I. K. Rubtsov and R. D. Zhilina</u>	2683	2604

BOOK REVIEWS

New Synthetic Materials. <u>Z. V. Pushkareva</u>	2685	2607
--	------	------



USE OF MANGANESE DIOXIDE TO REMOVE HYDROGEN SULFIDE FROM GAS WITH SUBSEQUENT EXTRACTION OF ELEMENTARY SULFUR

Ya. Ya. Dodonov, L. D. Borzova, V. S. Kolosova,
and V. S. Pokaevskaya

N. G. Chernyshev State University, Saratov

Many methods for the removal of hydrogen sulfide from gas are known in the trade literature. The most widespread methods of purification are based either on the oxidation of the hydrogen sulfide to elementary sulfur [1-6] or on the neutralization of the hydrogen sulfide using basic compounds [2, 3, 7-9].

The use of manganese dioxide to remove hydrogen sulfide from gas was first proposed in 1931 [10]. However, based on our perusal of the literature, the use of this method failed to receive further development.

The purpose of Chagunava's investigation of the desulfurization of gases with manganese compounds [11] was to remove sulfur compounds from the gas without attempting to recover and reuse the manganese compounds.

We describe the cyclic use of manganese dioxide to remove hydrogen sulfide from gas with a subsequent extraction of elementary sulfur.

The experiments were run with a manganese dioxide that contained not more than 0.95% MnO , not more than 5.78% Mn_2O_3 , and not more than 80.07% MnO_2 . The MnO_2 content, calculated from the "active oxygen", ranged from 74.70 to 87.02%.

To run the experiments we used the apparatus shown in the diagram, consisting of hydrogen sulfide generator 1, where the gas was generated by mixing 10% solutions of sodium sulfide and hydrochloric acid, chambers for the mixing of hydrogen sulfide with nitrogen or some other gas (2), reaction column containing manganese dioxide 3, Drexel wash bottles containing cadmium acetate solution 4, manometers 5, flow meters 6, air blower 7, and gas meter 8.

To study the oxidation of hydrogen sulfide, we used pure manganese dioxide, contained in the reaction column (Expt. Nos. 1-7), manganese dioxide that had been deposited on a carrier (Expt. Nos. 8 and 9), and a suspension of manganese dioxide in water (Expt. Nos. 10 and 11). In the last case, we replaced the reaction column by two bubblers, which contained the aqueous suspension of finely divided manganese dioxide. Magnetic stirrers were used to keep the manganese dioxide suspended.

The experimental results are summarized in Table 1.

The data in Table 1 show that, depending on the experimental conditions used, the oxidation-reduction reaction $\text{MnO}_2 + 2\text{H}_2\text{S} = \text{MnS} + 2\text{H}_2\text{O} + \text{S}$ goes with a variable yield. The least degree of hydrogen sulfide oxidation is observed in the experiments using manganese dioxide suspension.

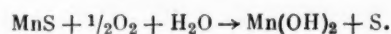
A slight decrease in the extent of gas oxidation is observed when the height of the absorbent layer is decreased, or when either the gas passage rate or the amount of hydrogen sulfide in the original gas is increased. The use of carriers has a favorable effect on the removal of hydrogen sulfide from gas.

TABLE 1

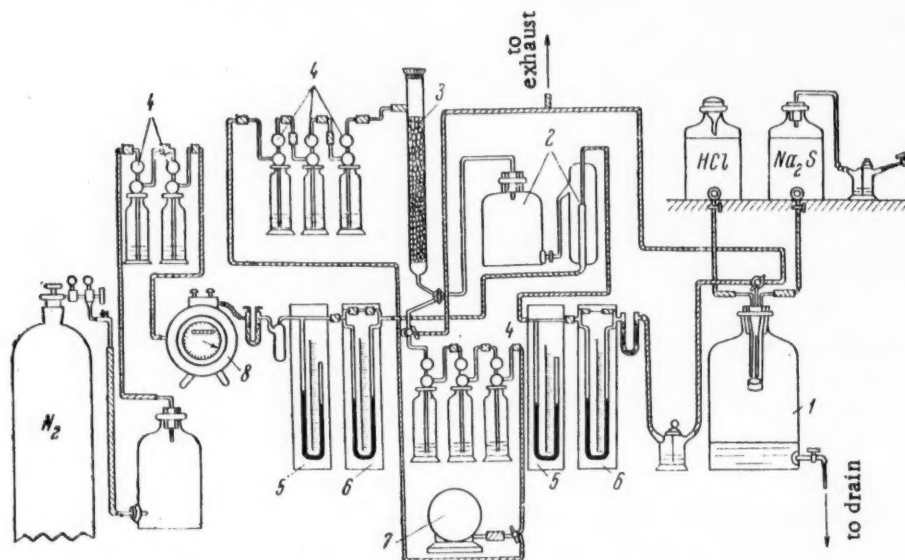
Oxidation of Hydrogen Sulfide with Manganese Dioxide

Expt. No.	Composition of absorbent mass (in g)				Rate of gas passage (in ml/min)	Amount of H ₂ S in original gas (in g/liter)	Time of gas passage (in min)	H ₂ S oxidized by MnO ₂ (in g)			Oxidation
	MnO ₂	H ₂ O	lime	carrier				theoretically possible	found experimentally		
1	35.0	—	—	—	31.4	0.30	2110	20.44	19.96	97.85	
2	10.0	—	—	—	36.2	0.52	314	6.40	5.88	91.90	
3	30.0	—	—	—	34.4	0.38	1896	19.20	19.20	100.00	
8	4.0	12.0	0.1	125.6	50.0	0.32	180	2.72	2.72	100.00	
9	4.0	12.0	0.1	chamotte 125.6	12.0	0.34	930	2.72	2.60	95.58	
10	35.0	350.0	5.0	chamotte	21.0	0.11	931	20.44	2.29	11.20	
11	4.0	340.0	0.1	—	10.7	0.46	112	2.72	0.55	20.22	

The manganese sulfide formed is oxidized by atmospheric oxygen with the liberation of still another atom of sulfur, according to the reaction



Either dichloroethane or trichloroethylene was used to extract the sulfur in an ordinary Soxhlet apparatus, followed by distilling off the solvent. The sulfur was also extracted with superheated steam in an apparatus composed of a steam generator, steam superheater (a porcelain tube filled with pieces of porcelain), reaction column, and cooled receiver for the sulfur.



The results of the experiments are given in Table 2.

TABLE 2

Isolation of Sulfur from the Products of Oxidizing Manganese Sulfide with Atmospheric Oxygen

Expt. No.	Starting product	Extraction method	Amount of free sulfur theoretically possible, based on H_2S (in g)	Amount of sulfur isolated	
				in g	in %
1	Manganese dioxide	Dichloroethane	2.20	2.13	96.82
2		Trichloroethylene	5.02	5.05	100.50
3		Steam	18.79	18.57	98.83
4	Manganese dioxide on chamotte	Steam	4.67	4.35	93.14

As can be seen from the data in Table 2, both extraction methods yield a complete removal of sulfur. The purity of the isolated sulfur was entirely satisfactory.

The most important factor in determining the practicality of using manganese dioxide in the "dry" method of removing hydrogen sulfide from gas is the recovery of manganese dioxide, i.e., the possibility of its reuse in the cyclic purification of the gas. The regeneration of manganese dioxide using atmospheric oxygen proceeds with great difficulty; the products obtained from the air oxidation possess a low oxidative capacity toward hydrogen sulfide (the amount of "active" manganese dioxide does not exceed 32-36%).

Investigation of the regeneration conditions established that the use of chlorine gas and steam leads to an acceleration of the oxidation process and to an increase in the amount of "active" manganese dioxide.

We used slaked lime to create an alkaline medium and to reduce manganese losses due to elution of water-soluble bivalent manganese salts.

The experiments on the removal of hydrogen sulfide from gas, with subsequent regeneration of the spent manganese dioxide and its recycling, were run in the following manner: a known weight of manganese dioxide was placed in the apparatus (Figure) and hydrogen sulfide containing gas was passed through until all of the manganese dioxide had been reduced. After air oxidation, the sulfur was extracted with trichloroethylene. The steam-chlorine heat treatment was run before starting cycle II, which in turn was preceded by preparing a mixture composed of 30% slaked lime and 70% of the air-oxidation product of manganese sulfide, tentatively named "manganese dioxide".

After the steam-chlorine treatment, which raised the amount of "active" manganese dioxide from 30.81 to 81.53%, we ran analogous experiments, which we have labeled cycles II and III, using the "active" manganese dioxide to remove hydrogen sulfide from gas.

Replacing the chlorine by other oxidizing agents proved unsuccessful in raising the oxidative capacity.

The summarized results on the use of manganese dioxide to remove hydrogen sulfide from gas are given in Table 3.

A perusal of the data given in Table 3 permits concluding that the addition of 30 weight percent of slaked lime leads to a practically complete elimination of manganese losses; reaction between hydrogen sulfide and manganese dioxide goes to completion in all three cycles, which is confirmed by the 100% yields of sulfur; the steam-chlorine heat treatment permits increasing the "active" content of the recycled manganese dioxide up to 75-85%.

TABLE 3

Summarized Results of Using Manganese Dioxide to Remove Hydrogen Sulfide from Gas

Composition of absorbent mass	Amount of "active" MnO_2 (in %)	Cycle I			Treatment I			Cycle II			Treatment II			Cycle III		
		Yield of sulfide in % of theoretical	"Active" MnO_2 content at end of cycle	Oxidizing agent	"Active" MnO_2 content (in %)	Mn losses (in %)	Yield of sulfide in % of theoretical	Yield of sulfide in % of theoretical	Yield of sulfide in % of theoretical	Yield of sulfide in % of theoretical	"Active" MnO_2 content (in %)	Mn losses (in %)	Yield of sulfide in % of theoretical	Yield of sulfide in % of theoretical	Yield of sulfide in % of theoretical	Yield of sulfide in % of theoretical
Original MnO_2	83.11	100	30.91	Chlorine	99.47	1.25	100	100	100	100	85.62	53.40	100	100	46.60	46.60
80% MnO_2 + 20% Ca(OH)_2	83.11	100	33.96		87.72	35.22	100	100	100	100	—	—	—	—	—	—
70% MnO_2 + 30% Ca(OH)_2	83.11	100	38.70		76.25	9.31	100	100	100	100	—	—	—	—	—	—
50% MnO_2 + 50% Ca(OH)_2	83.11	100	36.05		81.53	0	100	100	100	100	—	—	—	—	—	—
70% MnO_2 + 30% Ca(OH)_2	83.11	100	38.70		74.03	2.23	100	100	100	100	—	—	—	—	—	—
70% MnO_2 + 30% Ca(OH)_2	83.11	100	37.27	Air	81.53	0	100	100	100	100	74.23	1.55	100	100	98.45	98.45
70% MnO_2 + 30% Ca(OH)_2	83.11	100	37.27		40.25	5.40	100	100	100	100	—	—	—	—	—	—
70% MnO_2 + 30% Ca(OH)_2	83.11	100	37.27	Oxygen	42.67	4.17	100	100	100	100	—	—	—	—	—	—

SUMMARY

1. A study of the use of manganese dioxide to remove hydrogen sulfide from gas revealed that the oxidation-reduction reaction between the hydrogen sulfide and manganese dioxide goes to completion. The reaction product is elemental sulfur, capable of being extracted either by chlorinated organic solvents or by superheated steam; 1 kg of manganese dioxide, containing 83.11% "active" MnO_2 , is capable of oxidizing 760.9 g of hydrogen sulfide in one cycle, with the isolation of 737.7 g of sulfur.

2. Conditions for the regeneration of manganese dioxide were established. It was shown that the steam-chlorine heat treatment permits increasing the oxidative capacity of manganese dioxide after its reaction with hydrogen sulfide, followed by air oxidation. The use of slaked lime practically eliminates manganese losses.

LITERATURE CITED

- [1] G. O. Nusinov, Methods for Extraction of Sulfur from Industrial Gases [In Russian] (Goskhimtekhnizdat, Moscow-Leningrad, 1933).
- [2] N. I. Egorov, et al., Removal of Sulfur from Coke and Other Fuel Gases [In Russian] (State Sci.-Tech. Press, Moscow, 1950).
- [3] A. S. Smirnov, Transport and Storage of Gases [In Russian] (Gostoptekhnizdat, Moscow-Leningrad, 1950).
- [4] G. U. Hopton, Gas World 128, 538 (1948); also in Gas J. 254, 100-2, 105-6, 111, 158-160, 163-4, 169, 218, 223 (1948).
- [5] F. I. Ivanovskii, V. A. Dontsova, and T. A. Semenova, Khim. Prom. 4, 26 (1955).
- [6] G. O. Nusinov and A. N. Andrianov, Arsenic Process for Gas Purification [In Russian] (ONTI, Moscow-Leningrad, 1937).
- [7] M. V. Gofman, et al., Trudy Khar'kov, Nauchno-Issled, Uglekhim. Inst. 20, (1941).
- [8] M. S. Litvinenko, Coke Chemical Industry in the United States of America [In Russian] (Metallurgical Press, 1947).
- [9] Removal of Hydrogen Sulfide from Gas and Production of Sulfuric Acid [In Russian] (Central Institute of Information of the Ministry of Ferrous Metallurgy of the USSR), Bulletin 23, (283) (1955).
- [10] S. Hunyady and K. Koller, German Patent 529,698, Class 26, Dated September 2, 1928, Issued July 16, 1931; Chem. Zentr. 2, 1801 (1931).
- [11] V. T. Chagunava, Author's Abstract of Doctoral Dissertation [In Russian] Tbilisi (1954).

Received June 10, 1958

RATE OF DECOMPOSITION OF KARA-TAU PHOSPHORITES WITH PHOSPHORIC ACID

M. E. Pozin, B. A. Kopylev, and D. F. Zhil'tsova

Lensovet Technological Institute, Leningrad

The unique nature of Kara-Tau phosphorites and the difficulty of obtaining a qualitatively simple superphosphate from them are the reason for making a special study of the production of concentrated phosphate fertilizers from this type of raw material. However, the phosphoric acid obtained from Kara-Tau phosphorites by extraction differs in its composition from the acid obtained by heat treatment, and also from the acid obtained by extraction from apatite concentrate. The degree of neutralization of the first hydrogen ion in this acid reaches as high as 20-22% [1] due to the large amount of magnesium in the system. For this reason the decomposition of such an acid from phosphorites should proceed slowly. In addition, a high degree of phosphoric acid neutralization is linked with a large consumption of acid to decompose the phosphate.

The decomposition of Kara-Tau phosphorites with pure phosphoric acid goes at a rapid rate when the ratio solid:liquid is equal to 1:20 by weight [2]. The degree of decomposition reaches approximately 100% when the decomposition is run at 60° for 30 minutes with acid containing 40% P_2O_5 . When the phosphoric acid is neutralized with magnesium compounds to the extent of 50%, the decomposition rate of the apatite concentrate at 40° shows a 14-fold decrease, while when neutralization is to the extent of 20 and 30% the decrease in the decomposition rate is 2- and 3-fold, respectively [3].

The rate and mechanism of the decomposition of apatite concentrate with phosphoric acid had been studied by us earlier [4, 5]. It seemed interesting to determine if the rules derived in this study could be applied to the reaction of Kara-Tau phosphorite with phosphoric acid.

Our objective in the present paper was to determine the rate and mechanism for the decomposition of Kara-Tau phosphorites with phosphoric acid. The ratios of phosphate to acid used in our study corresponded to those used in the production of double superphosphate.

EXPERIMENTAL

In our experiments we used both the pure acid and the extraction grade, the latter in its composition corresponding to that of the evaporated acid obtained by the sulfuric acid extraction of Kara-Tau phosphorites [6]. The phosphorite had the following composition: P_2O_5 26.7%, CaO 42.7%, MgO 3.1%, CO_2 7.8%, R_2O_3 2.2%, F 2.4%, and insoluble residue 12.1%. In its granular composition the phosphorite represented approximately 80% of particles with a size of 75-150 μ and about 12% of particles with a size smaller than 75 μ . The experimental technique was the same as that used by us in investigating the decomposition of apatite concentrate with phosphoric acid [4].

As usual, the amount of acid taken was based on the composition of the phosphorite.

The principal experiments on determining the effect of various factors on the process were run using pure (thermal) acid, diluted to the desired concentration.

Effect of acid concentration. The relation between the degree of phosphorite decomposition and the phosphoric acid concentration at 20° is shown in Fig. 1. As can be seen, the degree of decomposition effected in 180 minutes by acid, containing 36.6% P_2O_5 , is 63.3%, while with 44.8% acid it is 73.5%, and with 49.1% acid it is 74.7%. In this connection the degree of phosphorite decomposition increases very rapidly during the first 15-20 minutes. Then the degree of decomposition increases at a much slower rate. The maximum degree of decomposition in these experiments was obtained using acid with a P_2O_5 content of 54.1%. The phosphorite decomposition is less intense using acids of higher concentration. The degree of decomposition in 60 minutes decreases by 2.5% when the acid concentration is increased from 54.1% to 57.0% P_2O_5 , while when acid with a P_2O_5 content of 64.9% was used the amount of phosphorite decomposed in this length of time was only 65.5%, i.e., it was less than when using 44.8% acid.

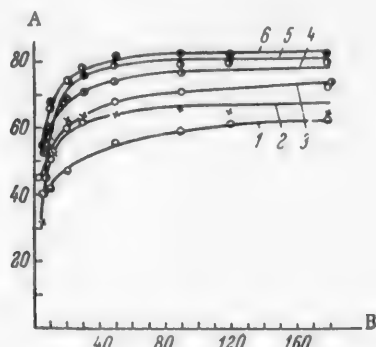


Fig. 1. Degree of decomposition of Kara-Tau phosphorites with acids of different concentration at 20° and a stoichiometric norm. A) Degree of decomposition (in %); B) time (in min). Acid concentration (in % P_2O_5): 1) 36.6, 2) 64.9, 3) 44.8, 4) 49.1, 5) 57.0, 6) 54.1.

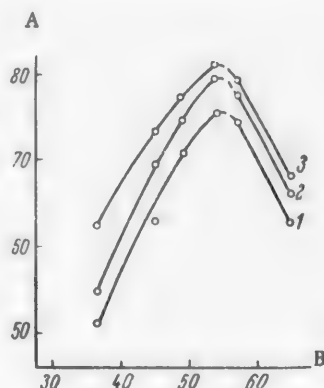


Fig. 2. Isothermal isochrones for the relation between the degree of decomposition of Kara-Tau phosphorite and the phosphoric acid concentration at 20° and a stoichiometric norm. A) Degree of decomposition (in %); B) acid concentration (in % P_2O_5). Time (in min): 1) 30, 2) 60, 3) 180.

The isothermal isochrones for the decomposition of the phosphorite as a function of the acid concentration are shown in Fig. 2. The optimum acid concentration of 54.1% P_2O_5 is retained for all of the isochrones.

Measuring the change in the decomposition rates as reaction progresses indicates that the decomposition rates decrease by a matter of some 20-30 and even a hundred times in 2-3 hours. For example, using the acid with a P_2O_5 content of 54.1%, the decomposition rate in 7.5 minutes after the start of experiment drops to 1.82 g/min, and after 160 min it is only 0.006 g/min., i.e., it is nearly 300 times slower. The more concentrated the acid, the greater the difference between the velocity values. In the indicated time interval the rate of the process, using acid with a P_2O_5 content of 36.6%, after 7.5 min is nearly 25 times greater than the rate after 150 minutes, while for 44.8% acid it is approximately 65 times greater, for 52.5% acid it is approximately 100 times greater, for 57.0% acid it is 300 times greater, and for 64.9% acid it is 580 times greater. This is apparently due to the fact that increasing the acid concentration leads to an impairment of the diffusion conditions because of an increase in the viscosity of the system, and also because of the probable formation of a denser film on the surface of the phosphate particles.

Beginning 7.5 minutes from the start of experiment, the decomposition rate using acid with the optimum P_2O_5 content of 54.1% is not higher, but in some cases is even lower than the decomposition rate using other concentrations of acid. The maximum degree of decomposition obtained with this acid is achieved as the result of higher rates at the very start of the process, which can be explained by the fact that the acid with a P_2O_5 content of 54% has the maximum concentration of hydrogen ions [5].

Effect of acid norm. The experiments on determining the relationship between the degree of decomposition and the acid norm were run at 20° using acid with a P_2O_5 content of 54.7%.

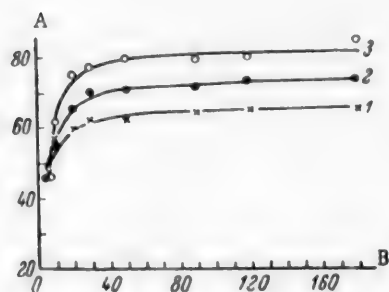


Fig. 3. Degree of decomposition of Kara-Tau phosphorite by phosphoric acid with a P_2O_5 content of 54.7% at 20° and different acid norms.

A) Degree of decomposition (in %);
B) time (in min.). Acid norm (in % of the stoichiometric): 1) 75, 2) 90, 3) 110.

At the start of reaction (approximately first 5 minutes) the degree of decomposition is practically independent of the acid norm. By analogy with the decomposition of apatite, this is apparently due to the fact that at the start of the process there is present in all cases a large excess of acid when compared with the reacting phosphate portion. As was to be expected, the degree of decomposition in the same length of time increases as the acid norm is increased (Fig. 3).

The degree of decomposition in 180 minutes using norms of 75, 90 and 110% is, respectively, 64.1, 73.0, and 84.6%. In other words, increasing the amount of acid by, for example, $90/75 = 1.2$ times, leads to increasing the degree of decomposition by a matter of only 1.14 times. The increase in the degree of decomposition is not proportional to the increase in the acid norm.

In contrast to apatite, a higher decomposition coefficient is retained for the higher acid norm over a long period of time, nearly from the very start of the experiment up to its completion (up to 3 hours).

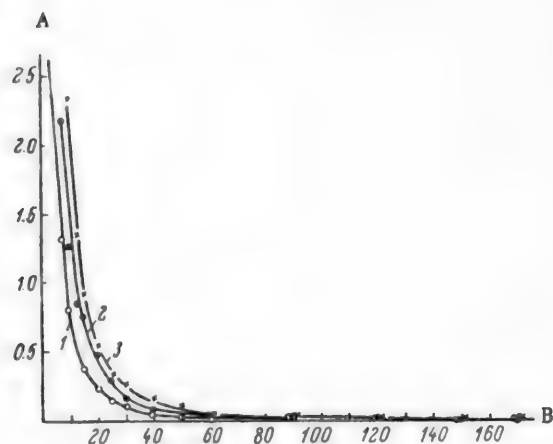


Fig. 4. Rate of decomposition of Kara-Tau phosphorite by phosphoric acid with a P_2O_5 content of 54.7% at 20° and different acid norms. A) Decomposition rate (in g/min); B) time (in min.). Acid norm (in % of the stoichiometric): 1) 75, 2) 90, 3) 110.

The higher the acid norm, the steeper the curves for the change in the degree of decomposition during the first 10-20 minutes. The main portion of the phosphorite is decomposed during the first 10-20 minutes. Thus, 20 minutes after the start of experiment, the degree of decomposition using 75, 90, and 110% of the acid norm is 59, 66 and 74%, respectively, and in the next 160 minutes it increases by only 6, 7, and 6.5%, respectively.

The difference between the values of the degree of phosphorite decomposition for different acid norms is smaller when the reaction time is shorter. But increasing the norms leads to an increase in the length of the period during which a comparatively rapid increase in the degree of phosphorite decomposition occurs. Beginning

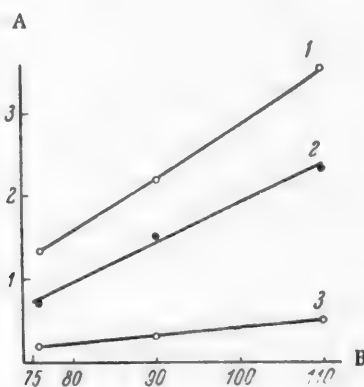


Fig. 5. Isothermal isochrones expressing the decomposition rate of Kara-Tau phosphorite by acid with a P_2O_5 content of 54.7% at 20° as a function of the acid norm. A) Decomposition rate (in g/min); B) acid norm (in % of the stoichiometric). Time (in min): 1) 7.5, 2) 10, 3) 30.

with a decomposition time of approximately 50-60 minutes, the curves become practically parallel. As a result, within the studied limits, the acid norm exerts a substantial influence only in the initial stage of the decomposition. Apparently, increasing the acid norm postpones somewhat the start of crystallization of the salts, resulting in an increase in the time of the first stage of the decomposition [5]. The change in the decomposition rates with time for different acid norms is shown in Fig. 4. As reaction progresses, the rate decreases. Thus, for an acid norm of 75% the decomposition rate at the end of 10 min is 0.8 g/min, while at the end of 170 min it is only 0.006 g/min; for a 90% norm the corresponding values are 1.27 and 0.007 g/min, and for a 110% norm they are 2.34 and 0.008 g/min. The decomposition rates are especially different for different acid norms at the start of decomposition. After 60-90 minutes the rates for all of the taken norms become nearly the same. Thus, for acid norms of 110 and 90% the difference in the rates at the end of 10 minutes is $\frac{2.34}{1.35} = 1.76$ times, at the end of 30 minutes it is $\frac{0.25}{0.18} = 1.35$ times, and after 1 hour it is $\frac{0.038}{0.037} \approx 1.03$, i.e., the rates are nearly equal.

From Fig. 5 it can be seen that the slope of the isothermal isochrones becomes smaller the greater the time from the start of experiment. This graph also shows that changing the acid norm within the indicated limits exerts an effect only in the initial period of decomposition.

Effect of temperature. Increasing the temperature from 20 to 40° results in a slight increase in the degree of phosphorite decomposition (Fig. 6). At 20° the phosphorite decomposes to the extent of 46.7% in 5 minutes, and to the extent of 72.0% in 30 minutes, while at 40° the corresponding values are 63.8 and 77.8%. As a result, in the indicated temperature interval, the degree of decomposition in the first 5 minutes increases by a matter of 1.4 times, and in 30 minutes by a matter of 1.1 times. Increasing the temperature further does not lead to an increase in the degree of decomposition.

Moreover, the absolute values of the decomposition rates for the same length of time even decrease when the temperature is increased. Thus, after 10 minutes the decomposition rate at 40° is 0.8 g/min, at 50° it is 0.57 g/min, and at 80° it is 0.44 g/min, while after 30 minutes the corresponding values are 0.189, 0.133, and 0.077 g/min; at 20° the rates for the same lengths of time are 1.37 and 0.273 g/min, respectively, i.e., they are considerably higher. The rates tend to become equal toward the end of experiment.

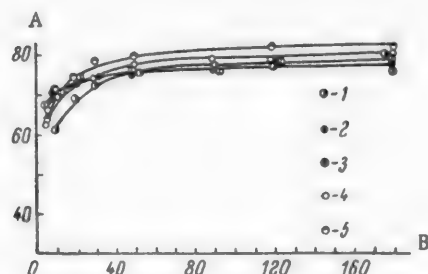


Fig. 6. Degree of decomposition of Kara-Tau phosphorite by phosphoric acid with a P_2O_5 content of 52.5% at different temperatures and the stoichiometric norm. A) Degree of decomposition (in %); B) time (in min). Temperature (in °C): 1) 20, 2) 80, 3) 60, 4) 50, 5) 40.

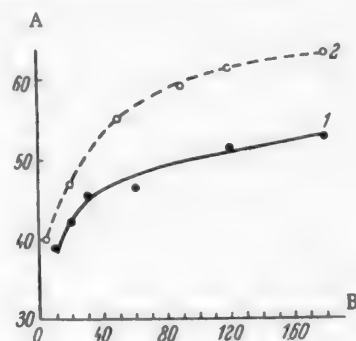


Fig. 7. Degree of decomposition of Kara-Tau phosphorite by extraction acid with a P_2O_5 content of 34.0% at 20° and the stoichiometric norm. A) Degree of decomposition (in %); B) time (in min.). 1) Extraction acid with a P_2O_5 content of 34.0%; 2) thermal acid with a P_2O_5 content of 36.6%.

The above can be explained by the fact that in the examined process an increase in the reaction rate occurs only in the first moment of reaction when the temperature is raised. This results in a rapid accumulation of crystalline reaction products, which sharply retards the process even after the lapse of a short period of time. Under conditions excluding the formation of the solid phase, i.e., with a small solid:liquid ratio, the decomposition rate of Kara-Tau phosphorite increases with temperature increase [2, 3] during the entire experiment.

With comparatively large values for the solid:liquid ratio there also occurs, besides crystallization of the product, an increase in the absolute amount of salts in the liquid phase when the temperature is increased (due to increased solubility), which in turn leads to a reduction in the decomposition rate as the process progresses.

Decomposition of Kara-Tau phosphorite with extraction acid. In Fig. 7, we have shown the change (when compared to the pure acid) with time in the degree of decomposition of Kara-Tau phosphorite at 20° by phosphoric acid of composition [6]: P_2O_5 34.0%, SO_3 4.0%, MgO 4.0%, F 1.0%, R_2O_3 1.8%, and having a density of 1.5.

The "degree of decomposition vs. time" curve lies in a region of lower degrees of decomposition when compared with the decomposition obtained using the pure acid. With a small difference in the acid concentrations (2.6%), the degrees of decomposition differ by 10% after 3 hours. At the same time, for the two thermal acid concentrations of 26.4 and 36.6% P_2O_5 , differing by approximately 10%, the difference in the degrees of decomposition, with all of the other conditions constant, is equal to a total of only 7%.

The phosphorite is decomposed by the thermal acid at a faster rate for a matter of 30-50 minutes at the start of the process. The difference in the degrees of decomposition effected by the two acids is specifically due to the slower rate with which the extraction acid reacts with the phosphorite during this period. The presence of magnesium ions in the extraction acid is responsible for the high degree of advance neutralization of the phosphoric acid [1, 7]. Consequently, the greater the amount of magnesium in the system, the slower will be the rate of the chemical decomposition of the phosphorite. The presence of a variable amount of magnesium in the liquid phase also exerts an effect on the time when crystallization of the salts begins. The greater the amount of magnesium, the sooner the crystallization of monocalcium phosphate begins, i.e., it begins to crystallize at a lower degree of decomposition. As a result, when extraction acid is used to decompose the phosphorite, the period of a comparatively rapid reaction rate is shortened and a retardation of the process begins sooner. As can be seen from Fig. 7, a retardation of the process begins sooner for the extraction acid than for the thermal acid.

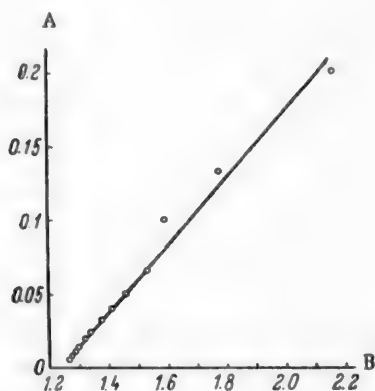


Fig. 8. Relation between $1/y$ and $1/\tau$. A) Value of $1/y \times 10^{-2}$; B) value of $1/\tau$.

Mechanism of the decomposition of Kara-Tau phosphorite by phosphoric acid. The experimental data obtained for the decomposition of Kara-Tau phosphorite with either thermal or extraction phosphoric acid indicate that the mechanism of this process is the same as the mechanism for the decomposition of apatite [5]. In both cases, based on the rate of progress, the process can be subdivided into two stages, each determined by the reaction conditions and the composition of the reactants.

The first stage represents decomposition in phosphoric acid solutions, which become saturated with calcium and magnesium salts as reaction progresses. The decomposition rate in this very short stage is directly proportional

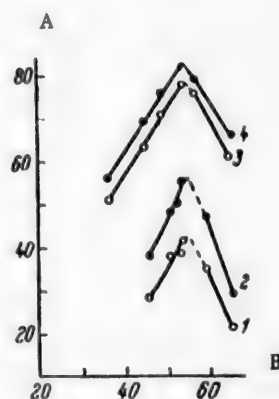


Fig. 9. Isothermal isochrones for the decomposition of apatite and Kara-Tau phosphorite with phosphoric acid at 20°. A) Degree of decomposition (in %); B) acid concentration (in % of P_2O_5). Time (in min): apatite: 1) 30, 2) 60; phosphorite: 3) 30, 4) 60.

to the hydrogen-ion activity [3], and is greater the smaller the amount of salts in solution. As the liquid phase becomes saturated with salts, and they begin to crystallize from solution, the decomposition process begins to be hindered by the resistance offered by the formed crust of salts.

The same as in the decomposition of apatite, where conditions for the rapid removal of the formed salts into the main bulk of the system are absent, the salts deposit in the immediate proximity of their place of origin, i.e., on the surface of the phosphate grains. In this case, the rate of the process will be determined by the diffusion rate of the reactants through the layer of reaction products. In contrast to the decomposition of apatite concentrate, the decomposition of Kara-Tau phosphorite over nearly the entire duration of experiment in the limits from approximately 5 to 150 minutes is described well by a linear function (Fig. 8) in the coordinates $\frac{1}{y}$ and $\frac{1}{\tau}$, where y is the degree of decomposition of Kara-Tau phosphorite by 52.5% acid (in %), and τ is the time (in min). Evidently, the reason for this is that, with magnesium compounds present in the solution, saturation of the solution and crystallization of salts probably begins much before the time of making the first determination. However, assuming that the precipitate has a constant structure and thickness, this should lead to a retardation of phosphorite decomposition by pure phosphoric acid when compared to the apatite concentrate. Actually, as can be seen from Fig. 9, the isothermal isochrones for Kara-Tau phosphorite lie considerably above the corresponding isothermal isochrones for apatite. The difference is of the order of 25-30%. This is evidently explained by the finer and less-dense structure of the phosphorite when compared with apatite, by the presence of a substantial amount of easily decomposed dolomite, and also by the salt deposits assuming a friable nature as the result of carbon dioxide evolution.

SUMMARY

1. The degree of decomposition of Kara-Tau phosphorite by thermal phosphoric acid increases when the acid concentration is increased from 22.0 to 54.1% P_2O_5 . Further increase in the acid concentration to 64.9% P_2O_5 leads to a decrease in the degree of decomposition.
2. The decomposition rate of the phosphorite decreases by some 20-30 and even 100 times as reaction progresses. For example, for acid with a P_2O_5 content of 54.1%, the decomposition rate 160 minutes after the start of experiment shows a decrease of nearly 300 times when compared with the rate at the end of 7.5 minutes. The more concentrated the acid, the greater the difference between the initial and final rates.
3. The same as in the decomposition of apatite, the acid norm affects the decomposition rate of the phosphorite mainly at the start of the process.
4. The degree of decomposition of Kara-Tau phosphorite by thermal phosphoric acid increases when the temperature is raised from 20 to 40°. Thus, at 20° the phosphorite decomposes to the extent of 46.7% in 5 min, and at 40° to the extent of 63.8% in the same length of time, while in 20 minutes the corresponding values are 72.0 and 77.8%. Further increase in the temperature from 40 to 80° fails to raise the degree of decomposition.
5. The degree to which Kara-Tau phosphorite is decomposed by extraction acid (from the same phosphorite) with a P_2O_5 content of 34.0% is lower than when thermal acid of the same concentration is used. The rates of the process are especially different in the first 30-50 minutes of decomposition, and then they tend to become approximately the same. This is explained by the large extent to which the original acid is neutralized.
6. The mechanism for the decomposition of Kara-Tau phosphorite is the same as the mechanism for the decomposition of apatite. However, due to the presence of magnesium compounds in the phosphorite solution, causing a salting out of calcium salts, the time of the first stage is greatly reduced. For this reason, the decomposition of Kara-Tau phosphorite over nearly the entire duration of experiment in the limits from approximately 5 to 150 min is described well by a linear function in the coordinates $1/y$ and $1/\tau$.
7. The isothermal isochrones for Kara-Tau phosphorite lie considerably above the corresponding isothermal isochrones for apatite. The difference is of the order of 25-30%. This is evidently explained by the less-compact and less-dense structure of the phosphorite mineral when compared with apatite, by the presence of a substantial amount of easily decomposed dolomite, and also by the crust of monocalcium phosphate acquiring a friable texture as the result of carbon dioxide evolution.

LITERATURE CITED

- [1] S. K. Milovanova, Nauchno-Tekhn. Inform. Byull. Nauchnyi Inst. po Udobreniyam i Insektofungitsidam 9, 58 (1957).
- [2] A. B. Bekturov and S. G. Trofimova, Izvest. Akad. Nauk Kazan SSR 72, 62 (1949).
- [3] E. V. Yuzhnaya, Author's Abstract [In Russian] (Moscow, 1956).
- [4] M. E. Pozin, B. A. Kopylev, and D. F. Zhil'tsova, Zhur. Priklad. Khim. 32, 3, 509 (1959). *
- [5] M. E. Pozin, B. A. Kopylev, and D. F. Zhil'tsova, Zhur. Priklad. Khim. 32, 10, 2161 (1959). *
- [6] S. K. Milovanova, Nauchno-Tekhn. Inform. Byull. Nauchnyi Inst. po Udobreniyam i Insektofungitsidam 9, 65 (1957).
- [7] M. L. Chepelevetski and E. B. Brutskus, Superphosphate, Physicochemical Principles of Production [In Russian] (Goskhimizdat, 1958).

Received June 12, 1959

*Original Russian pagination. See C.B. Translation.

THE DECOMPOSITION OF ALUMINATE SOLUTIONS WITH ACTIVE SEED

S. I. Kuznetsov, A. N. Stolyarov, V. A. Derevyankin,
O. V. Serebrennikova, and S. F. Vazhenin

S. M. Kirov Ural Polytechnical Institute

The bottleneck in the production of alumina by either the Bayer or the combined Bayer — sinter method is the operation of decomposing the supersaturated aluminate solutions. This decomposition operation is characterized by the following: a long duration (2.2-3.5 days), a comparatively low degree of decomposition of the solutions (approximately 50%), a very inefficient utilization of the equipment capacity, the need to use a large amount of aluminum hydroxide as seed in production, and other disadvantages. Eliminating the indicated principal disadvantages represents a practically important problem.

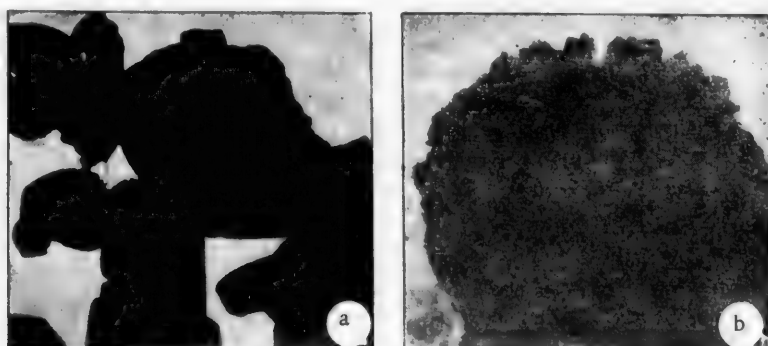


Fig. 1. Electron photomicrographs of aluminum hydroxide. a) Obtained in the decomposition of aluminate solution under production conditions. Magnification 6125. b) Obtained by the spontaneous decomposition (without seeding) of aluminate solution with a low caustic ratio for 2-3 days. Magnification 8750.

Studies made in recent years in the search for methods of intensifying the decomposition process have yielded several interesting recommendations, including the use of seed with a high seeding activity. This type of seed has received the name of active seed.

Active seed represents aluminum hydroxide that has been freshly precipitated from aluminate solutions. When compared with the conventional seed (Fig. 1, a), active seed consists of fine particles with a much more highly developed surface area (Fig. 1, b). Having a high concentration of active sites on the surface (peaks, crystal edges, flaws), the particles of the indicated hydroxide grow more rapidly by a matter of 1.5-2 times and, at the same time, they grow more uniformly during the crystallization process. As a result of this, at the proper temperatures, the fine crystals of active hydroxide seed succeed in growing to the desired size during the time of decomposition.

The use of freshly precipitated, finely crystalline aluminum hydroxide as seed permits a sharp reduction in the seed ratio (ratio of Al_2O_3 in the seed to the Al_2O_3 in solution). If the customary seed ratio is 1.0-1.9, then using active seed it drops down to 0.05-0.1. Such a substantial reduction in the amount of seed does not cause a lengthening of the time of decomposition, since here a quite high total surface of the seed particles is retained, while the rate of their becoming coarser increases.

Different methods can be used to prepare active seed. For example, at the Lautawerk plant (in Germany) the active seed was prepared by taking a portion (5-10%) of the aluminate solution, destined for decomposition, and decomposing it with stirring, but without seeding,* at 40° for 6 days [1]. In this length of time the solution suffered decomposition to a caustic ratio (mole ratio $\text{Na}_2\text{O}_{\text{Cst}}^{**} : \text{Al}_2\text{O}_3$) equal to 6. The finely crystalline aluminum hydroxide, or active seed, obtained in the first stage was used without separating from the mother liquor to decompose the remaining 90-95% of the original solution. Decomposition of the solution with this seed was conducted in the temperature range 60-40°. The yield of alumina was about 55%. All of the decomposition product was salable.

The chief disadvantage of the decomposition method used at the Lautawerk plant is the fact that an insufficiently coarse grade of production aluminum hydroxide was obtained. For this reason the indicated decomposition method failed to find wide commercial acceptance.

In Yugoslavia [2] the active seed was also prepared by the technique of decomposing a portion of the aluminate solution, cooled to 40°, for a matter of 10-14 days. During this time the temperature of the pulp is reduced to 35-30°. The obtained pulp is concentrated. The concentrated product is used to decompose the remainder of the solution. The average seed ratio is 0.05. The time of decomposition with the active seed is 7-8 days. The extent of solution decomposition reaches 50-52%. Here a comparatively coarse hydroxide is obtained, with 60-70% of the material having a mesh size exceeding 270.

The decomposition of aluminate solutions using active seed was also investigated in our country (both at the Ural Aluminum Plant (UAP) and at the All-Union Aluminum-Magnesium Institute). In these investigations the active seed was prepared by the technique of decomposing the aluminate solutions at low temperatures (25 to 40°) in several stages. A very fine aluminum hydroxide was obtained in the first stage by decomposing the solution for a long time: from 8 to 15 days without seeding, or by seeding with small amounts of aluminum hydroxide, obtained in different ways. In the subsequent stages, the product of the first cycle was made coarser by the technique of employing it as seed for either 2 or 3 times. The length of stirring in each stage was 4-6 days. The technological indices of the decomposition process using active seed prepared by the indicated procedure proved to be unsatisfactory: when the coarseness of the hydroxide was satisfactory the amount of solution suffering decomposition was small, or, in reverse, the product had a fine structure when the degree of solution decomposition was satisfactory.

The described methods of using active seed to decompose aluminate solutions possess serious disadvantages. In all cases the preparation of the active seed requires much time. A sufficiently coarse production hydroxide can be obtained only by resorting to a longer time of stirring than that employed in conventional decomposition.

In this paper we give the results of investigating a method for the decomposition of aluminate solutions using active seed that is quite different from existing methods. The main difference consists in the method of preparing the active seed. To obtain the latter, we capitalized on the known property shown by the dust from calcination furnaces to substantially accelerate the decomposition rate of aluminate solutions [3]. The use of this dust as seed is practical for the reason that it causes the formation of large amounts of highly dispersed aluminum hydroxide during the decomposition process.

Results of Laboratory Investigations

The main objective in this portion of the work was to establish both the optimum technological regime of preparing the active seed and the optimum decomposition conditions using active seed. The dust from the calcination furnaces, collected in the multicyclones and electrofilters, was used as the primary seed in all cases.

* Actually, decomposition of the solution proceeded under the influence of small amounts of seed, representing hydroxide particles that had fallen into it from the deposits on the walls of the pipe lines and decomposers.

** cst = caustic.

The main bulk of the dust particles from the multicyclones had a size of 10-25 μ , while the main portion from the electrofilters had a size of 5-10 μ . In both cases, the dust consisted of γ -alumina and boehmite. A small amount of hydrargillite was found in some of the dust samples.

The decomposition of the aluminate solutions was run in three, and at times, in four stages. In each stage, except the first, the aluminum hydroxide obtained in the previous stage served as the seed. The seed ratios were different, ranging from 0.01 to 0.1.

Both synthetic aluminate solutions, obtained by dissolving Al_0 aluminum in chemically pure alkali, and commercial aluminate solutions, obtained from the Bogoslov Aluminum Plant (BAP), were subjected to decomposition. The indicated solutions contained 100-130 g/liter $\text{Na}_2\text{O}_{\text{total}}$ and 95-120 g/liter Al_2O_3 (the mole ratio $\text{Na}_2\text{O}_{\text{total}}:\text{Al}_2\text{O}_3$, denoted by α_{total} , was 1.60 to 1.8, and the caustic ratio, denoted by α_{cst} , was 1.58 to 1.78).

The stirring of the aluminate solutions with seed was done in 100 ml glass flasks or in 250 ml steel autoclaves, set up in thermostats with air agitation. The stirring rate ranged from 12 to 28 rpm.

In the first series of experiments we subjected synthetic aluminate solution, containing 120 g/liter of Al_2O_3 ($\alpha_{\text{total}} = 1.74$; $\alpha_{\text{cst}} = 1.72$), to decomposition. The temperature was maintained constant (25°) in the first stage. The second and third stages were run at different temperature regimes (Fig. 2).

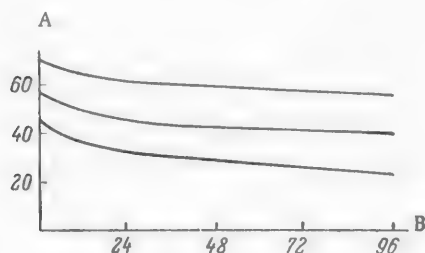


Fig. 2. Temperature regime of decomposition in second and third stages. A) Temperature (in °C); B) time of stirring (in hr).

Pulp samples for analysis were removed after 24, 48, and 96 hours. The aluminate solutions were analyzed volumetrically [4], while the dispersity of the obtained hydroxide was determined by the Figurovskii method [5], as well as microscopically.

In the first stage the extent of solution decomposition in 96 hours was 50-60%. The experimental results obtained in studying the decomposition rate in the second and third stages are plotted in Fig. 3. According to Fig. 3, quite satisfactory yields of alumina are obtained in the second and third stages in 48-96 hours.

The temperature regime of decomposition exerts an important influence on the extent of solution decomposition, especially in the second stage. The highest yields of alumina are observed at low temperatures.

The decomposition rate increases with increase in the seed ratio. Especially noticeable differences in the decomposition rate are observed in the initial period of the process. At the end of 3 to 4 days the extent of solution decomposition becomes the same.

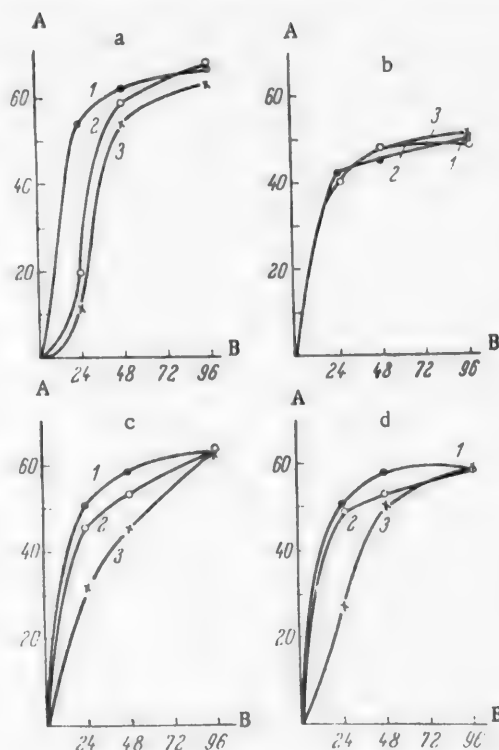


Fig. 3. Decomposition rate of aluminate solution, containing 120 g/liter of Al_2O_3 ($\alpha_{\text{total}} = 1.74$, $\alpha_{\text{cst}} = 1.72$), in the second (a and b) and third (c and d) stages. A) Yield of alumina (in %); B) time of decomposition (in hr). Temperature (in °C): a and c) 45-25; b) 70-55; d) 56-40. Seed ratio: 1) 0.10; 2) 0.05; 3) 0.01.

Determining the dispersity of the precipitates revealed the following.

An exceedingly fine hydroxide, 85% of the material having a size of $10\ \mu$, was obtained in the first stage. In the second stage the average size of the hydroxide particles proved to be $15-30\ \mu$.

It was established that a substantial increase in the coarseness of the hydroxide in the second stage of the process can be achieved by raising the decomposition temperature and decreasing the seed ratio. However, even under the most favorable conditions, it proved impossible to obtain a sufficiently coarse hydroxide. Thus, for example, at a temperature of $70-55^\circ$ and a seed ratio of 0.01 the amount of material with a size of $52\ \mu$ was 60-70% (the main portion of the particles had a size of $20-35\ \mu$).

A sufficiently coarse hydroxide, having an average particle size of $30-60\ \mu$, was obtained in the third stage under the indicated conditions.

As a result, the preparation of seed in the first stage at a low temperature proved to be unwise, since a very fine hydroxide is obtained under these conditions, which fails to become sufficiently coarse in the second stage. Consequently, in subsequent experiments the decomposition of the solution in the first stage was run at elevated temperature, in the range $56-30^\circ$.

In this case, a coarser hydroxide ($8-15\ \mu$) was obtained in the first stage, the use of which as seed in the second stage led to obtaining a fairly coarse product ($30-60\ \mu$). The coarsest hydroxide in the second stage was obtained at a seed ratio of 0.01 and a temperature range of $65-38^\circ$.

As a result, the laboratory experiments revealed that it is possible to prepare active seed, using the dust from calcination furnaces, in one stage, the duration of which is comparatively short (3 days).

The use of this seed in the decomposition process permits reducing the seed ratio sharply. The duration of the decomposition could not be shortened.

It should be mentioned that a substantial increase in the decomposition rate using active seed can be achieved by increasing the seed ratio up to 0.2. In this case, it proves possible to obtain a quite high yield of alumina, approximating 50%, with a stirring time equal to 1 day. However, a finely divided hydroxide is obtained here.

Commercial aluminate solution, obtained from the Bogoslov Aluminum Plant, was subjected to decomposition in the second series of experiments (the experiments were performed in the Central Chemical Laboratory of this plant with the assistance of the co-workers in the laboratory). The solution had the following composition: Al_2O_3 115-130 g/liter ($\alpha_{\text{total}} = 1.75-1.8$, $\alpha_{\text{cst}} = 1.65-1.7$).

The commercial aluminate solution differed from the synthetic in that it contained impurities, which exerted a substantial effect on the decomposition process using active seed. For example, it was established that both the decomposition rate and the crystal size of the obtained hydroxide decrease with increase in the amount of organic impurities in the solution. In the first stage, a decrease in the solution decomposition rate occurs mainly as the result of an increase in the length of the induction period (Fig. 4).

For this reason the need arose, as applied to the commercial solution, of defining more accurately both the optimum technological regime of preparing the active seed and the optimum decomposition conditions using this seed.

The experimental results revealed that the commercial aluminate solution, in contrast to the synthetic solution, showed little decomposition in the first stage at low seed ratios (0.01-0.02). The yield of alumina increases with increase in the amount of seed. A quite practical extent of solution decomposition is achieved using a seed ratio of 0.05. A similar situation is observed in the second stage.

Investigating the decomposition of commercial aluminate solution using active seed made it possible to establish the following interesting phenomenon. It proves that the decomposition results are quite dependent on the source of the dust used for seeding in the first stage. The very fine dust collected in the electrofilters possesses a higher seeding activity than does the dust from the multicyclones. However, an exceedingly fine hydroxide deposits in this case, together with small amounts of coarse particles (exceeding $80-100\ \mu$). It proves impossible to increase the coarseness of this hydroxide to the necessary size in the second, third, or even the fourth stage.

Using the coarser dust, collected in the multicyclones, as the primary seed makes it possible to obtain a sufficiently coarse hydroxide even in the second stage provided both stages are run at elevated temperature: the first stage in the temperature range of 56-60° to 30-35°, and the second stage in the range from 60-65° to 40-45°.

In addition, it was established that the dust from the calcination furnaces loses its seeding activity when stored for a long time. Dust that had been stored for several months caused practically no decomposition of the aluminate solution in 72 hours. The seeding activity of the dust was restored when the dust was stirred for 3 days with aluminate solution. Unfortunately, we were unable to establish a reason for this interesting phenomenon.

The results of the laboratory investigations gave a basis to recommend the discussed decomposition method, using active seed, for testing on an industrial scale.

Results of Industrial Tests

The industrial testing of our proposed method of preparing active seed, and also the decomposition using this seed, was done mainly at the Bogoslov Aluminum Plant.*

In all cases the active seed was prepared in agitators having a capacity of 200 m³, equipped with a chain of stirrers. For seeding in the first stage we used the dust from the calcination furnaces that had been collected in the multicyclones. The seed ratio was 0.05-0.08. The time of stirring the aluminate solution (composition of the solution given above) with

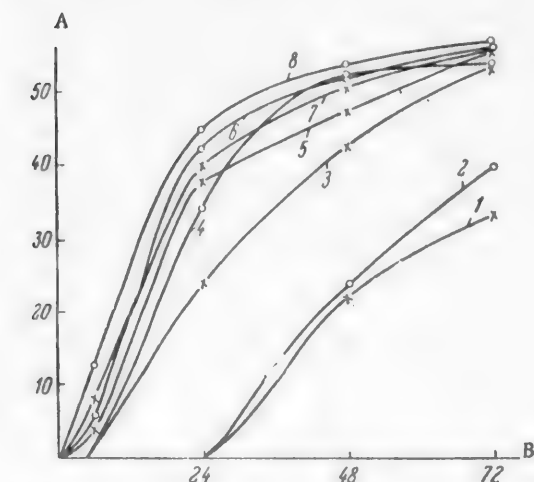


Fig. 4. Effect of concentration of organic impurities on the decomposition rate in the first stage. A) Yield of alumina (in %); B) time of decomposition (in hr). Amount of organic impurities (in % O_2 on Na_2O_{total}) and seed ratio, respectively: 1) 0.95 and 0.05; 2) 0.95 and 0.08; 3) 0.65 and 0.05; 4) 0.6 and 0.08; 5) 0.55 and 0.05; 6) 0.55 and 0.08; 7) no impurities and 0.05; 8) no impurities and 0.08.

the seed was 55-72 hours. The temperature of the solution during stirring was reduced in accordance with the curve shown in Fig. 5.

The extent of aluminate solution decomposition in the first stage proved to be 50-60% (the decomposition rate of the solution is shown in Fig. 5). In all of the experiments, the obtained precipitates consisted of finely crystalline hydrargillite, having the following dispersion composition:

—10 μ 0%	—20 μ 38—47%	—30 μ 84—90%	—52 μ 96—100%	—62 μ 98—100%	—74 μ 100%
-----------------	---------------------	---------------------	----------------------	----------------------	-------------------

Attempts to separate this hydroxide from the mother liquor either by concentration or by filtration proved unsuccessful. It proved that a fine active seed filters poorly and its suction-filtration proceeds very slowly. For this reason, it was used for decomposition without prior separation from mother liquor.

The decomposition of aluminate solution with active seed was run in the same agitators as described above, and also in decomposers with a capacity of 1000 m³, in which stirring was accomplished by aeration using an air-lift pump. The time of stirring the solution with seed was 57-72 hours. The seed ratio was equal to 0.05-0.08.

The same as for the first stage, the graph for reducing the temperature was based on the results of the laboratory investigations (Figs. 6 and 7).

The extent of aluminate solution decomposition under the indicated conditions was 48-52% in the agitators (Fig. 6) and 46-48% in the decomposers (Fig. 7). The higher extent of solution decomposition obtained in the

* The workers of the Bogoslov Aluminum Plant who took an active part in running the industrial tests were I. V. Konovalov, B. G. Chernikov, V. S. Miichenko, and V. K. Belikov.

agitators was due to the actually longer time of decomposition in this equipment when compared with the decomposers. For technical reasons the cooling of the aluminate solution to the initial decomposition temperature was effected in the first case by keeping it in the agitators without seed and without stirring for a matter of 5.5-15 hours. The solutions suffered some decomposition (approximately 5-10%) in this length of time.

The aluminum hydroxide obtained by decomposition using active seed had a satisfactory coarseness:

-20 μ 0.4-5.0%	-30 μ 9.0-21.5%	-52 μ 52.5-83.5%	-62 μ 63.0-89.0%	-74 μ 75.0-89.5%
-----------------------	------------------------	-------------------------	-------------------------	-------------------------

In many of the experiments, it proved to be coarser than the production hydroxide, obtained in the same length of time in the plant when using conventional seed for the decomposition, and having the following dispersion composition:

-20 μ 0-10%	-30 μ 5-40%	-52 μ 25-85%	-62 μ 55-90%	-74 μ 80-95%
--------------------	--------------------	---------------------	---------------------	---------------------

Consequently, the results of the industrial trials proved to be encouraging. A quite high yield of alumina with a satisfactory coarseness of the crystals could be achieved in individual experiments. However, the average yield proved to be somewhat lower than that obtained in conventional decomposition.*

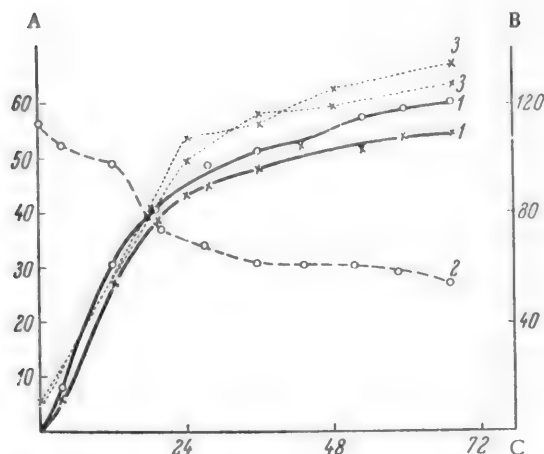


Fig. 5. Decomposition course of aluminate solutions in the first stage. A) Yield of alumina (in %) and temperature (in °C); B) amount of precipitate (in g/liter); C) time of decomposition (in hrs). 1) Extent of solution decomposition; 2) temperature; 3) amount of precipitate.

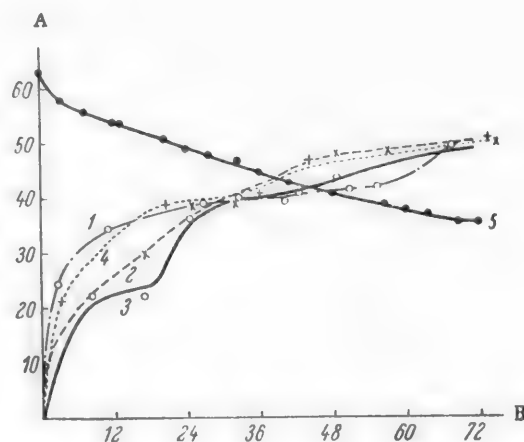


Fig. 6. Course of the decomposition of aluminate solutions in the second stage. A) Yield of alumina (in %) and temperature (in °C); B) amount of precipitate (in g/liter); C) time of decomposition (in hrs). Experiment: 1) No. 4; 2) No. 3; 3) No. 2; 4) No. 5; 5) temperature.

* Similar trials were run at the experimental plant of the Ural Aluminum Plant. The results obtained here proved to be less satisfactory. In not a single experiment was it possible to simultaneously obtain a degree of solution decomposition and a hydroxide coarseness equal to that obtained in the trade. A fine hydroxide separated when the yields of alumina were comparatively high, and, in reverse, it proved possible to obtain a sufficiently coarse hydroxide only at low degrees of solution decomposition. The reasons for obtaining such results were the following: 1) for technical reasons the seed used in the first stage was the dust from the calcination furnaces that had been collected in the electrofilters, and not in the multicyclones; 2) the aluminate solution at the Ural Aluminum Plant was characterized by having a high content of organic impurities (0.9 to 1.38% O_2 on Na_2O_{total}) when compared with the solution from the Bogoslov Aluminum Plant (0.5-0.7% O_2 on Na_2O_{total}).

An attempt to increase the alumina yield by raising the seed ratio or by reducing the decomposition temperature gave negative results. Thus, the yield of alumina, with a stirring time of 72 hours, rose to 55% when the seed ratio was increased to 0.17. However, an insufficiently coarse hydroxide was obtained under these conditions. The same situation was observed when the initial decomposition temperature was reduced to 51°. Simultaneously increasing the seed ratio to 0.14-0.17 and the initial decomposition temperature to 67-69°, and the final temperature to 45°, also failed to give the desired effect, and neither the alumina yield nor the hydroxide coarseness proved to be satisfactory.

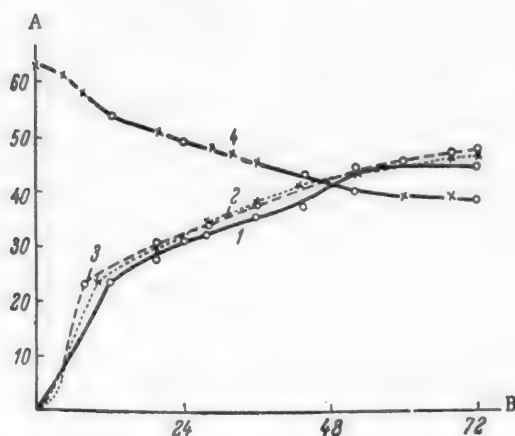


Fig. 7. Course of the decomposition of aluminate solutions in the second stage. A) Yield of alumina (in %) and temperature (in °C); B) time of decomposition (in hours). 1, 2, 3) Yield of alumina; 4) temperature. Amount of Al_2O_3 in solution (in g/liter), α_{total} , α_{cst} and seed ratio, respectively: 1 and 2) 129.5, 1.84, 1.69, and 0.07; 3) 132.2, 1.79, 1.65, and 0.062.

Separate experiments revealed that increasing the decomposition time in the second stage to 88-90 hours makes it possible to obtain both a satisfactory yield of alumina, equal to 50-51%, and a sufficiently coarse crystalline product. However, increasing the alumina yield in this manner is not acceptable, since the length of the operation is increased by approximately a day when compared with conventional decomposition.

The main reason for the industrial trials giving less-favorable results than those obtained in the laboratory consists of the following.

Under plant conditions, the active seed was used without separating from the mother liquor. As a rule, under laboratory conditions, it was separated from the solution by filtration.

Both calculations and analysis revealed that mixing the original aluminate solution with active seed, not separated from mother liquor, raises the caustic ratio of the former by approximately 0.3-0.4. Consequently, under industrial conditions, the solution subjected to decomposition in the second stage actually had a caustic ratio of 2.0-2.1, and at times even higher.

Investigation of conventional decomposition, and also the operating practice of aluminum plants, both show that increasing the caustic ratio of the starting aluminate solution by 0.1 causes, with the other conditions kept constant, an average reduction of approximately 3-4% in the yield of alumina. The results of the laboratory experiments revealed that increasing the caustic ratio of the starting solution also leads to a substantial decrease in the alumina yield when decomposition is with active seed. Thus, increasing the caustic ratio of solution destined for decomposition from 1.7-1.8 to 2.0-2.1 causes the alumina yield to drop by 6-10% (for a stirring time of 72 hours).

As a result, to obtain satisfactory indices for the decomposition process when using active seed it is necessary that the latter be separated in some manner from the mother liquor.

Good results under production conditions can be obtained only by using centrifuge separators, for example, models NOGSh-600 and NOGSh-800 [6]. Unfortunately, the manufacture of these centrifuges in our country has been retarded.

A substantial increase in the alumina yield is achieved if the active seed is separated from the mother liquor. It becomes necessary to define the optimum conditions for running the second stage more accurately when this is done. Here it may prove quite possible to increase the decomposition temperature somewhat, and, consequently, obtain a coarser hydroxide.

The industrial trials revealed that the hydroxide obtained using active seed for the decomposition can be satisfactorily concentrated, filtered, and washed free of mother liquor. A noticeable decrease in the coarseness of the hydroxide is not observed here. During calcination this hydroxide fails to suffer any more pulverization than does ordinary hydroxide.

The results of the present investigation indicate that the proposed decomposition method may find industrial use. The final decision as to the practicality of using this method on an industrial scale can be made only after additional trials, which will be run as soon as we find a practical way of separating the active seed from the mother liquor. It is quite possible that here the proposed method can also be used for the decomposition of aluminate solutions with a high content of organic impurities, for example, the solution from the Ural Aluminum Plant.

The introduction into industry of the proposed method for the decomposition of aluminate solutions using active seed makes it possible to sharply reduce the seed ratio to 0.06-0.08, which increases the useful capacity of the decomposers, i.e., it increases the productive output of the entire decomposition equipment. Calculations reveal that using the indicated decomposition method permits increasing the productivity of the decomposers by approximately 10%. The entire decomposition product will be salable.

In the absence of a practical method for separating the active seed from mother liquor, it is possible to use the given decomposition method for the design of tentative production in the building of new alumina plants. This makes it possible to eliminate the transport of hydroxide from other plants and is limited only by the availability of small amounts of dust from calcination furnaces.

LITERATURE CITED

- [1] A. I. Belyaev, *Tsvetnye Metal.* 19, 1 (1946).
- [2] A. N. Lyapunov and A. V. Pavlov, *Legkie Metal.* 3, 75 (1957).
- [3] F. F. Vol'f and S. I. Kuznetsov, Soviet Author's Certificate No. 8,422,319, Class 12, Subclass T, Group 5 (1949).
- [4] N. I. Bogolepov, *Legkie Metal.* 4, 22 (1936).
- [5] A. I. Lainer and M. A. Brovman, *Sbornik Trudy Moskov. Inst. Tsvetnye Metal. i Zolota im. M. I. Kalinina* 22, 182 (1952).
- [6] *Centrifuges, Catalog and Handbook [In Russian]* (Mashgiz, 1955), p. 55.

Received August 23, 1958

PHYSICOCHEMICAL PROPERTIES OF TRIPOTASSIUM PHOSPHATE SOLUTIONS*

L. S. Bezdel', V. P. Teodorovich, and V. V. Ipat'ev

All-Union Scientific Research Institute of Petroleum Chemical Processes

Whereas various methods are used to remove hydrogen sulfide from gases, only three methods are known for the purification of the propane-propylene fraction (PPF): purification using solutions of sodium hydroxide, ethanolamine [1], and tripotassium phosphate (TPP).

Only caustic soda is used in the Soviet Union for the purification of liquefied hydrocarbons. The sodium hydrosulfide that is formed here cannot be regenerated, which necessitates a large consumption of caustic, making the cost of the finished commercial product expensive.

Because of its good water solubility, it is possible for TPP to yield solutions that have a high absorption capacity for hydrogen sulfide, while its nonvolatility and lack of solubility in hydrocarbons makes it especially suitable for the purification of liquid products.

In connection with the design and construction of plants in the Soviet Union for the removal of hydrogen sulfide from gases and liquefied hydrocarbons using TPP solution it proved necessary to collect some data for calculating the apparatus design. The use of sodium salts of phosphoric acid to remove hydrogen sulfide was first proposed by Rosenstein [2]. However, this process, making it possible to utilize a relatively cheap chemisorbent like trisodium phosphate, failed to find commercial use.

In 1938, a paper was published by Rosebaugh [3], in which the use of TPP solution as an active chemisorbent for hydrogen sulfide was mentioned for the first time. TPP can be used to remove hydrogen sulfide from both gases and liquefied hydrocarbons, since due to its excellent solubility in water it can give solutions that have a high absorption capacity for hydrogen sulfide, and, at the same time, they are easily regenerated.

Rosebaugh described the principal technological schemes for running this process. The chemical reaction for binding the hydrogen sulfide is the following:



This reaction is reversible, and the equilibrium is shifted in the direction of hydrogen sulfide evolution from solution when the temperature is raised.

The use of this process to purify cracking gases was described by Mullen [4], while La Croix described its use for the purification of liquefied hydrocarbons [5].

The laboratory studies made by Pletneva [6] on the use of TPP solutions to remove hydrogen sulfide from gasolines bear a qualitative nature. The results of the work on regenerating the spent solutions are such that they cannot be used in calculating the design of the production equipment.

The purpose of the present study was to investigate the properties of TPP solutions. In this connection, we determined the densities, boiling points, heat capacities and the equilibrium concentrations of hydrogen sulfide in the systems H_2S - liquefied PPF - TPP solutions.

*Communication I.

Preparation of tripotassium phosphate solutions. TPP solutions of different concentration were prepared by the neutralization of either monopotassium phosphate (KH_2PO_4) or orthophosphoric acid with potassium hydroxide. For the quantitative determination of the amount of either free alkali or dipotassium phosphate, and also of TPP, in the solution we employed the potentiometric titration method, using a glass electrode.

In the future we will tentatively use the terms: a) a solution containing 1 mole of TPP (212 g) in 1 kg of solution will be called "monomolar", and b) a solution containing 2 moles of TPP (424 g) in 1 kg of solution will be called "bimolar". Solutions containing hydrogen sulfide will be characterized by the degree of saturation z , equal to the molar ratio of hydrogen sulfide to TPP, $\frac{\text{moles H}_2\text{S}}{\text{moles K}_3\text{PO}_4}$. In the calculations, it is more convenient to use the degree of saturation than the molecular concentration, since the density of the solution changes when hydrogen sulfide dissolves in it.

The densities of the TPP solutions of different concentration were determined at 20 and at 30°. The data are given in Table 1.

TABLE 1
Physicochemical Properties of TPP Solutions

Concentration of TPP in solution (in mole/kg)	Density of solution (in kg/liter) at temperature		Boiling point (in °C)	Heat capacity (in cal/kg·deg) at temperature	
	20°	30°		20°	57°
0.510	1.0950	—	—	0.853	0.870
0.815	—	—	101.2	—	—
1.02	1.2210	—	—	0.749	0.789
1.18	1.2736	1.2714	102.8	—	—
1.51	1.3520	—	—	0.655	0.689
1.62	1.3953	1.3937	—	—	—
2.00	1.5203	—	108.5	0.575	0.618
2.20	1.5723	1.5708	109.5	—	—
2.54	1.6930	—	—	0.531	0.560
2.58	1.7024	—	116.0	—	—
2.77	1.7799	1.7787	122.0	—	—

The density of the solution decreases when hydrogen sulfide dissolves in TPP solution. The change in the density of the solutions as a function of their degree of saturation with hydrogen sulfide can be expressed by the equations: for the bimolar K_3PO_4 solution, $d = 1.5203 - 0.0930z$, and for the solution containing 1.5 moles K_3PO_4 and 0.5 mole K_2HPO_4 , $d = 1.4785 - 0.0664z$.

TABLE 2
Relation Between the Boiling Points of the Solutions and Their Composition

Composition of solution (in moles)	Density of solution	Boiling point of solution (in °C)
1.0 $\text{K}_3\text{PO}_4 + 0.5 \text{K}_2\text{HPO}_4$	1.440	105.8
1.5 $\text{K}_3\text{PO}_4 + 0.5 \text{K}_2\text{HPO}_4$	1.517	108.5
2.0 $\text{K}_3\text{PO}_4 + 0.5 \text{K}_2\text{HPO}_4$	1.620	112.5
2.5 $\text{K}_3\text{PO}_4 + 0.5 \text{K}_2\text{HPO}_4$	1.735	118.5

Determination of boiling points of phosphate solutions. A thermometer, immersed in the vessel containing the boiling solution, was used to measure the boiling points of the phosphate solutions at atmospheric pressure. This vessel was connected through a condenser to a monostat, by means of which a constant pressure was maintained in the vessel. We not only determined the boiling points of pure TPP solutions of different concentration (Table 1), but also of their mixtures with dipotassium phosphate. The boiling points of the solutions composed of mixtures of K_3PO_4 and K_2HPO_4 are given in Table 2.

Heat capacities of tripotassium phosphate solutions. To determine the heat capacities of aqueous TPP solutions we used the method of mixing the investigated liquid with mercury, the latter having an accurately known heat capacity. The scheme of the apparatus is shown in Fig. 1. The heat capacities of the solutions, and also the water number of the calorimeter, were determined in the following manner. For the determination, we took 300 ml of the test solution, weighed with an accuracy of ± 0.02 g, and poured it into a Dewar vessel. The mercury was weighed out with the same accuracy, after which it was poured into a pipet encased in a steam-heated jacket. The amount of mercury poured into the pipet was such that when it was added to the solution, the temperature of the latter rose by $1-2^\circ$.

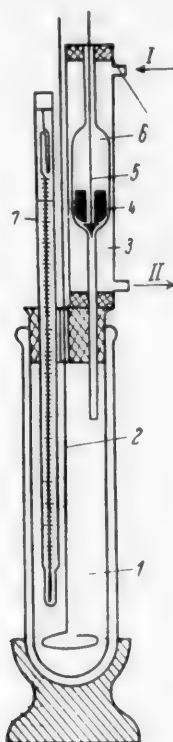


Fig. 1. Scheme of apparatus for determining the heat capacity of K_3PO_4 solutions. 1) Solution, 2) stirrer, 3) steam jacket, 4) mercury, 5) seal, 6) pipet, 7) thermometer. I) Steam inlet, II) steam outlet.

TABLE 3
Viscosity of Tripotassium Phosphate Solutions at Different Temperatures

Temperature	Viscosity (in centistokes) of K_3PO_4 solutions	
	1 Mole	2 Moles
20	1.68	5.56
30	1.36	4.16
40	1.14	3.28
50	0.96	2.70
60	0.81	2.30
70	0.70	1.98
80	0.62	1.72
90	0.57	1.44
99.8	0.54	1.17

TABLE 4
Viscosity of Tripotassium Phosphate Solutions, Saturated with Hydrogen Sulfide, at 20°

Degree of saturation of solution with hydrogen sulfide	Viscosity (in centistokes) of K_3PO_4 solutions	
	1 Mole	2 Moles
0.0	1.68	5.56
0.2	1.58	4.96
0.4	1.51	4.37
0.6	1.42	3.82
0.7	1.36	3.58
0.8	1.32	3.35
0.9	1.28	3.12
0.95	1.25	3.00

Viscosity of TPP solutions at 20° . An Ostwald-Pinkevich viscosimeter was used to measure the viscosity. The thermostat temperature was maintained constant with an accuracy of $\pm 0.1^\circ$. The results of measuring the viscosity of different tripotassium phosphate solutions are given in Table 3.

The results of measuring the viscosity at 20° of tripotassium phosphate solutions, saturated to variable degree with hydrogen sulfide, are given in Table 4.

Equilibrium Distribution of Hydrogen Sulfide Between Chemisorbent and Propane - Propylene Fraction (PPF)

Equilibrium distribution of hydrogen sulfide between aqueous TPP solution and PPF at 20° C. The equilibrium concentration of hydrogen sulfide in the system bimolar K_3PO_4 solution - H_2S - PPF was determined in the pressure apparatus usually used for this purpose [7].

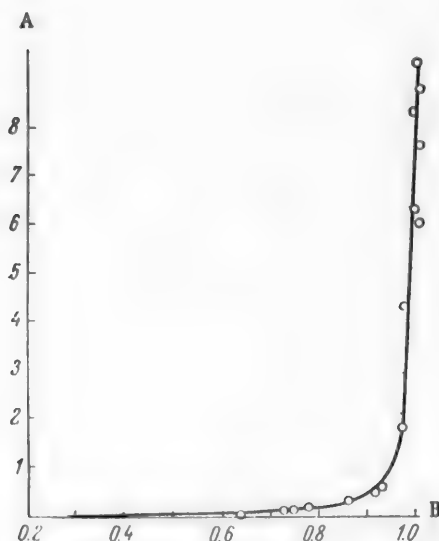


Fig. 2. Equilibrium curve for the distribution of hydrogen sulfide between bimolar K_3PO_4 solution and liquid propane-propylene fraction. A) Concentration of H_2S in PPF (in mole %); B) concentration of H_2S (in mole/mole K_3PO_4).

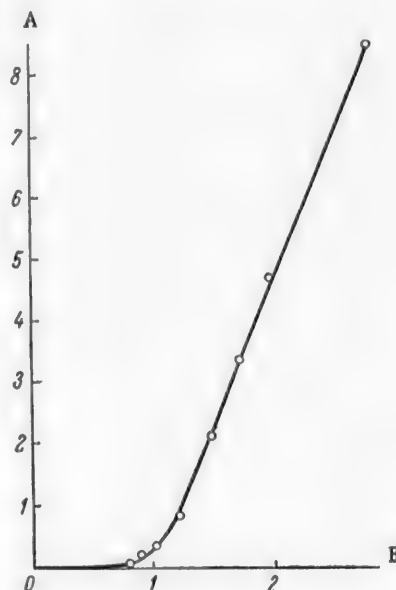


Fig. 3. Equilibrium curve for the distribution of hydrogen sulfide between liquid propane-propylene fraction and 0.18 molar Na_3PO_4 solution. A) Concentration of H_2S in PPF (in mole %); B) molar ratio H_2S/Na_3PO_4 .

The apparatus consists of a water thermostat, equipped with stirrer, into which the autoclave, designed for operating under pressure, is immersed. The autoclave was fitted with a stirrer and two tubes: one of the tubes descended to the bottom of the autoclave and served to remove samples from the lower phase (TPP solution), while the second tube reached to the middle of the autoclave and permitted removing samples from the upper phase (PPF).

The experiments were run in such a manner that equilibrium was approached from both sides, and specifically: a part of the experiments was run using a PPF that contained from 1 to 10 mole % of hydrogen sulfide, and a TPP solution that was weakly saturated with hydrogen sulfide, while another part of the experiments was run using a PPF that was free of hydrogen sulfide and a TPP solution that was saturated with hydrogen sulfide. The propane-propylene fraction used by us contained 31.2% propylene, 65% propane, and 3.8% butanes.

Using a liquid pump, a known amount of TPP solution was pumped from a buret into the autoclave, while the compressed PPF was admitted from a cylinder into the autoclave through the valve that also served to remove samples from the upper liquid layer; then the whole was stirred for 5-6 hours. After this, samples were removed from both phases and analyzed for their content of hydrogen sulfide. Stirring was resumed after taking the samples, and then new samples were taken. Agreement of the analysis results indicated that equilibrium had been reached.

The experimental results obtained in determining the equilibrium distribution of hydrogen sulfide between bimolar TPP solution and the PPF at 20° are given in Table 5. The equilibrium concentrations of hydrogen sulfide in the liquefied PPF as a function of \underline{z} are plotted in Fig. 2.

TABLE 5
Experimental Results Obtained
in Studying the Equilibrium
Distribution of Hydrogen Sulfide
Between PPF and Bimolar TPP
Solution

Concentration of hydrogen sulfide (in mole/mole K_3PO_4)	Concentra- tion of H_2S in PPF (in mole %)
0.290	0.0026
0.490	0.0033
0.630	0.0103
0.710	0.0201
0.740	0.0352
0.778	0.0528
0.830	0.0980
0.840	0.130
0.855	0.115
0.865	0.140
0.905	0.332
0.910	0.412
0.932	0.578
0.940	1.000
0.960	1.500
0.980	4.400
1.020	6.000
1.020	7.650
1.010	8.400
1.010	9.000
1.020	9.850

TABLE 6
Results Obtained in Studying
the Equilibrium Distribution
of Hydrogen Sulfide Between
PPF and TPP Solution at 20°

Amount of K_3PO_4 (in %)	H_2S Na_3PO_4	H_2S in PPF (in mole %)
5.04	0.32	—
	1.05	0.28
3.1	0.9	0.20
	1.47	2.1
	1.22	0.85
	1.22	0.93
2.62	1.68	3.43
	1.97	4.68
	2.3	8.56

As can be seen from Table 5, bimolar TPP solution, saturated with hydrogen sulfide to the extent of $z = 0.95$ to 0.97 , is practically incapable of absorbing any more hydrogen sulfide, despite the high concentrations of the latter in the PPF. Some increase in the amount of hydrogen sulfide in TPP solution at high partial pressures of the former can be explained as being entirely due to physical solution.

Equilibrium distribution of hydrogen sulfide between PPF and trisodium phosphate at 20°.

In view of the fact that the sodium salts of phosphoric acid are considerably cheaper than the potassium salts, it seemed intriguing to use them for the removal of hydrogen sulfide from hydrocarbons. However, because of the low solubility of trisodium phosphate (TSP), its use as a chemisorbent is impractical. In addition, the deposition of crystals is observed when hydrogen sulfide is dissolved in the more concentrated trisodium phosphate solutions, which also serves to discourage the use of trisodium phosphate as a chemisorbent. The concentrations of hydrogen sulfide in PPF, found in equilibrium with an aqueous solution of 0.18 mole of TSP in 1 kg of solution, were determined. The obtained data are given in Table 6 and plotted in Fig. 3. The equilibrium curve for the distribution of hydrogen sulfide in the system PPF — TSP has a more gentle slope at high values of z than is true of the corresponding curve for the TPP solution.

SUMMARY

The principal physicochemical constants of aqueous tripotassium phosphate solutions were determined. The design of equipment for the removal of hydrogen sulfide from the propane — propylene fraction can be based on the obtained results.

LITERATURE CITED

- [1] K. A. Edwards, D. I. Krzymuski, and co-workers, *Petroleum* (London) 19, 5 (1956).
- [2] L. Rosenstein and G. A. Kramer, U. S. Patent 1,945,163 (1934).
- [3] T. W. Rosebaugh, *Refiner Natural Gasoline Manufacturer* 17, 6, 245 (1938).

- [4] J. M. Mullen, Refiner Natural Gasoline Manufacturer 18, 159 (1939).
- [5] H. N. La Croix and L. J. Coulthurst, Refiner Natural Gasoline Manufacturer 18, 334 (1939).
- [6] O. V. Pletneva, Collected Works of Central Scientific Research Institute of Aviation Fuels and Oils [In Russian] (1944).
- [7] V. V. Ipat'ev and M. I. Levina, Khim. Tverdogo Topliva 100, 866 (1937).

Received November 5, 1958

SEA SYSTEM K, Na, Mg || Cl, SO₄ - H₂O AT 0°

O. K. Yanat'eva and V. T. Orlova

A study of complex systems of the sea type has great interest from the viewpoint of the chemistry, geochemistry and technology of mineral salts of oceanic origin.

As is known, the aqueous quinary reciprocal system containing the six salts (KCl , NaCl , MgCl_2 , K_2SO_4 , Na_2SO_4 , and MgSO_4) was subjected to partial study (in the region of NaCl saturation) by Van't Hoff and co-workers, and possesses great importance when the processes for the evaporation of sea water and natural brines are studied. There is hardly any information in the literature on this system at low temperatures, and all of the 5 points obtained by D'Ans at 0° also relate only to the region of saturation with sodium chloride [1]. Despite this, knowing the conditions under which salts crystallize, not only in the evaporation of brines, but also when brines are cooled, is of definite interest.

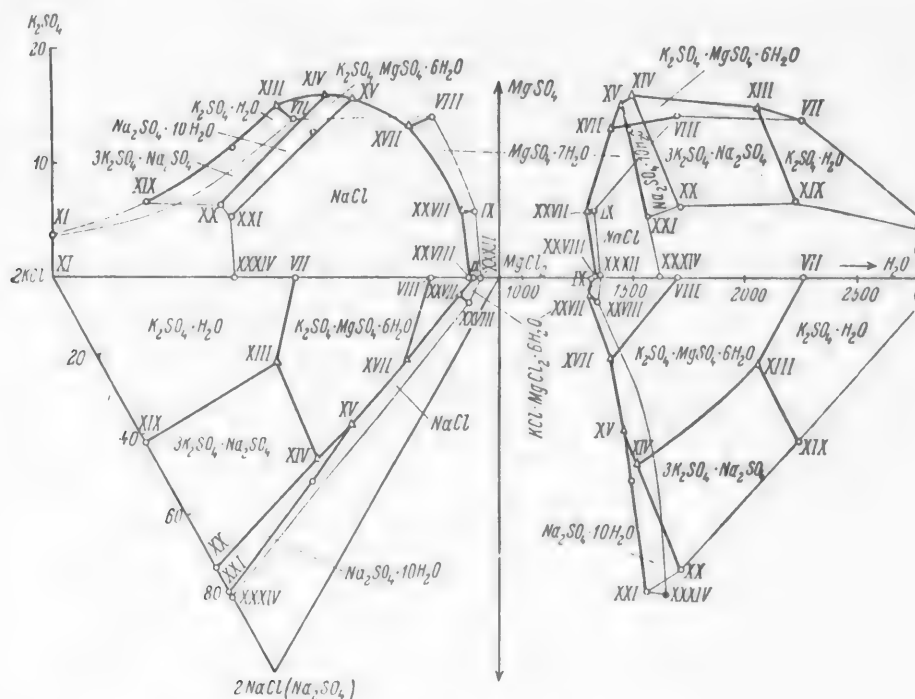


Fig. 1. Region of KCl crystallization in the system K, Na, Mg || Cl, SO₄ - H₂O at 0°.

Despite the slow rate with which salts dissolve at low temperatures and the need of maintaining a constant temperature in the cryostat for a long time, we made a complete study of the 0° isotherm of the quinary sea system as a component part of the polytherms of this system studied by us; equilibrium was reached in a matter of 15-25 days. First we restudied at 0° the simple systems (K, Na || SO₄-H₂O; K, Na, Mg || SO₄-H₂O; K, Na || Cl, SO₄-H₂O and K, Mg || Cl, SO₄-H₂O), entering into the composition of the quinary system, since

TABLE 1

System K, Na, Mg || Cl, SO_4 - H_2O at 0°

Point No.	Composition of liquid phase											Solution density (g/cc)	Solution viscosity (in centipoises)	Solid phase			
	Weight percent					Ionic percent (according to Jaenecke)											
	KCl	NaCl	MgCl ₂	K ₂ SO ₄	Na ₂ SO ₄	MgSO ₄	Total salts	H ₂ O	2K	2Na	Mg	2Cl	SO ₄	H ₂ O			
I-1	—	—	—	7.58	5.44	—	13.02	86.98	53.18	46.82	—	—	100.00	5900.7	1.1180	1.0152	K ₂ SO ₄ · H ₂ O + K ₂ NaSO ₄ · 10H ₂ O
II-2	—	—	—	7.89	5.28	8.51	21.68	78.32	29.57	24.28	46.15	—	100.00	2838.2	1.2205	2.3262	K ₂ SO ₄ · H ₂ O + + Na ₂ SO ₄ · 10H ₂ O + + schoenite
3	—	4.99	—	7.62	0.61	8.38	21.60	78.40	27.26	29.32	43.42	26.64	73.36	2714.0	—	—	K ₂ SO ₄ · H ₂ O + + Na ₂ SO ₄ · 10H ₂ O + + schoenite
XII-2	2.79	5.32	—	5.07	—	8.22	21.40	78.60	29.58	28.16	42.26	39.73	60.27	2699.1	1.1896	1.7645	K ₂ SO ₄ · H ₂ O + + Na ₂ SO ₄ · 10H ₂ O + + schoenite + glaserite
5	7.44	2.16	—	—	3.71	8.02	21.33	78.67	30.97	27.68	41.35	42.46	57.54	2709.9	—	—	K ₂ SO ₄ · H ₂ O + + schoenite + glaserite
6	8.01	2.88	—	—	2.84	7.93	21.66	78.34	32.70	27.17	40.13	47.69	52.31	2647.5	—	—	K ₂ SO ₄ · H ₂ O + + schoenite + glaserite
7	9.11	4.78	1.73	—	—	6.18	21.80	78.20	35.63	23.84	40.53	70.05	29.95	2530.6	—	—	K ₂ SO ₄ · H ₂ O + + schoenite + glaserite
XVIII-8	2.68	7.07	—	6.74	—	—	16.49	83.51	48.42	51.58	—	66.95	33.05	3957.4	1.1299	1.0300	K ₂ SO ₄ · H ₂ O + + Na ₂ SO ₄ · 10H ₂ O + + glaserite
9	3.53	6.30	—	5.28	—	3.31	18.42	81.58	39.88	39.81	20.31	57.31	42.69	3343.5	—	—	K ₂ SO ₄ · H ₂ O + + Na ₂ SO ₄ · 10H ₂ O + + glaserite
10	3.13	5.33	—	4.46	—	7.67	20.59	79.41	29.89	29.25	40.86	42.72	57.28	2826.6	—	—	K ₂ SO ₄ · H ₂ O + + Na ₂ SO ₄ · 10H ₂ O + + glaserite
11	2.77	5.52	—	4.83	—	8.16	21.28	78.72	28.71	29.26	42.03	40.79	59.21	2708.2	—	—	K ₂ SO ₄ · H ₂ O + + Na ₂ SO ₄ · 10H ₂ O + + glaserite

TABLE 1 (Continued)

Point No.	Composition of liquid phase										Solid phase					
	Weight percent					Ionic percent (according to Jaenecke)										
	KCl	NaCl	MgCl ₂	K ₂ SO ₄	Na ₂ SO ₄	MgSO ₄	Total salts	H ₂ O	2K	2Na		Mg	2Cl	SO ₄	H ₂ O	
12	7.46	7.73	1.58	—	—	7.34	24.11	75.89	25.80	34.11	40.09	68.48	31.52	2173.9	—	Na ₂ SO ₄ · 10H ₂ O + glaserite + schoenite
III-13	—	—	—	8.14	—	8.53	16.67	83.33	39.71	—	60.29	—	100.00	3935.5	1.7174	K ₂ SO ₄ · H ₂ O + schoenite
VIII-14	8.92	—	9.76	4.51	—	—	23.19	76.81	45.54	—	54.46	86.24	13.76	2264.8	—	KCl + K ₂ SO ₄ · H ₂ O + schoenite
15	11.94	3.32	5.64	—	—	3.42	24.32	75.68	40.85	14.48	44.67	85.52	14.48	2141.6	—	KCl + K ₂ SO ₄ · H ₂ O + schoenite
XI-16	21.50	—	—	0.90	—	—	22.40	77.60	100.00	—	—	96.52	3.48	2882.3	—	KCl + K ₂ SO ₄ · H ₂ O + schoenite
XIX-17	14.26	9.05	—	2.14	—	—	25.45	74.55	58.23	41.77	—	93.36	6.64	2231.5	1.1909	KCl + K ₂ SO ₄ · H ₂ O + glaserite
18	13.06	6.87	2.59	—	—	2.56	25.08	74.92	44.94	30.18	24.88	89.08	10.92	2134.4	—	KCl + K ₂ SO ₄ · H ₂ O + glaserite
XIII-19	11.90	5.07	4.68	—	—	3.70	25.35	74.65	39.31	21.38	39.31	84.88	15.12	2040.6	1.2097	KCl + K ₂ SO ₄ · H ₂ O + glaserite + schoenite
XX-20	6.91	19.86	—	2.51	—	—	29.28	70.72	26.32	73.68	—	93.75	6.25	1701.8	1.2126	KCl + Na ₂ SO ₄ · 10H ₂ O + glaserite
21	8.13	18.23	0.56	—	—	2.71	29.63	70.37	22.79	65.33	11.88	90.59	9.41	1635.2	—	KCl + Na ₂ SO ₄ · 10H ₂ O + glaserite
XIV-22	6.00	14.45	5.39	—	—	5.16	31.00	69.00	15.30	46.92	37.78	83.71	16.29	1454.6	1.2498	KCl + Na ₂ SO ₄ · 10H ₂ O + glaserite + schoenite
XXI-23 [2]	7.55	21.35	—	—	1.85	—	30.75	69.25	20.60	79.40	—	94.70	5.30	1560.1	1.2401	KCl + Na ₂ SO ₄ · 10H ₂ O + NaCl
24	6.01	15.45	4.70	—	—	4.01	30.17	69.83	15.80	51.80	32.40	86.94	13.06	1518.9	—	KCl + Na ₂ SO ₄ · 10H ₂ O + NaCl
V-25 [2]	—	—	—	3.60	3.95	19.70	27.25	72.75	9.71	13.15	77.14	—	100.00	1903.3	—	MgSO ₄ · 7H ₂ O + Na ₂ SO ₄ · 10H ₂ O + schoenite
26	—	—	6.28	3.75	6.11	9.74	25.88	74.12	10.18	20.35	69.47	31.19	68.81	1947.0	—	MgSO ₄ · 7H ₂ O + Na ₂ SO ₄ · 10H ₂ O + schoenite
27	—	—	9.78	3.99	6.76	5.10	25.63	74.37	10.62	22.08	67.30	47.63	52.37	1914.1	—	MgSO ₄ · 7H ₂ O + Na ₂ SO ₄ · 10H ₂ O + schoenite

TABLE 1 (Continued)

Point No.	Composition of liquid phase														Solid phase	Solution viscosity η (in centipoises)
	Weight percent							Ionic percent (according to Jaenecke)								
	KCl	NaCl	MgCl ₂	K ₂ SO ₄	Na ₂ SO ₄	MgSO ₄	Total salts	H ₂ O	2K	2Na	Mg	2Cl	SO ₄	H ₂ O		
IV-28	—	—	—	3.62	—	21.00	24.62	75.38	10.65	—	89.35	—	100.00	2142.0	MgSO ₄ · 7H ₂ O + +schoenite	5.4847
VIII-29	—	—	19.72	6.05	—	—	25.77	74.23	14.34	—	85.66	85.66	14.34	1703.5	MgSO ₄ · 7H ₂ O + + schoenite	—
XVII-30	4.73	1.87	18.10	—	5.30	—	30.00	70.00	11.52	19.39	69.09	86.44	13.56	1412.5	MgSO ₄ · 7H ₂ O + + schoenite + KCl + NaCl	—
XVII'-31 [1]	3.65	3.40	18.75	—	—	3.50	29.30	70.70	8.71	10.33	80.96	89.67	10.33	1393.2	MgSO ₄ · 7H ₂ O + +schoenite + KCl + NaCl	—
XXX-32 [2]	0.10	0.20	33.40	—	—	1.60	35.30	64.70	0.19	0.47	99.34	96.37	3.63	979.7	MgSO ₄ · 7H ₂ O + NaCl + + MgCl ₂ · 6H ₂ O + + camallite	—

the data given in the literature for them proved to be highly contradictory [2]. The results obtained in the process of studying the isotherms have been published in part by us as individual papers, in which we have also given a detailed description of the experimental portion of the work [3].

The solubility diagram of the system K, Na, Mg || Cl, SO₄-H₂O at 0° is considerably simpler than at 25 and 55° [4, 5]. If nine chemical compounds are known for the 55° isotherm, and six for the 25° isotherm, then only three compounds are formed in the system at 0°: schoenite, glaserite and carnallite, in which connection the crystallization regions of the last two salts are extremely small. A total of nine solid phases crystallize in the system at 0° (KCl, NaCl, MgCl₂·6H₂O, K₂SO₄·H₂O, Na₂SO₄·10H₂O, MgSO₄·7H₂O, glaserite - 3K₂SO₄·Na₂SO₄, schoenite - K₂SO₄·MgSO₄·6H₂O, and carnallite - KCl·MgCl₂·6H₂O), the regions for the existence of which were studied in detail by us.

The numerical data obtained relative to determining the solubility, viscosity and density in the quinary system at 0° are given in Table 1.

To graphically depict the equilibria in the system we used the method proposed by us, already described in a number of papers [4, 5], which made it possible to plot, without exception, all of the components of the system on the diagram; the region for the existence of each solid phase, represented as a volume on the isotherm of the quinary system, was drawn separately for greater clarity. In Figs. 1 and 2, we show the drawings for the volumes of crystallization of KCl, NaCl, and MgSO₄·7H₂O, where the fine lines delineate the fields in the simple systems, while the heavier lines correspond to the crystallization of three phases in the quinary system; in constructing the diagrams the solubility data were expressed in ionic percent by the Jaenecke method.

The potassium chloride crystallization volume, the drawing for which is given in four projections (Fig. 1), is bounded by only a few of the salt volumes in the system; it has seven internal boundaries, corresponding to the joint crystallization of KCl with glaserite (XIII - XIV - XIX - XX), schoenite (VII - VIII - XIII - XIV - XV - XVII), potassium sulfate (VII - XI - XIII - XIX), sodium sulfate (XIV - XV - XX - XXI), magnesium sulfate (VIII - IX - XVII - XXVII), sodium chloride (XV - XVII - XXI - XXVII - XXVIII - XXXIV) and carnallite (IX - XXVII - XXVIII - XXXII); its external boundaries are the KCl crystallization fields in the three quaternary systems K, Na, Mg || Cl-H₂O, K, Na, Mg || Cl-H₂O, K, Na || Cl, SO₄-H₂O and K, Mg || Cl, SO₄-H₂O entering into the composition of the quinary system.

The NaCl and $\text{MgSO}_4 \cdot 7\text{H}_2\text{O}$ crystallization volumes, drawn in one main projection (Fig. 2), each have six internal and three external boundaries. To draw the boundaries in the sodium chloride volume we made partial use of D'Ans' data [1] and also investigated several additional points; the values obtained for point XVII, corresponding to the joint crystallization of four salts (schoenite, NaCl, KCl, and $\text{MgSO}_4 \cdot 7\text{H}_2\text{O}$), do not agree with the data given in the literature (point XVII*, Table 1, Fig. 2, top). Sodium chloride crystallizes from its water solutions at 0° as the dihydrate, which suffers dehydration in the presence of the salts of the investigated quinary system. In the literature, some authors assert that $\text{NaCl} \cdot 2\text{H}_2\text{O}$ [6, 7] exists only in the ternary system $\text{NaCl} - \text{Na}_2\text{SO}_4 - \text{H}_2\text{O}$, while other authors, in contrast, reject its existence [8, 9]; for this reason we have shown the small dihydrate region in Figs. 2 and 3 by a tentative point.

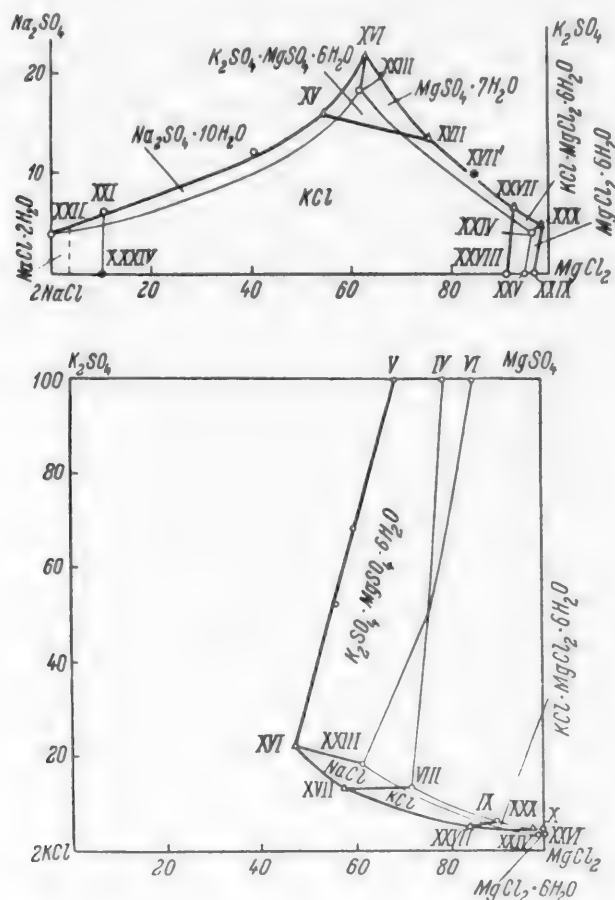


Fig. 2. Crystallization regions of NaCl (top) and $\text{MgSO}_4 \cdot 7\text{H}_2\text{O}$ (bottom) in the system K, Na, Mg || Cl, $\text{SO}_4 - \text{H}_2\text{O}$ at 0° .

Diagrams similar to those described above (Figs. 1 and 2), needed for practical use, were drawn by us for nine of the investigated salt crystallization volumes in the system, some of which have already been published (for schoenite, glaserite, $K_2SO_4 \cdot H_2O$ and $Na_2SO_4 \cdot 10H_2O$) [3]. For a very general characterization of the volumes of all of the salts in the system we give here only the scheme of their paragenetic relationships (Table 2) and a photograph of the space model of the system (photographed from three sides), showing at the same time the relative dimensions of the different volumes (Fig. 3, a, b, and c). As can be seen from Fig. 3, the crystallization volumes of the least-soluble sulfates in the system occupy almost the entire prismatic space diagram, but especially large among and nearly equal in size are the volumes of the sodium and potassium sulfates (Fig. 3, b; 1 and 2). Then follow the volumes of schoenite and of magnesium sulfate heptahydrate (Fig. 3, c; 7 and 4), which in size are nearly the same as at 25° [4]; in this connection it was shown by us [3] that the potassium content (4.73% KCl) in the solution for point XVII (final point for the crystallization of schoenite) should also remain nearly constant in the temperature interval from 0 to 25°, which bears importance in the technology of schoenite production.

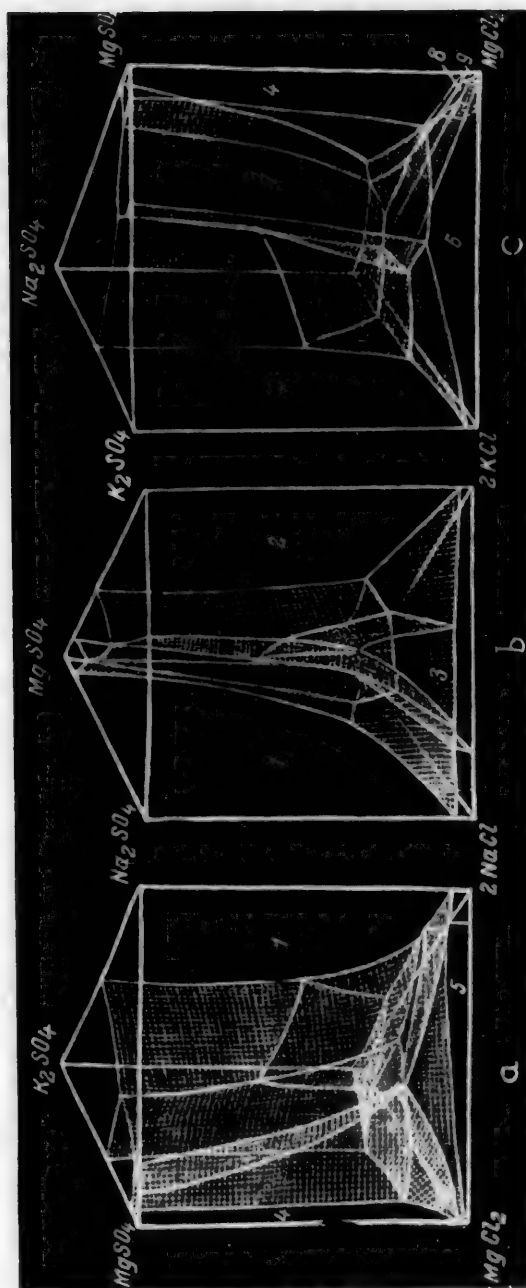


Fig. 3. Model of system K, Na, Mg \parallel Cl, $SO_4 - H_2O$ at 0° . 1) $Na_2SO_4 \cdot H_2O$; 2) $K_2SO_4 \cdot 10H_2O$; 3) $3K_2SO_4 \cdot Na_2SO_4$; 4) $MgSO_4 \cdot 7H_2O$; 5) $NaCl$; 6) KCl ; 7) $K_2SO_4 \cdot MgSO_4 \cdot 6H_2O$; 8) $KCl \cdot MgCl_2 \cdot 6H_2O$; 9) $MgCl_2 \cdot 6H_2O$.

The glaserite crystallization field occupies an extremely small portion of the prism (Fig. 3, b; 3); its small volume contains four internal "two-phase" surfaces and only one external boundary (Table 2), i.e., it wedges into the region of the other salts, forming at quaternary point XII (Table 1) the salt paragenesis: glaserite + schoenite + $K_2SO_4 \cdot H_2O$ + $Na_2SO_4 \cdot 10H_2O$, unknown for the other isotherms of the system [4, 5]. The carnallite and bischofite volumes are even smaller (Fig. 3, c), and depicting them is quite simple.

TABLE 2

Paragenetic Relationships of Crystallization Volumes of Salts in the System K, Na, Mg || Cl, SO_4-H_2O at 0°.

Investigated salt crystallization volumes	Bordering salt crystallization volumes	Number of facets	
		Internal	External
KCl	Schoenite, glaserite, carnallite, NaCl, $Na_2SO_4 \cdot 10H_2O$, $MgSO_4 \cdot 7H_2O$, $K_2SO_4 \cdot H_2O$	7	3
NaCl	Schoenite, carnallite, KCl, $Na_2SO_4 \cdot 10H_2O$, $MgSO_4 \cdot 7H_2O$, $MgCl_2 \cdot 6H_2O$	6	3
$MgSO_4 \cdot 7H_2O$. . .	Schoenite, carnallite, KCl, NaCl, $Na_2SO_4 \cdot 10H_2O$, $MgCl_2 \cdot 6H_2O$	6	3
$Na_2SO_4 \cdot 10H_2O$. . .	Schoenite, glaserite, KCl, NaCl, $K_2SO_4 \cdot H_2O$, $MgSO_4 \cdot 7H_2O$	6	3
Schoenite	Glaserite, NaCl, KCl, $K_2SO_4 \cdot H_2O$, $MgSO_4 \cdot 7H_2O$, $Na_2SO_4 \cdot 10H_2O$	6	2
$K_2SO_4 \cdot H_2O$	Glaserite, schoenite, KCl, $Na_2SO_4 \cdot 10H_2O$	4	3
Carnallite	KCl, NaCl, $MgSO_4 \cdot 7H_2O$, $MgCl_2 \cdot 6H_2O$	4	2
Glaserite	Schoenite, KCl, $K_2SO_4 \cdot H_2O$, $Na_2SO_4 \cdot 10H_2O$	4	1
$MgCl_2 \cdot 6H_2O$	Carnallite, NaCl, $MgSO_4 \cdot 7H_2O$	3	3

Thus, of the nine solid-phase crystallization volumes existing in the system K, Na, Mg || Cl, SO_4-H_2O at 0°, it is seen that six of them belong to pure salts. This indicates that it is possible to obtain mainly pure salts (potassium, sodium and magnesium sulfates) and, in addition, schoenite, being a valuable (chlorine-free) fertilizer for commercial crops, when sea brines are cooled to the indicated temperature (0°). In the conversion of complex natural deposits, for example, of astrakanite ($Na_2SO_4 \cdot MgSO_4 \cdot 4H_2O$) with potassium chloride or with sylvinit ($KCl + NaCl$), of carnallite with mixed salt ("Sel mixte", $MgSO_4 + NaCl$) or with astrakanite, and also of other salts, it will again be pure potassium and sodium sulfates that will crystallize from brines of the proper concentration when cooled to 0°, while with an accumulation of magnesium sulfate in the solution the separation of schoenite will also begin.

SUMMARY

1. When the 0° isotherm (solubility, viscosity, and density) of the five-component sea system K, Na, Mg || Cl, SO_4-H_2O was studied, we obtained the complete solubility diagram for the system, containing nine salt crystallization volumes that differ greatly in size ($K_2SO_4 \cdot H_2O$, $Na_2SO_4 \cdot 10H_2O$, $MgSO_4 \cdot 7H_2O$, $K_2SO_4 \cdot MgSO_4 \cdot 6H_2O$, $3K_2SO_4 \cdot Na_2SO_4$, $KCl \cdot MgCl_2 \cdot 6H_2O$, NaCl, KCl, $MgCl_2 \cdot 6H_2O$); the largest volumes, occupying almost the entire diagram, belong to the hydrated sulfates (potassium, sodium, magnesium) and schoenite.

2. A physicochemical analysis of the results obtained in investigating the 0° isotherm of the system indicates the conditions under which it is possible to obtain pure salts (mainly sulfates), and also schoenite, from natural salt mixtures and brines of oceanic origin.

LITERATURE CITED

- [1] J. D'Ans, Kali 15, 229 (1915).
- [2] Handbook on the Solubility of Salt Systems [In Russian] (GONTI, Leningrad, 1953-1954), Vols. 1 and 2.

- [3] O. K. Yanat'eva and V. T. Orlova, Zhur. Neorg. Khim. 3, 10, 2408 (1958); 4, 8, 1903 (1959).
- [4] O. K. Yanat'eva, Izvest. Sektora Fiz.-Khim. Analiza, Akad. Nauk SSSR 17, 370 (1949).
- [5] O. K. Yanat'eva and V. T. Orlova, Freiburger Forschungsh. - N. A., 123, 119 (1959).
- [6] A. Chrétien, Ann. Chim. [10], 12, 9 (1929).
- [7] H. W. Foote and J. F. Schairer, J. Amer. Chem. Soc. 52, 11, 4202 (1930).
- [8] N. S. Kurnakov and S. F. Zhemchuzhnyi, Izvest. Inst. Fiz.-Khim. Anal. 1, 1, 185 (1919).
- [9] W. C. Blasdale, Ind. Eng. Chem. 10, 344 (1918).

Received March 9, 1959

CALCULATION OF PHASE EQUILIBRIA IN MULTICOMPONENT GAS MIXTURES

I. G. Plit

Dnepropetrovsk Chemical Technological Institute

For multicomponent mixtures there is a lack of experimental data on the equilibria in the system, for which reason resort to calculation methods is made in most cases when analyzing the operation of industrial plants devoted to the processing of gaseous hydrocarbon mixtures. In this connection, the so-called phase equilibrium constants have found extensive use, with the aid of which it becomes a comparatively simple matter to determine the dew point, boiling point, and the composition and amount of the condensate formed in both the direct-flow and countercurrent condensation of a gas mixture. The phase equilibrium constants also find use in designing the dimensions of steam-condensation and rectification columns [1].

Calculation is based on the known rules of Raoult ($p_A = x_A \cdot P_A^0$) and of Dalton ($p_A = y_A \cdot P$), which permit obtaining for ideal mixtures an equation that links the phase compositions:

$$y_A = \frac{P_A^0}{P} \cdot x_A = K \cdot x_A, \quad (1)$$

where K is the phase equilibrium constant, which for ideal mixtures depends on the temperature and total pressure of the mixture.

In real systems, the saturated vapor pressure of component A over the solution (P_A^0) is determined not only by the temperature, but also by the correction for deviation from the ideal gas laws, i.e., by the coefficient of compressibility. In addition, the opinion exists [2] that when a high total pressure is reflected above a liquid mixture, the saturated vapor pressure of the component also depends on the total pressure. The enumerated factors are covered by the equation [2]

$$K = \frac{f_l}{f_v}$$

where f_l is the volatility of the pure liquid at the temperature and total pressure of the equilibrium, and f_v is the volatility of the vapor.

Taking into consideration the complexity and difficulty of determining f_l and f_v for a series of compounds in practical calculations, preference is given to phase equilibrium constants that either had been established experimentally or, in the limiting case, by the technique of qualified calculation with correction for the volatility.

The numerical values of such constants are given in the special literature [3] as the corresponding graphical functions of the temperature and total pressure. However, it is known that in most cases the indicated graphs do not embrace the entire span of possible temperature and pressure values, or even all of those encountered in the processing of gaseous hydrocarbon mixtures. Such a situation greatly limits the calculation possibilities and raises the need of systematizing the existing experimental and calculation material for the purpose of evolving some general rules that relate to phase equilibrium constants.

The saturated vapor pressure of the pure component (P_A^0) above the liquid is actually composed of the effect of two factors on the phase equilibrium constant, the temperature and the nature of the substance. In the case of a constant temperature for the process, it is obvious that the effect of the nature of the substance in this function can be expressed not only by the pressure of the saturated vapor, but also by some other physical parameter.

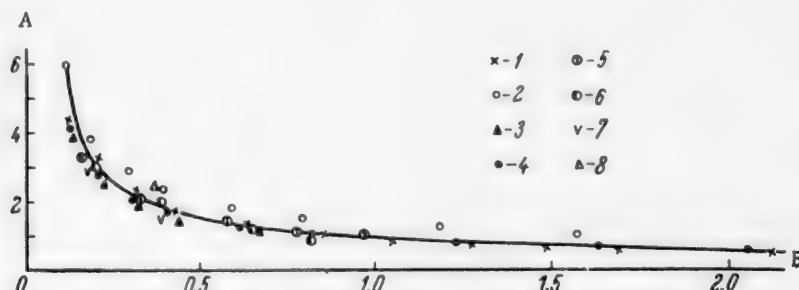


Fig. 1. Relation between the phase equilibrium constants (A) and the fictitiously transformed pressure (B) at transformed temperature $\theta = 1$.
1) Methane, 2) ethylene, 3) propylene, 4) ethane, 5) propane, 6) butane, 7) carbon monoxide, 8) nitrogen.

From the viewpoint of a possible generalization of the results, it is more convenient, for example, to use for this purpose the critical pressure of the substance (P_{Cr}), having replaced the saturated vapor pressure term P_A^0 in the expression for the constants by the term P_{Cr} , taken to be equivalent under the adopted conditions.

$$K_{1,t=\text{const}} = \frac{P_A^0}{P} = f\left(\frac{P_{Cr}}{P}\right).$$

Further, considering that the ratio of the pressures, $\frac{P}{P_{Cr}}$, can be regarded as the fictitiously transformed pressure P' , we obtain the functional relationship

$$K_{1,t=\text{const}} = f\left(\frac{1}{P'}\right),$$

in which the effect of the nature of the substance and the total pressure of the gas mixture at $t = \text{const}$ is characterized by the term P' . Since the transformed pressure, as is known, is a generalizing parameter, then functions of this type should bear a universal character.

To verify and evolve the final form of the function we plotted the values of the phase equilibrium constants as a function of the transformed pressure (P'), keeping the transformed temperature (θ) constant in all cases.

For this we used all of the experimental data available for such hydrocarbons as methane, ethylene, propylene, ethane, propane and butane.

The character of the obtained curve is shown in Fig. 1. The values of the constants at $\theta = 1$ are plotted along the ordinate, while the fictitiously transformed pressures are plotted along the abscissa.

The curve in Fig. 1 supports the existence of a universal relationship between K and P' , in that the phase equilibrium constants for different hydrocarbons at equal transformed parameters have the same values. The deviations of individual points from the general rule are very small and bear a haphazard character.

In addition to the hydrocarbons, we treated the available data relating to the constants for nitrogen and carbon monoxide. Due to the absence of reliable values for a wide range of pressures and temperatures, we were able to obtain only several points, in which connection these points show good agreement with the general rule observed for all hydrocarbons at $\theta = 1$.

Less successful results were obtained for carbon monoxide at transformed temperatures of $\theta < 0.8$ and for nitrogen at $\theta > 1.2$, although the agreement of the results on the other portions was good. This obviously confirms the fact that the accuracy of the values given in the literature for the mentioned constants [4] is not too high for all of the ranges.

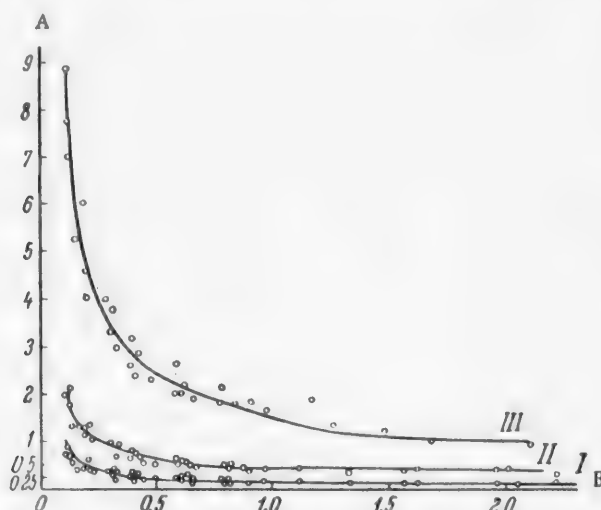


Fig. 2. Relation between the phase equilibrium constants (A) and the fictitiously transformed pressure (B). Transformed temperature θ : I) 0.7; II) 0.8; III) 1.2.

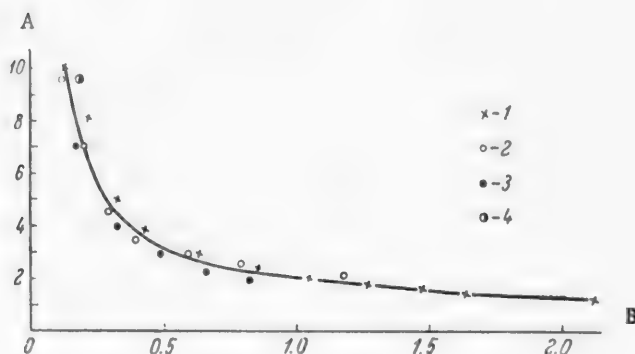


Fig. 3. Relation between phase equilibrium constants (A) and the fictitiously transformed pressure (B) at transformed temperature $\theta = 1.3$. 1) Methane, 2) ethylene, 3) propane, 4) carbon monoxide.

Curves illustrating the relationship between K and P' at different transformed temperatures are shown in Figs. 2 and 3 for a large number of tested materials. They all confirm the presence of a monotypical functional relationship between K and P' for different values of θ , and this in turn permits deriving some general rules pertaining to phase equilibrium constants. As can be seen, at $P' > 2$ or when the total pressure of the gas mixture $P > 2P_{Cr}$, the phase equilibrium constant is practically independent of the transformed pressure and remains constant with increase in the pressure. Consequently, it is impractical to employ the factor of pressure to intensify condensation that is fixed by a limit and the use of pressures greater than $2P_{Cr}$. Under such conditions, a reduction in the phase equilibrium constants can be achieved only by lowering the temperature.

A similar situation is also observed on the section where $P' \leq 0.1$. Here the values of the constants practically approach infinity, and to increase the efficiency of the process also requires a substantial reduction in the condensation temperature.

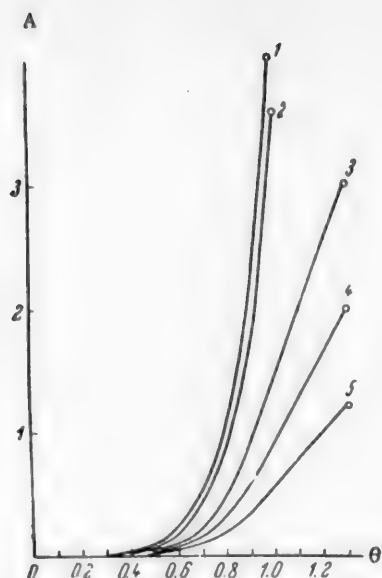


Fig. 4. Relation between the phase equilibrium constants (A) and the transformed temperature (θ). Transformed fictitious pressure P' : 1) 0.15; 2) 0.2; 3) 0.5; 4) 1; 5) 2.

The indicated characteristics are purely qualitative. For a quantitative expression of these changes it is necessary to have analytical equations, which can be derived from the generalized relationships. By using logarithmic coordinates to express the curves in linear form we derived the following equation:

$$\lg K = \lg a - 0.785 \lg P',$$

where a is a coefficient, the value of which depends on the transformed temperature; at $\theta = 1$, $a = 0.95$.

To show the form of the function $a = f(\theta)$, we have plotted in Fig. 4, using the data of Figs. 1-3, the curves for the relationship between the phase equilibrium constants and the transformed temperature at different transformed fictitious pressures. Using logarithmic coordinates to depict the curves in linear form, we establish that $a = 0.95 \cdot \theta^{2.85}$, and therefore finally

$$\lg K = \lg 0.95 + 2.85 \lg \theta - 0.785 \lg P'. \quad (2)$$

By virtue of its universality, the obtained Eq. (2) can be used in the preliminary orienting determination of the phase equilibrium constants under different conditions of running the process and for different industrial processes involving the processing of gaseous mixtures.

LITERATURE CITED

- [1] M. P. Malkov and K. F. Pavlov, Manual on Low-Temperature Cooling [In Russian] (Gostekhizdat, 1947).
- [2] K. F. Pavlov and M. P. Malkov, Cooling in the Chemical Industry [In Russian] (ONTI, 1937).
- [3] A. S. Smirnov, The Technology of Hydrocarbon Gases [In Russian] (State Sci.-Tech. Press, 1946).
- [4] S. Ya. Gersh, Low-Temperature Cooling [In Russian] ("Soviet Science" Press, 1947), Vol. 1.

Received January 30, 1959

EFFECT OF MINERAL SUBSTANCES ON THE RELATIVE VOLATILITY OF COMPONENTS IN LIQUID MIXTURES

V. B. Kogan, S. F. Bulushev, V. M. Safronov, and O. F. Moskovets

State Institute of Applied Chemistry

Azeotropic and extractive fractionation methods, in which organic liquids are used as the separating agents, are widely used at the present time to separate liquid mixtures. However, in a number of cases it proves difficult and even impossible to select an organic substance that has the desired volatility with respect to the components in a given mixture. In view of this, it becomes necessary to seek mineral substances that facilitate a separation of liquid mixtures by distillation and fractionation.

The possibility of using mineral substances to improve the conditions of separating mixtures was mentioned in the literature by Mariller [1], Longinov and Dzirkal [2], and others [3-13]. For the most part, the use of these substances was examined for the case of improving the conditions of making ethyl alcohol absolute [1, 2, 4, 5, 7]. Contradictory opinions exist in the literature regarding the criteria to be used in selecting mineral substances as separating agents. Some authors [3, 4] believe that the separation is improved if salts, soluble only in the high-boiling component, are added to the original mixtures. At the same time, Costa Novella and Moragues Tarraso [5], investigating the equilibrium between liquid and vapor in the system ethanol-water, in the presence of potassium acetate and cuprous chloride, came to the conclusion that the separation is improved if salts, soluble in both components, are added, while salts, soluble only in the high-boiling component, do not assure a favorable action.

As a result, the need arises of investigating the conditions under which mineral substances function as separating agents.

To solve this problem, it is necessary to start with an examination of the conditions for equilibrium between liquid and vapor in those ternary systems in which one of the components is a mineral substance. Up to now comparatively few systems of this type have been studied [4-6, 8-14]. In some of the investigations, the equilibrium conditions were studied only for saturated solutions [4, 12, 13], or at one concentration of the mineral substance [11], which does not permit elucidating the effect of its relative amount in solution on the volatility of the components of a binary solvent. For this purpose, it proved possible to use only the experimental data for the systems, ethyl alcohol-water-lithium chloride [8], formic acid-water-various salts [9], calcium chloride [10], and hydrogen chloride-water-sulfuric acid [14]. In view of the fact that in all of the enumerated systems, with the exception of the system ethyl alcohol-water-lithium chloride, one of the volatile components is an acid, it seemed timely to investigate the equilibrium between liquid and vapor in systems containing components of a basic character. As such systems we selected systems composed of pyridine and water, with the mineral additive being sodium hydroxide, the sulfates of ammonium, sodium, lithium and magnesium, and the chlorides of sodium and potassium.

A circulation apparatus was used to study the liquid-vapor equilibrium.

Both the pyridine and the mineral substances were of c. p. quality. The composition of the vapor condensate (mixture of pyridine and water) was determined from the refractive index using an IRF-22 refractometer. The composition of the equilibrium liquid phase was determined by calculation from the known amount and composition of the mixture poured into the apparatus prior to the start of experiment and the amount and com-

position of the vapor condensate. All of the experiments were run at a pressure of 760 mm Hg, which was maintained constant using a manostat.

To determine the effect of mineral substances on the relative volatility coefficient (α) of the binary solvent, we took the experimental data for the three-component systems and calculated the values of α_p , which were then compared with the values of α in the absence of mineral substance at the same relative concentration of the components of the binary solvent (x_i):

$$x'_i = \frac{x_i}{x_1 + x_2} = \frac{x_i}{1 - x_p},$$

where x_1 , x_2 , and x_p are, respectively, the mole fractions of volatile component, water and mineral substance.

The data obtained for the investigated systems are summarized in Table 1.

TABLE 1
Data for Equilibrium Between Liquid and Vapor in the Systems Pyridine - Water - Mineral Substance

x'_i	x_p	α	α_p	$\lg \frac{\alpha_p}{\alpha}$	x'_i	x_p	α	α_p	$\lg \frac{\alpha_p}{\alpha}$
K ₂ SO ₄					NaOH				
1.16	0.45	10.5	10.97	0.02	1.14	2.42	10.6	16.9	0.202
1.17	0.68	10.5	13.19	0.096	1.19	3.9	10.4	22.1	0.328
1.20	0.90	10.4	14.30	0.138	1.21	5.0*	10.4	28.4	0.456
					1.16	5.32*	10.5	33.14	0.5
Li ₂ SO ₄					NaCl				
1.17	0.90	10.5	13.75	0.117	1.17	1.67	10.5	12.84	0.088
1.25	2.29	10.3	19.01	0.266	1.22	3.47	10.3	16.94	0.218
1.29	2.98	10.2	23.64	0.355	1.29	5.4	10.2	18.9	0.288
1.31	3.42	10.2	27.02	0.422	1.35	7.5	10.0	28.4	0.453
MgSO ₄					CaCl ₂				
1.17	0.82	10.5	13.52	0.108	1.40	4.1	9.9	19.0	0.28
1.31	2.10	10.2	14.03	0.140	1.48	5.43	9.8	25.9	0.422
1.37	3.13	10.0	18.8	0.274	1.55	6.9	9.6	33.16	0.54
1.40	3.80	9.9	22.24	0.35	1.63	7.85	9.4	34.24	0.56
Na ₂ SO ₄					MgCl ₂				
1.17	1.3	10.5	14.44	0.14	1.18	1.14	12.0	10.5	0.06
1.22	1.96	10.3	17.3	0.226	1.36	3.43	11.6	10.0	0.065
1.24	2.31*	10.3	21.94	0.33	1.41	4.76	14.1	9.9	0.154
(NH ₄) ₂ SO ₄									
1.21	1.67	10.3	15.7	0.183					
1.30	2.47	10.2	16.9	0.22					
1.38	3.47	10.0	20.15	0.305					
1.44	4.6*	9.8	24.24	0.394					

* The data relate to the saturated solution.

The experimental data obtained for the systems: formic acid, water, and different salts; hydrogen chloride, water and sulfuric acid; acetic acid, water and calcium chloride; and ethyl alcohol, water and lithium chloride, have been plotted in Figs. 1 and 2 in the coordinates: logarithm of the ratio of the relative volatility coefficients of the first two components in the presence or in the absence of the third component ($\lg \frac{\alpha_p}{\alpha}$) vs. molar concentration of the third component (x_p , in mole percent).

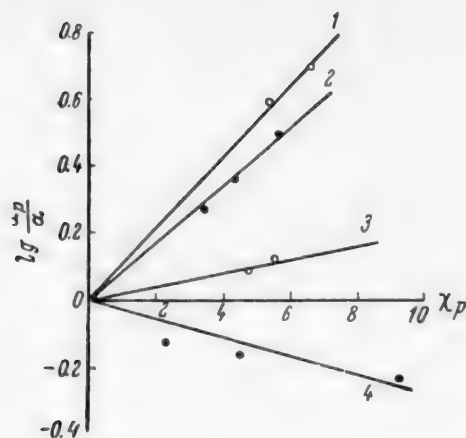


Fig. 1. Data on the equilibrium between liquid and vapor in systems composed of formic acid, water, and salts. Salt and relative concentration of formic acid to water (x'), respectively: 1) MgCl_2 , 8.9; 2) CaCl_2 , 8.9; 3) NaCl , 3.7; 4) NaHCO_3 , 8.9.

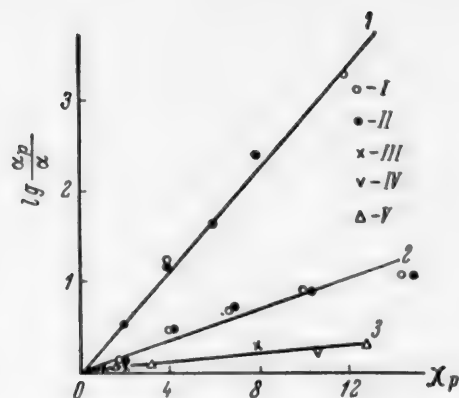


Fig. 2. Data on equilibrium between liquid and vapor. Systems: 1) hydrogen chloride-water-sulfuric acid; 2) water-acetic acid-calcium chloride; 3) ethyl alcohol-water-lithium chloride. Value of x' (in mole percent): I) 5; II) 10; III) 6.4; IV) 25; V) 50.

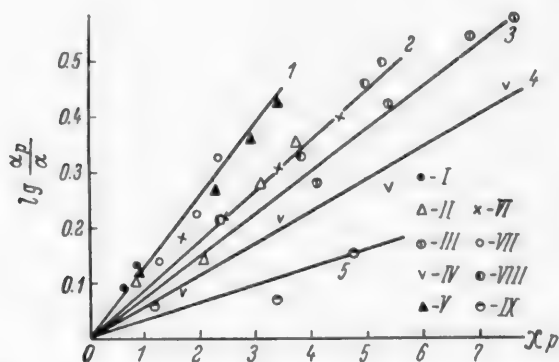


Fig. 3. Data on the equilibrium between liquid and vapor in systems composed of pyridine, water, and mineral substances. 1) K_2SO_4 , 2) MgSO_4 , 3) CaCl_2 , 4) NaCl , 5) MgCl_2 . I) K_2SO_4 , II) MgSO_4 , III) CaCl_2 , IV) NaCl , V) Li_2SO_4 , VI) $(\text{NH}_4)_2\text{SO}_4$, VII) Na_2SO_4 , VIII) NaOH , IX) MgCl_2 .

In a similar manner, we have plotted in Fig. 3 the experimental data obtained by us for the investigated systems composed of pyridine, water, and different mineral substances.

As can be seen from Figs. 1, 2, and 3, a linear relation between $\log \frac{\alpha_p}{\alpha}$ and the concentration of mineral substance exists in all cases. In all of the systems, except the system formic acid-water-sodium formate, a reduction in the relative volatility of the water occurs in the presence of mineral substance. To explain this difference in the behavior of the examined systems it seemed of interest to compare the solubility of the mineral substance in each of the components of the binary solvent.

In view of the absence of literature data on the solubilities of salts in formic and acetic acids, it became necessary for us to determine them experimentally. The 100% formic and acetic acids used by us were purified by fractional distillation. The c. p. sodium, calcium and magnesium chlorides were dehydrated by ignition. The sodium formate was prepared from the pure acid and c. p. sodium hydroxide. The solubilities were determined at 100° in the apparatus shown in Fig. 4.



Fig. 4. Apparatus for solubility determinations.

The salt and acid were placed in portion A, and the apparatus was mechanically shaken for 4 hours in a thermostat kept constant at 100° (boiling water). It was established first that this time is sufficient to reach equilibrium. After shaking had been stopped, the apparatus was allowed to stand for an hour in the thermostat, and then a certain portion of the clear solution was decanted into portion B, which was then cut off. The weighed sample, containing sodium formate, was analyzed for the amount of acid by titration with 0.1 N sodium hydroxide solution, using methyl red as indicator. The weighed samples, containing either sodium, calcium or magnesium chloride, were analyzed for the amount of salt by titration with standard silver nitrate solution.

TABLE 2
Comparison of Solubility of Mineral Substances in Components of Binary Solvent

Mineral substance	Second component	Solubility (in mole %)		Temperature
		in water	in the second component	
Magnesium chloride	Formic acid	12.09	8.95*	100°
Calcium chloride		20.51	19.86*	100
Sodium chloride		10.78	5.3*	100
Sodium formate		29.7	34.0	100
Sulfuric acid	Hydrogen chloride	—	—	—
Calcium chloride	Acetic acid	18.2	15.3	60.7
Magnesium chloride	Ethyl alcohol	26.18	22.19*	20

* Data of the authors.

The obtained data are summarized in Table 2, where the solubility of the mineral substance in water, taken from the handbook [15], is compared with its solubility in the other component of the binary solvent.

This comparison is not given for the systems: pyridine—water—mineral substance, since the solubility of the investigated mineral substances in pyridine is very small when compared to their solubility in water.

A comparison of the data on the equilibrium between liquid and vapor with the solubility data given in Table 2 reveals that in all cases the mineral substance raises the relative volatility of that component of the binary solvent in which it is least soluble.

According to Figs. 1-3, the effect of the mineral substance concentration on the relative volatility coefficient of a binary solvent can be described by the equation

$$\lg \frac{\alpha_p}{\alpha} = \text{const } x_p.$$

It is interesting to mention that in its form this equation coincides with the known Sechenov equation [16], describing the effect of electrolytes on the solubility of nonelectrolytes in water. In contrast to the Sechenov equation, valid only for dilute solutions, the present equation, as can be seen from the given experimental data, is also suitable for concentrated solutions.

The facts presented give a basis to assume that a relationship exists between solubility and relative volatility in systems composed of binary solvent - electrolyte, similar to that established for systems composed of nonelectrolytes [17]. A close similarity in the behavior of these two types of systems also follows from the fact that the linear function, $\log \frac{\alpha_p}{\alpha}$ vs. x_p , derives from general thermodynamic considerations [18, 19] and is independent of the nature of the system components.

As a result, the mineral substances that should be used as separating agents are the ones that are less soluble in the distilling component than in the components that remain in the residual liquid in the still. Since the

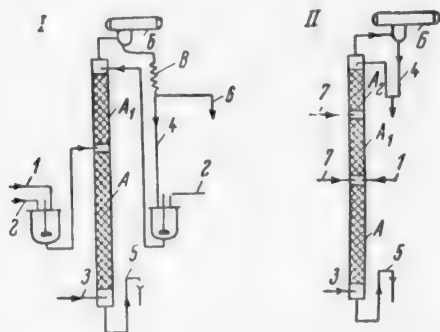


Fig. 5. Diagrams of the extractive fractionation process using mineral separating agents. General designations for both diagrams I and II. A and A₁) Stripping and rectifying portions of the column; A₂) rectifying portion of the column, operating without separating agent; B) dephlegmator; C) condenser. 1) Starting solution feed, 2) solid mineral substance feed, 3) steam feed, 4) reflux line, 5) bottoms of solution after stripping product, 6) distillate take-off, 7) mineral substance solution feed.

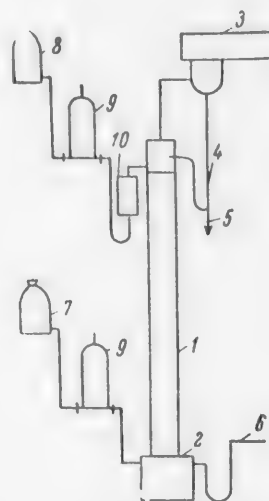


Fig. 6. Diagram of laboratory apparatus. 1) Column, 2) still pot, 3) dephlegmator, 4) reflux line, 5) distillate take-off, 6) still bottoms, 7) vessel containing aqueous pyridine solution, 8) vessel containing NaOH solution, 9) feed meters, 10) preheater for caustic solution.

efficiency of a separating agent increases with increase in its concentration, the most effective use of mineral separating agents for the isolation of substances from dilute solutions derives when the mineral substance has a sufficiently high concentration in the solution. On the other hand, at high concentrations of the distilling substance, the possible concentration of mineral separating agent, satisfying the above requirement, is small. In this case, the more effective will prove to be those mineral substances that are readily soluble not only in the distilling component, but also in the component removed as the still residue, since it is possible for the lower selective action shown by such mineral substances to be compensated by an increase in their concentration.

In principle, two methods may be used to run the process of extractive fractionation using mineral separating agents (Fig. 5). According to the first method, to create a sufficiently high concentration of the separating agent along the column height, the mineral substance is dissolved in the refluxing liquid and the starting mixture. According to the second method, the column is sprayed with a solution of the mineral substance in the component that is removed during the extractive fractionation process as the still residue. Regeneration of the separating agent is accomplished in both cases by evaporation.

The technological advantage of the second method over the first consists in the fact that it eliminates the need of operating with a solid phase. However, in this case, a component is introduced into the column that should be removed from the distillate. For this reason, application of the extractive fractionation process using a solution of a mineral substance as the separating agent is possible only for mineral substances that possess a high efficiency. In the separation of systems having an azeotropic boiling point it is important that the vapor in the portion of the fractionation column operating in the presence of the separating agent have a higher concentration of the distilling component than is present in the azeotrope. Then its subsequent isolation in the pure state can be done by conventional fractionation in the rectification portion of the column, situated above the extraction portion (A₂, Diagram II, Fig. 5).

As an example of the extractive fractionation process using a solution of a mineral substance as the separating agent we investigated the process of isolating pyridine from dilute water solution.

The experiments were run in the apparatus schematically depicted in Fig. 6. The main section of the apparatus was a continuously operating fractionation column with a diameter of 20 mm and a height of 1000 mm, filled with 3 × 3 × 0.5 mm metal Raschig rings. The column was electrically heated to compensate for heat losses to the surrounding medium. A 45% aqueous sodium hydroxide solution, preheated to 95°, was fed in at the top of the column, while a solution containing 2.9 wt. % (0.675 mole %) of pyridine was fed into the still pot.

The pyridine concentration in the distillate was determined from the refractive index. To determine the pyridine concentration in the still bottoms, we periodically removed 0.5 liter of the solution in the still pot and fractionated it until all of the pyridine had distilled. Calculation of the composition of the still bottoms was based on the analysis results. To calculate the reflux ratio we first determined the amount of water that vaporized from the still pot at various heat loads. The reflux ratio in our experiments was approximately 50.

Some representative results of the experiments are listed in Table 3.

TABLE 3
Results of Experiments on the Isolation of Pyridine From Dilute Water Solution by Extractive Fractionation With Aqueous Sodium Hydroxide Solution as the Separating Agent

Duration of experiment (in min)	Amt. of feed sol. (ml/hr)		Pyridine concentration in still pot (in wt. %)	Distillate	
	NaOH	Pyridine		Amount (in g)	Concentration (in wt. %)
175	243	258	0.5	23.05	71.0
180	253	540	0.46	29.5	79.4

From Table 3 it can be seen that despite the relatively small feed rate of the aqueous sodium hydroxide solution and the low concentration of pyridine in the still pot, still it proves possible to isolate pyridine in a more concentrated form than that existing in the azeotropic mixture (57% pyridine [20]). This demonstrates the high efficiency of the extractive fractionation method when mineral separating agents are used to isolate substances from dilute solutions.

SUMMARY

1. Based on an analysis of both our own data and that taken from the literature regarding equilibrium between liquid and vapor in systems of the binary solvent - mineral substance type, it was established that the effect of the mineral substance on the relative volatility coefficient of the binary solvent is described by the equation, $\log \frac{\alpha_p}{\alpha} = \text{const } x_p$.

2. By comparing the data on equilibrium between liquid and vapor with the data on the solubility of mineral substances in the components of a binary solvent it was shown that the mineral substances that should be used as separating agents in distillation and rectification processes are the ones that are more soluble in the component remaining as the still residue than in the component that distills.

3. It was established that running the rectification process in the presence of mineral separating agents finds its most effective use in the isolation of substances from dilute water solutions.

LITERATURE CITED

- [1] C. Mariller, *Distillation et Rectification* (Dunaud, Paris, 1925).
- [2] V. Longinov and V. Dzirkal, *Zhur. Priklad. Khim.* 7, 572 (1934).
- [3] W. H. Walker, W. K. Lewis, W. H. Mc Adams, and E. R. Gilliland, *Principles of Chemical Engineering* (McGraw-Hill Book Co., New York — London, 1937), 3rd edition.
- [4] R. R. Tursi and A. R. Thompson, *Chem. Eng. Progr.* 47, 304 (1951).
- [5] E. Costa Novella and J. Moragues Tarraso, *Anales real soc. espan. fis. y quim.* (Madrid) 48B, 441 (1952).
- [6] J. Proszt and G. Kollar, *Magyar Kém. Folyóirat* 60, 110 (1954).
- [7] C. E. Morrell and E. R. Gilliland, *Can. Patent* 516,100, August 30, 1955.
- [8] R. Shaw and J. A. V. Butler, *Proc. Roy. Soc. (London)* 129A, 519 (1939).
- [9] A. Guyer, A. Guyer, Jr., and B. K. Johnsen, *Helv. Chim. Acta* 38, 4, 946 (1955).
- [10] L. G. Garwin and K. E. Hutchison, *Ind. Eng. Chem.* 42, 4, 727 (1950).
- [11] É. L. Chernyak, *Zhur. Obshchei Khim.* 8, 14-15, 1341 (1938).
- [12] R. M. Rieder and A. R. Thompson, *Ind. Eng. Chem.* 42, 2, 379 (1950).
- [13] A. I. Johnson and W. F. Furter, *Canad. J. Technol.* 34, 7, 413 (1957).
- [14] A. V. Storonkin and M. P. Susarev, *Vestnik Leningrad. Gosudar. Univ.* 6, 119 (1952).
- [15] *Handbook of Chemistry*, Vol. 3 (1955).
- [16] I. M. Sechenov, *Ann. chim. et phys.* 6, 25, 226 (1892).
- [17] V. B. Kogan, *Zhur. Fiz. Khim.* 29, 1470 (1955).
- [18] A. M. Pozen, *Doklady Akad. Nauk SSSR* 81, 863 (1951).
- [19] V. B. Kogan, *Khim. Prom.* 6, 356 (1957).
- [20] L. H. Horsley, *Tables of Azeotropes and Nonazeotropes* (Russian translation) (IL, 1951).

Received February 27, 1959

INFLUENCE OF THE NATURE OF A BINARY SYSTEM ON THE EFFICIENCY OF A RECTIFICATION COLUMN*

I. N. Bushmakín

Leningrad State University

If the efficiency (number of plates) of a rectification column is determined using different binary systems, then different values are obtained for the efficiency. This fact was established by Peters as early as 1922 [1]. However, Peters did not have either accurate data on liquid-vapor equilibria or a reliable method for calculating the efficiency at his disposal. For this reason, the validity of the numerical data given in his paper is open to question. The work of Peters must be regarded as being the first indication that the efficiency of a column depends on the nature of the binary system used to determine the efficiency.

After the paper by Peters there were hardly any more studies made of the relationship between the efficiency of a column and the nature of the binary system used to determine the efficiency. The absence of sufficiently accurate data on liquid-vapor equilibria in binary systems was the reason for this. When such data are not sufficiently accurate, the efficiency of a column, determined using the same binary system, changes with change in the composition of the solution poured into the still pot.

The last circumstance leads to the situation that the relationships between efficiencies, determined using a number of systems, also change with change in the composition of the solutions taken for operation when going from a column with one efficiency to another column with a greater efficiency; as a result of this it proves impossible to establish any rules in the relationships between efficiencies.

A study of the relationship between the efficiency and the binary system was one of the main objectives in the present series of papers. In preparation for the study we investigated the efficiency of a column (when operating under total reflux), determined using the same system, as a function of various factors, and we also investigated the conditions under which a good reproducibility of the efficiency is obtained [2, 3]. Then we investigated the liquid-vapor equilibria in nine binary systems (for one of them at two pressures — 760 and 100 mm [4]), in which connection the obtained data were thoroughly checked. In addition, a rule was established by us, according to which the efficiency of a column is independent of the concentration of the solution in the still pot [5-10].

The present investigation of the relationship between the efficiency of a column and the binary system was made using 9 binary systems, 9 columns, and 4 kinds of packing. The binary systems were: benzene:carbon tetrachloride [5, 11], 1,2-dichloroethane: benzene [6], methanol: acetone,** n-heptane: benzene [7], acetic.

* Communication XII.

** In Communication VI [7], data are given in Table 4 for constructing the graph (number of plates vs. concentration) in the system methanol-acetone. In this table, the last line of up to azeotrope (77.4-45.4) and the last line of beyond azeotrope (77.4-61.7), both appearing in the table through misunderstanding, should be deleted. Otherwise, the table is correct.

acid; water, n-butyl acetate; acetic acid, acetic acid; ethyl acetate [8], methylcyclohexane; 2,2,4-trimethylpentane [9], and methylcyclohexane; n-heptane [10].

The internal diameter of the column was varied from 1.4 to 2.0 cm. The column construction was conventional, the same as in our study of the efficiency as a function of various factors [2] (Fig. 1). The columns differed in both the kind and height of the packing.

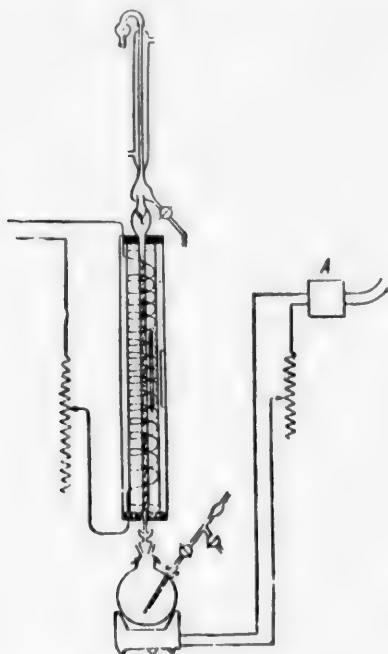


Fig. 1. Column. A) Voltage regulator.

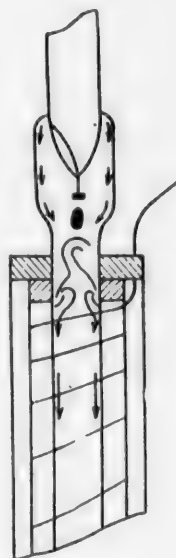


Fig. 2. Device for feeding reflux to the walls of an empty column.

Packing. Column No. 1. Single-turn triangles made of nichrome wire, inside height of triangle 1.3 mm, wire thickness 0.2 mm. Height of packing 53 cm. Efficiency* per meter of packing height, based on the system benzene-carbon tetrachloride, at a reflux rate of $2 \text{ ml/min} \cdot \text{cm}^2$, was 72 plates. Column No. 2. Single-turn helices made from constantan wire; inside diameter of helix 1.8 mm, wire thickness 0.3 mm. The packing was old and corroded, having operated for 8 years. Packing height 105 cm. The efficiency per meter of packing height was 54 plates. Column No. 3. Single-turn helices made from constantan wire, inside diameter of helix 3.5 mm, wire thickness 0.3 mm. Packing height 114 cm. Efficiency per meter of packing height 22 plates. Column No. 4. Glass Raschig rings $3.7 \times 3.7 \text{ mm}$, with a wall thickness of 0.9 mm. Packing height 173 cm. Efficiency per meter of packing height 17 plates. Column No. 5. No packing (empty column). In order to increase the efficiency, all of the reflux descending from the top of the column was directed by means of a special device (Fig. 2) along the walls of the column. The inside diameter of the column was 1.5 cm. The distance from the device for spreading the reflux to the lower drip device was 157 cm. The efficiency of the column at a reflux rate of 2 ml/min was 6.4 plates. Column No. 6. Glass Raschig rings $7 \times 6 \text{ mm}$, with a wall thickness of 1 mm. Packing height 250 cm. Efficiency per meter of packing height 10 plates. The column jacket was divided into two sections, each section having its own thermometer and heating coils. Column Nos. 7-9. The packings were the same as in No. 6. The packing height was 174, 58 and 32 cm, respectively. Column Nos. 8 and 9 had a height of 140 and 120 cm, respectively. The large number of columns with the same type of

* The efficiencies for all of the other packings listed in this paper are also based on using this same system and the same reflux intensity.

packing is due to two reasons: 1) the acetic acid-ethyl acetate system requires very few plates for a practically complete separation of the components, and consequently when working with this system we came to use a separate column with an efficiency of only 6.5 plates; and 2) with all of these columns, we determined the ratios of the efficiencies for systems with a large temperature gradient along the column height (heptane-benzene, acetic acid-water). Repeating the determination of the efficiency ratios for such systems using columns with the same heat-insulation design, but with different heights of the same kind of packing, should reveal whether adiabatic imperfection exerts an influence on the indicated efficiency ratios.

Materials. Purification of the materials and checking on their purity were done in the same manner as already described in earlier investigations of liquid-vapor equilibria [5-10].*

Design of experiments. All of the determinations of the efficiency were run with the column operating under total reflux.

At the start it wasn't clear to us what conditions should be used in making a comparison of the efficiencies. For this reason, we decided to obtain experimentally for each column the curves showing the relationship between the efficiency and the reflux intensity for 2-5 systems. These data can then be converted to any conditions (for example, either a mass or a linear vapor velocity).

The metallic packings were stabilized by repeated "cold" flooding. When determining the efficiency on these packings, the operation of the column was begun in all cases with a "cold" flooding. When determining the efficiency on the glass packings, the latter were first subjected to wetting either by a reflux stream or by "hot" flooding [2]. If the wetting was done with a reflux stream for one binary system, then the same type of wetting was also used for the other systems.**

To maintain a constant reflux intensity, the still heaters were connected to voltage regulators. We judged the constancy of the reflux intensity by the number of drops falling from the condenser into the column per unit of time (up to 200 drops a minute); no recording of the reflux constancy was made at reflux intensities greater than this, and we had to depend on the operation of the voltage regulators. The reflux intensity was expressed in milliliters per minute per cm^2 of column cross section. It was calculated either from the number and volume of the drops, or it was measured by the volume of reflux issuing from the condenser per unit of time. This measurement was made after taking the last liquid samples for determining the efficiency. Using the same drip device, the volume of the drops depends both on the binary system and the composition of the liquid. In the nature of an example, we have shown in Fig. 3 the relationship between the drop volume and the composition in the system benzene-carbon tetrachloride. In this work, the drop volume was found from the curve of drop volume vs. concentration, that portion of the curve corresponding to the desired concentrations having been obtained by us in advance by means of special experiments.

* In this paper we were able to obtain a more accurate value for the refractive index (n_D^{20}) of carbon tetrachloride; it proved to be 1.46026, instead of the 1.46037 reported in Communication I [11].

** A complete investigation of the conditions for obtaining a good reproducibility of the efficiency, described in Communication III [2], was made by us for the system benzene-carbon tetrachloride. Subsequent work with the other systems confirmed the results given in Communication III, but it also showed that "cold" flooding proceeds differently for different systems. On the basis of the accumulated experimental data we arrived at the following rule: just as soon as flooding has begun, to obtain a good reproducibility of the efficiency it is necessary to operate in such a manner that the column of liquid, with the vapor bubbling through it, rises from the very bottom of the column and covers the entire packing, and then give the column a chance to "flood", not permitting the reflux to drop below $0.5 \text{ ml/min} \cdot \text{cm}^2$. The efficiency obtained after such flooding is so easily reproducible that it is a characteristic value for the packing of the binary system and the reflux intensity. The efficiencies, obtained as the result of using other techniques to first wet highly efficient metallic packings (reflux stream, "hot" flooding), show much poorer reproducibility, since they depend on wetting nuances that are difficult to take into account. A preliminary wetting of glass packing by a reflux stream gives a quite good reproducibility of the efficiency; "hot" flooding gives a somewhat better reproducibility of the efficiency. It is impossible to use "cold" flooding with glass packing, since it disturbs the arrangement of the packing, making it more open.

The compositions were determined from the refractive indices, which were usually measured using an Abbe refractometer, and only for the high efficiencies were the compositions of the reflux in the condenser determined by the technique of differential recording on the drum of a Pulfrich refractometer [6]. In systems containing acetic acid, the latter was determined by titration with 0.1 N NaOH solution. Calculation of the number of plates from the data on the compositions of the liquid in the still pot and in the condenser was done employing our earlier calculated diagrams [5-10].

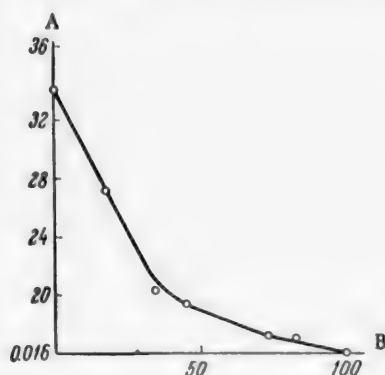


Fig. 3. Relation between the "hot" drop volume and the liquid composition. System benzene-carbon tetrachloride. A) Drop volume (in ml); B) amount of carbon tetrachloride in the liquid (in mole %).

During the experiment, temperature in the space between the column and the jacket (half way up the column) was maintained equal to the temperature of the vapors entering the condenser. As a result, the lower portion of the column always operated with some fractionation.

It seemed of interest to determine where and how the curves expressing the relationship between the efficiency and the reflux intensity end for different binary systems. It was convenient to do this using column Nos. 1, 2, and 4. Column Nos. 1 and 2 had a fine metallic packing, while column No. 4 had a fine glass packing. Such packings, possessing a comparatively high efficiency, have a somewhat low passage capacity. Using columns with these packings, we determined the reflux intensities at which flooding begins (points of flooding), and in the case of column No. 2, we also determined the efficiency of the flood point.

In addition to the above-discussed investigations, we took three of the columns and several binary systems and determined the static holdups at the boiling points, and we also traced the relationships between the dynamic holdups and the reflux intensity (using special adaptations).

Results and their discussion. As a result of our study, we obtained curves expressing the relationship between the efficiency and the reflux intensity for different columns and different binary systems. In the nature of an example, we have shown the more interesting curves in Fig. 4 (the total number of plates possessed by the columns are plotted along the ordinate, without subtracting one plate for going from the still pot to the column).

$$\text{Coefficient } \beta = \frac{\text{Efficiency Based on the Given System}}{\text{Efficiency Based on the Benzene-Carbon Tetrachloride System}}$$

The Efficiencies are Determined Under Constant Reflux Intensities

Designation of lines in the Figures	System	β
I	Benzene— carbon tetrachloride	1.00
II	Methylcyclohexane—2,2,4-trimethylpentane	0.98
III	Methanol—acetone	1.00
IV	Acetic acid—ethyl acetate	1.0*
V	Methylcyclohexane—n-heptane	1.07
VI	1,2-Dichloroethane—benzene	1.18
VII	n-Heptane—benzene	0.76
VIII	n-Butyl acetate—acetic acid	0.80
IX	Acetic acid—water	0.52

* The value of β for the system acetic acid-ethyl acetate is given with an accuracy of up to a tenth of a percent, it being impossible to obtain a greater accuracy for this system, since the error in determining the concentration is quite large, while comparing the efficiencies has to be done at a total efficiency of only 6-7 plates.

As can be seen from Fig. 4, the curves obtained using the system benzene-carbon tetrachloride occupy an intermediate position among the different curves. In the future, the ratio of the efficiency, determined using any

one system, to the efficiency obtained using the benzene-carbon tetrachloride system, both determined at a constant reflux intensity, will be designated by the coefficient β . For each system, β , obtained using the same column, remains constant at all reflux intensities. For the same system, but using different columns, β fluctuates within the limits ± 0.05 (in the worst case) around the average value obtained for all of the columns, in which connection there is no correlation between the magnitude of the indicated fluctuations and the size of the packing elements. As a result, it is possible to state that β , within the limits of experimental error, is independent of the kind of packing material. For an empty column the value of β is quite different from the value of β for columns that contain packing; thus, the average value of β for the system dichloroethane-benzene, obtained using packed columns, is equal to 1.18; using an empty column, β is equal to 1.30; for the heptane-benzene system, using packed columns, $\beta = 0.76$, and for the empty column, $\beta = 0.67$. In other words, using an empty column, the difference in the efficiency for a given system when compared to that for the benzene-carbon tetrachloride system is somewhat greater than when packed columns are used.

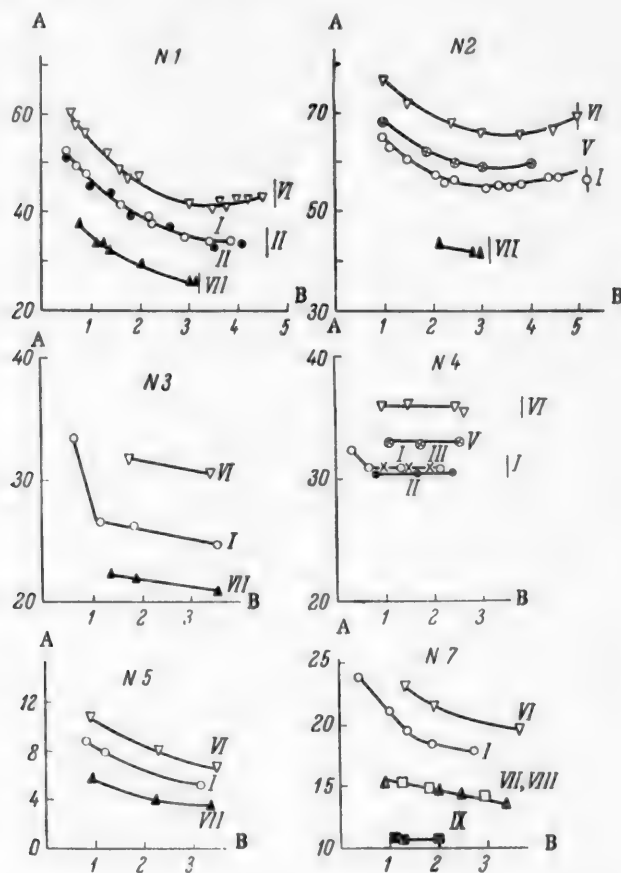


Fig. 4. Relation between the efficiency and the reflux intensity, obtained for different columns and different binary systems. A) Number of plates in the column (efficiency); B) reflux intensity (in ml/min·cm²). Nos. 1-5 and 7 represent the column numbers. Designation of the curves is given in the table. The vertical lines with numbers represent the points of flooding in the systems corresponding to the numbers.

The values of β for different systems are given in the table. These values represent the average of the values obtained for all of the packed columns.

Figure 5 represents a summary of the data obtained using an empty column and the columns with different kinds of packing, and in it the independence of β of the reflux intensity and the kind of packing material stands out more clearly than in Fig. 4.

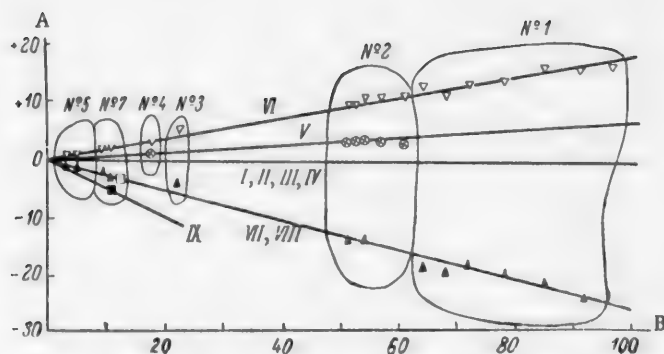


Fig. 5. Diagram representing a summary of the data obtained using different kinds of packing and an empty column. A) Value of Δ (difference between the number of plates when based on the given system and the number of plates when based on the benzene-carbon tetrachloride system, compared under the conditions of a constant packing and a constant reflux intensity); B) number of plates based on the benzene-carbon tetrachloride system. Designation of the straight lines is given in the table. Contours Nos. 1-5 and 7 were drawn from the data obtained using the same packing (column).

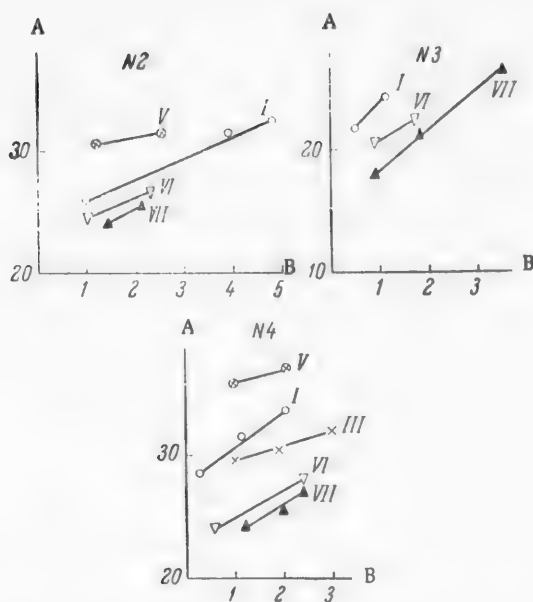


Fig. 6. Relation between the total holdup and the reflux intensity for different columns and different binary systems. A) Value of the total holdup in the column (in ml); B) reflux intensity (in ml/min·cm²). Designation of the straight lines given in the table. Nos. 2-4 represent column numbers.

To construct Fig. 5, the data of Fig. 4 were recalculated in the following manner: from the curves in Fig. 4 we found the interpolated efficiencies for reflux rates of 0.5, 1 ml/min·cm², etc. From these efficiencies, we subtracted 1 plate (going from still pot to column), and then the packing efficiencies obtained in this manner were recalculated to the efficiency per meter of packing height.* Subtracting from the efficiency of a meter of packing height, determined using any system, the efficiency obtained using the benzene-carbon tetrachloride system, both determined under the conditions of using the same packing and the same reflux intensity, we found the value of the difference in the efficiencies (Δ). In Fig. 5 we have plotted along the abscissa the values of the efficiency based on the benzene-carbon tetrachloride system, and along the ordinate we have plotted the corresponding values of Δ . Contours Nos. 1, 2, etc. were drawn from the data obtained using the same packing (column), but varying both the binary system and the reflux intensity.

Figure 5 shows that: 1) the ratio of Δ to the efficiency, based on the benzene-carbon tetrachloride system, for a given packing is independent of the reflux intensity (points within the limits of one contour); 2) this ratio is retained in going to other packings

* In Communication III [2] we had shown that the efficiency increases linearly with increase in the packing height.

(other contours); and 3) the efficiencies, obtained using systems I-III and IV, for all of the packings and at all reflux intensities, coincide.

If we designate the efficiency using a given system by eff_i , and the efficiency using the benzene-carbon tetrachloride system by eff_s , then the connection between the values of Δ and β is expressed by the equation

$$\Delta/\text{eff}_s = \frac{\text{eff}_i - \text{eff}_s}{\text{eff}_s} = \beta - 1 = \text{const.}$$

As had been indicated above, in determining the efficiency the columns always operated with internal fractionation. Studies, which we will not discuss here, revealed that the fractionation taking place in our experiments when determining β fails to exert any influence on the efficiency. On this basis, we postulate that the values of β given in the table will also retain their value when operating with vacuum-jacketed columns. Only for the acetic acid-water system do we lack sufficiently reliable data that the efficiency is not affected by the internal fractionation occurring in our experiments. For this reason, it is possible that the value of β for this system when using vacuum-jacketed columns will be somewhat higher than that given in the table.

Reasons responsible for the differences in the efficiencies when determined using different binary systems. In Fig. 6, we have shown the relationship between the total holdup (static and dynamic) values and the reflux intensity. This figure shows that there is no connection between the total holdup value and the efficiency. The efficiency, determined using the dichloroethane-benzene system, is greater, and that based on the n-heptane-benzene system is smaller, than the efficiency based on the benzene-carbon tetrachloride system; the holdup values for the first two systems lie very close to each other, and they are smaller than the holdup for the benzene-carbon tetrachloride system. In our opinion, the difference in the efficiencies when determined using various systems is due to the fact that in a column, operating under total reflux, a stationary state, and not equilibrium, is established between the vapor and the liquid. If equilibrium were established (as is the case in single vaporization apparatus), then the same efficiency would be obtained for all the systems. The span between the stationary state and the equilibrium state is different for different systems, and this difference is due to the different rates with which the processes of mass transfer between vapor and liquid take place.

The above-mentioned rule of the efficiency not being dependent on the concentration of the solution being rectified was established by us with complete certainty for 8 different binary systems. This rule shows that the span between the stationary state and the equilibrium state does not change with change in the concentration and the accompanying temperature change in the column.

SUMMARY

Using 8 columns with different packing materials and one empty column, we investigated the relationship between the efficiency (number of plates) and the reflux intensity for 9 different binary systems.

It was established that the ratio of the efficiency, determined using one system, to the efficiency, determined using another system, but maintaining both the column and the reflux intensity constant, is a constant value, not depending on either the reflux intensity or the kind of packing.

A table is given in which the efficiency ratios for 8 different binary systems are listed.

A difference in the efficiencies, determined using various systems, is explained by the fact that in a column, operating under total reflux, a stationary state, instead of an equilibrium state, is established between liquid and vapor. The span between the stationary state and the equilibrium state is different for different systems, which is explained by the different rate with which mass-transfer processes progress. A difference in the span between the stationary states and the equilibrium state is responsible for the difference in the efficiency.

LITERATURE CITED

- [1] W. A. Peters, Jr., Ind. Eng. Chem. 14, 476 (1922).
- [2] I. N. Bushmakina, R. V. Lyzlova, and O. I. Avdeeva, Zhur. Priklad. Khim. 25, 287 (1952).*

* Original Russian pagination. See C. B. Translation.

- [3] I. N. Bushmakin and R. V. Lyzlova, Zhur. Priklad. Khim. 25, 303 (1952).*
- [4] I. N. Bushmakin and N. V. Lutugina, Zhur. Priklad. Khim. 29, 1164 (1956). *
- [5] I. N. Bushmakin, Zhur. Obshchei Khim. 21, 1197 (1951).
- [6] I. N. Bushmakin, R. V. Lyzlova, and P. Ya. Molodenko, Zhur. Priklad. Khim. 26, 1258 (1953).*
- [7] I. N. Bushmakin, P. Ya. Molodenko, and R. V. Lyzlova, Zhur. Priklad. Khim. 26, 1268 (1953).*
- [8] I. N. Bushmakin and N. V. Lutugina, Zhur. Priklad. Khim. 29, 1169 (1956).*
- [9] I. N. Bushmakin, S. P. Versen, and N. P. Kuznetsova, Zhur. Priklad. Khim. 32, 6, 1274 (1959). *
- [10] I. N. Bushmakin and N. P. Kuznetsova, Zhur. Priklad. Khim. 32, 8, 1751 (1959).*
- [11] I. N. Bushmakin and E. D. Voeikova, Zhur. Obshchei Khim. 19, 1615 (1949).*

Received May 25, 1959

*Original Russian pagination. See C. B. Translation.

EQUATIONS AND SIMILARITY CRITERIA OF NONISOTHERMAL DIFFUSION*

A. A. Medvedev and P. G. Romankov

Lensovet Technological Institute, Leningrad

Many processes in chemical technology proceed under the conditions of a reciprocal development of a number of phenomena. For example, the extraction of matter in a system composed of solid and liquid is a process in which the interrelated phenomena of solution and the transfer of mass, heat and momentum are all present. Here the kinetics of the process depends simultaneously on several motive forces of different character.

We will derive a differential equation for nonisothermal diffusion, keeping in mind that in the system the gradients of the chemical potential and the temperature are not equal to zero ($\text{grad } \mu \neq 0$, $\text{grad } T \neq 0$), while the influence of the other motive forces can be neglected. The flow of mass for these conditions can be derived from the general linear equation for the thermodynamics of irreversible processes [1, 2] as the equation

$$I_m = -L_{21} \frac{\text{grad } T}{T} - L_{22} \left(\text{grad } \mu - \frac{\mu}{T} \text{grad } T \right), \quad (1)$$

where L_{21} and L_{22} are kinetic coefficients, respectively expressing the conductivity of the mass in the superimposed and principal effects (under the influence of heat and diffusional motive forces).

For the molecular mechanism of the transfer of matter the continuity equation had the form

$$\frac{\partial C}{\partial \tau} + \text{div } I_m = 0. \quad (2)$$

Substituting the density of flow I_m from Eq. (1) in Eq. (2), we obtain

$$\frac{\partial C}{\partial \tau} = \text{div} \left(L_{21} \frac{\text{grad } T}{T} + L_{22} \text{grad } \mu - L_{22} \frac{\mu}{T} \text{grad } T \right). \quad (3)$$

Regarding the divergence of each component as the difference of the product of the scalar by the vectorial, and expressing the volume concentration C by the concentration referred to the unit of mass \underline{c} , then from Eq. (3) at $\partial C = \rho \partial \underline{c}$, we have

$$\begin{aligned} \rho \frac{\partial \underline{c}}{\partial \tau} = & \frac{L_{21}}{T} \text{div grad } T + \text{grad } T \text{ grad } \frac{L_{21}}{T} + L_{22} \text{div grad } \mu + \\ & + \text{grad } \mu \text{ grad } L_{22} - \frac{L_{22}\mu}{T} \text{div grad } T - \text{grad } T \text{ grad } \frac{L_{22}\mu}{T}. \end{aligned} \quad (4)$$

* Communication II.

After certain transformations, Eq. (4) can assume the form

$$\begin{aligned} \frac{\partial \mu}{\partial \tau} = & \frac{L_{22}}{\rho \frac{\partial \mu}{\partial \mu}} \left(\frac{L_{21}}{L_{22}} \cdot \frac{\nabla^2 T}{T} - \frac{L_{21}}{L_{22}} \cdot \frac{\nabla T \nabla T}{T^2} + \frac{\nabla T \nabla L_{21}}{L_{22} T} + \nabla^2 \mu + \frac{\nabla \mu \nabla L_{22}}{L_{22}} \right) - \\ & - \frac{L_{22}}{\rho \frac{\partial \mu}{\partial \mu}} \left(\frac{\mu \nabla^2 T}{T} - \mu \frac{\nabla T \nabla T}{T^2} + \mu \frac{\nabla T \nabla L_{22}}{T L_{22}} + \frac{\nabla T \nabla \mu}{T} \right). \end{aligned} \quad (5)$$

Here $\frac{L_{21}}{L_{22}}$, due to the relationship of the reciprocity $L_{21} = L_{12}$, is numerically equal to the heat of transfer. In [3] we had shown that the complex term $\frac{L_{\mu}}{\rho \frac{\partial \mu}{\partial \mu}}$ is a complete analog of the coefficient of heat conductivity and expresses the conductivity of the chemical potential of component \underline{i}

$$\frac{L_{\mu}}{\rho \frac{\partial \mu}{\partial \mu}} = a_{\mu}, \quad (6)$$

where a_{μ} is the conductivity coefficient of the chemical potential of component \underline{i} in the system.

Employing the conductivity value of the chemical potential, Eq. (5) as applied to a two-component system, after certain simple transformations, can be written in the following form:

$$\begin{aligned} \frac{\partial \mu_1}{\partial \tau} = & a_{\mu} \frac{L_{21}}{L_{\mu}} \left(\frac{\nabla^2 T}{T} - \frac{\nabla T \nabla T}{T^2} + \frac{\nabla T \nabla L_{21}}{L_{21} T} \right) + a_{\mu} \left(\nabla^2 \mu_1 + \frac{\nabla \mu_1 \nabla L_{\mu}}{L_{\mu}} \right) - \\ & - a_{\mu} \frac{\mu_1 - \mu_2}{T} \left(c_2 \nabla^2 T - \frac{c_2 \nabla T \nabla T}{T} + c_2 \nabla T \nabla L_{22} + \frac{\nabla T \nabla \mu_1}{\mu_1 - \mu_2} \right). \end{aligned} \quad (7)$$

Equation (7) is a differential equation for nonstationary and nonisothermal molecular diffusion in a binary system. It describes the general case of molecular transfer, regarding the phenomenological coefficients as variable terms. For calculation purposes, where it is more convenient to use these coefficients as physical constants (which is fully permissible in the limits of slight changes in the chemical potentials and the temperature), Eq. (7) simplifies and assumes the form

$$\frac{\partial \mu_1}{\partial \tau} = a_{\mu} \frac{L_{21}}{L_{\mu}} \left(\frac{\nabla^2 T}{T} - \frac{\nabla T \nabla T}{T^2} \right) + a_{\mu} \nabla^2 \mu_1 - a_{\mu} \frac{\mu_1 - \mu_2}{T} \left(c_2 \nabla^2 T + \frac{\nabla T \nabla \mu_1}{\mu_1 - \mu_2} - c_2 \frac{\nabla T \nabla T}{T} \right). \quad (8)$$

For a particular case, under isothermal conditions, Eq. (8) becomes much simpler, as was shown by us earlier [3]

$$\frac{\partial \mu_1}{\partial \tau} = a_{\mu} \nabla^2 \mu_1. \quad (9)$$

Taking convective transfer of the material into account, Eq. (8) is easily transformed under certain conditions ($\text{div } \underline{w} = 0$, where \underline{w} is the linear velocity) to the following form:

$$\frac{D \mu_1}{d \tau} = a_{\mu} \frac{L_{21}}{L_{\mu}} \left(\frac{\nabla^2 T}{T} - \frac{\nabla T \nabla T}{T^2} \right) + a_{\mu} \nabla^2 \mu_1 - a_{\mu} \frac{\mu_1 - \mu_2}{T} \left(c_2 \nabla^2 T + \frac{\nabla T \nabla \mu_1}{\mu_1 - \mu_2} - c_2 \frac{\nabla T \nabla T}{T} \right), \quad (10)$$

where the left side of the equation represents a substantial derivative of the chemical potential of component 1.

The differential equations obtained by us for nonisothermal diffusion, namely (7), (8), and (10) do not lend themselves in general form to analytical integration. But solving complex boundary problems here can be represented in the form of functional relationships between similarity criteria.

For example, as the result of a similar transformation of differential Eq. (10) and boundary conditions of the form

$$\alpha_\mu \Delta \mu_1 + \alpha_T \Delta T = -L_{21} \frac{\text{grad } T}{T} - L_{22} \text{grad } (\mu_1 - \mu_2) + L_{23} \frac{\mu_1 - \mu_2}{T} \text{grad } T \quad (11)$$

we obtained the following similarity criteria:

$$K_1 = \frac{\alpha_\mu \Delta \mu_1}{\alpha_T \Delta T}, \quad (12)$$

$$K_2 = \frac{L_{21}}{\alpha_T \Delta T l}, \quad (13)$$

$$K_3 = \frac{\alpha_\mu \Delta \mu_1 l}{L_{21}}, \quad (14)$$

$$K_4 = \frac{L_{\mu} \mu_2 c_2}{\alpha_T \Delta T l}, \quad (15)$$

$$K_5 = \frac{L_\mu \Delta \mu_1}{\alpha_T \Delta T l}, \quad (16)$$

$$K_6 = \frac{L_{21}}{L_\mu \Delta \mu_1}, \quad (17)$$

$$K_7 = \frac{\Delta \mu_1}{\mu_2 c_2}, \quad (18)$$

$$K_8 = \frac{\alpha_\mu l}{L_\mu}, \quad (19)$$

$$K_9 = \frac{\alpha_\mu \tau}{l^2}, \quad (20)$$

$$K_{10} = \frac{wl}{a_\mu}, \quad (21)$$

$$K_{11} = \frac{\Delta \mu_1}{\Delta \mu_2}. \quad (22)$$

Criteria K_8 , K_9 , and K_{10} are, respectively, complete analogs of the classical heat-similarity criteria of Nusselt, Biot, Fourier and Peclet.

For this reason it is possible to write

$$Nu_D = K_8 = \frac{\alpha_\mu \cdot l}{L_\mu}, \quad (19a)$$

$$Bi_D = K_9 = \frac{\alpha_\mu \cdot \tau}{L_\mu}, \quad (19b)$$

$$Fo_D = K_9 = \frac{\alpha_\mu \cdot \tau}{l^2}, \quad (20a)$$

$$Pe_D = K_{10} = \frac{wl}{a_\mu}. \quad (21a)$$

Criterion K_{11} expresses the relationship between the chemical potentials of the components.

The first 7 criteria, K_1 , K_2 , K_3 , K_4 , K_5 , K_6 , and K_7 are new criteria [4, 5], characterizing the specific nature of the similarity in the molecular and molar-molecular forms of transfer in the process of nonisothermal diffusion under different conditions. The physical meaning of these similarity criteria can be discovered from an analysis of connecting Eqs. (10) and (11).

Criterion K_1 is a measure of the intensity of molecular-molar (convective) mass transfer under isothermal conditions when compared with the same form of transfer under the influence of a temperature head.

Criterion K_2 characterizes the relationship between molecular mass transfer under the influence of the heat motive force (according to Onsager) and its convective transfer under the influence of a temperature head.

Criterion K_3 shows the intensity of the convective isothermal transfer of the mass when compared with its molecular transfer under the influence of the heat motive force (according to Onsager).

Criterion K_4 is a measure of the ratio of the molecular forms of mass transfer under the influence of the diffusional motive force (its temperature gradient) and the convective transfer, corresponding to the total temperature head.

Criterion K_5 shows the relationship between the molecular isothermal mass transfer under the influence of the diffusional motive force and the convective mass transfer resulting from the action of the temperature head.

Criterion K_6 characterizes the relationship between the molecular forms of mass transfer under the influence of the heat and diffusional ($\text{grad } \mu$) motive forces.

Criterion K_7 is a measure of the intensity of the molecular forms of mass transfer, determined by the diffusional motive force ($\text{grad } \mu$ and $\mu/T \text{ grad } T$).

The form of the functional relationship between the similarity criteria and their number is established according to the general rules of the similarity theory. Thus, to form the criterial function, corresponding to the system of Eqs. (10) and (11), it is sufficient to have a total of seven criteria, the combination of which is determined by the concrete conditions of the problem (with a testing of the criteria for compatibility). However, the fact must not be forgotten that this system of equations, regarded by us as an example, is open. Consequently, even a combination composed of the similarity criteria (12) - (22) cannot fully reflect the investigated phenomenon. In solving a concrete problem of the nonisothermal diffusion process using experiment it is necessary to have, in addition to the differential equation of mass transfer, a complete characterization of the boundary conditions (spatial, including the geometry of the system, and auxiliary) and a characterization of the hydrodynamic conditions (equations of motion and of continuity).

If, let us say, in the investigated problem the hydrodynamics of the process is completely characterized by criterion Re , while the geometric similarity is characterized by simplex Γ_1 , then the criterial function can have the following form:

$$\varphi(Fo_D, Pe_D, Bi_D, Re, K_2, K_3, K_4, K_{11}, \Gamma_1) = 0. \quad (23)$$

The explicit form of this function can be found experimentally.

In conclusion we will examine the physical meaning of certain phenomenological coefficients. A number of investigators [2, 6], discussing the equation of the thermodynamics of irreversible processes as applied to diffusion phenomena, believe that the kinetic coefficients L_{ik} in this case are the ordinary coefficients of diffusion, thermal diffusion, etc.

In our opinion, this concept is incorrect. The diffusion coefficient, for example, expresses the total diffusional conductivity of the system under isothermal conditions. In the physical sense it is the coefficient of the concentration conductivity of the system [3]. Quantitatively the diffusion coefficient takes into account both the mass conducting and the inertia properties of the system. Coefficients L_{ik} , in the given case L_{22} and L_{21} , are a measure of only the mass conducting properties of the system when reference is to the diffusional and superimposing (heat) effect, respectively. Consequently, the L_{ik} coefficients differ from the diffusion coefficients not only quantitatively, but also qualitatively.

SUMMARY

1. Differential equations of general form were obtained for molecular nonisothermal diffusion. Taking into account convective transport, a differential equation of nonisothermal diffusion was derived for a two-component system (liquid - solid).

2. A number of new similarity criteria were obtained, characterizing the peculiarities of molar - molecular mass transfer in the nonisothermal diffusion process as applied to the system liquid - solid, and their physical meaning was disclosed.

3. The physical meaning of certain phenomenological coefficients in the thermodynamics of irreversible processes was made more precise.

LITERATURE CITED

- [1] L. Onsager, Phys. Rev. 37, 405 (1931); 38, 2265 (1931).
- [2] S. R. de Groot, Thermodynamics of Irreversible Processes (Amsterdam, 1952).
- [3] A. A. Medvedev and P. G. Romankov, Zhur. Priklad. Khim. 32, 1021 (1959).*
- [4] P. G. Romankov, Paper delivered at the 8th Mendeleev Convention [In Russian]. Data of Section No. 16 (Moscow, 1959); Abstracts of Papers, Section No. 16 (Moscow, 1958).
- [5] A. A. Medvedev, Paper delivered at the 8th Mendeleev Convention [In Russian]. Data of Section No. 16 (Moscow, 1958).
- [6] J. Meixner, Ann. Physik [5], 39, 333 (1941).

Received June 5, 1959

*Original Russian pagination. See C. B. Translation.

RESISTANCE OF THE LIQUID AND GAS PHASES IN ABSORPTION ON SIEVE AND BUBBLE-CAP PLATES

M. Kh. Kishinevskii and L. A. Mochalova

Laboratory of Physical and General Chemistry of the Astrakhan Technical Institute
of the Fish Industry and Economy

Despite the broad use of absorption processes in the chemical industry, very approximate methods have been used up to now in the design of absorption equipment. Such a situation is linked with the complexity of studying mass-transfer processes under industrial conditions. The mathematical problem here is linked with solving equations that include such physical constants as are inherent only to a given concrete experiment.

In the design of absorption equipment, it is obviously necessary to proceed along the lines of generalizing the experimental data on the coefficients of mass transfer, referred to the unit area of the plate and to the unit volume of the gas-liquid stream. Usually, the various types of bubble-cap and sieve plates are compared from the standpoint of the intensity of transfer achieved in them by comparing the partial coefficients of mass transfer in the liquid and gas phases, referred to the unit area of the plate. However, this comparison is possible only if the indicated coefficients were determined under the same physicochemical conditions, since, for example, the presence of even trace amounts of surface-active substances as impurities can lead to increasing the height of the foam layer, and in this way also the mass-transfer coefficient, referred to one square meter of the plate.

To a lesser degree this difficulty is also inherent for the partial coefficients of mass transfer, referred to the unit volume of the gas-liquid stream, since these coefficients change less substantially with increase in the foam layer resulting from the chance presence of surface-active substances or for some other reason. At the same time the height of the foam layer is determined by the apparatus conditions, as well as by the physicochemical conditions. Consequently, to solve the problem of which of the compared apparatus operates most intensely, it is necessary to have available both the first and the second coefficients.

A number of papers have appeared in the literature devoted to a study of the kinetics of absorption on bubble-cap and sieve plates [1-12].

Resistance of the Liquid Phase

The studies of Pozin and co-workers [10] have shown that one of the principal parameters of the process is the velocity of the gas in the total cross section of the column. Foss and Gerster [4] came to the same conclusion. Proceeding from this, in order to find general rules we treated the experimental material of the mentioned studies as coefficients of mass transfer, referred to the unit volume of the gas-liquid stream k_{La} and to the unit area of the plate k_{Laz} , and plotted this information as functions of the gas velocity in the total cross section of the column. The data are plotted in Figs. 1 and 2 (Tables 1 and 2). In Table 1, we have given the main structural details of the plates and some of the parameters of the process. The experimental data of Gerster and co-workers [8] are plotted in Figs. 3 and 4. In Figs. 5 and 6 (Tables 3 and 4) we have plotted, respectively, k_{La} and k_{Laz} as a function of the input of liquid.

TABLE 1

Literature reference	Process	Temperature (°C)	Cross-section area of plate (in sq m)	Free cross-section area (in %)	Height of overflow weir (in cm)	Number of openings in plate	Diameter of openings (in cm)	Height of liquid on plate in absence of gas (in cm)	Coefficient of gas loading	Input of liquid (kg-mole/hr-sq m)	Foam height (in cm)	Curve No. in Figure
[1]	Absorption of CO ₂ by water	11.5	0.18 · 10 ⁻²	—	—	18—19	0.318	2.54	0.789	3390	—	1
[1]								4.25	0.634	3390	—	2
[1]		22.4	0.715 · 10 ⁻²	—	—	83	0.318	5.84	0.570	3390	—	3
[1]								2.54 and 5.08	0.70—0.80	2140	—	4
[2]	Desorption of CO ₂ from water	28.0	2.28 · 10 ⁻²	6.07	2.5	—	0.3 and 0.09	—	—	1240	—	5
[4]	Desorption of O ₂ from water	25—30	0.11	4.2	5.08	—	0.47	—	—	2700	15.2	6
[4]	Likewise	25—30	0.11	4.2	5.08	—	0.47	—	—	6350	15.2	7
[4]	» »	25—30	0.11	10.6	5.08	—	0.47	—	—	2700	15.2	8
[4]	» »	25—30	0.11	10.6	5.08	—	0.47	—	—	6350	15.2	9
[5]	» »	—	—	10.0	—	—	0.318	—	—	8200	15.2	10 ^a
[5]	» »	—	—	10.0	—	—	0.318	—	—	4400	—	10 ^b
[6]	Desorption of CO ₂ from water	15.0	0.203 · 10 ⁻²	Plate with porous bottom	—	—	—	61	—	10800	—	11
[6]	Likewise	15.0	0.203 · 10 ⁻²		—	—	—	—	—	2700	—	12
[7]	» »	—	0.90 · 10 ⁻²	7.9	1.27	41	0.475	—	—	2720	—	13

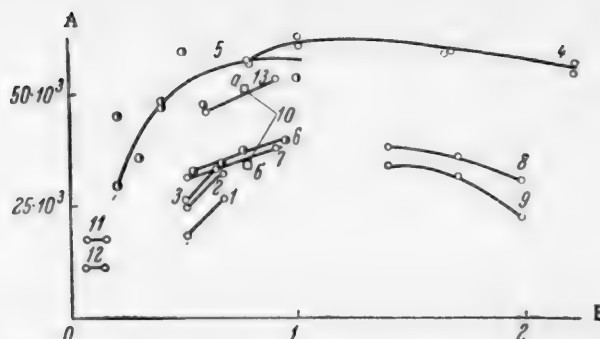


Fig. 1. Relation between mass-transfer coefficient and gas velocity. A) Mass-transfer coefficient in the liquid phase (in kg-mole/hr·m³); B) gas velocity in cross section of column (in m/sec). The designations are given in Table 1.

TABLE 2

Curves	Source of data	Type of plate	Input of liquid (in kg-mole/hr·cm ²)	Liquid level in absence of gas (in cm)	Free cross section (in %)	Literature reference
1, 2	West and co-workers	Sieve 83	2100	{ 2.54 5.08 }	—	[1]
3, 4, 5	West and co-workers	Sieve 19	3440	{ 2.54 4.32 5.85 }	—	[1]
6, 7, 8, 9, 10	Gerster and co-workers	Bubble-cap plate	{ 2030 4050 6100 8120 10300 }	{ 9.2 9.9 10.4 10.9 }	—	[8]
11, 12, 13	Foss and Gerster	Sieve	2560	{ 4.2 8 10.6 }	—	[4]
14, 15	Garner and co-workers	Sieve	{ 2720 815 }	—	—	[7]
16	Kuz'minykh and coworkers	Sieve	1240	—	—	[3]

Analysis of the graphs reveals that $k_L a$ is determined mainly by the gas velocity in the total cross section of the column. Such factors as the input of liquid, height of the overflow weir, and diameter of the openings fail to exert substantial effect on its value.

Although the gas velocity remains an important factor for $k_L a$, still it fails to be the determining value. This can be judged from Fig. 2, where it can be seen that under some conditions an increase in the gas velocity leads to an increase in $k_L a$, while under other conditions it leads to a decrease. Here it is obvious that the character of the relation between the mass-transfer coefficient and the gas velocity is determined by other factors, the influence of which on the bulk mass-transfer coefficient is imperceptible. As can be seen from Fig. 2, one of these factors is the initial level of the liquid on the plate, which, in turn, is determined by the height of the overflow weir, the input of liquid, and other less important factors. Thus, for example, with a comparatively

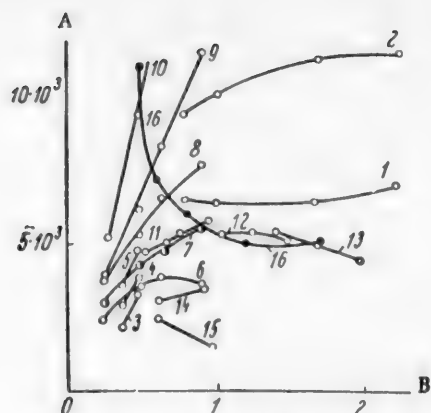


Fig. 2. Relation between mass-transfer coefficient and gas velocity. A) Mass-transfer coefficient in the liquid phase (in $\text{kg-mole/hr}\cdot\text{m}^2$); B) gas velocity in total cross section of column (in m/sec). The designations are given in Table 2.

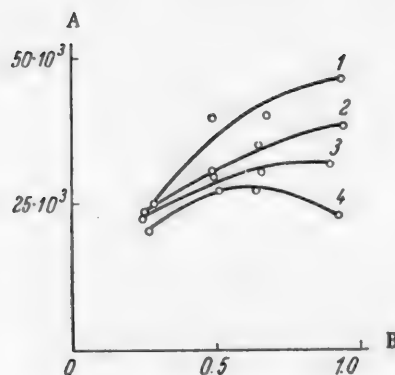


Fig. 3. Relation between mass-transfer coefficient and gas velocity. A) Mass-transfer coefficient in the liquid phase (in $\text{kg-mole/hr}\cdot\text{m}^2$); B) gas velocity in cross section of column (in m/sec). Experimental data of Gerster and co-workers [8]. Input of liquid (in $\text{kg-mole/hr}\cdot\text{m}^2$): 1) 10,300; 2) 6050; 3) 4050; 4) 2020.

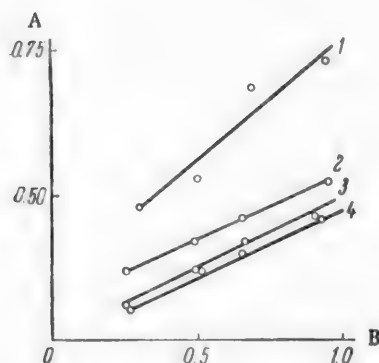


Fig. 4. Relation between gas-loading coefficient and gas velocity. A) Gas-loading coefficient; B) gas velocity in cross section of column (in m/sec). Experimental data of Gerster and co-workers [8]. Input of liquid (in $\text{kg-mole/hr}\cdot\text{m}^2$): 1) 10,300; 2) 6050; 3) 4050; 4) 2020.

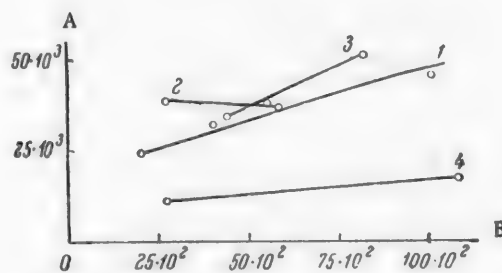


Fig. 5. Relation between mass-transfer coefficient and input of liquid. A) Mass-transfer coefficient in the liquid phase (in $\text{kg-mole/hr}\cdot\text{m}^2$); B) bulk input of liquid (in $\text{kg-mole/hr}\cdot\text{m}^2$). The designations are given in Table 3.

high initial liquid level (experimental data of West and co-workers — curve 2, Gerster and co-workers — curves 7-10, and Foss and Gerster — curve 11), k_{Laz} increases continuously in the interval of gas velocities ranging from zero to 1-2 m/sec . With a small initial liquid level (experimental data of Kuz'minykh and co-workers — curve 15), k_{Laz} passes through a maximum even before the gas velocity reaches a value of 0.5 m/sec . The bulk input of liquid exerts an important influence on k_{Laz} , in which connection, as can be seen from Fig. 6, this influence proves to be the same for both bubble-cap and sieve plates.

In Fig. 1 it is shown that k_{La} reaches a limiting value at a gas velocity of approximately 1 m/sec , independent of the bulk input of liquid and free cross section of the plate. A tendency for this coefficient to decrease

somewhat appears with further increase in the gas velocity. This is probably linked with a reduction in the specific area of the foam. At a gas velocity of 1 m/sec, k_{LA} changes from approximately $40 \cdot 10^{-3}$ kg-mole/hr·m³ in the experiments of Foss and Gerster [4] up to $60 \cdot 10^{-3}$ in the experiments of West and co-workers [1], and those of Kuz'minykh and co-workers [3].

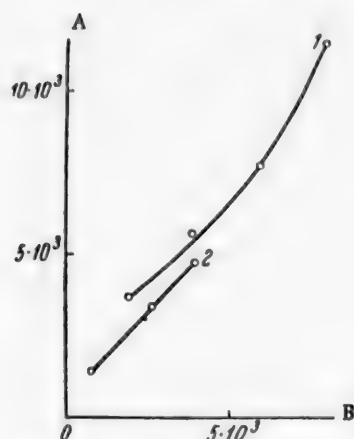


Fig. 6. Relation between mass-transfer coefficient and input of liquid. A) Mass-transfer coefficient in the liquid phase (in kg-mole/hr·m³); B) consumption of liquid (in kg-mole/hr·m³). The designations are given in Table 4.

It is difficult to relate this discrepancy to a difference in either the regimes or the structural characteristics of the apparatus. It is probably determined by physicochemical factors (impurities of surface-active substances, temperature), as well as by natural errors, assumed in determining the efficiency of the plates and in estimating the height of the foam, needed for the calculation of k_{LA} . The bulk input of liquid exerts some influence on k_{LA} , but it is completely impossible to explain the indicated discrepancy in the values of k_{LA} as due to this factor, since in the experiments of Foss and Gerster the input of liquid in some cases was more than 6000 kg-mole/hr·m³, in the experiments of West and co-workers it was 2140, and in the experiments of Kuz'minykh and co-workers, it was even less. As a result, in calculating the efficiency of a plate or the NTU (number of transfer units) it is possible to consider k_{LA} as being known and equal to approximately 50,000 kg-mole/hr·m³ (in the temperature range 15-30°).

The influence of the bulk input of liquid on k_{LA} and k_{LAZ} is shown in Figs. 5 and 6. As can be seen, increasing the bulk input of liquid leads to a slight increase in the first coefficient and to substantial increase in the second coefficient. However, it should be mentioned that the increase in k_{LAZ} with increase in the input of liquid does not compensate for the negative effect associated with a reduction in the time of contact between the phases, and, as a rule, an increase in the bulk input of liquid is accompanied by a reduction in the NTU and the efficiency of the plate relative to the liquid phase.

TABLE 3

Curves	Data	Gas velocity (in m/sec)	Literature reference
1	Gerster and co-workers	0.9	[8]
2	Foss and Gerster	0.9	[4]
3	Calderbank	0.78	[5]
4	Shulman and Molstad	0.15	[6]

TABLE 4

Curves	Data	Type of plate	Linear velocity of gas (in m/sec)	Literature reference
1	Gerster and co-workers	Bubble-cap	0.9	[8]
2	Garner and co-workers	Sieve	0.91	[7]

From Fig. 2 it can be seen that the value of the gas velocity corresponding to the maximum value of k_{Laz} depends on the original level of the liquid on the plate and the input of liquid. The region of optimum gas velocities shifts toward smaller values (below 0.5) as these parameters decrease, which is evidently linked with a maximum development of the interfacial area of the phases in this region of the velocity values. Since in the absorption of difficultly soluble gases on sieve and bubble-cap plates the objective is to achieve the greatest saturation of the liquid, then increasing the input of the latter is impractical, for the reason that this leads to a reduction in the time of contact of the liquid with the gas. It is also impractical to have a high weir level, since then the hydraulic resistance to the gas flow increases. Consequently, it is possible to conclude that in the process of saturating liquids with difficultly soluble gases on bubble-cap and sieve plates, operating with small liquid inputs and low weir levels, the optimum gas velocities lie below 0.5 m/sec.

Resistance of the Gas Phase

In Figs. 7 and 8 (Tables 5 and 6) we have given, respectively, the mass-transfer coefficients in the gas phase per unit volume of the gas-liquid stream and per unit area of the plate at different gas velocities in the total cross section of the column. As can be seen from the presented data, the mass-transfer coefficients in the gas phase, in contrast to the mass-transfer coefficients in the liquid phase, do not show a tendency to reach a limiting value in the interval of gas velocities ranging from 0 to 2 m/sec. This can be explained by the fact

TABLE 5

Curves	Data	Type of plate	Initial liquid level (in cm)	Literature reference
1,2,3	West, et al.	Sieve (based on the humidification of air)	$\left\{ \begin{array}{l} 1.27 \\ 2.54 \\ 5.08 \end{array} \right.$	$\left\{ \begin{array}{l} [1] \end{array} \right.$
4	Gerster, et al.	Bubble-cap (based on the humidification of air)	9.15	[8]
5, 6	Solomakhina and Matrosov (average)	Sieve (based on the absorption of ammonia from ammonia-air mixture)	—	[9]

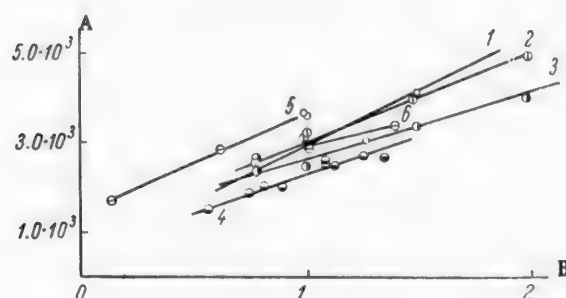


Fig. 7. Relation between mass-transfer coefficient and gas velocity. A) Mass-transfer coefficient in the gas phase (in kg-mole/hr·m³); B) gas velocity in the total cross section of the column (m/sec). The designations are given in Table 5.

that an increased turbulence in the gas phase masks a certain reduction in the specific area. That this is true is also indicated in the paper by Solomakha and Matrozov [9]. From Figs. 7 and 8 it can be seen that k_{GA} , the same as k_{LA} , is determined by the gas velocity in the total cross section of the column. Despite the different structural characteristics of the plates, in the studies of West, et al., Gerster and co-workers, and Solomakha and Matrozov, the values of k_{GA} differ but slightly from each other. Solomakha and Matrozov arrived at the same conclusion for the interval of gas velocities ranging from 0 to 0.8 m/sec. From Fig. 7 it follows that this conclusion can be extended to cover a much broader range of velocity values. In Fig. 8, it is shown that k_{GAz} rises more sharply than does k_{GA} with increase in the gas velocity. The same as k_{LAz} , the value k_{GAz} is not determined clearly by the gas velocity in the cross section of the column.

TABLE 6

Curves	Data	Type of plate	Original level (in cm)	Weir height (in cm)	Free cross-section (in %)	
1, 2, 3	West and co-workers	Sieve (based on the humidification of air)	1.27 2.54 5.08	—	—	[1]
4	Gerster and co-workers	Bubble-cap (based on the humidification of air)	9.15	—	—	
5	Kuz'minykh and co-workers	Sieve (based on the humidification of air)	—	2.5	—	
6	Pozin and Kopylev	Sieve based on absorption with cupro-ammoniacal solution)	—	1	—	[11]
7	Pozin and Kopylev	Sieve (based on absorption with 1N sodium hydroxide solution)	—	20—25	—	[11]
8	Solomakha and Matrozov	Sieve (based on the absorption of ammonia from ammonia-air mixture)	—	3.2	6.95	[9]
9			—		14.6	[9]

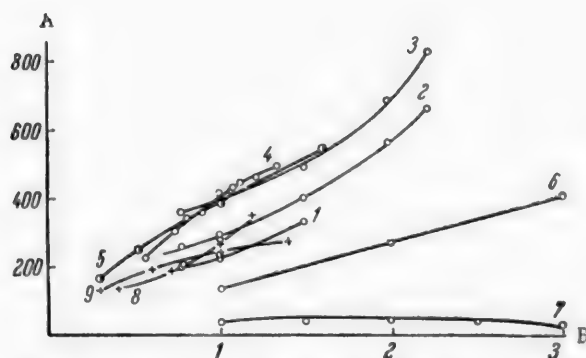


Fig. 8. Relation between mass-transfer coefficient and gas velocity. A) Mass-transfer coefficient in the gas phase (in kg-mole/hr·m²); B) gas velocity in the total cross section of the column (in m/sec). The designation are given in Table 6.

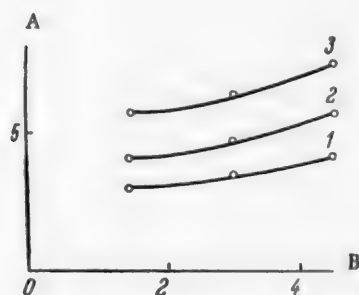


Fig. 9. Relation between mass-transfer coefficient and input of liquid. A) Mass-transfer coefficient in the gas phase (in m/hr·10⁻³); B) input of liquid per meter of weir length (in m/hr·m). Experimental data of Solomakha and Matrozov [9] for a sieve plate based on the absorption of ammonia from an air-ammonia mixture; diam. of openings 0.2 cm, overflow level 3.2 cm. Linear gas velocity in cross section of column (in m/sec): 1) 0.4; 2) 0.7; 3) 1.

Sherwood and Pigford [12] give graphs for the relationship between the N_{tu} relative to the gas phase and the velocity, constructed from the data of Gerster and co-workers [8], for the bubble-cap plate at different liquid inputs. From these graphs it follows that the N_{tu} relative to the gas increases from 2 to 4 when the input of liquid is increased from 3 to 50 gallons/min·ft. An increase in N_{tu} in this case is apparently due to an increase in k_{Gaz} as the loading relative to the liquid increases. That the input of liquid exerts an important influence on k_{Gaz} can also be concluded from the experimental data of Solomakha and Matrozov (Fig. 9).

Analysis of the experimental material discussed in this paper leads to still another interesting result. On sieve plates the mass-transfer coefficients in both the gas and liquid phases differ but slightly from the mass-transfer coefficients on bubble-cap plates. This indicates that the intensity of transfer in these two types of apparatus is approximately the same.

SUMMARY

1. The main factor determining the magnitude of the mass-transfer coefficient in the liquid phase, referred to the unit volume of the gas-liquid stream, is the gas velocity in the total cross section of the column. The structural characteristics of the plate and the gas-loading coefficient are practically without effect on the value of this coefficient. Some increase in k_{La} is observed as the bulk input of liquid is increased. For gas velocities exceeding 0.5 m/sec it is possible to take k_{La} approximately equal to 50,000 kg-mole/hr·m³.

2. The mass-transfer coefficient in the liquid phase, referred to the unit area of the plate, is not determined clearly by the gas velocity in the total cross section of the column. Together with this factor, both the bulk input of liquid and the weir height exert an important influence on k_{Laz} .

3. The optimum regime for the absorption of difficultly soluble gases in plate columns corresponds to values of less than 0.5 m/sec for the gas velocity in the total cross section of the column.

4. The same as for the liquid phase, the main factor determining the magnitude of the mass-transfer coefficient in the gas phase, referred to the unit volume of the gas-liquid stream, is the gas velocity in the total cross section of the column. For gas velocities ranging from 0 to 2 m/sec, it is possible to calculate this coefficient (in kg-mole/hr·m³) using the formula

$$k_{Ga} = 2600 w.$$

5. The mass-transfer coefficient in the gas phase, referred to the unit area of the plate, rises sharply with increase in the gas velocity. For the case where the resistance of the gas phase is controlling, this makes it possible to operate at higher loads relative to the gas without reducing the efficiency of the plate.

6. Approximately the same intensity of mass transfer in the liquid and gas phases is achieved on both bubble-cap and sieve plates.

LITERATURE CITED

- [1] F. B. West, W. D. Gilbert, and T. Shimizu, *Ind. Eng. Chem.* 44, 2470 (1952).
- [2] I. N. Kuz'minykh, L. S. Aksel'rod, Zh. A. Koval', and A. I. Rodionov, *Khim. Prom.* (1954), 86.
- [3] I. N. Kuz'minykh and Zh. A. Koval', *Zhur. Priklad. Khim.* 28, 21 (1955). •
- [4] Alan S. Foss and J. A. Gerster, *Chem. Eng. Progr.* 52, 28 (1956).
- [5] P. H. Calderbank, *Trans. Inst. Chem. Engrs. (London)* 34, 79 (1956).
- [6] H. L. Shulman and M. C. Molstad, *Ind. Eng. Chem.* 42, 1058 (1950).
- [7] F. H. Garner, S. R. M. Ellis, and D. C. Freshwater, *Trans. Inst. Chem. Engrs. (London)* 35, 61 (1957).
- [8] J. A. Gerster, A. P. Colburn, W. E. Bonnet, and T. W. Carmody, *Chem. Eng. Progr.* 45, 716 (1949).
- [9] T. P. Solomakha and V. I. Matrozov, *Kislород* 10, 2, 16 (1957).

•Original Russian pagination. See C. B. Translation.

[10] M. E. Pozin, I. P. Mukhlenov, E. S. Tumarkina, and É. Ya. Tarat, Foam Methods for the Treatment of Gases and Liquids [In Russian] (Goskhimizdat, 1955).

[11] M. E. Pozin and B. A. Kopylev, Zhur. Priklad. Khim. 31, 3, 387 (1958). •

[12] T. K. Sherwood and R. L. Pigford, Absorption and Extraction (1952).

Received February 16, 1959

•Original Russian pagination. See C. B. Translation.

INFLUENCE OF THE OPERATING CONDITIONS OF GAS LIFTS ON THEIR HYDRAULIC RESISTANCE*

M. L. Varlamov, G. A. Manakin, and Ya. I. Starosel'skii

Heterogeneous processes, progressing at the interface of gas - liquid phases, play an important role in chemical technology.

The design of new apparatus, securing good contact of the phases in a gas - liquid system, with the apparatus having as low a hydraulic resistance as possible, is a practical problem and permits intensifying many technological processes. A number of new types of absorption and reaction apparatus have been proposed recently, including mechanical, foam, having perforated plates, Venturi scrubbers, etc. [1-5].

The use of gas-lift apparatus as absorbers and reaction equipment is of interest [6-10]. They have been used for a long time in the transport of liquids, especially in obtaining petroleum from oil wells [11-14]. Lopatto suggested their use for the absorption and treatment of gases [6].

Gas lifts are characterized by a high intensity of the reaction volume due to the strong turbulence of the gas-liquid flow. The simplicity of construction and the ease of maintenance, the absence of moving parts and pumps for transferring the circulating liquid, and the low capital expense, all make this type of equipment look promising for operation with gases and liquids containing suspended solid particles. Due to the influence exerted by a large number of factors on the process, both the theory and the methods for designing gas lifts as transport machines have been inadequately developed, if we omit reference to gas-lift absorbers, the literature on which is extremely meager. The theory of similarity is still not applicable to this type of apparatus, and without special investigations, it is impossible to use the information obtained on laboratory models in the erection of plant installations.

Serious disadvantages of currently used gas-lift apparatus are: a high hydraulic resistance, the gas and liquid flowing in the same direction, the narrow limits within which it is possible to vary the ratios of the amounts of gas and liquid entering the gas lift, and the interdependence of the input of these components, which to a substantial degree is linked with the structural characteristics of the apparatus and the mode of assembling.

Below we give some new designs of gas-lift apparatus and we also discuss the results of investigating their hydraulic resistance under different operating conditions. The described apparatus possess a lower hydraulic resistance and permit varying the input ratios of gas and liquid within wide limits independently of each other.

A total of five different pieces of equipment was tested, which differed in the length and diameter of the lift tubes and the number of operating passages. The structural dimensions of the different kinds of apparatus** are given in the table.

* Communication I in a series of papers on new designs in gas-lifts as reaction and absorption apparatus.

** Certificate No. 7302, dated July 30, 1957, of registration with the Committee on Inventions and Discoveries of the Council of Ministers of the USSR.

Structural Dimensions of Gas Lifts

Parameters of gas lifts	Gas lift No.				
	1	2	3	4	5
Diameter of gas-lift tube (in mm) .	17	17	17	17	9**
Number of operating passages	1	1	1	2	7
Total height of operating passages (in m)	0.475	1.8	3.4	6.2	4.954
Total length of lift tube (in m) . . .	0.475	1.8	3.4	9.9	9.2
Input (in liters/ min) of gas (in studying the hydrodynamics):*					
minimum	40	105	31	40	50
maximum	370	170	170	360	660

* The equivalent diameter is given for this gas lift (the lift tube had a rectangular cross-section).

** At very low gas inputs the gas lifts operate in spurts and their hydraulic resistance changes with time.

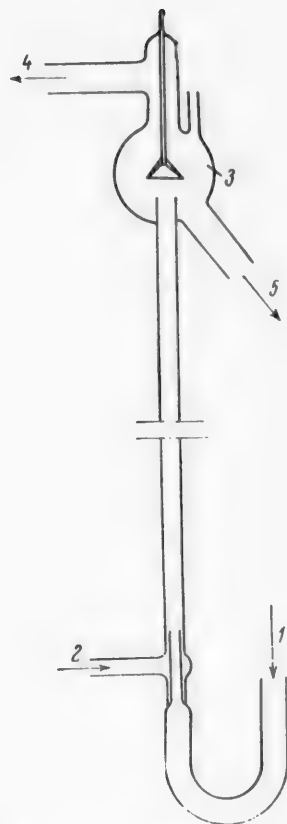


Fig. 1. Apparatus No. 1, representing a type of gas lift with modified design of the shoe. 1) Gas inlet; 2) liquid inlet; 3) separator; 4) gas outlet; 5) liquid outlet.

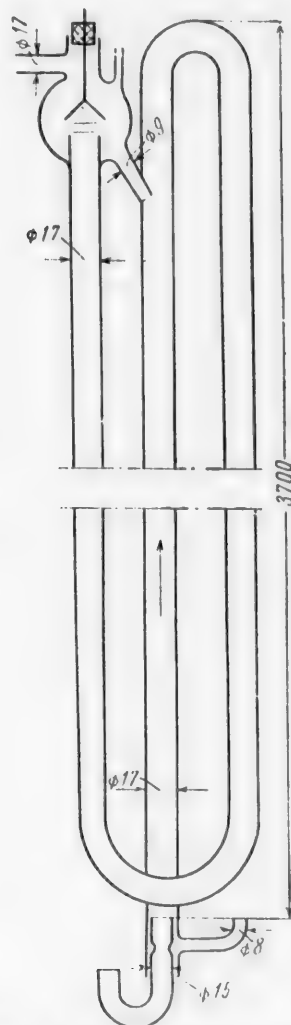


Fig. 2. Apparatus No. 3, with two operating passages in the lift tube.

The gas rate (w) in the apparatus reached 30 m/sec, while the ratio gas:liquid ($G:L$) went as high as 10,000, whereas in conventional equipment $w = 1-5$ m/sec, while $G:L \approx 5-100$.

Gas lifts with a modified design of the shoe, a spiral gas lift and a flat-walled multipassage apparatus are shown in Figs. 1-3. The other apparatus differ in the construction of the shoe and the lift tube. The gas and liquid are fed into the apparatus at the bottom and escape at the top. The phases are separated in a separator, and the liquid may be recycled.

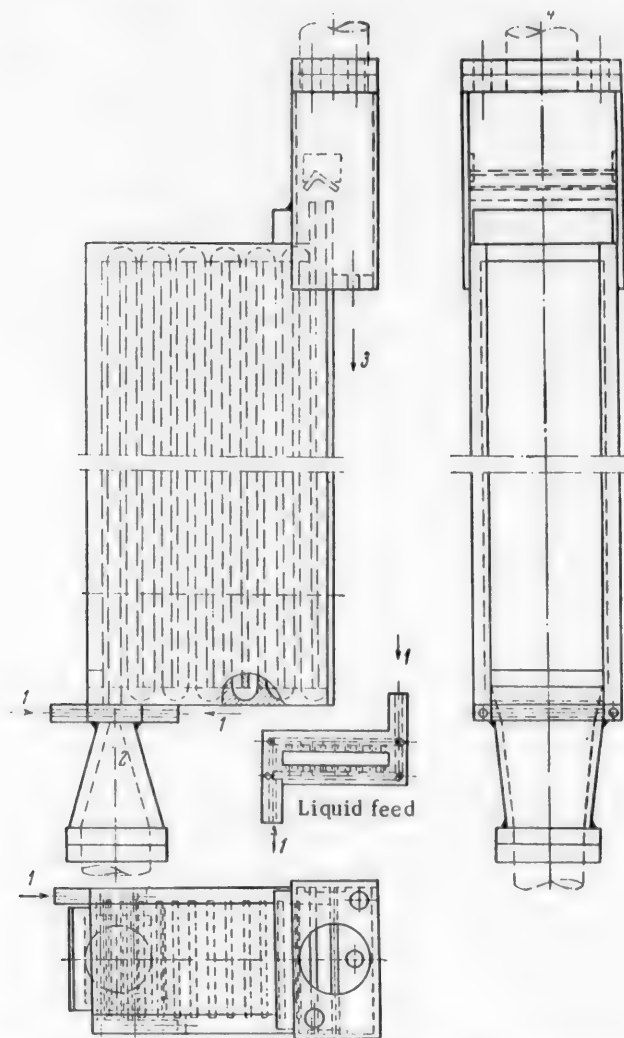


Fig. 3. Multipassage apparatus No. 5, with the lift tube having a rectangular cross section. Inlet: 1) liquid, 2) gas; outlet, 3) liquid, 4) gas.

In the flat-walled gas lift (Fig. 3) the gas is fed into the apparatus through a nipple connection at the bottom, while the liquid is brought in along the periphery of the same nipple. Then the gas - liquid emulsion is circulated through all of the sections, after which it escapes from the apparatus into the separator, where a separation of the gas and liquid phases occurs. An important advantage of this type of design is the possibility of erecting a plant with a high capacity, if the design is based on the study results obtained with the experimental unit (assuming that diameters of equivalent cross section are used).

It is characteristic for the gas lifts described in the literature to have several hydrodynamic regimes, determined by the input of gas and the so-called depth of immersion of the nozzle, feeding the gas into the lift tube.

Ordinary bubbling occurs when the gas feed rate is very small and the liquid hardly rises along the lift tube, while the hydraulic efficiency is equal to zero. Increasing the gas input Q_G leads to an "unsteady" regime, characterized by the presence of alternate gas and liquid plugs in the tube, which vanish when Q_G is increased. This leads to the formation of a turbulently moving gas-liquid emulsion. The maximum input of liquid (Q_L) is reached at a certain value for the gas input (Q_G), after which a further increase in Q_G leads to some reduction in Q_L . It is important to mention that Q_G and Q_L are interdependent values, i.e., a certain value of Q_L corresponds to a given value of Q_G and the depths of immersion of the nozzle. Finally, at very high values for the gas input (Q_G) the uniformity with which the liquid enters the apparatus vanishes, and the apparatus operates erratically, with pulsations, especially at low depths of nozzle immersion. The apparatus designs proposed by us permit operating at high gas rates.

The hydrodynamic experiments performed by us revealed that the input of liquid can be regulated independently of the gas input. Raising the gas input to a certain limit causes a reduction, and not an increase in the hydraulic resistance (Δp), and at the same time it causes an increase in the coefficients of the rate of absorption. This greatly expands the possible industrial applications of gas lifts and permits selecting the most rational operating conditions, under which a high intensity will be coupled with relatively low values for Δp . A regime approaching film conditions is observed at high linear gas velocities, in which connection most of the liquid is found on the inside walls of the apparatus as a thin film with a series of thick places (rings), slowing movement upwards along the walls of the lift tube. Intense mixing of the liquid occurs inside each of these thick places due to the friction forces of the gas and liquid at the tube walls interacting with gravity.

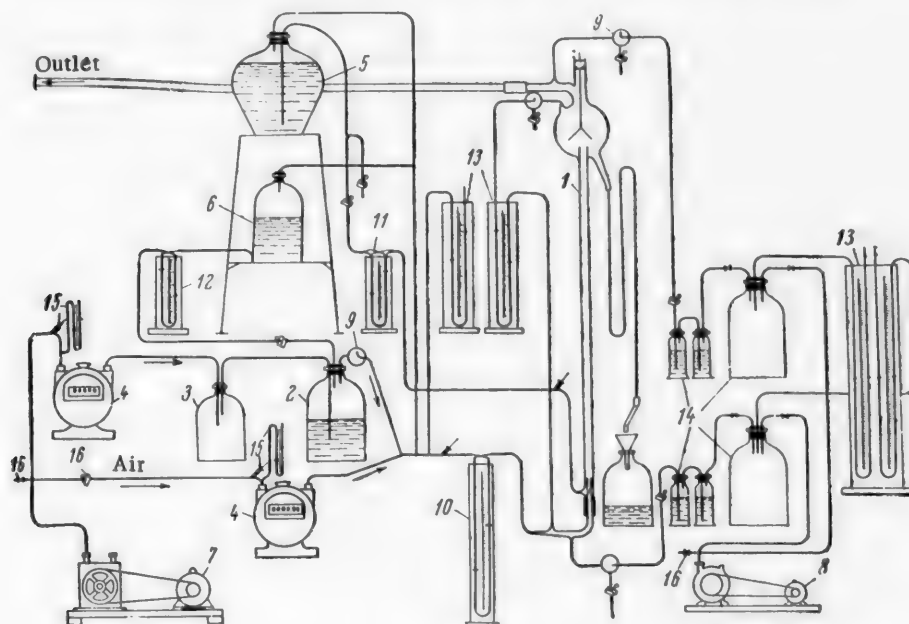


Fig. 4. Diagram of experimental setup. 1) Gas-lift apparatus; 2) nitrore solution; 3) receiver; 4) gas meters; 5) soda solution; 6) sodium nitrite solution; 7) compressor; 8) vacuum-pump; 9) spray traps; 10, 11, and 12) flow meters; 13) manometers; 14) analysis of sample for amount of nitrogen oxides in the gas entering and escaping from the gas lift; 15) thermometers and manometers; 16) regulating clamps and stopcocks.

A diagram of the large-scale experimental laboratory setup, which we used to study the hydrodynamics and absorption of nitrogen oxides by soda solutions in gas-lift apparatus, is shown in Fig. 4. A compressor was used to force previously purified air into the shoe of the gas lift. The amount and rate of input were controlled using gas meters and flow meters.

While the hydrodynamics was studied, water from the supply tank passed through the input meter and was also fed into the shoe of the apparatus.

From the separator the gas was vented to the outside, while the liquid was collected in a receiver, in which connection the consumption of water was measured at periodic intervals using a graduated cylinder. The hydraulic resistance in the apparatus was measured using a differential manometer, which was connected to both the gas inlet and outlet lines.

Increasing the liquid input at a constant gas input leads to an approximately linear increase in the hydraulic resistance, but beginning with a specific load of approximately $1-2.5 \text{ m}^3$ of liquid per running meter of internal perimeter of the gas lift, the slope of the lines decreases sharply.

The effect of the gas input on Δp is not clear-cut: in some cases Δp increases with increase in the gas input, and in other cases, to the contrary, it decreases. To show this relationship we plotted the curves of the function $\Delta p = \varphi(Q_G)$ at $Q_L = \text{const}$ (Fig. 5). The curves have extreme points, at one of which Δp is minimum. A decrease in Δp with increase in Q_G is caused by a reduction in the amount of liquid found at one time in the tube of the lift, which lowers γ_{cm} , the specific gravity of the gas-liquid emulsion.

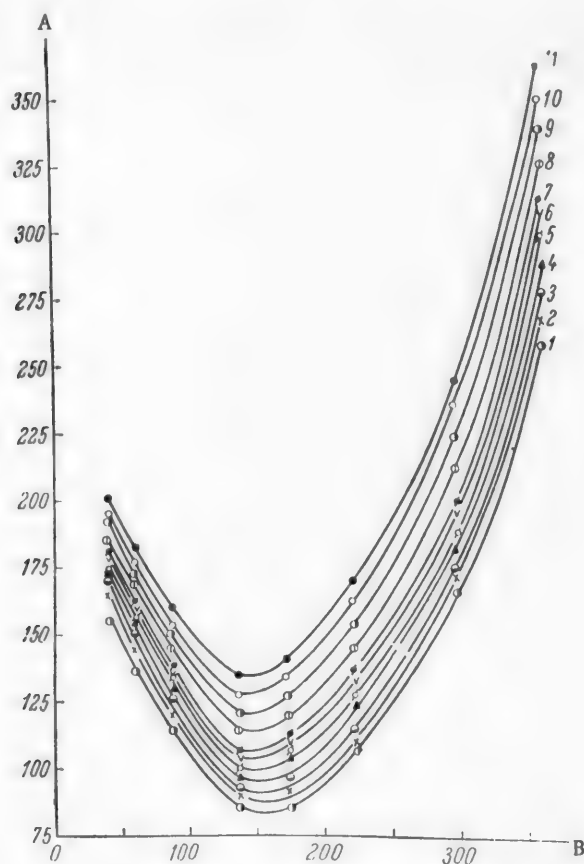


Fig. 5. Relation between the hydraulic resistance Δp of apparatus No. 1 and the input of gas at a constant liquid input. A) Value of Δp (in mm of water); B) input of gas (in liters/min). Input of liquid (in ml/min): 1) 50, 2) 75, 3) 100, 4) 150, 5) 200, 6) 250, 7) 300, 8) 400, 9) 500, 10) 600, 11) 700.

With further increase in the gas input, γ_{cm} approaches the γ of the gas, while increasing Q_G leads to an increase in Δp that nearly obeys the quadratic rule. The given relationship is observed for both single passage and flat-walled gas lifts. The presence of a minimum Δp at a certain Q_G permits selecting the optimum regime, under which the consumption of energy is minimum. It is important to mention that a gas:liquid ratio is established inside the lift tube which usually does not coincide with the ratio of the same components when entering the tube. For gas-lift apparatus of conventional design, with the depths of nozzle immersion maintained constant, a proportional increase in Δp is observed with increase in the gas input, which is associated with a simultaneous increase in the liquid input, characteristic for such apparatus. A minimum value for Δp is not observed in apparatus of this type.

A comparison of Δp for different types of apparatus in the region of minimum value as a function of the length of the lift tube is given in Fig. 6.

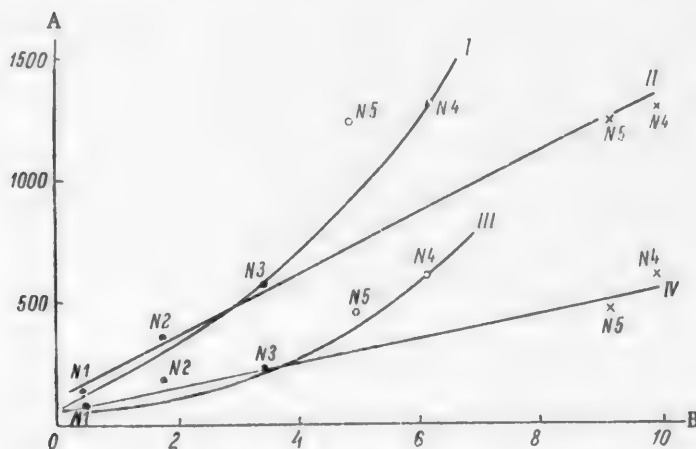


Fig. 6. Comparison of the hydraulic resistance Δp for different types of gas-lift apparatus in the region of minimum Δp as a function of the height of the lift tubes and the total height of the apparatus. A) Value of Δp (in mm of water column); B) height (in m). I) $\Delta p = f(H_{\text{operating}})$, $d_e = 0.017$ m, $Q_L = 700$ ml/min; II) $\Delta p = f(H_{\text{total}})$, $Q_L = 700$ ml/min; III) $\Delta p = f(H_{\text{operating}})$, $Q_L = 50$ ml/min; IV) $\Delta p = f(H_{\text{total}})$, $Q_L = 50$ ml/min. The numbers near the points designate the number of the gas lift.

At a liquid input of approximately 50 ml/min, Δp is a linear function of the total height of the lift tube H and increases proportionally to the operating height of the lift, the portion of the tube in which the liquid moves upward with the gas. This can be expressed approximately by the equation

$$\Delta p = (49 + 0.115 Q_L) \cdot H \text{ mm of water column.}$$

The influence of the equivalent diameter of the lift proved to be negligible in the investigated interval.

At a liquid input of 700 ml/min the character of the relationship is similar, but the value of Δp is greater. In this connection the point for the operating height of multipassage apparatus No. 5, in which, apparently, it is also necessary to take into account the length of all of the bends in the gas lift, drops out from the general rule.

The design of the shoe and of the baffle in the separator of the investigated gas lifts have little effect on the hydrodynamic regime.

SUMMARY

1. An investigation of gas lifts of modified design with different diameters and length of the lift tubes, and with a variable number of operating passages and shape of the cross section, revealed that the designed

apparatus permit varying the input ratios of gas and liquid within wide limits independently of each other, and they also permit operating at high linear gas velocities with quite low hydraulic resistances when compared with the usual designs of gas lifts, described in the literature.

2. The optimum gas inputs, at which the hydraulic resistance is at a minimum, while the coefficients of the rate of absorption have their highest values, were determined for the proposed type of gas-lift apparatus.

3. Based on the results obtained with the laboratory models, it is possible to use the construction of the flat-walled gas lift to design equipment having both a high capacity and a high intensity, assuming that the equivalent diameters of the cross sections of the lift tubes can be prorated without impairment of the efficiency.

LITERATURE CITED

- [1] V. M. Ramm, Absorption Processes in the Chemical Industry [In Russian] (Goskhimizdat, 1951).
- [2] M. E. Pozin, I. P. Mukhlenov, E. S. Tumarkina, and É. Ya. Tarat, Foam Methods for the Treatment of Gases and Liquids [In Russian] (Goskhimizdat, 1955).
- [3] M. L. Varlamov, G. A. Manakin, and Ya. I. Starosel'skii, Zhur. Priklad. Khim. 31, 178 (1958) *
- [4] S. N. Ganz and S. B. Kravchinskaya, Zhur. Priklad. Khim. 28, 145 (1955). *
- [5] I. N. Kuz'minykh, Khim. Prom. 4 (1956).
- [6] É. K. Lopatto, Author's Certificate Application No. 39,957, June 24, 1949; Trudy Odesskogo Gosudarst. Univ. 15 (1952).
- [7] A. G. Bol'shakov and G. O. Grigoryan, Nauchn. Zapiski Odesskogo Polytekh. Inst. 2, 1 (1955).
- [8] Ch. N. Gasyuk, Candidatal Dissertation [In Russian] Odessa Polytechnical Institute (1956).
- [9] M. L. Varlamov and Ya. I. Starosel'skii, Zhur. Priklad. Khim. 32, 8, 1716 (1959). *
- [10] Ya. I. Starosel'skii, Candidatal Dissertation [In Russian], Odessa Polytechnical Institute (1958).
- [11] V. G. Bagdasarov, Theory, Design and Operation of Gas Lifts [In Russian] (Gostoptekhizdat, 1947).
- [12] S. F. Shou, Theory and Operation of Gas Lifts [In Russian] (Gostoptekhizdat, 1948).
- [13] N. N. Konstantinov, Collected Works of Tekhratsnefti** [In Russian] (Gostoptekhizdat, 1950), Vol. 2.
- [14] N. M. Murav'ev and A. P. Krylov, Course in the Exploitation of Petroleum and Gas Deposits [In Russian] (Moscow-Leningrad, 1940).

Received July 14, 1958

*Original Russian pagination. See C. B. Translation.

**All-Union Technical Production Office for Efficient Utilization of Petroleum Products.

A STUDY OF THE ABSORPTION OF NITROGEN OXIDES BY SODA SOLUTIONS IN GAS-LIFT EQUIPMENT*

M. L. Varlamov, G. A. Manakin, and Ya. I. Starosel'skii

In this paper we discuss the results of investigating the absorption of nitrogen oxides by mainly dilute soda solutions in gas-lift equipment of modified design.

The absorption of nitrogen oxides by alkaline solutions in equipment of other design has been investigated in a series of papers [1-12].

In industry, the absorption of nitrogen oxides is usually done in mammoth, superficially operating, packed towers, the erection of which involves large capital expense.

An investigation of mass transfer in the absorption of nitrogen oxides and of sulfur dioxide, and also in the carbonation of ammoniacal salt solutions, in gas-lift equipment of conventional design, described in the literature, is given in [13-16]. As had already been mentioned [17], the disadvantages of this type of equipment are high hydraulic resistances and an interdependence of the inputs of gas and liquid entering the apparatus, in which connection the ratio of these inputs can be varied only within narrow limits.

Some new designs of gas-lift equipment, described in the previous communication [17], have been proposed by us, which to a large degree permit eliminating the indicated disadvantages. In the same communication, we have given a diagram of the experimental installation used by us to study the hydrodynamics and absorption of nitrogen oxides by soda solutions.

Our purpose in the present investigation was to establish the effect of such factors as the input of gas mixture, the concentration of nitrogen oxides in the mixture, the ratio of the gas and liquid inputs ($G:L$), and the diameter, height and cross-sectional shape of the lift tubes in the equipment, on the course of the absorption process. The proposed designs of gas-lift equipment permit varying the inputs of gas and liquid within wide limits independently of each other, and they also permit operating at high linear gas velocities.

In the experimental installation, the nitrogen oxides were generated by the addition of sodium nitrite solution to a vessel containing nitrose solution. The nitrogen oxides formed in this manner were then blown out of the vessel with a stream of air and mixed with additional air. The gas mixture of desired composition was then fed into the gas lift. The gas mixtures were analyzed in conventional manner for the amount of nitrogen oxides.

Using evacuated bottles, the one at the inlet side having a capacity of 10 liters, and the one at the exit side of the apparatus, a volume of 20 liters, samples of gas were removed at the same time and the nitrogen oxides were oxidized with hydrogen peroxide. The bottles were shaken periodically for about an hour, and then their contents were titrated with standard caustic solution using methyl red as indicator.

In some of the experiments, we made control determinations of the nitrogen dioxide by drawing a sample of the gas through a Drechsel wash bottle containing potassium iodide solution. The liberated iodine was titrated with sodium thiosulfate solution [9]. The analyses revealed that the degree to which oxidation of the nitrogen

* Communication II in a series of papers on new designs in gas lifts as reaction and absorption apparatus.

oxide in the gas occurred was somewhat greater than 0.6 and varied but slightly from experiment to experiment.

Absorption of the nitrogen oxides in the gas lifts was done using soda solutions with concentrations up to 100 g/liter, which were circulated through the gas lift several times.

According to [1], the effect exerted by the presence of nitrite-nitrate salts in solution on the absorption of nitrogen oxides is quite small, and consequently this parameter was not investigated further.

All of the experiments were run at 18-20°.

To calculate the coefficients of absorption K , we used the Eq. (1)

$$K = \frac{Q}{qf} \ln \frac{C_0}{C} = \frac{Q}{B} \ln \frac{C_0}{C}, \quad (1)$$

where Q is the space velocity of the gas mixture (in m^3/sec), q is the surface of the packing (in m^2/m^3), f is the free space of the packing (in m^3/m^3), C_0 is the initial concentration of nitrogen oxides (in %), and C is the final concentration of nitrogen oxides (in %).

In our case, under intense working conditions, the liquid in the apparatus is found mainly as a thin layer on the walls with wave formation being present. For this reason, the product qf is taken equal to the internal surface area of the lift tube (B).

We will now pass to a discussion of some of the obtained results.

The relation between the degree of absorption of nitrogen oxides by soda solutions in gas-lift apparatus No. 2 and the gas input is shown in Fig. 1. From the graph it follows that the degree of absorption decreases almost linearly with increase in the gas input. In Fig. 2, we have shown the coefficients of absorption for the same experiments.

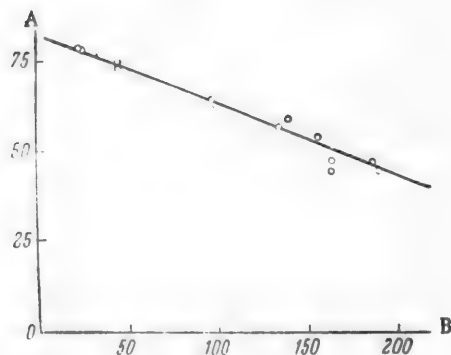


Fig. 1. Relation between the degree of absorption of nitrogen oxides by soda solutions and the gas input for gas lift No. 2. Concentration of nitrogen oxides 2.5-3.5%, degree of NO oxidation $\alpha \approx 0.6$, liquid input 163-194 liters/min. A) Degree of absorption (in %); B) gas input (in liters/min).

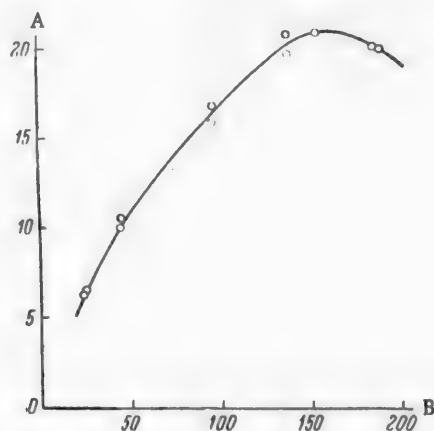


Fig. 2. Relation between the coefficients of absorption K of nitrogen oxides by soda solutions and the gas input in gas-lift apparatus No. 2. Concentration of nitrogen oxides 2.5-3.5%, degree of NO oxidation $\alpha \approx 0.6$, liquid input 163-194 liters/min. A) Value of $K \cdot 10^3$; B) gas input (in liters/min).

From Fig. 2 it can be seen that the absorption coefficients have a limiting value and reach a maximum at a gas input of about 160 liters/min. As follows from the results of studying the hydrodynamics of this gas-lift apparatus [17], such a gas input corresponds to a minimum hydraulic resistance of 80-135 mm of water column, depending on the liquid input.

In Fig. 3, we have shown the relation between the degree of absorption of nitrogen oxides η and the liquid input in the same gas-lift apparatus, maintaining the gas input practically constant and with but slight variation in the nitrogen oxides concentration. If the latter is equal to 1-1.3%, while the liquid input exceeds 50 ml/min, then the degree of absorption depends but slightly on the liquid input in the interval up to 800 ml/min. A similar relationship exists at lower concentrations of nitrogen oxides in the gas, but η proves to be smaller.

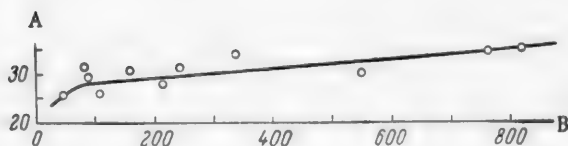


Fig. 3. Relation between the degree of nitrogen oxides absorption and the liquid input in gas lift No. 2. Concentration of nitrogen oxides 1-1.35%, gas input 144 to 152 liters/min. A) Degree of absorption (in %); B) liquid input (in ml/min).

ranging from 39 to 45 liters/min and liquid inputs ranging from 400 to 450 ml/min. From the graph, it follows that increasing the nitrogen oxides concentration up to 1.5-2% leads to a substantial increase in the degree of absorption. Further increase in the concentration of oxides has little effect on the degree of absorption. At low gas inputs, the efficiency in this gas-lift apparatus reaches approximately 75%.

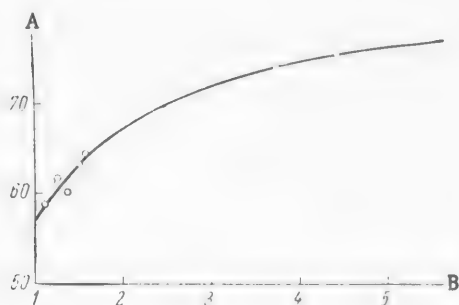


Fig. 4. Relation between the degree of absorption of nitrogen oxides and their concentration in gas lift No. 3. Gas input 39-45 liters/min, liquid input 400-455 ml/min. A) Degree of absorption (in %); B) concentration of nitrogen oxides (in %).

Independent of the nitrogen oxides concentration in the gas, η drops sharply when the input of liquid is less than 50 ml/min, which is apparently due to an insufficiency of soda in the surface layer of the liquid for neutralizing the acid formed in the absorption of the nitrogen oxides. The ratio of the inputs of gas and liquid (G:L) in these experiments reached 3000-12,000.

In Fig. 4, we have shown the relation between the degree of absorption of nitrogen oxides in gas lift No. 3 and their concentration at gas inputs

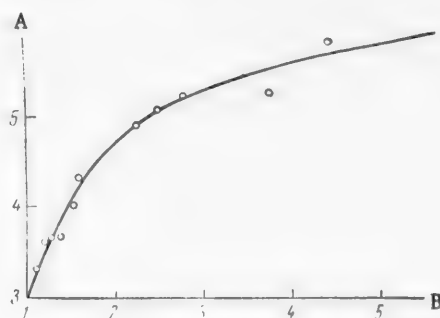


Fig. 5. Relation between absorption coefficient K and nitrogen oxides concentration in gas lift No. 3. Gas input 39-45 liters/min, liquid input 400-455 ml/min. A) Value of $K \cdot 10^3$; B) concentration of nitrogen oxides (in %).

In Fig. 5, we have shown the relation between the absorption coefficient of nitrogen oxides in gas lift No. 3 and their concentration for the same experiments. As follows from the graph, the absorption coefficient K is approximately proportional to the square root of the initial nitrogen oxides concentration. Closely similar results were obtained with the other gas-lift equipment investigated by us.

In Fig. 6, we have shown the relation between the absorption coefficient of nitrogen oxides and their concentration in the different types of gas-lift equipment described above.

All of the gas lifts were investigated in the region of their minimum hydraulic resistance.

Curve 1 corresponds to gas lift No. 2 ($d_{\text{lift}} = 17$ mm, $H_{\text{lift}} = 1.8$ m). The gas input rate was 146-164 liters/min, and that of the liquid was 19-820 ml/min. Curve 2 corresponds to gas lift No. 3 ($d_{\text{lift}} = 17$ mm, $H_{\text{lift}} = 3.44$ m). The gas input rate was 137-172 liters/min, and that of the liquid ranged from 130-761 ml/min. Curve 3 corresponds to gas lift No. 4 ($d_{\text{lift}} = 17$ mm, $H_{\text{lift}} = 6.22$ m, and the apparatus has two operating passages in the lift tube). The gas input rate was 146-175 liters/min, and that of the liquid ranged from 30 to 255 ml/min.

Curve 4 corresponds to gas lift No. 5 (diameter equivalent to the rectangular cross section of the lift tube = 0.009 m, $H_{\text{lift}} = 4.95$ m, number of operating passages in the lift = 7). In apparatus Nos. 2, 3, and 4, the gas rate in the lift tube ranged from 10 to 13 m/sec, while in apparatus No. 5 it ranged from 14.7 to 18.6 m/sec.

From the different graphs, it follows that the general character of the relation between K and the nitrogen oxides concentration is the same for all of the different types of gas lifts investigated. Raising the nitrogen oxides concentration increases the absorption coefficient, in which connection the greatest increase is observed at low concentrations of nitrogen oxides.

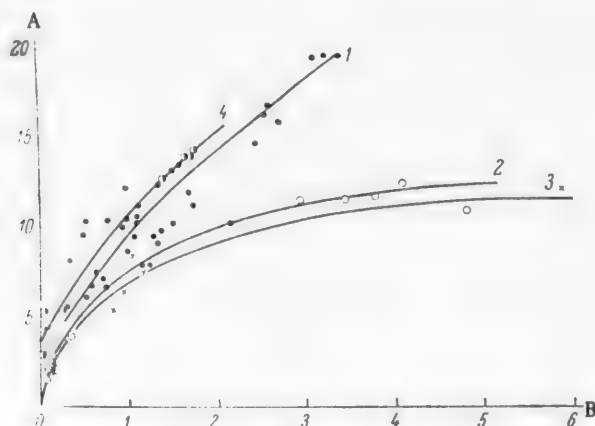


Fig. 6. Comparison of coefficients of absorption of nitrogen oxides by soda solutions for different gas-lift equipment as a function of the nitrogen oxides concentration in the gas. A) Value of $K \cdot 10^3$; B) concentration of nitrogen oxides in the gas (in %). Designation of the curves is given in the text.

The higher values of K are observed in apparatus Nos. 2 and 5, which have a short height of the operating passage in the lift tube. For apparatus Nos. 3 and 4, the absorption coefficient at high values of nitrogen oxides concentration is much higher than for the other two pieces of equipment. Apparatus Nos. 3 and 4 have a height exceeding 3 m for the operating passage in the lift tube, whereas for apparatus No. 2 this height is 1.8 m, and for No. 5 it is 0.7 m.

This phenomenon may be associated with the influence of the entrant effect or it may be due to disturbance of the normal operation of the gas lift when the lift tubes are exceedingly long. It is also possible that the higher value obtained in apparatus No. 5 for the absorption coefficients is due to the fact that in this apparatus we used a flat cross section of the lift tube, which permitted reducing the equivalent diameter of the cross section with the retention of both a comparatively high productive output for the apparatus and a high gas velocity.

We will not present a detailed comparison of our results with those obtained using conventional gas-lift equipment, since the operating conditions using the newly designed gas lifts are quite different from those employed in the conventional equipment, and, in addition, in our equipment, the absorption coefficients were calculated on the basis of per unit of internal surface of the lift tube, and not on the basis of per unit volume. Calculation reveals that in the proposed designs of gas lifts the absorption coefficients are much higher than for the case of packed towers and exceed them by a factor of 100.

SUMMARY

1. The absorption of nitrogen oxides by soda solutions was investigated in some newly designed gas-lift equipment as a function of the height, diameter, and cross-sectional shape of the lift tube, the concentration of nitrogen oxides, and the gas and liquid inputs.

2. The proposed designs of gas-lift equipment possess a higher intensity and smaller hydraulic resistances than is true of the conventional gas-lift equipment described in the literature.

3. The experimental data obtained on the absorption of nitrogen oxides in the newly designed equipment represent practical interest for the purification of the waste gases from nitric acid and sulfuric acid plants, especially if these gases are vented under pressure, which can be utilized in operating the gas lifts.

LITERATURE CITED

- [1] V. I. Atroshchenko and S. I. Kargin, The Technology of Nitric Acid [In Russian] (Goskhimizdat, 1949).
- [2] I. N. Kuz'minykh, E. P. Aigina, and M. Babushkina, *Khim. Prom.* 8 (1953).
- [3] N. M. Zhavoronkov, et al., *Zhur. Khim. Prom.* 7, 35 (1955).
- [4] V. I. Atroshchenko, *Zhur. Priklad. Khim.* 12, 167 (1939); 13, 6, (1940); 25, 11, 1143 (1952).*
- [5] Z. S. Perel'man and L. Kantorovich, *Zhur. Priklad. Khim.* 17, 6, 3 (1940).
- [6] I. N. Kuz'minykh, *Khim. Prom.* (1956), 234.
- [7] V. E. Gorfunkel and Ya. P. Kil'man, *Trudy Gosudarst. Inst. Azot. Prom.* 5 (1956).
- [8] Transactions of Conference at NIIOGAZ** on the Removal of Nitrogen Oxides from Waste Gases [In Russian] (1956).
- [9] N. M. Zhavoronkov, S. I. Babkov, Yu. M. Martynov, and G. N. Chernykh, *Khim. Prom.* (1954), 419.
- [10] M. L. Varlamov, G. A. Manakin, and Ya. I. Starosel'skii, *Zhur. Priklad. Khim.* 31, 178 (1958).*
- [11] M. E. Pozin, B. A. Kopylov, and G. V. Bel'chenko, *Trudy Leningrad. Tekhnol. Inst. im. Lensovet* 35 (1956).
- [12] S. N. Ganz and S. B. Kravchinskaya, *Zhur. Priklad. Khim.* 28, 145 (1955).*
- [13] A. G. Bol'shakov and G. O. Grigoryan, *Nauchn. Zapiski Odesskogo Polytekh. Inst.* 2, 1 (1955).
- [14] G. N. Gasyuk, *Candidatal Dissertation* [In Russian], Odessa Polytechnical Institute (1956).
- [15] M. L. Varlamov and Ya. I. Starosel'skii, *Zhur. Priklad. Khim.* 32, 8, 1716 (1959).*
- [16] É. K. Lopatto and L. I. Aleksandrova, *Trudy Odesskogo Gosudarst. Univ.* 15 (1952).
- [17] M. L. Varlamov, G. A. Manakin, and Ya. I. Starosel'skii, *Zhur. Priklad. Khim.* 32, 11, 2436 (1959).

Received March 9, 1959

*Original Russian pagination. See C. B. Translation.

**State Scientific Research Institute of Gas Purification for Industry and Sanitation.

CONVERSION OF ORGANIC SULFUR COMPOUNDS ON COBALT-MOLYBDENUM CATALYST IN GAS PURIFICATION

N. I. Brodskaya and V. P. Teodorovich

All-Union Scientific Research Institute of Petrochemical Processes

Organic sulfur compounds present in coal gas include thiophene, carbon disulfide and carbonyl sulfide. A possible method for removing these impurities from the gas is their conversion on catalysts. The thus-obtained hydrogen sulfide is then easily removed by conventional techniques.

It is indicated in the literature that thiophene is converted with the greatest difficulty. However, thermodynamic data on the hydrogenation of organic sulfur compounds are absent in the literature. It seemed of interest to us to make an experimental study of the conversion of the indicated compounds on cobalt molybdenum catalyst and then evaluate the obtained results by calculating thermodynamically the free energies of the reactions for the hydrogenation of thiophene, carbon disulfide and carbonyl sulfide.

EXPERIMENTAL

The experiments were run in the following manner: 15-20 ml of a cobalt-molybdenum catalyst [1] was charged into a U-shaped tube, which served as the reactor. The reactor was placed in a saltpeter bath, which was electrically heated to the desired temperature. Gas from the line was passed through absorbers to remove hydrogen sulfide and ammonia, then through a gas meter, and into the reactor. In the reactor the organic sulfur compounds were converted to hydrogen sulfide, which was then absorbed in an absorber containing cadmium chloride. The thus-purified gas was then burned to determine the amount of organic sulfur. The total amount of sulfur remaining in the gas was determined as usual by titration of the hydrogen peroxide solution, which absorbs the combustion products, with alkali. The total amount of sulfur in the line gas was determined at the same time.

Two methods were used to determine the total sulfur and the group composition of the organic sulfur compounds: the combustion method and the gravimetric method described by Avdeeva [2, 3].

The two methods gave good agreement for the total amount of carbonyl sulfide and carbon disulfide in the gas, but the results obtained by the first method for carbonyl sulfide alone were somewhat high, which was probably due to the fact that a part of the carbon disulfide failed to be absorbed by the oil and escaped with the gas, destined for combustion in order to determine the amount of carbonyl sulfide.

As a result, it is more correct to speak of the total amount of carbonyl sulfide and carbon disulfide in the gas, which by both methods averaged about 75-80% of the total amount of organic sulfur in the gas (Table 1).

In running the experiments, both the temperature in the reactor and the space velocity of the gas were varied.

The results obtained in our experiments are summarized in Table 2. The obtained data reveal that raising the temperature leads to a substantial increase in the degree of gas purification.

TABLE 1

Group Composition of Organic Sulfur Compounds in the Gas From the Leningrad Coke-Gas Plant *

Method	Analysis No.	Mercaptans	Thiophene		CS ₂		COS		Total sulfur g/100 cu m	COS + CS ₂ (in %)
			in g/100 cu m	in %	in g/100 cu m	in %	in g/100 cu m	in %		
1	1	None	2.38	22	3.18	29.5	5.24	48.5	10.8	78.0
	2		1.30	10	3.00	23.6	8.40	56.2	12.7	79.8
2	3	—	—	—	5.2	38.5	5.3	38.9	13.6	77.1
	4	—	—	—	5.9	45.5	3.5	27.0	12.95	72.5
	5	—	—	—	8.9	67.0	1.0	7.5	13.85	74.5

* The analysis results show some variation, since the analyses were run on different days, and the composition of the illuminating gas was not entirely constant in respect to the amount of organic sulfur compounds.

TABLE 2

Degree of Gas Purification as a Function of the Temperature and the Space Velocity

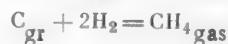
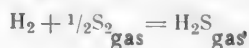
Temperature (in °C)	Space velocity (volume of gas/volume of catalyst per hr)	Contact time (in sec)	Amount of sulfur in gas (in g/100 cu m)		Degree of purification (in %)
			Before purification	After purification	
500	710	5.1	10.7	2.72	74.8
	700	5.1	11.7	2.24	80.9
	675	5.3	12.0	2.56	78.7
	470	7.6	13.3	2.61	80.4
	430	8.4	12.1	2.18	82.0
470	410	8.8	13.1	2.04	84.4
	860	4.2	11.8	2.81	76.2
	1500	2.4	12.65	3.75	70.4
430	850	4.2	12.2	2.8	77.4
	710	5.1	10.8	2.66	75.6
	700	5.1	13.1	3.0	77.4
	1600	2.2	12.5	3.85	69.0
400	1450	2.4	14.5	4.13	71.6
	1000	3.6	13.2	2.7	79.7
	1000	3.6	12.1	4.0	66.7
	1000	3.6	11.7	3.7	68.7
	960	3.8	13.9	3.7	73.5
	800	4.5	12.5	3.7	70.2
	800	4.5	15.0	5.0	66.2
	750	4.8	15.0	4.6	69.4
	750	4.8	12.6	4.0	67.9
	670	5.4	13.3	3.0	77.5
370	510	7.1	12.2	3.3	72.9
	460	7.9	10.8	3.1	71.6
	1200	3.0	12.7	6.3	50.5
	1000	3.6	12.5	5.0	59.8
	850	4.3	13.4	5.0	62.8
310	310	11.6	11.8	3.3	72.0
	320	11.6	12.55	3.8	67.7
	740	4.9	13.1	5.6	57.2

In discussing the obtained results, it is necessary to point out that the gas was not purified from any one certain chemical compound, as, for example, is the case when hydrogen sulfide is removed from the gas, but instead it was separated from a mixture of sundry organic sulfur compounds. It is fully known that such compounds as thiophene, carbon disulfide and carbonyl sulfide differ sharply from each other in chemical stability and therefore in their hydrogenation rate, and consequently, the purification conditions for the individual compounds will be substantially different.

For comparison, we will make some calculations.

The heat of formation of carbon disulfide from graphite and gaseous sulfur (taking into account the heat for the transition of sulfur from the rhombic to the gaseous state) is 3600 cal [4]: $C_{gr} + S_{2gas} = CS_{2gas}$; $\Delta H = -3600$ cal. The heat of formation of methane [5], $C_{gr} + 2H_2 = CH_{4gas}$, is $\Delta H_{298} = -18,070$ cal. The heat of formation of H_2S [6]: $H_2 + \frac{1}{2} S_2 gas = H_2S gas$, is $\Delta H = -19,610$ cal.

Consequently, based on the existing data relative to the heats of formation of the compounds



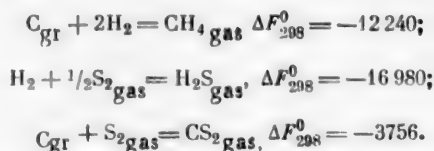
it is possible to calculate the heat of the reaction



At 25° C it will be

$$\Delta H_{\text{reaction}} = 2\Delta H_{\text{H}_2\text{S}} + H_{\text{CH}_4} - H_{\text{CS}_2} = -2 \times \\ \times 19\,610 - 18\,070 + 3600 = -53\,690 \text{ cal}$$

Making use of the free energy values for CH_4 , H_2S and CS_2 , the change in the free energy for reaction (1) can be determined for different temperatures:



In Table 3 we have given the free energies of the reacting gases, CH_4 , H_2S and CS_2 , and the free energies of reaction (1) at 25 and 500° C, calculated from the data given above. The values of the reaction constants for (1) were determined using the thermodynamic equation:

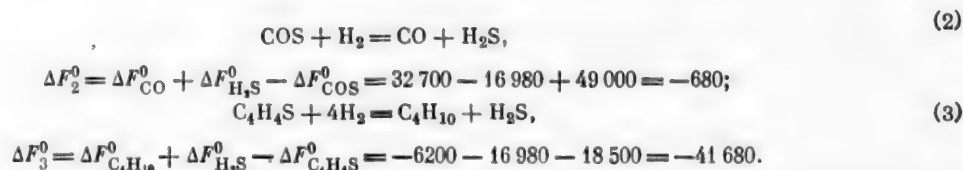
$$\begin{aligned} \Delta F_T^0 &= -RT \ln K, \\ \lg K &= \lg \frac{P_{\text{CH}_4} \cdot P_{\text{H}_2\text{S}}^2}{P_{\text{CS}_2} \cdot P_{\text{H}_2}^4} = -\frac{\Delta F^0}{4.571 T}. \end{aligned}$$

The large numerical values of the equilibrium constants indicate that thermodynamically the given reaction in the temperature range 298-773° K should go to completion from left to right. Lowering the temperature favors progress of this reaction, but the reaction rate at low temperatures is very slow, and consequently, only the use of a catalyst makes it possible to run this reaction at a sufficiently fast rate at low temperatures.

TABLE 3
Equilibrium Reaction $\text{CS}_2 + 4\text{H}_2 = \text{CH}_4 + 2\text{H}_2\text{S}$

(in °K)	t(in °C)	$\Delta F_{\text{CS}_2}^0$	$\Delta F_{\text{H}_2\text{S}}^0$	$\Delta F_{\text{CH}_4}^0$	$\Delta F_{\text{reaction}}^0$	lg K	K
298	25	-3750	-16980	-12240	-42450	31.08	$1.2 \cdot 10^{31}$
773	500	-4470	-12278	-1679	-20765	5.81	$6.46 \cdot 10^5$

Similar calculations for the hydrogenation of carbonyl sulfide and thiophene gave the following values for the free energies:



The free energy values obtained for the examined reactions indicate that all three processes should go spontaneously. However, the hydrogenation of carbonyl sulfide goes with considerably greater difficulty, since the free energy value for reaction (2) is very small.

This conclusion is supported by the experimental data. From Table 4 it can be seen that within the experimental error the amount of carbonyl sulfide in the gas coincides with the amount of sulfur compounds remaining in the gas after purification, i.e., on the average it represents about 3 g/100 m³.

TABLE 4
Amount of Carbonyl Sulfide in Purified Gas

Date	CO _S (in g/100 m ³)	Total amount of sulfur in purified gas (in g/100 m ³)
June 14	2.7	2.8
June 15	2.8	3.3
June 16	2.9	3.3

represents carbonyl sulfide, which is hydrogenated with the greatest difficulty and consequently, remains in the gas under the given conditions.

To verify the above, we determined the group composition of the gas after its passage through the reactor. The experiments revealed that carbon disulfide is practically absent in the purified gas, while the amount of carbonyl sulfide ranges from 2.9 to 2.7 g per 100 m³ of gas. On the corresponding days, the amount of sulfur remaining in the purified gas ranged from 2.8 to 3.3 g per 100 m³ (Table 4).

As a result, it may be concluded that all of the sulfur remaining in the gas after purification

SUMMARY

1. Determination of the group composition of the organic sulfur compounds in the gas from the Leningrad Coke and Gas Plant revealed that mercaptans are absent in the gas, that the thiophene content is 20-25%, and that the sum of the carbon disulfide and carbonyl sulfide content is 75-80% of the total amount of sulfur in the gas.

2. The suitability of using a cobalt-molybdenum catalyst to remove organic sulfur compounds from the gas was examined. It was shown that the organic sulfur remaining in the gas after purification is carbonyl sulfide. This was confirmed by making a thermodynamic calculation of the free energies for the reactions of hydrogenating thiophene, carbon disulfide and carbonyl sulfide.

LITERATURE CITED

- [1] Gas J. 285, 11/1 (1956).
- [2] A. V. Avdeeva and M. A. Lyudkovskaya, Zhur. Khim. Prom. 14, 824 (1937).
- [3] A. V. Avdeeva, Gas Sulfur (Goskhimizdat, 1950), p. 93 [in Russian].
- [4] G. N. Lewis and M. Randall, Chemical Thermodynamics (Russian translation) (ONTI, 1936), p. 480.
- [5] F. D. Rossini, Bur. Standards J. Research 6, 49 (1931).
- [6] A. R. Gordon and C. Barnes, J. Chem. Phys. 1, 297 (1933).

Received February 4, 1959

USE OF THE ION-EXCHANGE METHOD FOR THE REMOVAL OF IMPURITIES FROM ARSENIC

G. A. Kataev, A. G. Grigor'eva, and L. N. Rozanova

The specifications for the arsenic used in the preparation and alloying of different semiconductors call for a very high purity. Together with this, the existing methods for the purification of arsenic are either tedious or not very efficient as regards the removal of micro amounts of impurities. The ion-exchange method possesses great promise for the purification of metals. It is indicated in [1] that the chromatographic method may be used successfully to purify zirconium, and also to separate the rare-earth and radioactive elements.

We made an attempt to use the ion-exchange method in the purification of arsenic. The impurities usually present in arsenic are iron, copper, antimony and bismuth, and in trace amounts, the impurities of many other elements.

In essence our method consists of passing a solution of arsenic as arsenic acid through a column filled with the hydrogen form of a cationite. Here, the arsenic acid passes into the filtrate, and then metallic arsenic can be isolated from the arsenic solution by the use of a suitable reducing agent. The cations of the impurities are retained in the column. In order to find a suitable method for the purification of arsenic, it was necessary to ascertain the order and find the conditions for the most complete adsorption of the contaminating ions from the arsenic solution on the cationite, study the conditions for regeneration of the cationite, and find the conditions for the most efficient method of isolating arsenic from the solution.

EXPERIMENTAL

We used KU-2 resin as the cationite. The resin was pulverized first. The fraction with a grain size of 0.25-0.50 mm was repeatedly digested with pure concentrated hydrochloric acid (5 N) on the water bath to remove various contaminants (especially iron).

The glass column used for the adsorbent had an internal diameter of 1 cm and a height of 60-70 cm. A glass filter was sealed in the bottom of the column, which also served as a support for the cationite.

The column was filled with the resin in the usual manner; the height of the resin layer was 30-45 cm. To obtain the hydrogen form, the cation-exchange resin was washed with hydrochloric acid at a rate of 1 ml/min, after which the excess acid was removed by washing with distilled water (until neutral). Both the polarographic and the photocolorimetric methods were used to determine the contaminating ions.

A visual PV-5 polarograph was used for the polarographic determinations. A solution composed of sodium potassium tartrate (0.5 M) and ammonia (0.5 M) was used as the support, on which the joint determination of many contaminating ions (by groups) proved possible.

The half-wave potentials on this support relative to the saturated calomel electrode are (in v): copper (II) -0.38 (first wave) and -0.54 (second wave); nickel (II) -1.19; zinc -1.40; lead -0.72; iron -1.62; cadmium -0.81; antimony (III) -1.18; bismuth (II) -1.0; cobalt (III) -1.40.

To determine copper and iron we had worked out [2] a polarographic determination method involving their advance separation from arsenic by the ion-exchange technique.

For the photocolorimetric determination of antimony, copper and iron, we used the methods worked out by Kristaleva. Brilliant Green was used to determine antimony. The method is based on the formation in hydrochloric acid medium of a complex between the complex anion of antimony (V) chloride and the cation of Brilliant Green, which complex can be extracted with benzene (toluene, xylene) to yield a blue-green extract.

The iron was determined using o-phenanthroline [3]; the method permits running the determination in the presence of arsenic and a number of other impurities.

Copper was determined by the diethyl dithiocarbamate method, which also permits running the determination in arsenic solution. A FEK-M photocolorimeter was used to make the readings.

Adsorption of some ions on KU-2 cationite and regeneration of column samples. To determine the order of adsorption on cationite KU-2 and evolve the conditions for the most complete adsorption of the separate ions we used solutions of the appropriate metal salts, prepared by dissolving the metals in acids or by using c. p. salts.

The ionic concentration in the starting solution was of the order of 10^{-3} - 10^{-4} molar. The first experiments were run in the absence of arsenic. The solution of salts with a known pH was passed through the cationite at a definite rate. The pH values were varied from 1.0 to 3.0, while the rate was varied from 0.5 to 5.0 ml/min. The original solution, the filtrate after passage of the original solution, and the filtrate after elution of the ions were all subjected to polarographic analysis. All of the ions were subdivided into the following groups (for analysis convenience): zinc (II), copper (II), nickel (II) - group I; lead (II) and iron (III) - group II; zinc (II), nickel (II), lead (II) and copper - group III; lead (II), nickel (II) and antimony (III) - group IV; cadmium (II), zinc (II), cobalt (II) and nickel (II) - group V. All of these ions give well-defined waves on a support composed of a mixture of 0.5 M sodium potassium tartrate solution and 0.5 M ammonia solution, with the half-wave potentials indicated above.

In group III, in the presence of chloride ion, the lead half-wave potential (-0.72) shifts toward the half-wave potential of copper (-0.54). Since the heights of both the first and second waves of copper are equal on this support, the copper concentration was determined from the first wave, while the lead concentration was determined from the total lead wave and the second copper wave after subtracting the first copper wave.

In group V the half-wave potentials of cobalt and zinc lie close to each other. These elements were determined from the total wave.

TABLE 1
Adsorption Efficiency of Some Ions on Cationite KU-2

Analyzed ions	Found (in mg)	
	in original solution	in filtrate after elution with 3N HCl
Cu ⁺²	16.00	16.0
Ni ⁺²	16.00	15.5
Zn ⁺²	8.13	8.10
Pb ⁺²	10.35	10.30
Fe ⁺²	13.20	13.20
In the presence of arsenic acid		
Cu ⁺²	0.37	0.36
Fe ⁺³	2.38	2.36

To determine the extent to which the ions of the impurities are adsorbed, we passed a solution of the salts (by groups) through the column (in 250 ml portions). The adsorbed ions were eluted with 50 ml of 3 N hydrochloric acid solution. For analysis we took 10 ml aliquots of the solution.

Based on the polarographic-analysis results, we have given in Table 1 the ion-exchange results obtained under the optimum conditions: pH = 1.5 (controlled either by using methyl violet or by measuring with a pH-meter), passage rate 0.5 ml/min, column diameter 1 cm, and room temperature.

The polarographic analysis was run with a galvanometer sensitivity of 1/1000 (original solution, elution) and 1/500 (filtrate after passage of original solution).

As can be seen from Table 1, even a single filtration under the described conditions leads to a good purification of the solution.

It should be mentioned that a strict control of the pH of the medium is necessary, since deviations of the pH from the indicated values lead to the passing through of individual ions (especially iron).

In most cases, hydrochloric acid was used to elute the ions, which at the same time functioned to regenerate the cationite for the next cycle. It proved that 3 N hydrochloric acid was the most satisfactory for this purpose (other concentrations were also tested). During elution the filtrate was collected in separate beakers (up to 5 beakers with 10 ml in each beaker).

Polarographic analysis of the separate filtrate portions revealed the order in which the different ions were eluted, and consequently permitted us to compose the approximate order in which the ions are desorbed on cationite KU-2. This order is similar to the adsorption orders obtained by other authors [4] on different resins of this type:



After this series of experiments, we checked the possibility of separating the foreign ions from solutions containing arsenic (V). The analyses were run using the polarographic technique. The data for copper and iron are given in Table 1. Elution in this case was run using sodium potassium tartrate solution, to which ammonia solution had been added [2].

As the data in the table show, arsenic does not change the adsorption results: the amounts of impurities introduced in the original solution coincide with those eluted from the column.

Removal of impurities from technical arsenic. The original arsenic solution was prepared by dissolving technical arsenic in a little concentrated nitric acid with moderate heating (on the water bath). Here the arsenic, on going into solution, is oxidized to arsenic acid. To remove excess nitric acid, the solution was evaporated, and then it was diluted with distilled water. Some difficultly soluble hydroxides and basic salts deposited when the water was added. The precipitate was filtered, and the filtrate, containing arsenic as arsenic acid, was brought to the desired acidity (pH = 1.5, to the blue color of methyl violet, which was added to the solution). The obtained solution (containing about 17 g of arsenic per liter) was passed through the column, containing cationite KU-2 in the hydrogen form, at a rate of 0.5 ml/min. The contaminating ions (iron, copper, zinc, lead) are adsorbed on the cationite, while the arsenic acid passes into the filtrate.

TABLE 2
Amount of Some Impurities in Technical Arsenic and in the
Filtrate After Passage Through a Column Containing
Cationite KU-2

Filtrate	Contaminating ions (in % on arsenic)		
	Antimony	Copper*	Iron*
After the first passage	0.0390	Not found	0.034
After the second passage	0.0037	Not found	0.003
Amount of impurities in technical arsenic	0.172	0.008	0.100

* The polarographic method was used to make the determinations.

To appraise the efficiency of this method for the removal of impurities from arsenic, we present in Table 2 the results obtained in the photocolorimetric analysis of the filtrate for the amount of antimony, copper and iron after one and two passes through the cationite.

Lead, zinc, nickel and other ions were not found in the filtrate even after the first passage (polarographic analysis and sensitive color reactions).

The amount of impurities decreases by approximately one order after each alternate passage. Consequently, the process should be repeated 3-4 times to achieve the desired purity of the arsenic solution.

Isolation of arsenic from solution. To isolate the arsenic from solution we used the technique of reducing it with potassium hypophosphite in hydrochloric acid medium [5].

The filtrate obtained from the column was evaporated on the water bath, and then it was treated with concentrated hydrochloric acid (d 1.19) until the content of the latter was 19-20 wt. %.

Then a solution of potassium hypophosphite (2-4 times the theoretical amount) was added gradually and with vigorous stirring. After this the solution was heated to the boil and boiled for 2-3 hours until the precipitate had coagulated completely.

The precipitate was filtered and washed well with hydrochloric acid (1:3), after which it was washed with hot water to remove excess reducing agent and hydrochloric acid. The arsenic obtained in this manner was dried in an oven at 70°.

SUMMARY

1. In the described ion-exchange process arsenic remains in solution as arsenic acid and is not adsorbed by the resin, whereas the impurities, present in the form of positive ions, are removed.
2. Some polarographic and photocolorimetric analysis data are given in the paper, illustrating the efficiency with which iron, copper, antimony, zinc, lead and nickel are removed from arsenic.
3. Based on the polarographic analysis of the filtrate obtained in the elution process, it was concluded that the adsorption order of the contaminating ions on cationite KU-2 is the same as that given in the literature for the adsorption of the same ions on ionites of the KU-2 type.

LITERATURE CITED

- [1] Chromatographic Method of Separating Ions. Collection of Papers [In Russian] (IL, Moscow, 1949); Ion Exchange. Collection of Papers [In Russian] (IL, Moscow, 1951).
- [2] L. N. Rozanova and G. A. Kataev, Zhur. Priklad. Khim. 32, 11, 2576 (1959). *
- [3] E. B. Sandell, Colorimetric Determination of Traces of Metals (Russian translation) (Goskhimizdat, 1949).
- [4] Khim. i Khim. Tekhn. 12, 182 (1953).
- [5] S. Yu. Fainberg, Analysis of Ores of Nonferrous Metals [In Russian] (Metallurgical Press, 1953).

Received November 13, 1958

*Original Russian pagination. See C. B. Translation.

CHEMISTRY OF THE ACID AUTOCLAVE LEACHING OF THE MONOSULFIDES OF NICKEL, COBALT, AND IRON

G. N. Dobrokhotov

Design and Scientific Research Institute of the Nickel-Cobalt and Tin Industry

The existing explanations regarding the chemistry of the acid autoclave leaching of the monosulfides of nickel, cobalt and iron reduce to two principal versions. The first of them assumes a surface oxidation of the minerals by dissolved (molecular) oxygen [1-4], while the second assumes an oxidation of the sulfides via the ionic compounds present in solution [5-7]. The version of a topochemical oxidation is supported by the large decreases in the thermodynamic potentials of the reactions and by the properties possessed by the sulfides of Group VIII metals to catalytically (irreversibly) adsorb large amounts of oxygen [8].

The version of oxidation via ionic compounds includes the stage of a surface solution of the sulfides and the stage of an oxidation and hydrolysis of the products formed. It is probable that the reactions in this case are:



In this paper we describe the results obtained in investigating the conditions for the progress of reactions (1) - (6) in the autoclave leaching of nickel mattes.

As is known, the solubility of sulfides in water solutions is determined by the product of the activities (S), which in respect to reaction (1) is expressed by the equation

$$S_{\text{MeS}} = a_{\text{Me}^{++}} \cdot a_{\text{S}^{--}} = a_{\text{Me}^{++}} \cdot \frac{K \cdot a_{\text{H}_2\text{S}}}{a_{\text{H}^+}^2}, \quad (7)$$

where K is the complete ionization constant of hydrogen sulfide. Reorganization of Eq. (7) gives

$$\text{pH} = \frac{\lg S_{\text{MeS}}}{2} + \frac{\text{p}K}{2} + \frac{\text{p}a_{\text{H}_2\text{S}}}{2} - \frac{\lg a_{\text{Me}^{++}}}{2}. \quad (8)$$

According to the recent and most accurate data [9], under standard conditions $\text{p}K_{\text{H}_2\text{S}} = -\log K_{\text{H}_2\text{S}} = 19.88$, while the change in the heat content for the ionization of hydrogen sulfide is $\Delta H^0 = 17.2$ kcal/mole. From this

it follows that at 115°, $pK_{115} = 16.95$. The solubility of hydrogen sulfide in salt solutions [10] and its activity [11] both change but slightly with change in the concentration of extraneous ions. For this reason, it is possible to write with a sufficient degree of accuracy, $pa_{H_2S} = -\log a_{H_2S} = -\log C_{H_2S}$. From this, according to [12], pa_{H_2S} at 25 and 115° is, respectively, equal to $0.990 - \log P_{H_2S}$ and $1.465 - \log P_{H_2S}$, where P_{H_2S} is the H_2S pressure in absolute atmospheres. Substituting the values of pK and pa_{H_2S} in Eq. (8) gives:

$$pH_{25} = 10.44 + \frac{\lg S_{25}}{2} - \frac{\lg P_{H_2S}}{2} - \frac{\lg a_{Me^{++}}}{2}, \quad (9a)$$

$$pH_{115} = 9.21 + \frac{\lg S_{115}}{2} - \frac{\lg P_{H_2S}}{2} - \frac{\lg a_{Me^{++}}}{2}. \quad (9b)$$

Literature data regarding the values of S for NiS , CoS , and FeS are usually based on direct analytical determinations of the solubility of sulfides in acid solutions. According to these data, the monosulfides of nickel, cobalt and iron are usually ascribed several crystalline modifications each, which is erroneous. Thus, for example, the existence of the α -, β -, γ -, and β^* -form, each of a different solubility, is mentioned for nickel sulfide. Actually, the indicated modifications are the compounds $Ni(SH)_2$, $Ni(OH)(SH)$, and NiS [13-15]. The first is formed from alkaline solutions and is amorphous, the second is formed from neutral or weakly acid solutions and is slightly crystalline, while the third is an equilibrium form in acid solutions and corresponds to native crystalline millerite. β^* - NiS is a high-temperature modification formed at 390° and above [15].

A more accurate method for the determination of S was proposed by A. F. Kapustinskii [16]. According to this method, the product of the activities S is regarded as being an ordinary thermodynamic constant, linked with the change in the standard isobaric thermodynamic potential ΔZ^0 and the standard heat content ΔH^0 of the ionization reaction by the equations:

$$\Delta Z^0 = -RT \ln S = -4.575 \cdot T \cdot \lg S, \quad (10)$$

$$\frac{\lg S_2}{\lg S_1} = \frac{\Delta H^0}{4.575} \left(\frac{1}{T_1} - \frac{1}{T_2} \right). \quad (11)$$

The thermodynamic functions ΔZ^0 and ΔH^0 in Eqs. (10) and (11) can be determined with a high degree of accuracy at the present time. The most reliable values of the constants needed to calculate ΔZ^0 and ΔH^0 for the ionization of monosulfides are summarized in Table 1.

The results of determining S are given in Table 2.

TABLE 1

Values of Thermodynamic Potentials ΔZ^0 and Heat Contents ΔH^0 Under Standard Conditions

Substance	ΔZ^0 (in kcal/mole)	ΔH^0 (in kcal/mole)	Substance	ΔZ^0 (in kcal/mole)	ΔH^0 (in kcal/mole)
Ni^{++}	-11.5	-15.2	SO_4^{--}	-177.3	-216.9
Co^{++}	-12.8	-16.5	NiS	-20.6	-20.2
Fe^{++}	-20.3	-20.6	CoS	-21.7	-21.1
S^{--}	-20.6	7.8	FeS	-22.7	-23.0

* At a temperature of 119° and above, the elemental sulfur that is liberated in the autoclave leaching becomes molten and dissolves a part of the unreacted sulfides. For this reason, it is usually recommended to run the autoclave treatment of sulfides at temperatures lower than 119°. In our work we selected a temperature of 115°.

TABLE 2
Values of $pS = -\log S$ for Monosulfides
of Nickel, Cobalt and Iron

Formula of sulfide	25°	115°
NiS	21.75	19.57
CoS	21.62	19.52
FeS	16.86	15.12

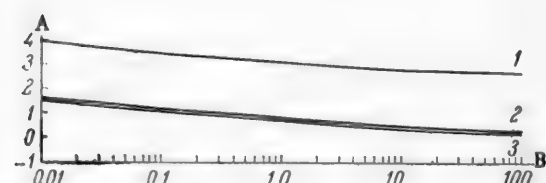


Fig. 1. Value of the pH for the solution (precipitation) of the monosulfides of nickel, cobalt, and iron at 25° and $P_{H_2S} = 1$ atm. A) Hydrogen ion concentration, pH; B) metal concentration (in g/liter). 1) FeS; 2) CoS; 3) NiS.

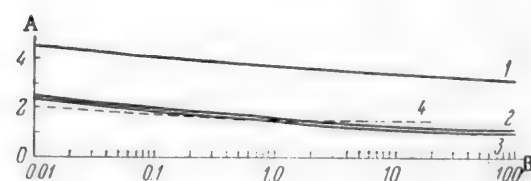


Fig. 2. Value of the pH for the solution (precipitation) of the monosulfides of nickel, cobalt and iron at 115° and $P_{H_2S} = 0.01$ atm. A) Hydrogen ion concentration, pH; B) metal concentration (in g/liter). 1) FeS; 2) CoS; 3) NiS; 4) $Fe(OH)_3$.

Substituting the values of S in Eqs. (9a) and (9b) leads to the following resultant expression:

$$pH = A - \frac{P_{H_2S}}{2} - \frac{\lg a_{Me^{++}}}{2} \quad (12)$$

in which coefficient A for the sulfides of nickel, cobalt and iron is respectively equal to, at 25°: -0.44 , -0.37 , and 2.01 ; and at 115°: -0.58 , -0.55 , and 1.65 . The diagram of the equilibrium pH values for the solution (precipitation) of the sulfides corresponds to Eq. (12). The general appearance of the diagram for the sulfate solutions, constructed using the activity coefficients taken from Harned and Owen [11], at 25° and $P_{H_2S} = 1$ atm, is shown in Fig. 1.

As follows from the obtained data, the properties of the monosulfides of Group VIII metals are such that they permit a selective salt leaching of iron at practically any composition of the solution. This reaction



can go to completion and is restricted only by kinetic factors. The sulfides of nickel and cobalt possess almost like properties; the selective salt leaching of these metals is thermodynamically impossible. Changing the temperature has very little effect on changing the difference in the solubility (precipitation) values of the sulfides and consequently, it can exert an influence only kinetically.

Reducing the hydrogen sulfide pressure raises the equilibrium pH values. These conditions are created when hydrogen sulfide is oxidized under the conditions prevailing in the autoclave leaching of sulfides in an oxygen atmosphere under pressure. At sufficiently low H_2S concentrations the plots of the pH for the solution of the sulfides and the precipitation of ferric hydroxide [17] coincide (Fig. 2). In this case, the solution of the sulfides, the oxidation of the sulfide and ferro ions, and also the precipitation of ferric hydroxide, all occur simultaneously.

EXPERIMENTAL

Method of study. The acid leaching experiments were run in a 3.0 liter autoclave [18]. Technical oxygen, containing 96-98% O_2 , was used to oxidize the sulfides. The composition of the mattes is given in Table 3.

TABLE 3
Composition of Mattes

Specimen	Coarseness (in mm)	Content (in %)					
		Ni	Co	Cu	Fe	S	Remainder
Matte I. . . .	-0.600	19.26	0.78	0.22	55.98	21.63	2.19
Matte II. . . .	-0.385	7.46	0.49	14.29	49.00	24.01	4.75

Experimental Data and Their Discussion

The leaching experiments were run using 400 g samples of the mattes and a starting solution volume of 2.1 liters. The admission of oxygen was begun after the experimental temperature of 115° had been reached. The results of the experiments on the leaching rates of the mattes are plotted in Figs. 3 and 4; the coordinate origin in the graphs corresponds to the start of oxygen admission. As can be seen from the obtained results, only the ferrous sulfide dissolves when the mattes are processed in the absence of oxygen. These experimental results are in full agreement with the theoretical concepts regarding the chemistry of salt leaching, presented above.

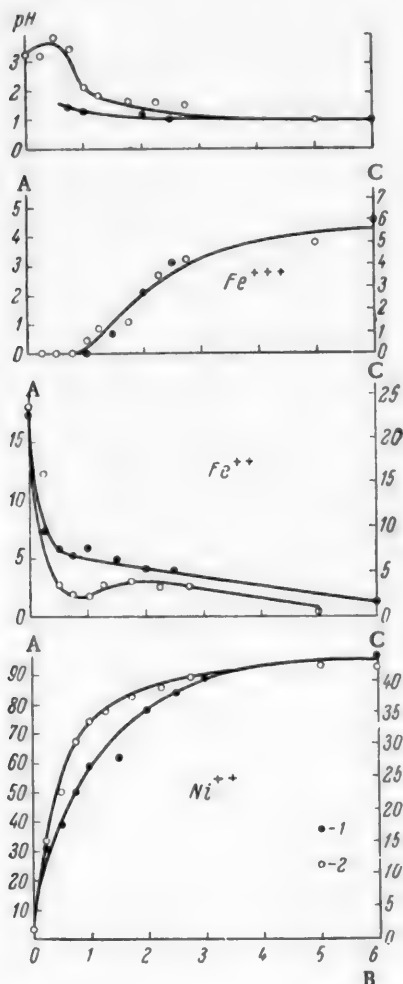


Fig. 3. Leaching of matte I with 0.9 N sulfuric acid solution at 115°. A) Extraction (in %); B) time (in hours); C) concentration (in g/liter). Oxygen pressure (in atm): 1) 10, 2) 20.

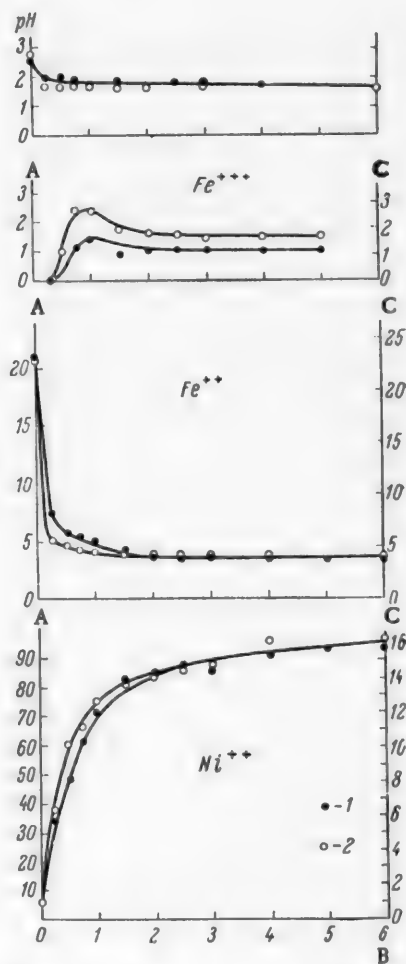
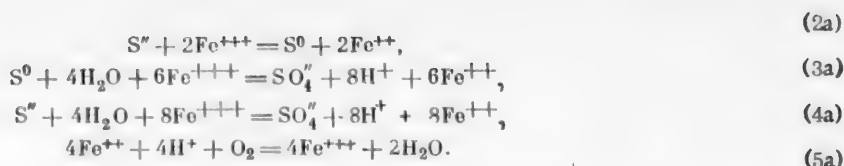


Fig. 4. Leaching of matte II with 0.9 N sulfuric acid solution at 115°. A) Extraction (in %); B) time (in hours); C) concentration (in g/liter). Oxygen pressure (in atm): 1) 15; 2) 20.

The admission of oxygen leads to a vigorous oxidation of the ferrous sulfate and a dissolving of the nickel and cobalt sulfides. The absence of ferric sulfate ions in the initial periods of oxidative leaching and the peculiar change in the ferric sulfate concentration during subsequent processing both indicate that the oxidation of sulfide ions according to reactions (2) - (4) goes mainly with involvement of the iron ions. As a result, the principal general reactions involved in the oxidative leaching of sulfides are the following:



Determining the conditions for the oxidation of sulfur according to the three possible variations possesses interest in connection with discovering a new method for obtaining elemental sulfur from artificial troilite [5] and the working out of methods for the autoclave leaching of nickel-cobalt mattes [6, 7, 18]. The oxidation-reduction potentials of reactions (2) - (4) are expressed by the equations:

$$\varphi_2 = \varphi_2^0 + \frac{0.0001984 \cdot T}{2} \cdot \lg \frac{a_{H^+}}{K \cdot a_{H_2S}}, \quad (2b)$$

$$\varphi_3 = \varphi_3^0 + \frac{0.0001984 \cdot T}{6} \cdot \lg \frac{a_{H^+}^8 \cdot a_{SO_4^{''}}}{K \cdot a_{H_2S}}, \quad (3b)$$

$$\varphi_4 = \varphi_4^0 + \frac{0.0001984 \cdot T}{8} \cdot \lg \frac{a_{H^+}^{10} \cdot a_{SO_4^{''}}}{K \cdot a_{H_2S}}, \quad (4b)$$

where φ_2^0 , φ_3^0 and φ_4^0 are the standard oxidation-reduction potentials of reactions (2) - (4), equal to $\varphi_T^0 = \Delta Z_T^0 / 23060 \cdot n$, and K is the complete ionization constant of hydrogen sulfide. The values of φ^0 , calculated from the data in Table 1, are given in Table 4.

TABLE 4
Values of Standard Oxidation-Reduction Potentials (in v) of
Reactions (2) - (4)

Reaction	25°	115°
$S'' = S^0 + 2e$	-0.447	-0.532
$S^0 + 4H_2O = SO_4^{''} + 8H^+ + 6e$	+0.356	+0.414
$S'' + 4H_2O = SO_4^{''} + 8H^+ + 8e$	+0.156	+0.124

The functional dependence of the potentials φ_2 , φ_3 and φ_4 on the hydrogen sulfide concentration ($pH = 1.0$, $a_{SO_4^{''}} = 0.1$) is shown in Fig. 5. The graph for the standard potential of the system Fe^{++}/Fe^{+++} is given here. As can be seen from Fig. 5, changing the hydrogen sulfide pressure causes a substantial change in the difference of the potentials. The most favorable conditions for the progress of reaction (2), i.e., for the formation of elemental sulfur, are created at a low temperature and a high hydrogen sulfide pressure. Low hydrogen sulfide concentrations favor both reaction (3) - the oxidation of elemental sulfur - and reaction (4) - the oxidation of sulfide ions to sulfates. Increasing the temperature favors reaction (4).

The conclusion regarding the predominant oxidation of sulfide ions to elemental sulfur at low temperature and a high hydrogen sulfide concentration is supported by the experimental results obtained by Downes and Bruce [5].

The oxidation of sulfur according to reaction (3) proceeds very slowly. The experimental results obtained in treating pure elemental sulfur with an acid solution of ferric sulfate in an oxygen atmosphere under pressure are given in Table 5. In running these experiments the autoclave charge was 50 g of sulfur, ground to a coarseness of less than 100μ , and 2 liters of a solution containing about 17.5 g/liter of Fe^{+++} . The length of the experiments was 3 hours, and the total pressure of the gas mixture was maintained equal to 10 ± 1 atm.

TABLE 5

Change in the SO_4^{2-} Concentration When Elemental Sulfur is Treated with Ferric Sulfate Solution

Time of Leaching 3 hours, Total Oxygen Pressure 10 ± 1 Atm.

Temperature (in °C)	SO_4^{2-} Content (in g/ liter)		Change in SO_4^{2-} concentration (in g/ liter)
	Starting solu- tion	Final solution	
80	88.68	89.22	0.54
100	89.55	90.00	0.45
125	88.80	89.46	0.66
145	88.20	88.74	0.54

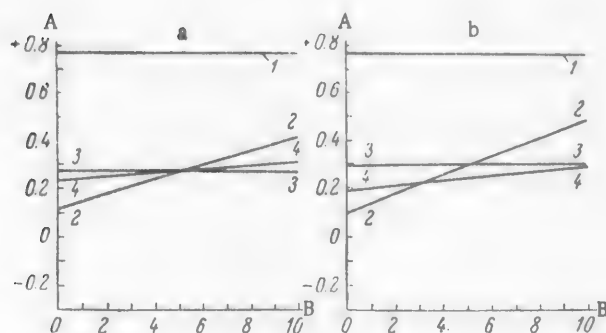


Fig. 5. Effect of hydrogen sulfide pressure on oxidation-reduction potentials of reactions. pH = 1.0, $a_{\text{SO}_4} = 0.1$. A) Oxidation-reduction potential φ (in v); B) value of log P. 1) $\text{Fe}^{3+} + e = \text{Fe}^{2+}$; 2) $\text{S} = \text{S}^0 + 2e$; 3) $\text{S}^0 + 4\text{H}_2\text{O} = \text{SO}_4^{2-} + 8\text{H}^+ + 6e$; 4) $\text{S}^{2-} + 4\text{H}_2\text{O} = \text{SO}_4^{2-} + 8\text{H}^+ + 8e$. a) At 25°; b) at 115°.

The slow rate with which elemental sulfur is oxidized in an autoclave is also supported by the examples of the acid leaching of troilite, low-grade mattes, and pyrrhotitic concentrates [5, 6], the processing of which goes with the formation of substantial amounts of molten sulfur. All of this information permits regarding the formed sulfur as being a practically inert material.

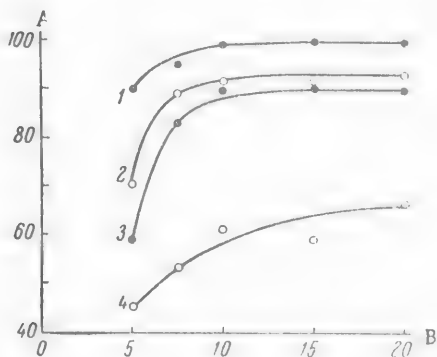


Fig. 6. Extraction of iron, nickel, cobalt, and sulfur into solution when matte I is leached with 0.9 N sulfuric acid solution at 115°. Time of leaching 6 hours. A) Extraction (in %); B) oxygen pressure (in atm). 1) Fe, 2) Ni, 3) Co, 4) S.

A study of reaction (4) under the conditions most favorable for its progress is difficult because of the complexity of determining low H_2S concentrations analytically. It is logical to assume that increasing the oxygen pressure will favor a reduction in the H_2S concentration, and consequently, a predominant progress of reaction (4). The experimental data plotted in Fig. 6 lend good support to this assumption. Consequently, it could be expected that in a continuous process, with a slow feed rate for the sulfides, the oxidation of the latter will go with the predominant formation of sulfates. In contrast to this, the conditions of a cyclic leaching are more favorable for obtaining elemental sulfur.

SUMMARY

1. The chemistry of the acid autoclave leaching of the monosulfides of nickel, cobalt and iron is determined by their thermodynamic properties. It includes the existence of a number of dynamic equilibria, controlling the conditions of the experiments.

2. The oxidation of sulfide ions is accomplished by ferric sulfate ions. At high S^{2-} concentration the oxidation of sulfide ions goes to elemental sulfur, while at low S^{2-} concentration it goes to the SO_4^{2-} anion.

LITERATURE CITED

- [1] G. Neikhaus and F. Pavlek, *Problemy Sovremennoi Metallurgii* 3 (15), 86 (1954).
- [2] G. B'erling, *Problemy Sovremennoi Metallurgii* 3(21), 49 (1955).
- [3] E. Discher and F. Pawlek, *Z. Erzbergbau u. Metallhüttenwesen* 10, 4, 158 (1957).
- [4] F. Pawlek and H. Pietsch, *Z. Erzbergbau u. Metallhüttenwesen* 10, 8, 373 (1957).
- [5] K. W. Downes and R. W. Bruce, *Can. Mining Met. Bull.* 48, 127 (1955); 48, 791 (1955).
- [6] G. N. Dobrokhotoy and N. I. Onuchkina, *Tsvetnye Metal.* 30, 3, 35 (1957).
- [7] G. N. Dobrokhotoy and N. I. Onuchkina, *Tsvetnye Metal.* 31, 7, 35 (1958).
- [8] E. H. M. Badger, R. H. Griffith, and W. B. S. Newling, *Proc. Roy. Soc. (London)* A197, 184 (1949).
- [9] J. W. Kury, A. J. Zielen, and W. L. Latimer, *J. Electrochem. Soc.* 100, 10, 468 (1953).
- [10] *Handbook of Physical-Chemical Constants*, BTE Vol. 5, 416, 434 (1929).
- [11] H. S. Harned and B. B. Owen, *The Physical Chemistry of Electrolytic Solutions* (Russian translation) (1952).
- [12] B. P. Nikol'skii, *Handbook of Chemistry [In Russian]* 3, 210 (1952).
- [13] A. Mickwitz, *Z. anorg. allgem. Chem.* 196, 113 (1931).
- [14] G. S. Gritsaenko, G. S. Sludskaya, and N. Kh. Aidin'yan, *Izvest. Akad. Nauk SSSR, Ser. Geol.* 2, 112 (1950).
- [15] D. Lundqvist, *Arkiv Kemi, Mineral. Geol.* 24 A, 21 (1947).
- [16] A. F. Kapustinskii, *Zhur. Priklad. Khim.* 16, 1-2, 50 (1943).
- [17] G. N. Dobrokhotoy, *Zhur. Priklad. Khim.* 27, 1056 (1954).
- [18] G. N. Dobrokhotoy and N. I. Onuchkina, *Sbornik Tekhn. Inf. Inst. Gipronikel* 3, 3 (1958).

Received June 16, 1958

•Original Russian pagination. See C. R. Translation.

PHOSPHATATION OF STEELS IN THE PRESENCE OF NITRATES OF MONOVALENT METALS *

I. I. Khain

Phosphatation is one of the most widely used methods of protecting metals against corrosion. The principle of this method consists in producing a layer of an insoluble phosphate on the surface of the metal; the phosphate layer is produced as the result of a chemical reaction between the metal and dilute solutions of monophosphates of bivalent metals.

The main property of the phosphate layer is its capacity of increasing to a considerable extent the adhesion, and consequently the protection, of subsequently applied lacquers or oil paints.

The high degree of corrosion resistance, the simplicity of producing the phosphate coatings and the relatively low cost of the phosphatation process are responsible for its wide use in almost all branches of industry connected with protection of metals. However, the ordinary methods of phosphatation have an inherent drawback: the formation of the phosphate layer requires a considerable expenditure of time, up to two hours or more.

The amount of time required for the formation of the phosphate coating, which is accompanied by considerable evolution of hydrogen, leads not only to technological difficulties (slowing down of the industrial cycle) but also to the danger of inducing susceptibility to hydrogen embrittlement in the metal.

Thus, we are faced with the problem of increasing the speed of phosphatation and eliminating the susceptibility to hydrogen embrittlement.

In solving this problem we started with the following assumption: the formation of the phosphate coating is divided into two separate stages — 1) the dissolution of iron with formation on the surface of a layer of a supersaturated bi- and triphosphate solution, and 2) crystallization of phosphates from the supersaturated solution on the surface of the metal, the conditions of crystallization determining the formation and growth of the protective phosphate layer.

The first stage is the electrochemical dissolution of the metal; it results from the ionization of iron (anodic process) and the reduction of an equivalent amount of one of the components of the solution (cathodic process).

During the ordinary process of phosphatation the cathodic process consists in evolution of hydrogen. The rate of this process limits the dissolution of the metal, since the evolution of hydrogen proceeds at a relatively high overpotential. Consequently, the increase of the rate of formation of the phosphate layer can be achieved by facilitating the cathodic process; the easiest way to achieve this is by introducing special accelerating agents into the phosphate solution. These accelerating agents should create additional cathodic processes requiring less energy than that necessary for the evolution of hydrogen. The deposition of cations more positive than hydrogen (copper cations, for example, when copper compounds are used as accelerating agents) will represent such an additional cathodic process. The accelerated phosphatation process called Bonderizing is based on this principle. However, the addition of copper compounds leads to the formation, in the protective layer, of inclusions more positive than iron, which is always accompanied by the decrease of the protective properties of the phosphate layer. Therefore the addition of such elements appears to us undesirable.

* Part I.

Additional cathodic processes can also consist of reducing oxidizing agents (which are not cations) added to the phosphate solution. The most suitable oxidizing agents for this purpose are those which increase the rate of layer formation and form reduction products which do not decrease the corrosion resistance of the protective layer.

Taking into account the modern theory of formation of phosphate layers [1-5] and the results of our preliminary work [6, 7], we have assumed that the best method would consist of the use of nitrates as accelerating agents. However, the method of phosphatation with nitrates as accelerating agents has not yet been investigated.

The purpose of the present work was investigation of the effect of nitrates of mono-, bi-, and trivalent metals, and also free nitric acid, on the process of formation and properties of phosphate layers in view of determining the nature of the accelerating action of these compounds, choosing the best compounds, and developing on the basis of these findings an accelerated method of phosphatation applicable in industry.

In the first part we shall report the results of the investigation of the process of phosphatation of steel in the presence of nitrates of monovalent metals.

EXPERIMENTAL

Phosphate layers were deposited on $45 \times 45 \times 3$ mm plates of carbon steel of the following composition (in %): C = 0.31, Si = 0.09, Mn = 0.36, S = 0.054, P = 0.047, and traces of Ni and Cr.

The phosphatation solution was a mixture of manganese and iron monophosphates of the following composition (in %): $F^{2+} = 1.68$, $F^{3+} = 0.03$, Mn = 17.84, $PO_4 = 67.59$, $H_2O = 12.56$; the solution was free of SO_4 and Cl ions.

The accelerating agents were chemically pure nitrates of sodium, potassium and ammonium, used in the following concentrations: 20, 40, 60, 80, and 100 g/liter.

The layers were produced in aqueous phosphate solutions (30 g/liter) containing the respective proportions of nitrate. The temperature during the phosphatation process was kept constant at $98 \pm 0.5^\circ C$.

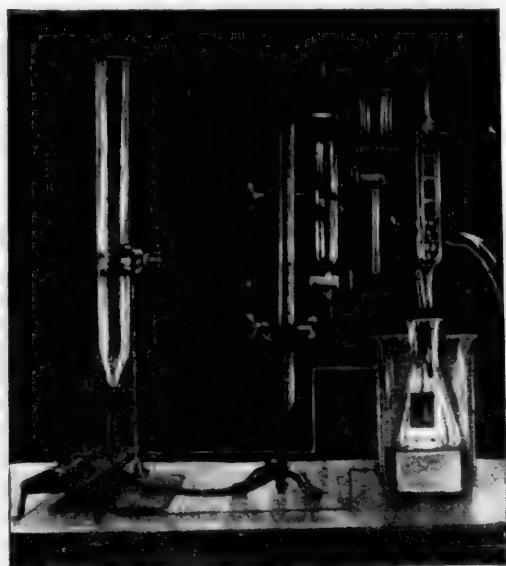


Fig. 1. Apparatus for determining the volume of hydrogen evolved during phosphatation.

loss of weight (g/m^2) of phosphated samples of a given surface state after 20 minutes in a 3% HCl solution containing a high concentration (150 g/liter) of an inhibitor ("Unikol" of the "PB" brand).

We investigated the effect of nitrates on the following factors: the acidity of the solution, the duration of the layer formation, and the weight, color, thickness, structure, and protective properties of the phosphate layer. In a number of cases we also determined the composition of the phosphate layer and its capacity of increasing the adhesion of lacquer coatings.

The acidity of the solution was determined by the general technique used in phosphatation, titration of samples of the solution (10 ml) with 0.1 N solution of sodium hydroxide in the presence of indicators: methyl-orange (when free acid was being determined), and phenolphthalein (when the general acidity of the solution was being determined). Also, we determined the pH of the solution by using a glass electrode.

The duration of the layer formation was determined by visually following the evolution of hydrogen from the surface of the samples and also by determining the volume of the evolved hydrogen; for this last purpose we used a special apparatus, shown in Fig. 1.

The phosphate layers were characterized by the

The color of the layer was determined visually and was compared with the color of the phosphate formed by the process of phosphatation in the absence of accelerating agents.

The thickness and structure of the phosphate layer were determined with a profilograph, an apparatus we developed earlier [8].

The protective capacity of the layers investigated was determined by subjecting the samples to a 3% NaCl solution and to a salt spray, the most suitable methods for testing phosphate layers [9].

RESULTS OF THE INVESTIGATIONS

Figure 2 shows that the acidity of the solution is not affected by sodium and potassium nitrates — strongly basic salts highly dissociated in solution and weakly hydrolyzed. The addition of ammonium nitrate (salt of a weak base and easily hydrolyzed) increases the general acidity of the solution.

The pH of the solution is not affected when the concentration of nitrates is increased.

The period of layer formation, determined by the duration of hydrogen evolution (Fig. 3) and by the volume of hydrogen evolved (Fig. 4), remains unaffected by the addition of sodium and potassium nitrates but decreases slowly under the effect of ammonium nitrate, i.e., the rate of the process of phosphate film formation increases.

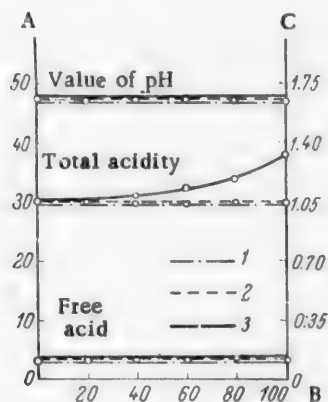


Fig. 2. Effect of concentration of sodium, potassium, and ammonium nitrates on the acidity of the solution. A) Volume of 0.1 N sodium hydroxide solution (ml); B) concentration of nitrates (g/liter): 1) NaNO_3 , 2) KNO_3 , 3) NH_4NO_3 ; C) value of the hydrogen indicator.

The change of weight of the phosphate layer follows the same pattern (Fig. 5).

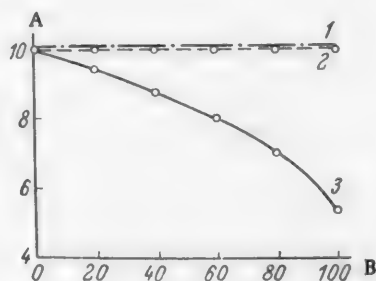


Fig. 3. Effect of the concentration of sodium, potassium, and ammonium nitrates on duration of hydrogen evolution. A) Duration (min.); B) Concentration of nitrates (g/liter): 1) NaNO_3 , 2) KNO_3 , 3) NH_4NO_3 .

The color of the layers formed in the presence of nitrates is dark gray, characteristic of phosphate layers obtained without the use of accelerating agents.

The thickness and the surface state of phosphate layers are not affected by the addition of sodium and potassium nitrate, but both decrease when ammonium nitrate is added to the solution, a result characteristic of the effect of easily hydrolyzed nitrates.

The protective capacity of phosphate layers remains unaltered when sodium and potassium nitrate are added to the phosphate solution (see Table) but decreases somewhat when ammonium nitrate is added.

The results show that the different nitrates affect the main factors of the process of formation and the properties of the phosphate layer differently. In the presence of sodium and potassium nitrate all the factors investigated remain unaltered. Under the effect of ammonium nitrate the acidity (total) of the solution is slightly increased, the time necessary for the formation of the layer decreases, and the weight, thickness, surface state, and protective capacity of the layer also change.

Effect of The Concentration of Sodium, Potassium, and Ammonium Nitrates on Corrosion Resistance of Phosphate Layers

Cation of the nitrate introduced	Concentration of nitrate (g/liter)	Tests in salt spray		Tests in 3% solution of sodium chloride		Remarks
		Duration of tests up to beginning of corrosion (hours)	Loss of weight ($\text{g}/\text{m}^2 \cdot \text{hr}$)	Duration of tests up to beginning of corrosion (hours)	Loss of weight ($\text{g}/\text{m}^2 \cdot \text{hr}$)	
Sodium	0	294	0.0023	102	0.0057	Control
	20	294	0.0023	103	0.0056	
	40	294	0.0023	102	0.0057	
	60	295	0.0022	103	0.0056	
	80	294	0.0023	102	0.0057	
	100	294	0.0023	102	0.0057	
Potassium	0	294	0.0023	102	0.0057	Control
	20	294	0.0023	102	0.0057	
	40	294	0.0023	102	0.0057	
	60	293	0.0024	101	0.0058	
	80	294	0.0023	102	0.0057	
	100	294	0.0023	102	0.0057	
Ammonium	0	294	0.0023	102	0.0057	Control
	20	240	0.0061	84	0.0128	
	40	203	0.0086	71	0.0176	
	60	176	0.0104	59	0.0210	
	80	159	0.0115	55	0.0232	
	100	146	0.0128	50	0.0247	

The difference in the effects of the nitrates is apparently due to the difference in their behavior in dilute solution, resulting from the difference in their degree of hydrolysis, with subsequent liberation of free nitric acid.

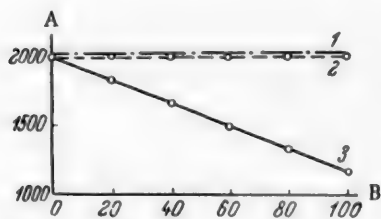


Fig. 4. Effect of concentration of sodium, potassium, and ammonium nitrates on volume of hydrogen evolved. A) Volume of hydrogen (ml/m^2); B) concentration of nitrates (g/liters): 1) NaNO_3 , 2) KNO_3 , 3) NH_4NO_3 .

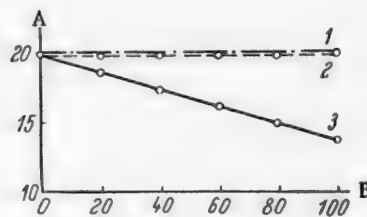


Fig. 5. Effect of concentration of sodium, potassium, and ammonium nitrates on the weight of phosphate layer. A) Weight of the layer (g/m^2); B) concentration of nitrates (g/liters): 1) NaNO_3 , 2) KNO_3 , 3) NH_4NO_3 .

One may assume that the effect of these nitrates on the main factors of the process of phosphatation is determined by their tendency to become hydrolyzed and the effect of the free nitric acid subsequently liberated.

SUMMARY

1. Sodium, potassium, and ammonium nitrates added to the phosphating solution have different effects on the main factors of the process of formation and properties of phosphate layers.

2. Sodium and potassium nitrate do not affect these factors. Ammonium nitrate, however, increases the acidity (total) of the solution and increases the rate of formation of the phosphate layer and affects its basic properties (thickness, surface state, protective capacity).

3. To explain the difference in the effects of the nitrates investigated one must assume that this difference is due to the degree of hydrolysis and the subsequent liberation of free nitric acid, which apparently has a direct effect on the investigated factors of the process of formation and the properties of the phosphate layer.

LITERATURE CITED

- [1] V. I. Vul'fson, *Corrosion and Protection* 5, 1-2, 7 (1939).
- [2] W. Machu, *Korrosion und Metallschutz* 17, 5, 157 (1941).
- [3] A. Wustefeld, *Archiv für Metallkunde* 7, 253 (1949).
- [4] I. V. Krotov, *ISFKhA AN SSSR* 26, 304 (1955).
- [5] V. S. Lapatukhin, *Phosphatation of Metals*, Mashgiz 17 (1958).
- [6] I. I. Khain, *Zhur. Priklad. Khim.* XVIII, 4-5, 264 (1945).
- [7] I. I. Khain, *Zhur. Priklad. Khim.* XIX, 5-6, 527 (1946).
- [8] I. I. Khain, *Factory Labs.* 7, 864 (1957).
- [9] E. I. Dyrmont and S. D. Gol'denberg, *Communications of the Central Institute of Metals* 16, 158-164 (1934).

Received April 20, 1958

PROTECTION OF STEEL AGAINST GASEOUS CORROSION BY GLASS-METAL COATINGS

E. A. Antonova and A. A. Appen

Institute of Chemistry of Silicates of the Academy of Sciences, USSR

The problem of protecting steel against gaseous corrosion at high temperatures gains importance every year. Recently, the method of protection consisting in enrichment of the surface of iron and steel articles with silicon, chromium, and other elements by diffusion has found wide application. Protective coatings of this type provide resistance against gaseous corrosion [1-4]. However, it must be noted that when exposed to high temperatures for long periods of time these protective coatings obtained by thermal diffusion progressively lose their protective properties due to the diffusion of the components of the coating into the metal and the diffusion of metal atoms to the surface layer.

One of the possible methods of protecting steels against oxidation is enameling; this method is already being applied. Heat resistant enamels [5-9] consist essentially of slightly alkaline or nonalkaline silicate enamels mixed with heat-resistant elements during grinding. The elements added are usually oxides (Cr_2O_3 , Al_2O_3 , SiO_2 , ZrO_2 , CeO_2) or other minerals (zircon, diaspore, mellilites, chromium ore, etc.). By their composition these enamels belong to the oxide-type enamels. The resistance of oxide enamels to sharp changes of temperature is very small. Having a low coefficient of thermal expansion and low thermal conductivity, they rapidly chip off the surface of steel articles, especially in areas with a small radius of curvature. The general characteristics of oxide enamels make them unsatisfactory for many uses.

In 1951, Moore and his collaborators [10, 11] described a new and interesting method of protection. They used glass-chromium coatings of mixtures of glass-type frit and finely ground chromium metal powder to protect molybdenum. Later they proposed the same type of protective coating for steels [12]. In this case, they used as the metallic component a cermet powder of a complicated composition which contained Cr, Ni, B, Si, C, Fe. The binder was glass of the following composition (in % weight): $\text{SiO}_2 = 37.5$, $\text{B}_2\text{O}_3 = 6.5$, $\text{BaO} = 44.0$, $\text{CaO} = 3.5$, $\text{ZnO} = 5.0$, $\text{Al}_2\text{O}_3 = 1.0$, $\text{ZrO}_2 = 2.5$. The relative proportion of the cermet and the glass varied widely. The best protection was found to be 90 parts cermet and 10 parts glass, by weight. Surface layers of this composition protected iron against oxidation in air over a long period at temperatures around 900°C .

Aside from heat resistance, this protective layer had high resistance to temperature changes and good adhesion to iron.

Glass-metal coatings which combine the properties of glass and metals represent a new type of enamel. They have significant advantages with respect to pure oxide enamels. A detailed study of their nature and properties, their composition, and the area of their applicability appears to be an important problem.

In the present work we give the first results concerning this problem obtained in our laboratory.

The object of our first investigation was the "chromium-glass" system. Chromium was used in powder form; the particle-size distribution is given in Table 1.

In glass-chromium mixtures glass plays the role of binder. The composition of this binder, which is of great importance, has not been investigated.

It is known [12] that the glass-metal protective coating itself is very susceptible to separating by layers. During the firing of the protective coating glass tends to melt out on the surface. It was noted that the phenomenon of separation by layers manifests itself very strongly in the case of low melting point homogeneous glasses; therefore these represent a poor medium for the distribution of chromium particles. It is preferable to use nonhomogeneous media possessing structural viscosity. We used as binder material a nonalkaline borosilicate slag-type glass of the following composition (weight %): $\text{SiO}_2 = 58.0$, $\text{Al}_2\text{O}_3 = 5.0$, $\text{B}_2\text{O}_3 = 20.0$, $\text{TiO}_2 = 6.0$, $\text{ZrO}_2 = 3.0$, $\text{BeO} = 3.0$, $\text{CoO} = 5.0$.

TABLE 1
Sedimentation Analysis of Metallic Chromium Powder

Particle size (in μ)	Amount (in %)
up to 4	12.8
4-6	18.0
6-8	27.2
8-10	16.0
10-12	12.8
12-15	8.0
15-20	3.6
20-30	0.4
>30	1.2

The glass-chromium coatings were used for the protection of low-carbon steels.

First we prepared water suspensions of powder mixtures of different compositions (Table 2). Bentonite (2%) was added to prevent precipitation of particles. The materials were ground to a thin powder until the solid components could pass completely through a sieve of 10,000 holes/cm². The amount of water in the suspension was varied according to the ratio of glass to chromium, within the limits of 30 and 40%. The specific gravity varied correspondingly from 2.0 to 2.65.

TABLE 2
Composition and Properties of Glass-Chromium Enamels

Coating No.	Composition (parts by wt.)		Softening temperature (in °C)	Density (in g/cm ³)	Modulus of elasticity E (in kg/mm ²)	Poisson coeff.	Coefficient of linear expansion, α_{20-600} 10 ⁻⁷	Specific volume resistance, ρ_{22} (in ohm · cm).
	Glass	Chromium						
1	50	50	1090	2.93	7930	0.245	72.0	16.8
2	40	60	1120	3.92	8400	0.305	76.0	2.7
3	30	70	1150	4.54	10740	0.291	78.0	0.62
4	20	80	1190	4.97	13380	0.257	87.0	0.60
5	10	90	1250	5.48	—	—	95.0	—
6	5	95	1330	—	—	—	96.5	—

These coatings were spread over samples of steel No. 3. This steel has the following composition: C = 0.14 - 0.22, Si = 0.12 - 0.35, Mn = 0.35 - 0.60, S < 0.055, P < 0.05 %.

The dimensions of the samples were 20 × 10 × 3 mm. At both ends of each sample were drilled holes for the suspension of samples during firing. The samples were sandblasted before being coated.

After application of the coatings, the samples were dried at 105-110° C and fired in a special electrical furnace in an atmosphere of argon for 1.5 to 2.0 minutes. The firing temperatures varied from 1200 to 1350° C. The thickness of the coatings was 0.15-0.30 mm. We used technically pure argon, containing 12 % nitrogen and 0.6 % oxygen. Oxygen was eliminated by passing the gas through copper shavings at 550° C.

Properties of the Protective Coatings

Firing temperature and adhesion. Tests have shown that the higher the chromium concentration the higher the firing temperature must be.

The ratio between glass and chromium has a great effect on the quality of the protective layer. Protective layers with high concentration of glass (> 50%) peel off from the steel during cooling of the samples. Apparently, this is due to the strain resulting from the difference between the thermal expansion of the protective coating and the underlying steel; the coefficient of thermal expansion of steel ($\alpha_{20-500} = 133 \cdot 10^{-7}$) is considerably higher than that of the protective layers (Table 2).

The tendency of the protective layer to peel off decreases when the concentration of chromium increases. Optimum adhesion to steel was shown by coatings No. 4 to No. 6 (Table 2), containing a high concentration of chromium. Therefore, further experiments were made with protective layers of this type.

To determine the degree of adhesiveness, samples carrying coatings of No. 4 were subjected to impact tests on a special apparatus. The layer resisted chipping up to 0.8 kg-m. Only very small cracks not reaching the surface of the steel could be detected. Silicate enamels can resist an impact of 0.3 kg-m at best.

Heat resistance. The corrosion of steel protected by glass-chromium layers always has a local character. As a rule, the corrosion of samples begins not over the whole surface but only at isolated points where accidental defects occur in the protective layers (porosities, bubbles, foreign inclusions, etc.). Where there are such defects the method of determining the heat resistance of the protective layers by the variation of weight of the samples is not representative. Only samples with perfect protective layers should be subjected to this test.

Tests of heat resistance of steel samples protected by glass-chromium layer No. 4 were made by subjecting the samples to the atmosphere in an electric furnace at 900 and 1000° C for long periods of time (100 hours and more).

The heat resistance of the protective layers was measured by the increase in weight of the samples. The minimum increase in weight or its absence was considered as the indication of high quality in the protective properties of glass-chromium layers.

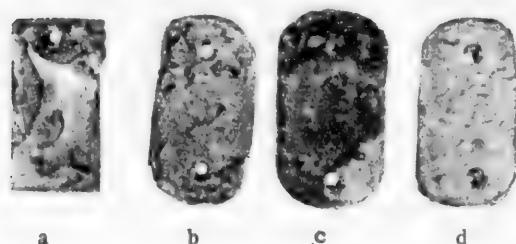


Fig. 1. Surface of steel samples after tests of heat resistance at 900° C. a) Unprotected sample (50 hours); b) surface enriched in chromium (50 hours); c) surface enriched in silicon (50 hours); d) glass-chromium coating (600 hours).

The results of the tests showed that glass-chromium enamels have a considerably higher heat resistance than the oxide-type enamels or diffusional coatings. Enrichment in silicon by thermal diffusion [1] can be used for the protection of steel and iron parts against atmospheric corrosion up to 700° C; enrichment in chromium by thermal diffusion [3] can be used up to 850° C; enameling with glass-chromium coatings insures the protection of steel up to 1000° C.

Table 3 shows that steel protected with glass-chromium layers remains almost unoxidized in air up to 1000° C. The increase in the period of testing heat resistance did not lead to any change in the surface of the samples (Fig. 1 d).

TABLE 3
Heat Resistance of Steels

Type of coating or type of steel	Temperature (in °C)	Change in weight (in mg/cm ² ·hr)
Steel No. 3, without coating	700	from + 1.0 to + 2.0
Low-carbon steel, thermo-diffusional silicon coating [1]	700	from + 0.06 to + 0.08
Low-carbon steel, thermo-diffusional chromium coating [3]	850	from - 0.02 to - 0.2
Steel No. 3, protected by glass-chromium coating No. 4	1000	+ < 0.01
Heat resistant steel [13]:		
ÉI-602	1100	+ 0.06
ÉI-435	1100	+ 0.04

Resistance to sharp temperature changes. To investigate the resistance of glass-chromium layers to sharp changes in temperature the protected samples were subjected alternately to heating and cooling at the following temperatures: $20^{\circ} \rightarrow 900^{\circ} \rightarrow 20^{\circ}$. The samples were cooled by being plunged in water.

The resistance of the protective layers to abrupt changes of temperature depends on the chromium concentration. High resistance to temperature changes was achieved with layers containing 80% and more chromium. It must be emphasized that under the effect of temperature change the upper layers of the glass-chromium coating, consisting mainly of melted glass, chip off. The lower layer, enriched in chromium, remains firmly adherent to steel and continues to protect the steel against oxidation. In the case of coating No. 4 obvious signs of destruction, in the form of cracks reaching the steel, occurred only after several tens of thermal cycles.

Thermal expansion. The coefficient of expansion of the glass-chromium mixture was determined on samples 70-90 mm long and 4-6 mm thick. The measurements were made with a quartz dilatometer [14].

Table 2 shows that the addition of chromium to glass increases the melting point and the coefficient of expansion. Thus, one can obtain high melting point coatings with high expansion coefficients, which is very important for successful enameling of steel.

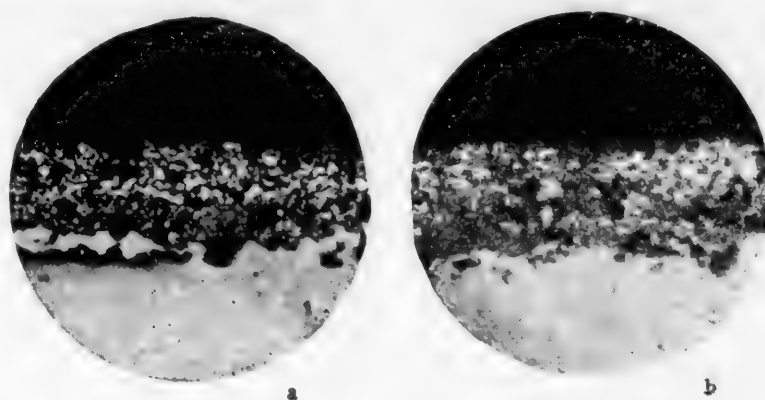


Fig. 2. Normal structure of the glass-chromium layer. a) Before test of heat resistance; b) after 100 hour exposure in air at 1000° . Magnification 133 x.

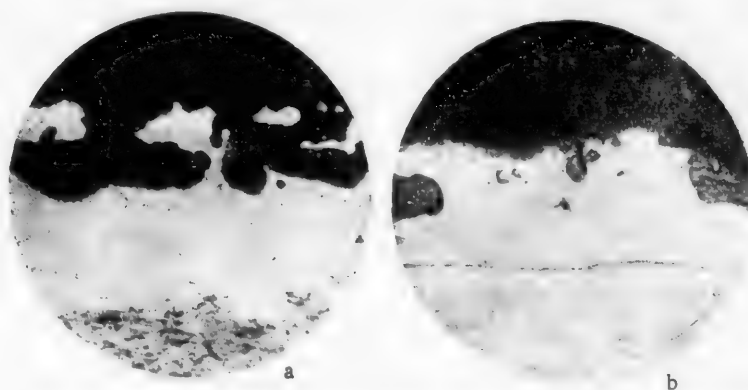


Fig. 3. Structure of the glass-chromium layer resulting from overheating during firing. Stages of separation into layers: a) first, b) second. Magnification 133 x.

Mechanical and electrical properties. The elastic modulus, E , of glass-chromium layers is considerably higher than that of silicate enamels. The values of E and of the Poisson coefficient measured by the ultrasonic method are given in Table 2.

The specific electrical resistance of glass-chromium layers is higher than that of chromium and considerably lower than that of glass. It decreases with the increased concentration of chromium in the layer.

Structure of the protective layer. Glass-chromium layers consist of a heterogeneous layer composed of a glass phase, or of the products of its crystallization, and of particles of chromium. When the melting conditions of the layer are correct the particles of chromium are distributed evenly within the mass of glass (Fig. 2a).

The structure of the protective layer does not change significantly after being exposed to 1000° C for long periods (Fig. 2b).

The firing temperature has a decisive effect on the structure of the protective layer. If the coating is overheated during firing, it becomes separated into layers. In this case, one must distinguish two stages of layer separation. First there occurs the aggregation of chromium particles, as a result of which the structure acquires the form represented in Fig. 3 a. Then the glass almost completely detaches from chromium and becomes molten on the surface. Chromium, together with a small amount of binder, is deposited on steel in the form of a continuous layer 100 microns thick or thicker (Fig. 3, b). The expansion coefficient of the glass molten on the surface is different from that of steel and consequently chips off easily. Nevertheless, the protective property of the layer remains after this upper layer of glass has chipped off.

SUMMARY

The general properties of glass-chromium protective layers, particularly their protective properties and their capacity to withstand sharp changes of temperature, make them more advantageous than the silicate enamels. Glass-chromium layers give better protective characteristics than metallic protection and have a higher heat resistance than protective layers produced by diffusion (thermal diffusion of silicon or chromium).

LITERATURE CITED

- [1] N. S. Gorbunov and A. S. Akopdzhanyan, *J. Appl. Chem.* XXIX, 655 (1956).*
- [2] N. S. Gorbunov and I. D. Yudin, *Diffusional Chromium Coating* [In Russian] (Acad. Sci. USSR Press, 1946).
- [3] N. S. Gorbunov, *Vacuum Method of Thermodiffusional Chromium Coating* [In Russian] (Acad. Sci. USSR Press, 1955).
- [4] Z. G. Ordina, *Reports of Leningrad Technical Institute of the Food Industry* 12, 290 (1955).
- [5] W. Harrison, D. Moore, and J. Richmond, *J. Nat. Bur. Stand.* 38, 293 (1947).
- [6] W. Plankenhorn, *J. Amer. Cer. Soc.* 31, 145 (1948).
- [7] G. V. Kukolev and V. N. Tarasenko, *Reports of the Kharkov Polytechnic Institute* VIII (3), 195 (1956).
- [8] A. Petzold, *Email, Berlin*, 371 (1955).
- [9] J. Richmond, H. Lefort, C. Williams, and W. Harrison, *J. Amer. Cer. Soc.* 38, 2, 72 (1955).
- [10] D. Moore, L. Bolz, J. Pitts, and W. Harrison, *National Advisory Committee Aeronaut. Techn. Note* 2422, 39 (1951).
- [11] *Nat. Bur. Stand., Technical News Bulletin* 36, 140 (1952).

*Original Russian pagination. See C. B. Translation.

[12] D. Moore and J. Cuthill, Amer. Cer. Soc. Bull. 34, 11, 375 (1955).

[13] A. P. Boyarinova and A. R. Krylova, Reports presented at the 11th Scientific-Technical Conference on Heat Resistant Materials 85 (1957).

[14] V. V. Vargin and R. I. Rylova, Industrial-Technical Conference on Enameling [In Russian] (Metallurgy Press, 1956), 298.

Received February 4, 1959

PROCESS OF PHOSPHATATION OF STEEL IN THE PRESENCE OF NITRATES OF BIVALENT METALS*

I. I. Khain

In our previous publication [1] we described the results of the investigation of the process of phosphatation of steel in the presence of ammonium nitrate and of nitrates of monovalent metals, namely sodium and potassium. We have shown that these salts affect differently the main factors in the process of formation and the properties of phosphate layers.

In our present publication, we shall describe the results of the investigation of the process of formation of phosphate layers on steel in the presence of nitrates of bivalent metals.

EXPERIMENTAL

The initial samples, the phosphatating reagent and the method of investigation used in this work were the same as those described previously [1].

The accelerating agents added to the phosphate solution were chemically pure nitrates of the following bivalent metals: manganese, zinc, cadmium, calcium, strontium, and barium.

Preliminary experiments showed that these nitrates can be divided into two groups in terms of their effect on the factors investigated. The first group contains the nitrates of manganese, zinc, and cadmium, and the second the nitrates of calcium, strontium, and barium.

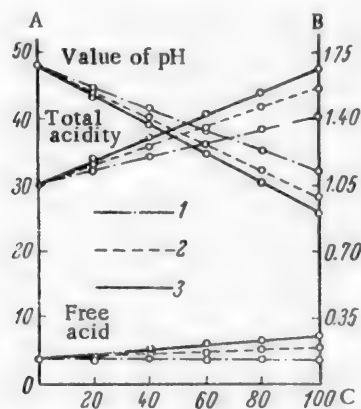


Fig. 1. Effect of the concentration of manganese (1), zinc (2), and cadmium (3) nitrates on the acidity of the solution. A) Quantity of 0.1 N sodium hydroxide solution (ml); B) value of pH; C) concentration of nitrate (g/liter).

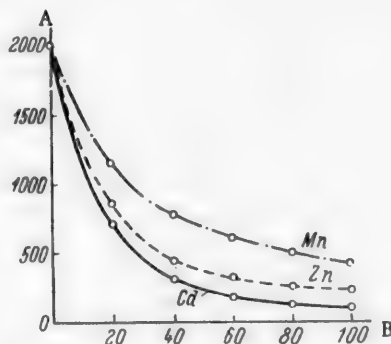


Fig. 2. Effect of the concentration of manganese, zinc, and cadmium nitrates. A) Volume of hydrogen (ml/m²); B) concentration of nitrate (g/liter).

* Part II.

The results of the investigation are presented separately for each group.

Effect of manganese, zinc, and cadmium nitrates. Figure 1 shows that the acidity of the solution increases with the concentration of the nitrates; it must be noted that the increase of total acidity of the solution is accompanied by an increase in the concentration of free acid, so that the pH value decreases.

The acidity of the solution is lowest in the presence of manganese and highest in the presence of cadmium; this is apparently due to the progressively increasing hydrolysis of this series of salts. It is well known that in the series zinc-cadmium the degree of hydrolysis of normally dissociated salts increases from zinc to cadmium [2].

The period of layer formation, judging by the volume of hydrogen evolved (Fig. 2) and by the duration of its evolution (Fig. 3), decreases sharply when the concentration of nitrates is increased; this indicates that the formation of phosphate layers is considerably accelerated. When the concentration of zinc and cadmium reaches 100 g/liter the duration of phosphatation is shortened 10-12 times.

The weight (Fig. 4) and the thickness of the phosphate layers progressively decrease as the concentration of nitrates increases. The order in which the weight of the phosphate layers decreases is the same as the order in which the layer-formation rate changes under the effect of the different nitrates.

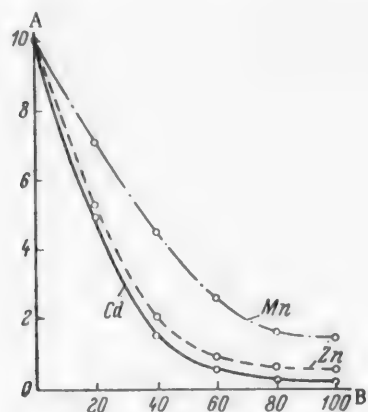


Fig. 3. Effect of the concentration of manganese, zinc, and cadmium nitrates on the duration of hydrogen evolution. A) Duration of hydrogen evolution (min); B) concentration of nitrate (g/liter).

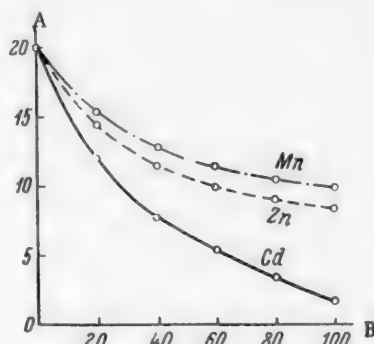


Fig. 4. Effect of the concentration of manganese, zinc, and cadmium nitrates on the weight of the phosphate layer. A) Weight of phosphate layer (g/m^2); B) concentration of nitrate (g/liter).

The color of the phosphate layer does not change when manganese or cadmium nitrate is added. As the concentration of zinc nitrate increases, the dark-gray color of the layer becomes lighter, apparently due to the inclusion of white zinc phosphate in the layer.

The microrelief of the layer formed is uniform, with very small irregularities.

Under the effect of manganese and cadmium nitrates the protective properties of the surface layers deteriorate (see Table 1). The addition of zinc nitrate has no significant effect on the anticorrosion properties of the phosphate layer.

Effect of calcium, strontium, and barium nitrates. The acidity of the solution increases progressively as the concentration of the nitrates is increased (Fig. 5). This increase of the acidity in the presence of these nitrates, which are generally weakly hydrolyzed in water solutions, can apparently be explained by increased hydrolytic decomposition of these salts under the effect of phosphoric acid and primary phosphates, with which these nitrates can form compounds insoluble in water.

TABLE 1

Effect of the Concentration of Manganese, Zinc, and Cadmium Nitrates on the Corrosion Resistance of Phosphate Layers

Cation of the nitrate introduced	Concentration of nitrate (g/l)	Tests in salt spray		Tests in a 3% solution of sodium chloride		Remarks
		Duration of tests up to the beginning of corrosion (hrs)	Loss of weight (g/m ² · hr)	Duration of tests up to the beginning of corrosion (hrs)	Loss of weight (g/m ² · hr)	
Manganese	0	294	0.0023	102	0.0057	Control
	20	158	0.0117	54	0.0236	
	40	113	0.0148	40	0.0300	
	60	86	0.0162	31	0.0328	
	80	65	0.0178	22	0.0365	
	100	58	0.0187	19	0.0373	
Zinc	0	294	0.0023	102	0.0057	Control
	20	294	0.0023	102	0.0057	
	40	295	0.0022	103	0.0056	
	60	295	0.0022	103	0.0056	
	80	294	0.0023	102	0.0057	
	100	294	0.0023	102	0.0057	
Cadmium	0	294	0.0023	102	0.0057	Control
	20	152	0.0123	51	0.0243	
	40	108	0.0153	38	0.0303	
	60	80	0.0169	27	0.0351	
	80	61	0.0184	19	0.0373	
	100	54	0.0192	16	0.0378	

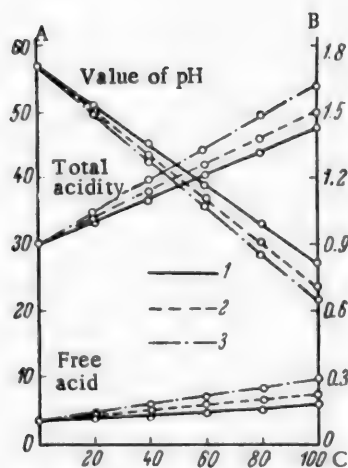


Fig. 5. Effect of the concentration of calcium (1), strontium (2), and barium (3) nitrates on the acidity of the solution. A) Quantity of 0.1 N sodium hydroxide solution (ml); B) value of pH; C) concentration of nitrate (g/liter).

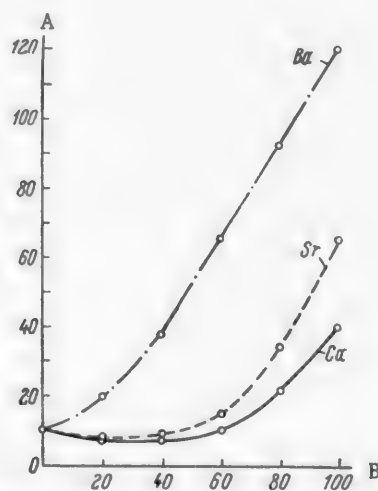


Fig. 6. Effect of concentration of calcium, strontium, and barium nitrates on the duration of hydrogen evolution. A) Duration of hydrogen evolution (min); B) concentration of nitrate (g/liter).

When the concentration of calcium and strontium increases, the duration of hydrogen evolution (Fig. 6) and the volume of hydrogen evolved (Fig. 7) first decrease and then increase, i.e., when the concentration of these salts is small the rate of film formation increases, while for high salt concentrations it decreases. In the presence of barium nitrate the period of phosphate film formation increases.

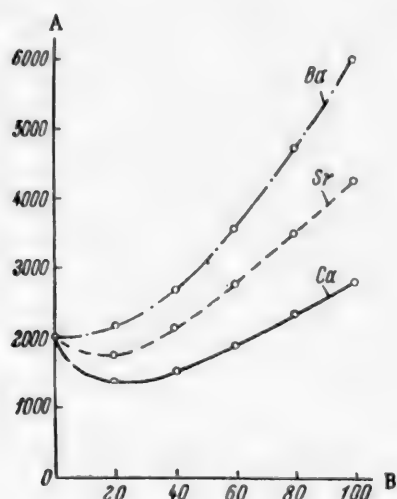


Fig. 7. Effect of concentration of calcium, strontium, and barium nitrates on the volume of hydrogen evolved. A) Volume of hydrogen (ml/m^2); B) concentration of nitrate (g/liter).

In the presence of calcium, strontium, and barium nitrates the weight of the phosphate layers decreases and reaches $1-3 \text{ g/m}^2$ (Fig. 8) when the concentration of the salts is maximum (100 g/liter).

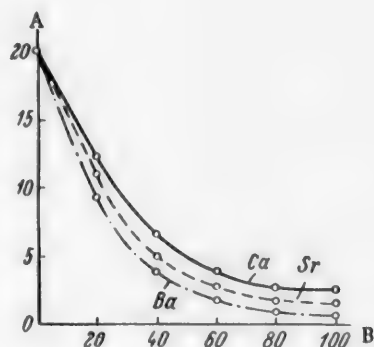


Fig. 8. Effect of concentration of calcium, strontium, and barium nitrates on the weight of phosphate layer. A) Weight of phosphate layer (g/m^2); B) concentration of nitrate (g/liter).

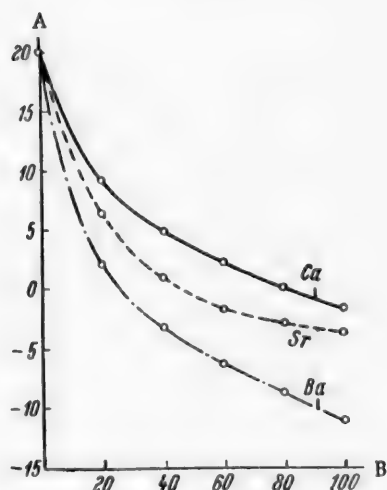


Fig. 9. Effect of concentration of calcium, strontium, and barium nitrates on the change of weight of samples after phosphatation. A) Change in weight of samples (g/m^2); B) concentration of nitrate (g/liter).

Under the effect of the nitrates the amount of nitric acid in the solution increases due to hydrolysis, and as a consequence etching of the metal is intensified; this is indirectly proved by the increase in weight of the samples subjected to phosphatation (Fig. 9). The minimum weight loss occurs in the presence of calcium nitrate and the maximum in the presence of barium nitrate. It is characteristic that the acidity of the solution changes in the same order, calcium nitrate inducing minimum increase of the acidity while barium nitrate induces maximum acidity (Fig. 5).

The surface irregularity characteristic of phosphate layers disappears progressively and the layer becomes smooth as the concentrations of calcium, strontium, and barium increase. The color of the phosphate layer passes from the characteristic dark gray to dark blue, becoming black after the sample is oiled. The phosphate layers obtained look very much like oxide layers obtained on steel in alkaline oxidizing solutions [3]. We obtained these layers, called phosphate-oxide layers, for the first time [4].

At the present time our method of obtaining phosphate-oxide layers (alkali-free oxidation) is described

in the literature here [5-7] and abroad [8-10] with reference made to our authorship. It is also indicated in foreign literature that up to now phosphate-oxide layers were unknown either in Europe or America.

The protective properties of the layers obtained in the presence of calcium, strontium, and barium nitrates deteriorate as the concentration of the salts in the solution increases (Table 2). Table 2 shows also that the corrosion resistance of these layers increases somewhat from calcium nitrate to barium nitrate. This can be explained by the order of the solubility of the phosphates — calcium, strontium, barium — entering into the composition of the surface layer. As the solubility of the phosphate forming the layer decreases, the resistance of the layer to corrosion must increase in the same order.

Thus, our investigation of Mn, Zn, Cd, Ca, Sr, and Ba nitrates showed that the acidity of the solutions increases with the concentration of these nitrates, in the order indicated.

TABLE 2

Effect of the Concentration of Calcium, Strontium, and Barium Nitrates on the Corrosion Resistance of Phosphate Layers

Cation of the nitrate introduced	Concentration of nitrate (g/l)	Tests in salt spray		Tests in a 3% solution of sodium chloride		Remarks
		Duration of tests up to the beginning of corrosion (hrs)	Loss of weight ($\text{g}/\text{m}^2 \cdot \text{hr}$)	Duration of tests up to the beginning of corrosion (hrs)	Loss of weight ($\text{g}/\text{m}^2 \cdot \text{hr}$)	
Calcium	0	294	0.0023	102	0.0057	Control
	20	108	0.0153	37	0.0309	
	40	59	0.0186	22	0.0365	
	60	28	0.0201	10	0.0415	
	80	17	0.0212	7	0.0424	
	100	12	0.0217	4.5	0.0432	
Strontium	0	294	0.0023	102	0.0057	Control
	20	111	0.0148	38	0.0303	
	40	62	0.0182	24	0.0360	
	60	32	0.0203	13	0.0408	
	80	22	0.0208	9	0.0417	
	100	16	0.0213	6	0.0430	
Barium	0	294	0.0023	102	0.0057	Control
	20	116	0.0141	41	0.0297	
	40	66	0.0176	26	0.0353	
	60	35	0.0196	17	0.0376	
	80	26	0.0205	11	0.0412	
	100	21	0.0210	8	0.0420	

The period of formation of the surface layer changes with the concentration of the acidity of the solution; under the effect of manganese, zinc, and cadmium nitrates it decreases (the rate of film formation increases) while in the presence of calcium, strontium, and barium nitrates it increases progressively (the rate of film formation decreases). At the same time all the properties of the surface layers formed — weight, thickness, surface irregularity, and other investigated properties — undergo a change.

The increase of the acidity of the solution is apparently the result of increased hydrolysis of the nitrates in increasing order from Mn to Ba, accompanied by the liberation of free nitric acid, which directly affects all the factors investigated.

SUMMARY

1. Nitrates of bivalent metals (Mn, Zn, Cd, Ca, Sr, and Ba) have an important effect on the main factors in the formation and properties of phosphate layers.

It is characteristic that the rate of layer formation is increased under the effect of manganese, zinc, and cadmium nitrates while it is decreased in the presence of calcium, strontium, and barium nitrates when the acidity of the solution of nitrates is increased; the acidity of the solution increases with the concentration of the salts in the solution in an increasing order from manganese nitrate to barium nitrate.

2. A new and decorative protective phosphate-oxide layer formed by phosphatation in the presence of calcium, strontium, and barium nitrates was obtained for the first time.

LITERATURE CITED

- [1] I. I. Khain, J. Appl. Chem. XXXII, 11, 2463 (1959). *
- [2] B. V. Nekrasov, Textbook of General Chemistry [In Russian] (State Chemistry Press, 1954), 654.
- [3] A. G. Samartsev, Protective Oxide Films [In Russian] (Acad. Sci. USSR Press, 1944).
- [4] I. I. Khain, Author's Certificate No. 66,887 (1946).
- [5] A. M. Yampol'skii, Oxidation and Phosphatation of Metals [In Russian] (State Scientific-Technical Press for Machine Construction Literature, 1950), 76.
- [6] G. M. Badal'yan, Protection of Metals by Phosphate and Oxide Films [In Russian] (Shipbuilding Industry Press, 1952), 36.
- [7] A. Ya. Drinberg, E. S. Gurevich, and A. V. Tikhomirov, Nonmetallic Protective Coatings [In Russian] (State Chemistry Press, 1957), 148.
- [8] H. A. Holden, Electroplating and Metal Finishing 9, 9, 291 (1956).
- [9] W. Roggendorf, Industrie-Anzeiger 78, 11, 191 (1956).
- [10] H. Tippmann, Metalloberfläche 11, 358 (1957).

Received July 20, 1959

*Original Russian pagination. See C. B. Translation.

TOWARD THE QUESTION OF THE DETERMINATION OF OXYGEN IN METALLIC CHROMIUM OF HIGH PURITY

N. V. Ageev, A. I. Ponomarev, and V. A. Trapeznikov

At present there is considerable interest in the possibility of producing heat-stable alloys based on chromium [1]; this has aroused interest in metallic chromium itself.

One of the main requirements for increasing the quality of chromium is its preparation with the minimum quantity of impurities, especially gases.

At present, methods of preparing chromium of high purity [1-5] are known, in which the content of gases is low, varying from ten-thousandths to hundredths of a percent. To find such quantities of gases, one must have reliable and accurate methods of analysis.

There are two methods for determining oxygen in metals: the vacuum fusion method and the chemical method.

In the determination of gases by the vacuum fusion method, the metal sample is dissolved in molten iron at 1600-1650° in a high vacuum. The molten iron, contained in a graphite crucible, is saturated with carbon which reduces the oxide to metal and combines with the oxygen to form carbon monoxide. This makes it possible to isolate the oxygen in the form of carbon monoxide. The gases extracted from the metal (H_2 , O_2 , and N_2) are collected and analyzed [6, 7]. However, this method requires complex apparatus and much time. In the case of the determination of gases in chromium it must be taken into account that chromium, having a high vapor pressure, evaporates in the process of fusion in vacuo, trapping part of the gases evolved from the sample being analyzed, and then condenses in the cool parts of the furnace in the form of a sorption-active film which also can absorb part of the gases evolved from the metal. As the extraction temperature rises, the amount of distilled chromium increases. In order to decrease the evaporation of chromium, it would be desirable to lower the temperature to which the metal is heated, but in this case the gases might not be completely extracted from the chromium.

In contrast to the vacuum fusion method, where oxygen is determined by reduction of the oxides occurring in the chromium with carbon, the proposed chemical method consists essentially in conversion of all the oxygen to a chemical compound — chromic oxide. In order to convert all the oxygen present in the chromium to a combined, analytical form, a special treatment is used, which leads to formation of a variety of chromic oxide which is insoluble in dilute hydrochloric acid.

In work [8] it was shown that the oxygen content in the chromium can be determined from the chromic oxide content by rapidly heating the chromium in vacuo at 800° for 2 hours, cooling, and dissolving it in dilute hydrochloric acid. In this case, the chromic oxide remains in the form of an insoluble precipitate.

The reliability of this method of determining the oxygen content in chromium was checked [9-11], and it was shown that under certain experimental conditions this simple method gives quite acceptable results. The optimum ignition temperature is considered to be 800° [8-10] or 750° [12] for an ignition time of 2 hours. Increase of the ignition time from 3 to 48 hours at 800° [10] has no substantial effect on the content of insoluble chromic oxide.

For solution of the sample, the use of hydrochloric acid with a concentration of 5-10% (but not over 10% [8, 9]) is recommended, since with higher concentrations the chromic oxide itself may dissolve [9].

On the question of the ignition time of the samples (2 hours), as well as the concentration of the hydrochloric acid (not over 10%) used to dissolve the chromium, there exists an established opinion. However, on the question of taking and preparing the sample or the conditions of heat-treatment in vacuo there are no detailed directions or explanations. In using the chemical method, therefore, we directed our attention [13] mainly to the indicated questions.

Taking and preparation of samples. Sufficiently pure chromium can be prepared by known methods in the form of a fine fraction, in the form of lamellae in the case of electrolytic chromium [5], and in the form of fine crystals in the case of iodide chromium [1, 2] or chromium prepared by sublimation [4]. For the determination of oxygen in samples of cast or deformed chromium a coarse sample may be taken — in the form of a separate small, broken-off piece with a clean surface or in the form of a large chip.

When a sample is taken for analysis, the established rules for its preparation must be observed.

The sample taken is thoroughly washed in chemically pure dichloroethane, benzene, or alcohol in order to remove foreign matter and grease. For removal of moisture the sample is washed with acetone and the residual acetone removed with ether (crystals of iodide chromium or chromium purified by sublimation are not subjected to the stated purification).

The sample weight is decided mainly on the basis of the expected amounts of oxygen in the chromium. The optimum sample weight is 2-5 g, but in the case where the expected oxygen content is less than 0.005 wt. %, an 8-10 g sample is recommended. The sample taken is weighed on an analytical balance.

Vacuum treatment of the sample. Gaseous impurities in the metal may be present in different forms.

Oxygen may be present in chromium in the form of a solid solution of intrusion, in the form of gaseous inclusions or bubbles in the pores (O_2 , H_2O), in the combined state in the form of various solid chemical compounds (Cr_2O_3 , Al_2O_3 , SiO_2 , etc.), and finally in the form of an adsorbate on the metal surface.

The sample is heated in vacuo at 850-900° for 2 hours. Oxygen, present in the chromium in the uncombined state (in the form of a solid solution or gaseous inclusions), combines with the chromium to form chromic oxide, and the latter is converted by heating to a form insoluble in 10% HCl. Oxygen present in the combined state in the form of Cr_2O_3 inclusions of varying dispersity in the chromium, which were formed in the course of preparation of the metal and its metallurgical treatment, and as a result of heat treatment (on ignition), is also converted to the form of chromic oxide Cr_2O_3 which is insoluble in dilute hydrochloric acid, and determined by chemical analysis.

In order to choose the optimum ignition temperature, we studied the stability of pure chromic oxide Cr_2O_3 on treatment with dilute hydrochloric acid (10% HCl) after heating the oxide at 850° for 2 hours both in air and in vacuo. For this, pure chromic oxide was prepared by decomposing ammonium bichromate (p.a.r. grade) [14]. The product obtained was thoroughly washed with hot water, after which the solution was decanted from the settled precipitate, and the latter was washed on a filter until a perfectly clear filtrate was obtained, placed in a drying oven, and dried at 140-160° for 10-15 hours. Finally, the precipitate was heated for 1.5-2 hours at 800 to 850° for removal of traces of moisture and volatile impurities. In order to study the solubility of the pure chromic oxide obtained, with respect to the temperature and conditions of ignition, it was subjected to special heat treatment under conditions similar to those required in the determination of oxygen in pure metallic chromium, i.e., at 850° for 2 hours in vacuo, and also in air. Ignition in air was carried out in porcelain crucibles in a muffle furnace. Ignition in vacuo was used because, in determining oxygen in metallic chromium, the latter must not be heated in air if oxidation is to be avoided. Ignition in vacuo (10^{-5} mm) was carried out in special previously ignited and degassed fused-silica ampules with narrow openings, in which losses of oxide through pulverization during the evacuation of air from the silica tube, in which the ampules containing the samples were placed, were excluded. The sample of pure chromic oxide (0.1-0.2 g) was weighed before ignition and again after ignition at 850° for 2 hours. The ignited chromic oxide was then treated with 100 ml of gently boiling 10% HCl for 1 hour; after cooling and standing not less than 2 hours the Cr_2O_3 precipitate was filtered out, dried, strongly heated until the filter paper was entirely consumed, and weighed.

The change in weight of the chromic oxide with respect to ignition at 850° and solution in 10% HCl is given in Table 1.

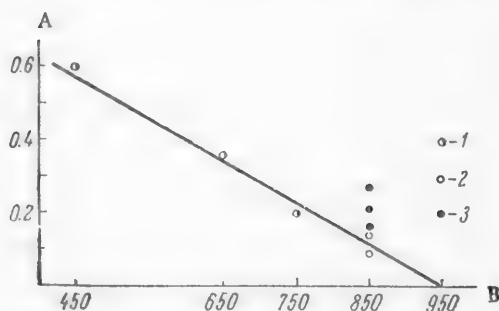
TABLE 1

before ignition (initial sample)	Weight of chromic oxide (in g)			Change in weight (in g)		
	After ignition at 850°		After solution in 10% HCl	After ignition	After solution in 10% HCl	Solubility (in rel. %)
	in air	in vacuo				
0.0930	0.0929	—	0.0927	—0.0001	—0.0002	0.21
0.1138	0.1137	—	—	—0.0001	—	—
0.1463	0.1462	—	0.1458	—0.0004	—0.0004	0.27
0.1257	0.1256	—	0.1254	—0.0001	—0.0002	0.16
0.1050	0.1049	—	—	—0.0001	—	—
0.1079	—	0.1078	0.1077	—0.0001	—0.0001	0.09
0.1456	—	0.1454	0.1452	—0.0002	—0.0002	0.14

It follows from the data obtained, that the selected ignition temperature of chromic oxide Cr_2O_3 does not affect its weight regardless of whether the oxide was ignited in air or in vacuo, and the observed variation in weight does not exceed admissible weighing deviations.

On studying the solubility of chromic oxide, ignited at 850°, in 10% HCl we found a very insignificant loss in weight (Table 1). The weight loss may be due either to the very slight solubility of Cr_2O_3 in dilute hydrochloric acid or to the passage of an insignificant quantity of submicroscopic oxide particles through the filter into the solution. In order to check the latter, the filtrate was evaporated to minimum volume and the content of chromic (Cr^{3+}) ions in the solution checked. However, no chromium ions were found in the solution by a colorimetric reaction.

Therefore the weight loss observed by us may be due to the very slight solubility of pure chromic oxide in 10% hydrochloric acid; this is also confirmed by the data of the cited work [15], where the solubility of pure chromic oxide Cr_2O_3 in dilute HCl after ignition in air at various temperatures for 2 hours was studied, and where it was shown that chromic oxide goes over to a form insoluble in dilute HCl when it is ignited at a temperature of 850° or higher. On turning to the graph (diagram) constructed from these data, it is seen that the solubility of



Effect of the ignition temperature of Cr_2O_3 on its solubility in dilute HCl. A) Solubility (in %); B) temperature (in °C). According to data of: 1) Budnikov [14]; 2 and 3) authors of the present article. Ignition: 2) in vacuo; 3) in air.

the oxide after ignition at 850°, determined by graphical extrapolation, is about 0.1-0.15 rel. %, which agrees with our experimental data. The solubility of the oxide in dilute hydrochloric acid may be reduced by raising the ignition temperature, for instance, to 950-1000° (figure). Taking into account the fact that the metallic chromium is ignited not in air but in vacuo, where a certain decrease in the loss in weight of the chromic oxide on solution in dilute hydrochloric acid (Table 1) is observed, one may use a somewhat lower ignition temperature than that given by the graph, namely 850-900°. At these temperatures chromic oxide Cr_2O_3 is more completely converted to a form which is stable to dilute hydrochloric acid, or nearly insoluble in it.

Thus, the optimum ignition temperature of very pure metallic chromium (with an oxygen content less than 0.01%) must be 850-900° instead of 750-800° as recommended in foreign works [8-12].

Vacuum ignition of the chromium sample (especially in the form of shavings or lumps) may be carried out in a fused-silica ampule from which the air is exhausted at room temperature to a pressure of 10^{-5} mm, after which the ampule is sealed off. Then the ampule containing the sample is placed in a furnace heated to 850 to 900° and kept at that temperature for 2 hours (in this case a more uniform distribution and partial coagulation of the chromic oxide particles in the metal are obtained), after which it is taken out of the furnace, cooled in air,

and opened in order to extract the sample. The next operation consists in solution of the metallic chromium sample; * for this the weighed sample is placed in a beaker, 100-200 ml of 10% HCl poured in, and the beaker covered with a watch glass and heated to boiling in a sand bath. If the acid evaporates, the beaker is refilled, the solution volume being kept within the stated limits. For better solution the contents of the beaker are periodically stirred. Heating is continued until the sample is completely dissolved, after which the solution is cooled to room temperature and left to stand at least 2-4 hours (preferably overnight) in order to ensure coagulation of the submicroscopic chromic oxide particles. The solution is filtered through a benzene-treated, dense paper filter (blue band) and the undissolved Cr_2O_3 precipitate washed on the filter with cold 4-5% HCl. Washing is continued until a negative reaction for chromic ion is obtained. Finally, the filter bearing the residue is washed with distilled water.

The washed precipitate, together with the filter, is dried in air and transferred to a porcelain crucible, the filter burned away, and the precipitate ignited to constant weight at 800-900° during 1.5 hours.

The chromic oxide precipitate obtained is weighed and the percentage of oxygen calculated by the formula

$$\% \text{ O} = \frac{\text{weight of } \text{Cr}_2\text{O}_3 \cdot 0.3157}{\text{weight of metal sample}} \cdot 100,$$

where 0.3157 is the gravimetric factor for oxygen in Cr_2O_3 [6].

From the practice of oxygen determination in metals it is known [6] that the results of chemical analysis depend to a considerable degree on the state of division and method of preparation of the sample. In Table 2 are given data showing the effect of the degree of division of the sample on the results of chemical analysis, these results being higher, the more finely divided is the sample. This may be due to adsorption phenomena. Powder, fine shavings, and fine grains, having high specific surface, are the most active forms of the metal in the case of gas adsorption.

TABLE 2

Degree of division of the sample	Sample wt. (in g)	Weight of Cr_2O_3 in pre- cipitate (in g)	O_2 content (in wt. %)
Powder	1.0562	0.0112	0.33
Fine shavings, ground finer in an Abich mortar.	1.5861	0.0161	0.32
	0.8925	0.0076	0.27
Medium shavings, taken with a cutting tool.	1.4118	0.0074	0.16
	1.3824	0.0084	0.19
	1.6784	0.0084	0.16
Coarse shavings	1.4508	0.0062	0.13

The method of preparing the sample by taking it with a drill or cutting tool also promotes adsorption phenomena. In this case, evolution of heat from the shavings and tarnishing of their surface as a result of oxidation are observed. In taking the sample, therefore, one must beware of heating of the metal, since this causes additional adsorption of oxygen.

There is also a certain amount of adsorbed oxygen and moisture on the inside walls of the silica ampule used for ignition of the sample, which may react with the chromium on ignition and may cause the results of the chemical analysis to be high. It should be noted that the use of ampules consisting of silica for ignition of the sample also may lead to high results. In work [2] on the preparation of iodide chromium by deposition of the latter in silica tubes, it was shown that the chromium is contaminated by gases, particularly oxygen, which diffuse through the walls of the silica tubes at 1100°, since silica glass is not reliably airtight in this case. The loss of

* P. P. Korostelev participated in the experimental part of the work on solution of the sample.

airtightness by silica at temperatures of 1000° and higher is pointed out in another work [6]; the absorption of hydrogen and carbon monoxide by silica at 700° is also known [16]. Furthermore, silica (SiO_2) is not chemically neutral and may react with the chromium, contaminating it in this case with oxygen, especially at high temperatures (above 1000°) and long ignition times. The high results, noted by certain authors [10], which are observed when ignition temperatures of 1000 and 1150° and times of 48 and 36 hours, respectively, are used, may be due partly to the indicated causes.

In the present work, in order to eliminate factors leading to high analytical results, different conditions of sampling and, especially, of vacuum treatment of the sample were used. The chromium sample was taken, as far as possible, in the form of coarse flakes, crystals, or a separate, detached piece with a clean surface. The sample was ignited in a silica boat fused in an oxygen flame, or in a metal boat,* placed in a qualitative silica tube with double walls, the space between which was filled with argon (or had a current of technical argon passing through it). The silica tube had to be ignited and degassed in a high vacuum beforehand and had to be rinsed with acetone and then ether for removal of moisture before it was loaded with the sample.

The tube was connected to the vacuum system and air pumped from it until a limiting, constant vacuum was reached; the system was checked for leaks, and heating of the silica tube and sample was begun. The sample was heated to 850-900°, kept at that temperature for 2 hours, and slowly cooled in the furnace, a high vacuum (10^{-5} mm) being maintained throughout by continuous pumping. Under these conditions of heat treatment, more complete removal of the adsorbed gas layer from the sample surface and the walls of the boat and silica tube is obtained.

The analytical results in this case are more stable and reliable. Shortcomings connected with the effect of the adsorbed gas layer on the sample surface were diminished but not completely eliminated, since the oxygen content is always higher at the surface of the sample than in the interior. This was found out through surface-layer etching of a sample prepared from cast chromium in the form of 10×10 mm cylinders with polished surfaces. The cylinder (or lump) was placed in a perforated glass bucket and put into a beaker containing 10% HCl, where its entire surface was uniformly etched.

The initial etching of the sample was continued for 15-20 minutes, after which the bucket with the remainder of the sample was transferred to another beaker for final solution of the latter. On analysis (by the method described above) the oxygen content in the surface (or outer) layer was obtained in the first case and the oxygen content in the interior of the specimen (or the remainder of the sample), in the second.

The results of several determinations of this kind are given in Table 3; for comparison the oxygen content in the shavings, obtained in the preparation of the cylinders, is also given.

TABLE 3

Form of sample	O ₂ content (in wt. %)			
Shavings, taken with a cutting tool	0.22	0.21	—	—
Separate lumps:				
surface	0.131	0.142	0.108	0.120
interior	0.091	0.114	0.077	0.092

The data of Table 3 show that the oxygen content in the indicated chromium samples is determined primarily by the amount of adsorbed oxygen present, and the more favorable the conditions for adsorption are, the higher the oxygen content is.

* The metal boat may be made of "Mo" or "Ta" sheet ignited in a high vacuum (10^{-5} - 10^{-6} mm) at 1500 to 1600°. A sample in the form of a separate piece may be ignited in an induction furnace in a basket made of molybdenum or tungsten wire.

The oxygen content is about 50% higher in shavings than at the surface of a separate lump, and twice as high in shavings as in the interior of the latter.

The excess oxygen content in the surface of a lump in comparison with that in the interior is about 30-40 rel. % on the average. On analyzing purer chromium specimens this excess increases and reaches 50%. The results of the experiments are given in Table 4.

TABLE 4

Wt. of layer dissolved in 10% HCl (in g)		Weight of chromic oxide in precipitate (in g)		Oxygen content (in wt. %)	
surface	interior	surface	interior	surface	interior
4.0140	10.3821	0.0031	0.0039	0.0244	0.0119
1.9771	7.4191	0.0018	0.0020	0.0288	0.0123

It was found, by using the method of surface-layer etching, that oxygen was nonuniformly distributed in the sample, the surface of the sample always containing more oxygen than the interior on account of adsorption of gases and moisture thereon. In order to eliminate the effect of oxygen adsorbed on the sample surface on the result of chemical analysis, the latter may be removed from the surface by brief, light pickling in concentrated hydrochloric acid provided the sample is in the form of an individual lump weighing at least 5 g.

The method of surface-layer analysis not only permits determination of oxygen on the surface and in the interior of a specimen, but also makes it possible to find the degree of distribution of oxygen with respect to depth in the specimen with sufficient accuracy. On analysis of cylindrical specimens by pickling each layer for 15 minutes, it was found that the oxygen in cast chromium specimens is distributed uniformly throughout the volume of the ingot. The results of one of these layerwise oxygen determinations are given below.

Layer	O ₂ content (in wt. %)
1	0.080
2	0.073
3	0.075
4	0.077
5	0.076
(remainder)	

The proposed chemical method of oxygen determination also permits one to determine, with a certain degree of accuracy, the form in which the oxygen may be present in the chromium. Electrolytic chromium, obtained by deposition from aqueous solutions, is usually contaminated with oxygen, the content of which sometimes reaches 0.8-0.9% [8].

On analysis of a sample in the form of flakes from one batch of electrolytic chromium, purified in a current of hydrogen, it was found that when the sample was dissolved in 10% HCl without ignition in vacuo, the oxygen content found was 1/10 as high as in the case where the sample was heat-treated in vacuo.

The amount of oxygen in the sample was 0.0028% before ignition and 0.030-0.034 wt. % after ignition.

Thus, the amount of oxygen in the chromium is increased after ignition in vacuo. This means that the amount of oxygen, combined in the form of chromic oxide Cr_2O_3 , in the flakes of the original electrolytic chromium before heat-treatment is negligible. Presumably, oxygen in the given type of chromium occurs mainly in the free state, i.e., uncombined, apparently in the form of gaseous inclusions (O_2 , H_2O) or as an adsorbate on the surface of the metal flakes.

The amount of free oxygen is determined as the difference between the amount of oxygen in the ignited chromium and the amount of oxygen in the original chromium. The accuracy of the method may be estimated from the data in Table 5.

TABLE 5

Weight of chromium sample (ing)	Weight of Cr_2O_3 obtained after ignition (in g)	O_2 content (in wt. %)	Value of absolute deviation from average result
4.9167	0.0007	0.0045	-0.0018
5.1792	0.0010	0.0061	-0.0002
5.0739	0.0010	0.0063	0.0000
5.0142	0.0010	0.0063	0.0000

SUMMARY

In the determination of oxygen in chromium the chemical method is perhaps the most acceptable method of analysis taking into account all forms of oxygen, and is more reliable than the vacuum fusion method, where difficulties are encountered in oxygen determination, owing to the high volatility of chromium under conditions of high vacuum and high temperatures.

The proposed method of oxygen determination is not prolonged, it is simple and convenient in use, and it does not require complex and costly equipment. The accuracy of the method is ± 10 rel. %, and the minimum determinable value is 0.001 wt. % when the sample is ignited at 850-900° for 2 hours.

The possibility of carrying out analysis by layers has been shown; this is an advantage of the chemical method, since the vacuum fusion method does not permit such analysis.

The determination of oxygen in commercial-grade chromium by the method described above will be less accurate, since in this case it is necessary to make a number of corrections in the result of determination, for oxygen combined in the form of $\text{Al}_2\text{O}_3 \cdot \text{SiO}_2$ and for the presence of carbides; this requires the use of special methods of analysis.

LITERATURE CITED

- [1] D. J. Maykuth and R. I. Jaffee, *Trans. ASM* 49, 948 (1957).
- [2] N. V. Ageev and V. A. Trapeznikov, *Collection: Investigations of Heat-stable Alloys* [In Russian] 1, 17 (1956).
- [3] *Met. Ind.* 90, 16, 309 (1957).
- [4] N. V. Ageev and V. A. Trapeznikov, *Collection: Investigations of Heat-Stable Alloys* [In Russian] IV, 237 (1959).
- [5] H. T. Greenaway, *J. Inst. Met.* 83 (4), 121 (1954).
- [6] Yu. A. Klyachko, A. G. Atlasov, and M. M. Shapiro, *Analysis of Gases and Inclusions in Steel* [In Russian] (1953).
- [7] J. T. Sterling, *Ductile Chromium*, Amer. Soc. Metals 188 (1957).
- [8] F. Adcock, *J. Iron Steel Inst.* 115, 369 (1927).
- [9] H. G. Chort, *Analyst* 75, 335 (1950).
- [10] A. H. Sully, E. A. Brandes, and A. G. Provan, *J. Inst. Met.* 81, 569 (1953).

- [11] Dieckmann and Hanf, *J. anorg. Chem.* 257, 73 (1949).
- [12] R. M. Fowler, T. C. Lancaster, and G. Porter, *Ductile Chromium*, *Amer. Soc. Met.* 121 (1957).
- [13] N. V. Ageev, A. I. Ponomarev, B. N. Melent'ev, and V. A. Trapeznikov, *Zhur. Priklad. Khim.* 30, 3, 474 (1957).*
- [14] B. V. Nekrasov, *Course in General Chemistry [In Russian]* 333 (1952).
- [15] P. P. Budnikov and Krauze, *Zhur. Priklad. Khim.* 4, 4 (1931).
- [16] V. G. Gruzin, *Control of the Temperature of Molten Iron Alloys [In Russian]* (1955).

Received January 12, 1959

*Original Russian pagination. See C. B. Translation.

INFLUENCE OF TEMPERATURE ON THE EFFECT OF POLARIZATION
IN THE CORROSION CRACKING OF V-95 ALLOY IN A 0.1 N
SOLUTION OF H_2SO_4 + 35 g/liter OF NaCl

V. V. Romanov and V. V. Dobrolyubov

In works of recent years the influence of polarization on the rate of corrosion cracking has been studied for a number of metals and corrosive media.

The data obtained in these investigations made it possible to determine [1] the characteristic shape of the polarization curve, which reflects the dependence of the rate of corrosion cracking on the cathodic and anodic current densities. The cathodic branch of this curve has three main sections: the first section, reflecting a certain increase in the rate of cracking at relatively low initial current densities, the second section, following the first and characterizing a very slight influence of increased current density on the rate of cracking of the metal, and the third section, characterizing a protective current which arrests the cracking process completely or for a long time in comparison with the cracking time in the absence of polarization. The anodic branch of the characteristic polarization curve consists of two main sections: the first section, showing substantial acceleration of corrosion cracking under the influence of low initial current densities, and the second section, following the first and characterizing a smaller effect of anodic polarization on the rate of corrosion cracking under the influence of relatively high current densities.

In one of the preceding works [2] it was found that temperature has a substantial effect on the form of the polarization curve in the corrosion cracking of MA-2 alloy in a solution containing 0.1 N H_2SO_4 + 35 g/liter of NaCl.

An analogous investigation for aluminum alloys is at least as important. Highly stable alloys based on aluminum, as a rule, are protected by plating; i.e., they may become corroded under stress in the presence of cathodic polarization. The use of aluminum parts in constructions, in contact with stainless steel, titanium, and certain other metals does not exclude the possibility of anodic polarization of those parts under similar conditions.

Thus, the probability of cathodic and anodic polarization of aluminum alloys subjected to corrosion cracking is as great as in the case of magnesium alloys. In connection with this, it is of definite practical interest to know the influence of temperature on the effect of polarization in the corrosion cracking of aluminum alloys.

The indicated data are no less important for development of the general theory of corrosion cracking of metals.

EXPERIMENTAL

The material used in the investigation was standard V-95 alloy sheet 1.5 mm thick, having the following chemical composition:

Alloy composition	Zn	Mg	Cu	Mn	Cr	Al
Amount (in %)	6	2.3	1.7	0.4	0.2	remainder

The alloy was subjected to preliminary heat treatment which decreased its stability to corrosion cracking: annealing to the solid solution during 3 hours at a temperature of 460-480°, quenching in water, aging at 120° for 4 hours, and cooling in air. The microstructure of the alloy after this heat-treatment is shown in Fig. 1.

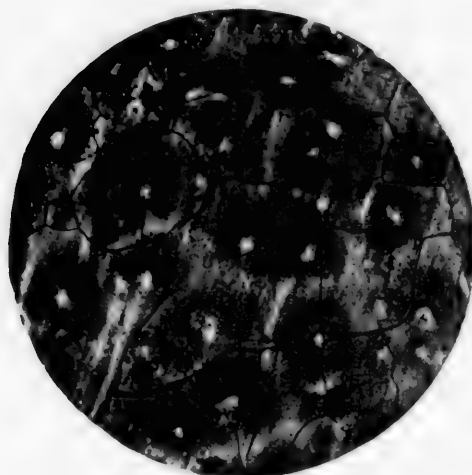


Fig. 1. Microstructure of the alloy under investigation after heat treatment which increased the rate of corrosion cracking. Magnification 200.

Before the experiment the samples were degreased and then treated with a solution of 6% HNO_3 + 1% $\text{K}_2\text{Cr}_2\text{O}_7$ for 3 minutes, washed, dried, and kept in a desiccator for 18-20 hours.

A platinum wire, wrapped around the working part of the samples in uniform loops, was used as an auxiliary electrode in polarization.

The stresses were produced by uniaxial elongation of the samples in a VP-8 machine, and were equal to 43 kg/mm² for the initial state.

In all other respects the investigation was carried out as before [2].

The data obtained, which are plotted in Fig. 2, show that in the absence of polarization a temperature rise causes a continuous decrease in the cracking time. This relation, expressed in semilogarithmic coordinates, is linear in character (Fig. 3).

Simultaneously with the increase in the rate of corrosion cracking on increase of temperature, the total corrosion rate of the alloy increased; these data will not be considered in the present work, however, since this question was specially investigated earlier by one of the authors together with Akimov [3].

The data plotted in Fig. 2, relating to the influence of temperature on the effect of cathodic polarization, show that the temperature has a substantial influence on the shape of the cathodic curves; the first section is about the same at 20 and 35°, somewhat greater at 50°, and absent at 70°. The second section varies in reverse order; i.e., it is greatest at 70° and least at 20°. The third section in the cathodic curves, which characterizes the protective current density,* increases linearly as the temperature rises (Fig. 4).

* The protective current density is arbitrarily taken to be that current density at which cracking does not occur during a period approximately 10 times as long as in the absence of polarization at the same temperature.

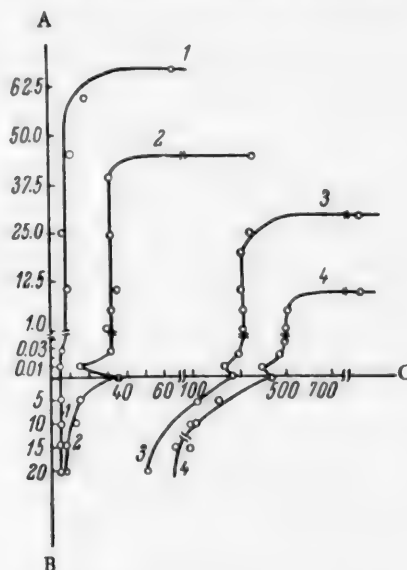


Fig. 2. Influence of temperature on the effect of cathodic and anodic polarization in the corrosion cracking of V-95 alloy in a solution containing 0.1 N H_2SO_4 + 35 g/liter of NaCl. A) D_c (in mA/cm²); B) D_a (in mA/cm²); C) cracking time (in minutes). Temperature (in °C): 1) 70; 2) 50; 3) 35; 4) 20.

In order to ascertain whether or not the increase in the "life" of the alloy on cathodic polarization is due to a possible change in the properties of the medium and the protective films, the protective current in a number of separate experiments was turned off before the arbitrarily chosen time characterizing protection of the alloy. After the current was turned off, the samples soon disintegrated — the more rapidly, the higher was the temperature.

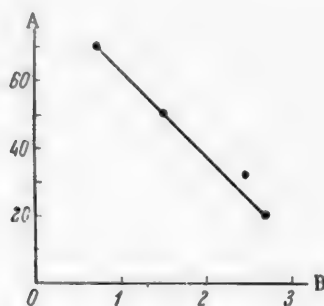


Fig. 3. Influence of temperature on the rate of corrosion cracking of V-95 alloy in a solution containing 0.1 N H_2SO_4 + 35 g/liter of NaCl. A) Temperature (in $^{\circ}\text{C}$); B) log of cracking time.

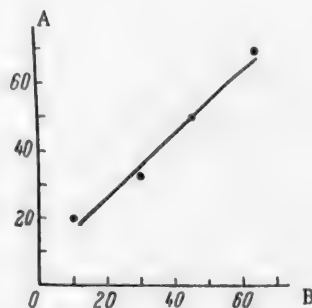


Fig. 4. Influence of temperature on the protective current density in the corrosion cracking of V-95 alloy in a solution containing 0.1 N H_2SO_4 + 35 g/liter of NaCl. A) Temperature (in $^{\circ}\text{C}$); B) protective current density D_c (in ma/cm^2).

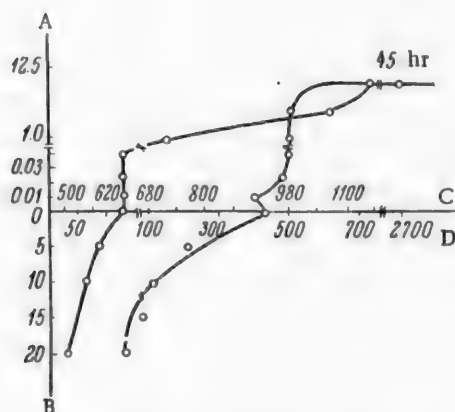


Fig. 5. Effect of cathodic and anodic polarization on the rate of corrosion cracking and the electrode potential of V-95 alloy in a solution containing 0.1 N H_2SO_4 + 35 g/liter of NaCl at 20 $^{\circ}$. A) D_c (in ma/cm^2); B) D_a (in ma/cm^2); C) electrode potential — E_h (in mv); D) cracking time (in minutes).

Data on the influence of temperature on the effect of anodic polarization show that this effect is observed at 20, 35, and 50 $^{\circ}$ but is absent at 70 $^{\circ}$. At lower temperatures (20 and 35 $^{\circ}$) a shortening of the cracking time occurs, which is continuous and is relatively greater than at 50 $^{\circ}$.

The influence of polarization on the electrode potential of the metal, which was measured with respect to a saturated calomel electrode by a compensation method and the readings converted to values on the hydrogen scale, was investigated at 20 $^{\circ}$.

In Fig. 5 are shown potentials at the corresponding current densities, selected for a time of 60 minutes, since this time corresponds to the maximum rate of cracking at an anodic current density of 20 ma/cm^2 .

These data show that in the case of cathodic polarization at initial current densities at which shortening of the cracking time is observed, the potential does not change. It begins to change at current densities corresponding to the beginning of the second section of the cathodic curve.

The anodic curve is characterized by continuous increase of potential with increase in the current density.

Cracking both with insufficient cathodic polarization and with anodic polarization took place as a result of the preferential growth of a single corrosion crack. Cracks parallel to the main one did not arise, so that the influence of polarization on the character (form) of the corrosion cracks could not be studied.

In the construction of the polarization curve, the deviation of the results was greatest in the second section of the cathodic branch and did not exceed 6%.

DISCUSSION OF RESULTS

The increase in the rate of corrosion cracking on increase of temperature in the absence of polarization may be explained by the increase in the activity of local microcouples, occurring in this case [3] in the regions of the walls and bottoms of growing corrosion cracks.

This also explains the observed increase in the protective current density with increase in temperature (the third section in the cathodic curves). The more active these couples are, the greater is the strength of the current that must be applied from outside in order to render them inactive.

The disappearance of the first section in the cathodic curves on increase of the temperature to 70° was observed earlier in the case of the magnesium alloy MA-2 [2]. In the present investigation this dependence was less pronounced, which is more readily explained by insufficiently careful measurement of the given section owing to the limited quantity of identically prepared samples than by any change in the character of the dependence itself. Therefore, the hypothesis proposed in order to explain the dependence, found on investigation of the magnesium alloy, may be used to explain the data obtained for the V-95 alloy.

The more pronounced influence of anodic polarization on the rate of cracking at relatively low temperatures, and also the absence of any effect of this polarization on the rate of cracking at 70°, may be due to enhancement of those factors, which inhibit cracking, with increase of temperature.

Anodic polarization in corrosion cracking causes acceleration of the process owing to a positive shift in the potential of the metal [4]; it may simultaneously cause an increase in the uniformity of the corrosion process. Increase in temperature apparently favors the latter effect by weakening the protective film and intensifying the action of local microcouples on the metal surface.

SUMMARY

1. Temperature substantially influences the shape of the polarization curve in the corrosion cracking of V-95 alloy in a solution containing 0.1 N H_2SO_4 + 35 g/liter of NaCl. The current density, required for protection of the alloy from corrosion cracking, increases linearly as the temperature rises.
2. The initial shortening of the time of corrosion cracking, which occurs at low initial current densities, is observed at the temperatures 20, 35, and 50°; it does not occur at 70°.
3. The accelerating influence of anodic polarization on the rate of corrosion cracking is most effective at 20 and 35°, less effective at 50° and absent at 70°.

LITERATURE CITED

- [1] V. V. Romanov, Collected Works, D. I. Mendelev Voronezh Chem. Soc. II [In Russian] (1959).
- [2] V. V. Romanov and V. V. Dobrolyubov, Zhur. Priklad. Khim. 31, 5, 743 (1958).*
- [3] G. V. Akimov and V. V. Romanov, Collection: Inst. Phys. Chem. of the Academy of Sciences, 4, 50 (1955).
- [4] V. V. Romanov, Collected Works, D. I. Mendelev Voronezh Chem. Soc. I, 105 (1957) [In Russian].

Received November 11, 1958

*Original Russian pagination. See C. B. Translation.

CORROSION OF LEAD IN CONTACT WITH GRAPHITE

V. A. Titov and É. N. Semkova

I. V. Stalin Moscow Steel Institute

In the production of chemical products which severely attack the apparatus at elevated temperatures and pressures, the question of the choice of corrosion-resistant materials for construction of the apparatus presents great difficulties.

The use of corrosion-resistant metallic materials alone, e.g. lead, or a nonmetallic material having high chemical stability, e.g., graphite, for the internal protective lining of the apparatus is not always possible owing to the characteristics of these materials in construction. Therefore, the cover and upper part of the apparatus are lined with lead, and the body is lined with graphite tile (Fig. 1). In the case of contact between the graphite and the lead, however, the useful life of the latter in corrosive media, e.g., hydrochloric acid, is greatly diminished owing to contact corrosion.

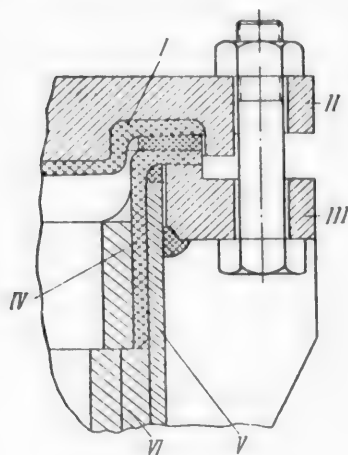


Fig. 1. Lining of the cover and body of a steel reaction vessel. I) Plating (S-1 lead); II) cover (steel 3); III) flange (steel 3); IV) collar (S-1 lead); V) shell (steel 3); VI) lining (graphal tile).

Contact corrosion is a rather common cause of corrosion of metals in the course of their use in electrolytes. This is due to the necessity of using dissimilar metals in construction, which leads to the formation of galvanic macrocouples. The rate of contact corrosion is proportional to the total current flowing through a cell consisting of an anode metal having a more negative electrode potential and a cathode metal having a more positive electrode potential.

Contact injurious to lead will exist in the case where the lead forms a couple with a material having a more positive electrode potential. Such materials include semimetal and noble metals (Cu, Ag, Au, Pt, etc.) and nonmetals, graphite in particular.

Cases of accelerated disintegration of parts, apparatus, and constructions composed of dissimilar metals are numerous [1-7]. However, in the literature examined by us we did not find any instances of contact corrosion of lead in a couple with graphite, unless indications of the qualitative effect of the ratio of areas of graphite and lead on the rate of corrosion of the latter [8] are considered. The increase in the rate of corrosion of lead in contact with graphite, observed when the area of the latter is greater than that of the lead, follows from the theory of galvanic cell operation [9, 10].

The corrosion resistance of lead is determined to a considerable extent, in the absence of a macrocontact, by the degree of its heterogeneity. For instance, such impurities in lead as: Sb, Sn, Bi, Cu, Ag, etc. cause microcurrents and increase the corrosion of the lead [8]. Therefore, the grade of the lead used in the lining of a steel reaction vessel is of substantial importance in determining the life of the lining. With regard to the corrosion resistance of lead in various media, a great number of works have been published in which this question is quite fully elucidated [1, 8-13]. Here, however, it is proper to note that the corrosion of lead and the rate thereof are functions of factors leading to the formation of a protective film on the surface of the lead.

The corrosion resistance of lead in the medium of interest to us — 99% HCl solution — amounts to $19.0 \text{ g/m}^2 \cdot \text{hour}$ at 20° , and the depth index of corrosion under these conditions is equal to 14.44 mm/yr [8]. According to other data, lead containing 99.7% Pb corrodes in anhydrous HCl at a rate of $0.32 \text{ g/m}^2 \cdot \text{hour}$ at 15° , $0.46 \text{ g/m}^2 \cdot \text{hour}$ at 40° , and $2.53 \text{ g/m}^2 \cdot \text{hour}$ at 100° [11].

Schikorr [14] made a rather thorough study of the stability of lead in hydrochloric acid and found that on treatment with concentrated acid (7.7 N HCl) the corrosion of lead continued during the entire time of the tests, even when they were prolonged, while with acid of low concentration (0.01 N HCl) the corrosion of lead quickly ceased. This is explained by the formation of a protective film on the lead in weak acid, which inhibits its corrosion, whereas in concentrated acid the film on the lead practically does not form.

Graphite is stable in hydrochloric acid of any concentration even at the boiling point of the acid [15, 16]. Graphite impregnated with phenol-aldehyde resins (graphal) is impermeable to liquids, including hydrochloric acid [8].

The purpose of the present work was to investigate the corrosion resistance of sheet lead, situated in contact with the graphite lining of the steel cover and body of a reaction vessel (Fig. 1), in hydrochloric acid containing methyl chloroformate.

EXPERIMENTAL

Materials. Type S-1 sheet lead containing 99.98% Pb.

The mechanical properties of this grade of lead are as follows: yield strength 1.8 kg/mm^2 , relative elongation 40-50%, hardness 4.0-4.6 H_B ; coefficient of linear expansion $0.0000273 \text{ degree}^{-1}$, specific gravity 11.25 [17].

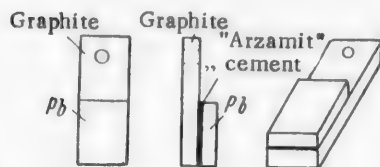


Fig. 2. Experimental samples after cementing the lead to the graphite.

Electrode graphite has the following properties: density $2.15\text{--}2.25 \text{ g/cm}^3$, compressive strength $400\text{--}500 \text{ kg/mm}^2$, porosity 20-30%, specific electrical resistance $8\text{--}20 \text{ ohm} \cdot \text{mm}^2/\text{m}$ [18].

Corrosive media. Chemically pure hydrochloric acid and methyl chloroformate — ClCOOCH_3 — were used as corrosive media; from them, 20 and 35% HCl solutions and 20 and 35% HCl solutions containing 3 and 10% methyl chloroformate were made up. The methyl chloroformate was added to the HCl solutions in order to approximate the operating conditions of the apparatus, in the experiments.

Lead samples measuring $20 \times 15 \times 5 \text{ mm}$ were cleaned with emery cloth, degreased with acetone, and weighed on an analytical balance with an error not greater than 0.0002 g , before testing.

Graphite samples measuring $40 \times 15 \times 5 \text{ mm}$ were cut out of an electrode and subjected twice to impregnation in a phenol-aldehyde mixture, followed by drying at $100\text{--}110^\circ$, beforehand. Before and after each drying, the samples were weighed to determine the degree of packing, which was calculated by the formula

$$\eta = \frac{\Delta P}{P} \cdot 100\%,$$

where ΔP is the change in weight after impregnation (in g) and P is the initial sample weight (in g).

In our experiments the "percent of impregnation" proved equal to 8.0, which corresponds to the degree of packing of the graphite, usually attained under production conditions.

After this the lead and graphite samples were cemented together (Fig. 2) with "Arzamid-4" cement in order to prepare an experimental lead-graphite couple.

The electrical contact between the cemented materials was checked by connecting the prepared sample into an electrical circuit with a signal lamp.

The prepared samples were again degreased and weighed. The ratio of working surfaces of the lead-graphite couple (S_{Pb}/S_C) was made equal to 1/2.3, approximately corresponding to the ratio of lead and graphite-tile surfaces in the reaction vessel.

The experiments were carried out in glass flasks, provided with reflux condensers, in a thermostat. The temperature did not vary more than $\pm 2^\circ$ from the set value. Three samples were put into each flask on glass hooks: graphite - lead in contact, graphite alone, and lead alone.

Three series of experiments were carried out, in which the temperatures of the media were 20, 40, and 71° . The experiments were performed continuously during 145 hours.

DISCUSSION OF RESULTS

On boiling, hydrogen chloride gives an azeotropic mixture with water as a rule [19].

The methyl chloroformate added to the acid hydrolyzes and decomposes on heating to form HCl, CO_2 , and some methanol [20].

In connection with this, the corrosive media were in-constant during the first hours, mainly owing to appreciable variations of the HCl concentration in the solutions. In the course of time the composition of the medium apparently approached that of an azeotropic mixture. The medium was not analyzed, since it was replaced with a fresh one every day.

In Fig. 3 is shown a graph of the effect of temperature on the rate of corrosion of lead in contact with graphite (curves 2, 4) and without such contact (curves 1, 3) in 20% and 35% hydrochloric acid. The path of the curves indicates an exponential relation between the rate of corrosion and the temperature, as well as the fact that the rate of corrosion of lead in contact with graphite (curves 2, 4) is much greater than without contact (curves 1, 3). Furthermore, the graph plainly shows that the rate of corrosion of lead in 35% hydrochloric acid (curves 3, 4) is increased in comparison with that in 20% acid (curves 1, 2), the increase becoming greater as the temperature rises. Analysis of the graph leads to the conclusion that contact of graphite with lead increases the corrosion of the lead more than 100% on the average in 20% HCl and about 50% in 35% HCl, owing to formation of the corrosion current of the galvanic couple C-Pb; on increase of the activating factor - the temperature of the acid solutions (from 20 to 71°) - the corrosion of lead, with or without contact with graphite, increases about sevenfold as a result of a decrease in the hydrogen overvoltage; as the acid concentration increases (from 20 to 35%), the corrosion of lead in contact with graphite increases on the average about nine-fold because of the decrease in the pH of the medium.

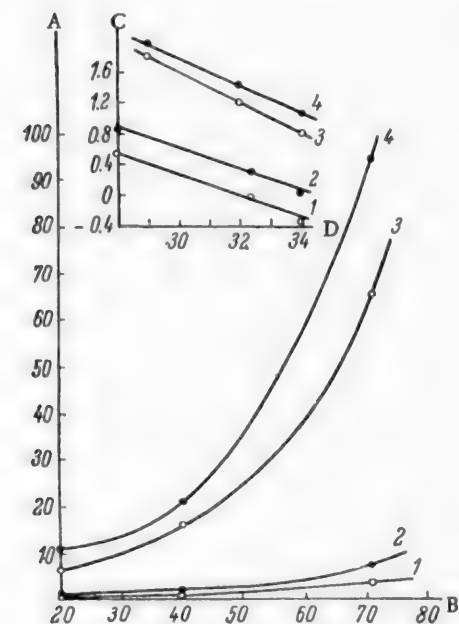


Fig. 3. Effect of temperature on the rate of corrosion of lead in 20% HCl (1, 2) and 35% HCl (3, 4) in contact with graphite (2, 4) and without such contact (1, 3). A) Rate of corrosion (in $g/m^2 \cdot hour$); B) temperature (in $^\circ C$); C) value of $\log K$; D) value of $\frac{1}{T} \cdot 10^4$.

By means of the graph of $\log k = f(1/T)$ (Fig. 3, top) the effective activation energy of the process (Q) was determined; its value varies between 7 and 9 kcal/mole and corresponds to chemical, but not concentration polarization.

At 20° the corrosion of lead in hydrochloric acid, as is generally known, is determined by the cathodic reaction. This also was found at a high temperature (70°). Hence, Q should be referred to the discharge process of H^+ ions, i.e., the characteristic of the hydrogen overvoltage. Values of Q for lead and graphite are nearly

alike; i.e., the latter have about the same temperature coefficient of hydrogen overvoltage. The difference between the slopes of the straight lines for experiments in 20% HCl (straight lines 1, 2) and 30% HCl (straight lines 3, 4) indicates an increase in the activation energy of the hydrogen-ion discharge process with increase in the HCl concentration.

The effect of temperature on the rate of corrosion of lead in contact with graphite in acid solutions of these same concentrations but with admixtures of methyl chloroformate is shown in Fig. 4. Analysis of the graph shows that as the amount of methyl chloroformate admixture in 20% HCl increases, the rate of corrosion of the lead increases insignificantly (curves 1, 2, 3). In more concentrated acid (35% HCl) the rate of corrosion of the lead is lowered insignificantly by a 3% admixture of methyl chloroformate and more appreciably by a 10% one (curves 4, 5, 6).

In order to explain the effect of contact with graphite on the corrosion of lead, the potential change of lead and graphite in 35% HCl at 25° was investigated. The experiments were performed with an ordinary potentiometric set-up. In order to exclude the effect of temperature on the potential change, the experiments were performed in a thermostat,

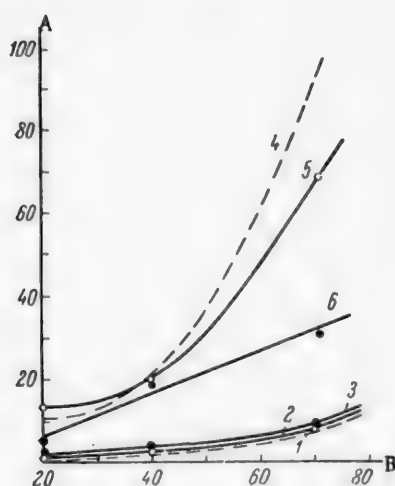


Fig. 4. Effect of the temperature of the medium on the rate of corrosion of lead in contact with graphite. A) Rate of corrosion (in $\text{g}/\text{m}^2\cdot\text{hour}$); B) temperature (in $^{\circ}\text{C}$). 1, 2, 3) Rate of corrosion in pure 20% HCl and in 20% HCl with admixtures of 3 and 10% CICOCH_3 , respectively; 4, 5, 6) the same in pure 35% HCl and in 35% HCl with admixtures of 3 and 10% CICOCH_3 , respectively.

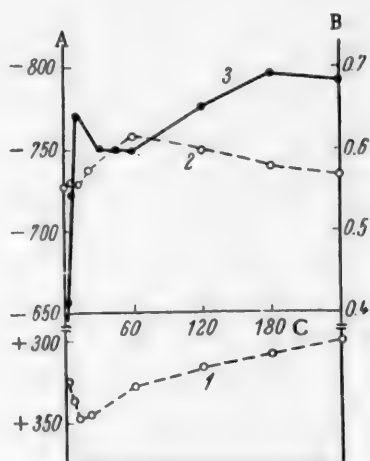


Fig. 5. Variation of the electrode potentials of graphite (1) and lead (2) and the current in the lead-graphite couple (3) with time in 35% HCl. A) Potential (in mv); B) current (in ma); C) time (in min).

In Fig. 5 are shown the results of the experiments, analysis of which shows that lead acts as an anode with respect to graphite (in contact with it) (Curve 2), the initial potential difference of the C-Pb couple being 1.054 v. Hence, it is no wonder that lead in contact with graphite is rapidly corroded in the beginning of the experiment. Subsequently, the potentials approach each other, but very slightly (after 4 hours of the experiment the potential difference of the couple is 1.040 v), as a result of polarization, under the experimental conditions; hence the corrosion of the lead will continue with only a slight drop in rate.

The negative shift in the potential of lead at the beginning of the experiment may be explained by destruction of the original protective film, and the subsequent positive shift, by polarization (curve 2).

The initial rise and subsequent fall of potential of graphite are due to aeration by absorbed atmospheric oxygen and polarization, respectively (curve 1).

The rate of corrosion of lead in contact with graphite is determined by the current in this couple. The corrosion current of the lead-graphite couple was measured in 35% HCl at 25°. The path of curve 3 in Fig. 5 indicates the presence of a large corrosion current in the couple, amounting to about 0.68 ma when the ratio of areas of anode (lead) and cathode (graphite) is equal to one. The corroding surface of the lead in the experiments amounted to 18 cm². After 4 hours of the experiment the lead sample weighed 0.2768 g less than at the beginning, which corresponds to a rate corrosion of 39 g/m²·hour or 30 mm/year. The maximum value of the depth index of corrosion of lead in contact with graphite was observed in the case of corrosion in 35% HCl, and corresponded to 72 mm/year. This indicates that a 5 mm thick lead lining in a reaction vessel will be removed from the structure in about one month under similar conditions of use.

Graphite remained essentially unchanged in the media tested by us.

SUMMARY

1. When graphite is combined with lead in hydrochloric acid solutions, an electrochemical couple is formed, in which the lead acts as anode and the graphite, as cathode.

The potential difference between lead and graphite in 35% HCl at 25° reaches 1.054 v, and the corrosion current amounts to 0.68 ma. Contact of graphite with lead increases its corrosion more than 100% in 20% HCl and about 50% in 35% HCl.

2. The rate of corrosion of lead in hydrochloric acid of 20 and 35% concentrations increases exponentially about sevenfold as the temperature rises from 20 to 71°.

3. It has been established that the degree of corrosion of lead in contact with graphite in 35% HCl is about 10 times as great as in 20% HCl.

4. Admixtures of methyl chloroformate in hydrochloric acid affect the corrosion of lead in different ways, depending on the acid concentration; in 20% HCl they increase the rate, whereas in 35% HCl they decrease it.

5. The maximum rate of disintegration of lead by corrosion was observed when the latter was in contact with graphite in 35% HCl at 71°, and amounted to 93.5 g/m²·hour. In this case, the depth index of corrosion was 72.0 mm/year.

6. The experiments showed that under the experimental conditions lead in contact with graphite will not protect a steel reaction vessel from corrosion for long.

It is recommended that the reaction vessel be lined only with graphal tiles in such cases.

LITERATURE CITED

- [1] U. R. Evans, Corrosion, Passivity, and Protection of Metals [Russian translation] Metallurgizdat (1941).
- [2] R. Heyn and O. Bauer, Mitt. Matt. Prief., Anit. 26, 526 (1935).
- [3] W. Hause and G. Gad, Gesundheits Eng. 58 (1935).
- [4] Corrosion of Metals, Collection of Translations of Articles from Foreign Periodical Literature (Russian translation). Edited by G. V. Akimov (IL, 1953).
- [5] W. McLaren, Prans. Inst. Marine Eng. 37, 485 (1925).
- [6] V. O. Krenig, Corrosion of Metals [In Russian] (ONTI - NKTP, 1936).
- [7] M. Shmidt and L. Wettermlk, Z. prakt. Metallbearb. 45 (1935).
- [8] Corrosion and the Chemical Stability of Materials, Handbook [In Russian] Edited by Dollezhal', (Mashgiz, 1954).
- [9] G. V. Akimov, Theory and Methods of Investigation of the Corrosion of Metals [In Russian] (Acad. Sci. USSR Press, 1945).

- [10] N. D. Tomashov, Theory of the Corrosion of Metals [In Russian] Metallurgizdat (1952).
- [11] V. P. Batrakov, Corrosion of Construction Materials in Aggressive Media [In Russian] Oborongiz (1952).
- [12] V. P. Barannik, Brief Handbook on Corrosion [In Russian] (Goskhimizdat, 1953).
- [13] Corrosion of Metals, 1. Edited by V. V. Skorchelletti [In Russian] (Goskhimizdat, 1952).
- [14] G. Schikorr, Korrosion und Metallschutz 6, 5181 (1940).
- [15] I. Ya. Klinov, Corrosion of Chemical Apparatus and Corrosion-Resistant Materials [In Russian] (Mashgiz, 1954).
- [16] G. V. Sagalaev, Nonmetallic Corrosion-Resistant Materials and Coatings [In Russian] Transactions of the Conference (Goskhimizdat, 1955).
- [17] Sulfuric Acid Technician's Handbook [In Russian] (Goskhimizdat, 1952).
- [18] L. Ya. Markovskii, et al., Chemical Electrothermics [In Russian] (Goskhimizdat, 1952).
- [19] Yu. V. Karyakin, Pure Chemical Reagents [In Russian] (Goskhimizdat, 1947).
- [20] V. Nekrasov, Chemistry of War Gases [In Russian] (Goskhimizdat, 1950).

Received December 22, 1958

THE INFLUENCE OF CURRENT DENSITY AND SULFURIC ACID CONCENTRATION ON THE MAGNITUDE OF THE INTERNAL STRAINS IN ELECTROLYTIC COPPER DEPOSITS

N. P. Fedot'ev and A. A. Khonikevich

An important problem of modern electroplating is the production of metal deposits with the smallest possible internal stresses. High internal stresses in galvanic deposits lead to lowering of the fatigue strength of components which are coated and to a higher percentage of rejects. Factors giving rise to internal stresses in galvanic deposits have been fairly closely studied in the case of chromium- and nickel plating but the problem has not been at all extensively discussed in the literature in the case of copper-plating [1-4]. Nothing at all has been published about the influence of reversed current on the mechanical properties of copper deposits — internal stresses, microhardness, etc.

In the present work we studied the influence of current density (D_K), H_2SO_4 concentration in the electrolyte and current reversal on the internal stresses and microhardness of copper deposits. We also determined the cathode potential (ϵ_K) and the cathodic current efficiency (η_K).

EXPERIMENTAL

Experimental Procedure

Measurement of the deflection of a flexible cathode, necessary for determination of the magnitude of the internal stresses, was effected with the help of a vertical optimeter by the technique developed by Fedot'ev, Glikman and Chernova [5].

Figure 1 is a line diagram of the set-up for determination of the deflection of a cathode.

By the term "positive internal stresses" (tension) is implied in this paper those stresses that subject the deposit to tension and cause it to tend to contract in volume (Fig. 2, Fig. 3 a); at the same time the base metal will be subjected to compressive strains. Negative or contractive stresses are those that contract the deposit so that the latter strives to increase in volume (Fig. 2, Fig. 3 b).

The flexible cathodes in the tests were L 67 brass plates measuring $75 \times 16 \times 1.1$ mm. The elastic modulus of the brass was determined experimentally and the mean value obtained was $E = 1.09 \cdot 10^4$ kg/mm².

Internal stresses (σ) were calculated from the formula

$$\sigma = \frac{4}{3} \cdot \frac{E \cdot (h + t)^3 \cdot f}{l^2 \cdot h \cdot t} \text{ (kg/mm}^2\text{)},$$

where f = deflection of cathode (in mm), h = thickness of plate (in mm), t = thickness of deposit (in mm), and l = datum [distance in mm between supports (Fig. 1)].

Electrolysis was carried out in a rectangular bath with a capacity of 100 cm³. Microhardness (H) was determined by the static pressure method with a type PMT-3 microdurometer as designed by Khrushchov and Berkovich [6]. Measuring procedure was based on the investigations of Vyacheslavov [7].

Cathode potentials were measured in relation to a saturated calomel electrode by the compensation method using a standard potentiometer. The cathodic current efficiency (η_K) was determined from the increase in weight of the cathode of a copper coulometer. The set-up for obtaining reversed current has been described in a paper by Fedot'ev and Khonikevich [8]. The plate functioned as an anode for a period (t_a) of one second, and as a cathode (t_K) for 10 seconds; hence $t_a:t_K = 1:10$. In all of the experiments the copper deposit had a thickness of about 20μ .

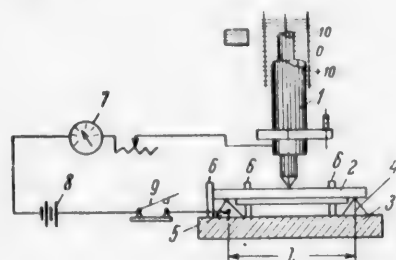


Fig. 1. Diagram of apparatus for determination of deflection of a cathode.

1) Vertical optimeter; 2) plate with deposit; 3) stage; 4 and 5) plate supports; 6) stops; 7) millimeter; 8) accumulator; 9) knife switch.

The dependence of internal stresses, microhardness, cathode potential and cathodic current efficiency on current density was studied with an electrolyte of the following composition (in g/liter): $\text{CuSO}_4 \cdot 5\text{H}_2\text{O}$ 250, H_2SO_4 50. Room temperature. Current densities were varied in the range of up to 6 a/dm^2 . The electrolyte was stirred mechanically in experiments with current densities above 3 a/dm^2 . A series of experiments was run with reversed current.

Experimental results are presented in the form of graphs in Fig. 4.

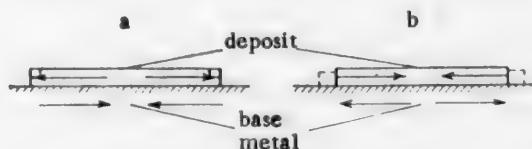


Fig. 2. Representation of internal stresses in deposit and base. a) Tensile stresses in deposit (positive); b) contractive strains in deposit (negative).

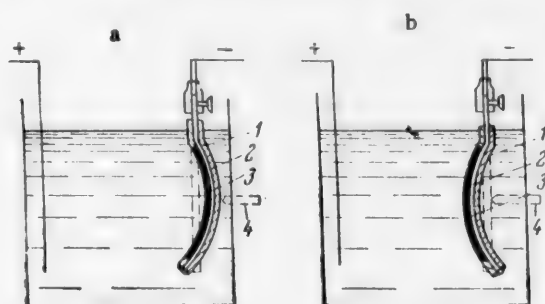


Fig. 3. Representation of deformation of plate during electrolysis. 1) Wax layer; 2) plate; 3) metal deposit; 4) optimeter probe (in arbitrary representation).

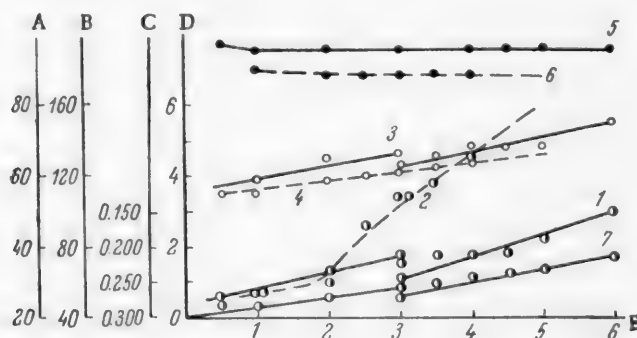


Fig. 4. Dependence of internal stresses, microhardness, cathode potential and cathodic current efficiency on current density. A) Current efficiency η_K (in %); B) microhardness H (in kg/mm^2); C) cathode potential ϵ_K (in V); D) internal stresses σ (in kg/mm^2); E) current density D_K (in a/dm^2). 1) Internal stresses σ , 2) ditto with 1:10 reverse current, 3) microhardness H , 4) ditto with reverse current, 5) current efficiency η_K , 6) ditto with 1:10 reverse current, 7) cathodic potential ϵ_K .

The experimental data show that in operations with nonreversed current the internal stresses and the microhardness increase with the current density; stirring slightly lowers them. We see from Fig. 4 that the dependence of the internal stresses and microhardness on the current density is the same as the dependence of the cathode potential on D_K . The cathodic current efficiency does not alter appreciably in the experimental D_K range. With reversed current the internal stresses in the D_K range of 0.5 to 2 a/dm² hardly differed from the stresses in a copper deposit resulting from operation with direct current, but in the range of 2-4 a/dm² they approximately doubled. With $D_K = 2-4$ a/dm² the deposits were lustrous. The character of the curves of microhardness versus current density also remained unchanged when the current was reversed. The cathodic current efficiency with reversed current was 8-10% smaller than with direct current.

The dependence of the internal stresses, the microhardness, the cathodic potential and cathodic current efficiency on the sulfuric acid concentration was studied with an electrolyte containing 250 g CuSO₄ · 5H₂O per liter at $D_K = 2$ a/dm² and room temperature. The H₂SO₄ concentration was varied over the range of 0 to 200 g/liter.

The experimental results are plotted in Fig. 5.

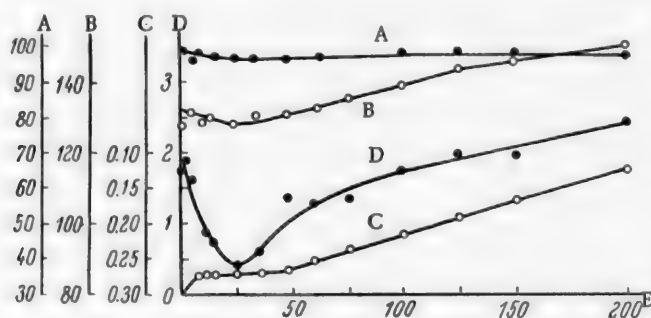


Fig. 5. Dependence of internal stresses, microhardness, cathodic potential and cathodic current efficiency on the sulfuric acid concentration in the electrolyte. A) Current efficiency η_K (in %); B) microhardness H (in kg/mm²); C) cathodic potential ϵ_K (in V); D) internal stresses σ (in kg/mm²); E) sulfuric acid concentration (in g/liter).

The curve of internal stresses versus H₂SO₄ concentration contains a minimum at an acid content of 25 g/liter. At the same concentration there is also a minimum on the microhardness curve, but not so well-developed. The cathodic current efficiency is independent of the sulfuric acid concentration in the electrolyte [9].

Evaluation of Experimental Results

Publications of many authors [4, 5, 10-17] put forward a series of theories to account for the development of internal stresses in galvanic deposits. On the basis of these theories and of the experimental material of the present work, we can attribute the development of internal tensile stresses in copper deposits to the following causes.

1. During formation of the deposit the initially deposited atoms of metal are not associated as crystals but are in a "quasiamorphous" state of lower density.

Such a metastable modification possesses much free surface energy which tends to decrease in the deposit. Recrystallization of the deposit therefore takes place with formation of larger crystals with a smaller specific volume.

2. In the instant of formation of a metal crystal at the cathode surface [14] the crystal must possess an expanded lattice (this is the Lennard-Jones effect).

Due to the stoppage of growth of the crystal and the continuing growth of the deposit, the growth process eventually proceeds inside the deposit. The parameters of the crystal must be correspondingly shortened and the volume of the deposit reduced. Due to the volumetric changes the deposit tends to contract but this process is hindered by the strength of the bond between deposit and base metal. The metal and the deposit retain their original volume but tensile strains are set up in the deposit (positive strains).

These ideas are supported by a study of the internal tensile stress as a function of the current density (Fig. 4). At low values of D_K the values of $\sigma_{\text{tens.}}$ set up in copper deposits are insignificant, while with increase of D_K the cathodic potential becomes more negative and the copper deposits become microcrystalline. The number of crystals in the deposit increases, the number of individual internal tensile stresses becomes larger, and consequently, the total internal tensile stresses increase.

If we designate by P the energy with which each crystallite tends to diminish in volume, then the total force F acting on the deposit will be

$$F = \Sigma n \cdot P,$$

where n is the number of crystals in the deposit.

The dependence of H on D_K is similar to that of $\sigma_{\text{tens.}}$ on D_K . This is because both $\sigma_{\text{tens.}}$ and H depend on the number of crystals in the deposit which increases with growth of D_K .

Internal stresses decrease to a very small extent in experiments with reversed current up to values of $D_K = 2 \text{ a/dm}^2$. In explanation of this, we may assume that active projecting particles of deposit undergo partial solution. At higher values of D_K than 2 a/dm^2 , the deposits become finely crystalline and lustrous and acquire an excellent appearance, but their internal stresses continue to increase and reach a value of 4.5 kg/mm^2 .

As Bakhvalov [18] points out, short-period functioning of the electrode as an anode interrupts the growth of the crystals and subsequent deposition of copper proceeds via development of new crystallization centers. This behavior explains the internal tensile stresses developed during operation with reverse current.

The main factors influencing the value of $\sigma_{\text{tens.}}$ are D_K and ϵ_K ; under otherwise identical conditions, we then have

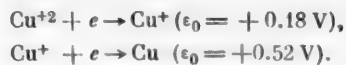
$$\sigma = f(D_K) \quad \text{or} \quad \sigma = f(\epsilon_K).$$

On the basis of analysis of experimental data [19] the following formula is proposed for approximate determinations of the magnitude of σ in copper deposits (obtained from sulfuric acid electrolytes without additives):

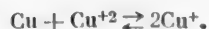
$$\sigma = A(D_K \pm B),$$

where A is the tangent of the angle between the σ versus D_K plot and the D_K axis, B is the section of the D_K axis from the origin to the point of intersection of the σ versus D_K plot with the D_K axis.

Influence of the acidity of the electrolyte. Formation of copper deposits in sulfuric acid electrolytes at low values of D_K can proceed by stepwise discharge of ions according to the equations:



As P. P. Fedot'ev points out [9], Cu^+ builds up in the electrolyte because a chemically reversible process takes place at the Cu/Cu^{2+} interface [20]



The equilibrium constant of this reaction at $t = 20^\circ$ is

$$K = \frac{C_{\text{Cu}^+}^2}{C_{\text{Cu}^{2+}}} = 0.5 \cdot 10^{-4}.$$

Rise in t occurs at the metal/solution interface and the reaction is shifted to the right.

The salt in the lower valence stage is hydrolyzed at low acidity of the electrolyte according to the equation



The dependence of σ and H of the copper deposit on the H_2SO_4 concentration has a complex character. A minimum occurs at an H_2SO_4 concentration of 25 g/liter. It may be suggested that at an H_2SO_4 concentration of up to 5 g/liter the values of σ and H are high because the cuprous oxide formed under these conditions at the cathode is in the colloidal state; it exerts the protective action usual for colloids and facilitates the formation of a finely crystalline deposit. At the same time the cathodic potential rises by 0.0237 V. At H_2SO_4 concentrations of over 5 g/liter the colloid ceases to exert an action and σ falls. Rise of the H_2SO_4 concentration to over 25 g/liter results in stoppage of hydrolysis, the active concentration of Cu^{2+} starts to fall and the electrical conductivity of the electrolyte increases. The cathodic potential rises, the deposit becomes more finely crystalline and its tensile stress σ and microhardness increase.

The above explanation of the influence of the acidity of the electrolyte is in harmony with the previous explanation of the causes of development of internal tensile stresses in copper deposits.

LITERATURE CITED

- [1] P. A. Jacquet, *Compt. rend.* 194, 456 (1932).
- [2] N. P. Fedot'ev and E. G. Kruglova, *Zhur. Priklad. Khim.* 28, 3, 275 (1955).*
- [3] Yu. S. Tsareva, V. G. Solokhina, N. T. Kudryavtsev, and A. T. Vagramyan, *Zhur. Fiz. Khim.* 29, 1 (1955).
- [4] A. T. Vagramyan and Yu. S. Tsareva, *Zhur. Fiz. Khim.* 29, 1 (1955).
- [5] N. P. Fedot'ev, L. A. Glikman, and A. P. Chernova, *Zavodskaya Lab.* 9, 1126 (1951).
- [6] M. M. Khrushchov and E. S. Berkovich, *Microhardness Determination by the Compression Method* [In Russian] (Acad. Sci. USSR Press, 1943).
- [7] P. M. Vyacheslavov, *Candidate's Dissertation*, Leningrad Lensovet Institute of Technology (1953).
- [8] N. P. Fedot'ev and A. A. Khonikevich, *Trudy Leningrad Tekh. Inst. im Lensovet* 40 (1957).
- [9] P. P. Fedot'ev, *Electrolysis in Metallurgy* [In Russian] (United Sci. Tech. Press, Theoretical Chemistry, Leningrad, 1935).
- [10] V. Kohlschütter, *Z. Electrochem.* 24, 300 (1918).
- [11] V. Kohlschütter and M. Vuillenmuier, *Z. Electrochem.* 24, 19/20 (1918).
- [12] V. Kohlschütter and Jakober, *Z. Electrochem.* 33, 7, 290 (1927).
- [13] A. N. Nemnonov, *Zhur. Tekh. Fiz.* 18, 2, 239 (1948).
- [14] V. S. Ioffe, *Uspekhi Khim.* 13, 1 (1944).
- [15] A. V. Rykova, *Investigation of Corrosion of Metals Under Stress* [In Russian] (Metallurgical Press, 1953).

*Original Russian pagination. See C. B. Translation.

- [16] A. Brenner and S. Senderoff, J. Nat. Bur. Stand. Res. 42, 2, 89 (1949).
- [17] A. G. Samartsev and Yu. V. Lyzlov, Zhur. Fiz. Khim. 29, 2, 374 (1955).
- [18] G. T. Bakhvalov, Jubilee Collection of Scientific Papers of the Moscow M. I. Kalinin Institute of Nonferrous Metals and Gold (Metallurgical Press, 1950).
- [19] A. A. Khonikevich, Candidate's Dissertation, Leningrad Lensovet Inst. Tech. (1957).
- [20] V. I. Lainer, Tsvetnye Metally 5 (1935).

Received January 20, 1959

CATHODIC POLARIZATION DURING FORMATION OF IRON - COBALT ALLOY AND THE CAUSES OF DEPOLARIZATION AND OVER-POLARIZATION

A. L. Rotinyan and E. N. Molotkova

Department of Electrochemistry of the Leningrad Lensovet Institute of Technology

In this communication we give the results of an investigation of the nature of the polarization during formation of an iron-cobalt alloy at a cathode.

EXPERIMENTAL

The polarization was studied by the method of partial polarization curves [1]. Six compositions of sulfate electrolyte, in all, were studied with various ratios of cobalt and iron concentrations but all with the same total concentration of $C_{CoSO_4} + C_{FeSO_4}$ of 1.25 moles/liter. Experiments were run at five thermostated temperatures between 25 and 85° at a pH value of 3.5. In each case 10 g/liter of sodium chloride and 30 g/liter of boric acid were added to the electrolytes. The current efficiency, reckoned on the total metals, was always close to unity.

The electrolyzer was a closed bath containing 400 ml of electrolyte. The cathodes were copper plates 0.5 mm thick and with a working surface of 10 cm². The anodes were high-purity cobalt and Armco iron. Potentials were measured by the usual compensation circuit. The compositions of the various solutions are shown in the table.

Constants a_{Co} and a_{Fe} in Eq. (1) with a Current Density of $i = 1$ amp/dm² and the Coefficients α_{Co} and α_{Fe} During Formation of Cobalt - Iron Alloy

Electro- lyte no.	Composition of electrolyte (mole/liter)	25°		40°		55°		70°		85°		Element
		α	α	α	α	α	α	α	α	α	α	
1	Co — 1.06, {	0.574	0.37	0.520	0.44	0.463	0.50	0.400	0.56	0.355	0.71	Co
	Fe — 0.19 }	0.616	0.37	0.550	0.50	0.490	0.59	0.426	0.71	0.385	0.83	Fe
2	Co — 1.03, {	0.590	0.35	0.518	0.42	—	—	—	—	—	—	Co
	Fe — 0.22 }	0.690	0.35	0.540	0.42	—	—	—	—	—	—	Fe
3	Co — 0.94, {	0.603	0.35	0.530	0.42	—	—	—	—	—	—	Co
	Fe — 0.31 }	0.630	0.35	0.540	0.42	—	—	—	—	—	—	Fe
4	Co — 0.83, {	0.645	0.41	0.592	0.46	0.546	0.59	0.508	0.62	0.473	0.79	Co
	Fe — 0.42 }	0.652	0.49	0.598	0.56	0.552	0.65	0.516	0.75	0.476	0.89	Fe
5	Co — 0.63, {	0.675	0.42	0.632	0.47	0.595	0.59	0.558	0.62	0.508	0.72	Co
	Fe — 0.62 }	0.657	0.42	0.618	0.56	0.583	0.65	0.545	0.74	0.496	0.86	Fe
6	Co — 0.19, {	0.732	0.37	0.672	0.44	0.616	0.50	0.568	0.59	0.510	0.72	Co
	Fe — 1.06 }	0.685	0.37	0.634	0.56	0.586	0.62	0.537	0.76	0.492	0.89	Fe

Due to the oxidation of bivalent iron and subsequent hydrolysis of the sulfate of trivalent iron with formation of $\text{Fe}(\text{OH})_3$, the electrolytes gradually turn cloudy. Any considerable oxidation of bivalent iron ions and subsequent hydrolysis were prevented by always conducting the electrolysis in freshly prepared transparent electrolyte. A fresh electrolyte was used after one or two experiments. The pH value of the solutions was measured with a glass electrode and hardly varied in the course of an experiment. The deposited alloys were dissolved in 30% sulfuric acid for analysis. Iron in the electrolyte and the deposits was determined volumetrically; the cobalt in the electrolytes was determined potentiometrically and in the alloys by the difference in weight between the alloy and the value found for iron.

Comparison of the partial polarization curves with the curves of deposition of the pure metals shows that the polarization curves of cobalt on deposition in an alloy are shifted in the direction of more negative potentials, whereas the polarization curves of iron are shifted in the direction of more positive potentials in comparison with the deposition of the pure metals. This picture is true of all of the investigated concentrations and temperatures.

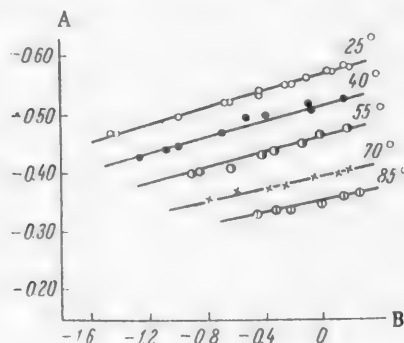


Fig. 1. Partial polarization curves of cobalt from electrolyte No. 1 (see table) in semilogarithmic coordinates. A) Potential φ_K (in V); B) value of $\log i_{\text{Co}}$.

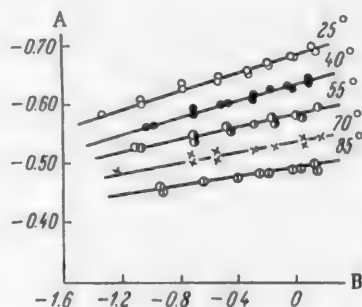


Fig. 2. Partial polarization curves of iron from electrolyte No. 6 (see table) in semilogarithmic coordinates. A) Potential φ_K (in V); B) value of $\log i_{\text{Fe}}$.

The partial polarization curves of cobalt and iron in all of the cases that we investigated are converted into straight lines in semilogarithmic coordinates. Typical plots are shown in Figs. 1 and 2. In view of this character of the graphs, we can omit the full experimental data and give only a summarizing table of the values of coefficients a and α in the equation

$$\varphi = a + \frac{2.3 RT}{\alpha z F} \cdot \lg i, \quad (1)$$

where φ is the cathodic potential in the hydrogen scale; a is the cathodic potential at current density i of one amp per dm^2 ; α is a coefficient with values between zero and unity; z is the valence of the discharging ions; F is the Faraday constant; R is the gas constant; T is the absolute temperature.

Evaluation of Results

1. The equation of separation of a pure component with chemical polarization (subscript M) is:

$$i_M = K_M a_M e^{-\frac{u_{0M}}{RT}} e^{\frac{\alpha_M z F \varphi_{\text{zdp}}^M}{RT}} e^{-\frac{\alpha_M z F \varphi_M}{RT}}, \quad (2)$$

where K_M = velocity constant of the electrochemical reaction;

u_{0M} = activation at zero discharge potential of the surface; and

φ_{zdp}^M = zero discharge potential of the surface in the hydrogen scale.

The remaining symbols have their former significance.

Since K_M , u_{0M} , φ_{zdp}^M and α_M are constants in this equation, the curves of Eq. (2) will naturally be converted into straight lines in semilogarithmic coordinates of φ_M and $\log i_M$. The situation alters if the separated component is not pure but in the form of an alloy. In this event two variants are possible even if the alloys are solid solutions. If the composition of the alloy depends on the ratio of the components in solution and on the temperature but does not depend on the current density, then K , u_{0M} , φ_{zdp} and α can acquire values on separation of a given component that differ from the values for the pure component although independent of the current density. In these circumstances, the partial polarization curves will therefore undergo parallel shifts, but in semilogarithmic coordinates they will remain rectilinear.

If, however, the composition of the alloy depends on the current density, the partial polarization curves are not necessarily converted into rectilinear plots since in general the magnitudes in question must change with the current density. Only if certain supplementary conditions are introduced can we expect Tafel's equation to be valid. In practice Tafel's equation is valid for the systems Co-Fe and Co-Ni [1] even when the alloy composition alters with the current density. It is therefore desirable to consider the possible explanation of this phenomenon more closely.

The available information on the relation between the zero discharge potential of a surface and the composition of the alloy does not provide us with a full explanation of the process. However, the data of Krasikov and Sysoeva [2] for the system Ni-Fe and some amalgam cells, and also the data of Antropov and co-workers [3-5], show that with gradual addition of a metal with a more negative zero discharge potential of the surface to a metal possessing a more positive zero discharge potential of the surface, the φ_{zdp} of the alloy at first alters sharply and quickly reaches the value of the zero discharge potential of the surface of the metal with the more negative value of φ_{zdp} . After this change, the zero discharge potential of the surface of the alloy no longer depends on the composition of the alloy.

All of our experiments were carried out on the assumption that the ratio of the alloy components did not approximate to zero or infinity. We can therefore assume that we worked in the region in which the φ_{zdp} was substantially independent of the composition of the alloy.

The activation energy of discharge of the ions at zero surface discharge potential and the constant K must depend on the composition of the alloy. Consequently, constancy of the angular coefficient of the semilogarithmic straight-line plots is only possible if the changes in the above magnitudes cancel one another or if these constants in the case of the iron group are little dependent on the alloy composition, i.e., if they remain approximately constant.

2. Depolarization of one of the components and over-polarization of the other takes place with all of the binary alloys of metals of the iron group [1-6].

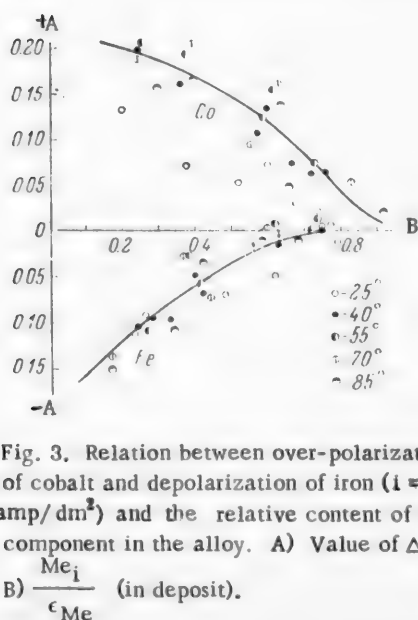


Fig. 3. Relation between over-polarization of cobalt and depolarization of iron ($i = 1$ amp/dm²) and the relative content of the component in the alloy. A) Value of $\Delta\varphi$; B) $\frac{Me_i}{\epsilon_{Me}}$ (in deposit).

Figure 3 shows the depolarization of iron and over-polarization of cobalt for potential values corresponding to a current density of 1 amp/dm² as functions of the alloy composition. The magnitudes of $\Delta\varphi$ were determined by comparison of the potentials of deposition of the metals in the alloy and in the pure form under conditions of equal concentrations of the deposited component in separate and in mixed solutions.

The magnitudes of over-polarization of cobalt and of depolarization of iron are weakly temperature dependent except at 25°, but strongly dependent on the composition of the cathodic deposit.

The value of constants a of iron-rich alloys is substantially equal to the value of a for separation of pure iron. And only after the cobalt concentration in the alloy has reached a value of about 30% does discharge of iron ions start to be facilitated by the simultaneous discharge of cobalt ions. The only difference is that over-polarization commences even when the iron content is still of the order of 15%.

The process of depolarization has previously [1] been associated with the energy of alloying and that of over-polarization with the superstructure of the crystal lattice. Precision can now be imparted to these ideas. X-ray studies [7, 8] have shown that on deposition of an alloy with a preponderating amount of one of the components, the alloy crystallizes with the lattice characteristic of that component. Iron-rich alloys can accordingly be regarded as solid solutions in which cobalt atoms replace some iron atoms in the crystal lattice of iron. Similarly, alloys with a predominating content of cobalt will have the cobalt lattice structure with some atoms replaced by iron. With equal amounts of components, the alloy may possess the lattices of both of the metals.

It is therefore to be expected that in the case of an iron-cobalt alloy the separation of small quantities of cobalt at sites in the iron lattice will take place at potentials close to the separation potential of iron and that it will not be accompanied by depolarization of iron, but by a large over-polarization of the more electropositive cobalt. Conversely, the entry of the more electronegative iron into the cobalt lattice will be accompanied by substantial absence of over-polarization when cobalt is deposited and by large depolarization on deposition of iron.

3. With the help of the chemical polarization equations we can correlate the process of depolarization and over-polarization with the fundamental electrochemical constants of the kinetics of electrode reactions.

Unlike Polukarov and Gorbunova [9], who studied the problem from the thermodynamic aspect, we shall consider the case when the potential shift on formation of an alloy is governed not by thermodynamic but by kinetic factors. By analogy with Eq. (2), for the separation of a given component into an alloy we can write the following kinetic equation for the partial polarization curve:

$$i_c = K_c a_c e^{-\frac{u_{0c}}{RT}} e^{-\frac{\alpha_c z F \varphi_{zdp}}{RT}} e^{-\frac{\alpha_c z F \varphi_c}{RT}}, \quad (3)$$

where the values of φ_c relate to the release of a metal from the mixed solution into the alloy.

Joint solution of Eqs. (2) and (3) leads to the expression:

$$\Delta \varphi = \frac{RT}{zF} \ln \frac{K_M^{\alpha_M}}{K_c^{\alpha_c}} + \frac{RT}{zF} \ln \frac{a_M^{\alpha_M}}{a_c^{\alpha_c}} - \frac{RT}{zF} \ln \frac{i_M^{\alpha_M}}{i_c^{\alpha_c}} + \\ + (\varphi_{zdp}^M - \varphi_{zdp}^c) - \frac{1}{zF} \left(\frac{u_{0M}}{\alpha_M} - \frac{u_{0c}}{\alpha_c} \right). \quad (4)$$

Here $\varphi_M - \varphi_c = \Delta \varphi$ characterizes the magnitude of depolarization ($\Delta \varphi < 0$) or over-polarization ($\Delta \varphi > 0$) when metal is released into alloy, in comparison with the value for its release in the pure form.

On the basis of the foregoing exposition of the nature of the dependence of φ_{zdp} on the alloy composition, we can determine the magnitude and sign of the fourth term of the right-hand part of Eq. (4). If we consider the potential shift when the alloy receives a metal possessing a more negative value of φ_{zdp} , then for not very small contents of this metal in the alloy, we shall have $\varphi_{zdp}^M - \varphi_{zdp}^c = 0$. On the other hand, if we consider the entry into the alloy of a metal with more electropositive φ_{zdp} , then for the same conditions we have $\varphi_{zdp}^M - \varphi_{zdp}^c = \varphi_{zdp}^{M_1} - \varphi_{zdp}^{M_2}$, i.e., we obtain the difference between the zero discharge potentials of the pure components of the alloy. This difference will be positive.

The fifth term of the right-hand part of Eq. (4) can be positive or negative, depending on the ratio between u_{0M} and u_{0c} and between α_M and α_c .

The potential shift on alloy formation, as we see from the equation in the general case ($\alpha_M \neq \alpha_c$), depends likewise on the current density at which the comparison is carried out. Here a ratio between α_M and α_c is possible such that some values of current density $i_M^{\alpha_M} / i_c^{\alpha_c} > 1$, while others < 1 . Consequently, the sign

in front of the third term of the right-hand side of Eq. (4) can change. Hence, if the value of this term is large in relation to the other terms of the right-hand side of the equation, then the sign of $\Delta \varphi$ may alter with changing current density, i.e., we get transition from depolarization to over-polarization or vice versa. With the aim of not complicating the problem by the influence of the current density on the magnitude of $\Delta \varphi$, it is desirable to determine the potential shift when $i = 1$, i.e., to actually compare the constants a of Tafel's equation.

In all previous work the objective has been to determine the shift of $\Delta \varphi$ with equal activities of the discharging ions in the electrolyte. It follows from Eq. (4) that this is valid if $\alpha_M = \alpha_C$. In the general case, however, it is necessary, for the purpose of elimination of the influence of active ions in solution on the magnitudes of depolarization or over-polarization, to carry out the comparison when $\frac{1}{a_M^{\alpha_M}} = \frac{1}{a_C^{\alpha_C}}$. If the magnitude of the second term of the right-hand side of Eq. (4) is large, then the determination of the value of $\Delta \varphi$ with equal activities of the metal in mixed and separate solutions with changing activity values can lead not only to change in the sign in front of this term of Eq. (4) but also to change of the sign in front of $\Delta \varphi$. This was observed in an earlier study [1].

The magnitude of the first term of Eq. (4) can also be either positive or negative, according to the value of the ratio between constants K and α .

Such a complex dependence of $\Delta \varphi$ on a whole series of factors, acting in various directions and changing the sign under specific conditions, enables us to assert that the formation of an alloy at a cathode can be associated with all the fundamentally possible cases of shift of the partial polarization curves which determine the positive, negative or zero value of $\Delta \varphi$.

SUMMARY

1. Cathodic polarization during formation of iron-cobalt alloy was investigated in the 25-85° temperature range from electrolytes with various ratios of concentrations of the coprecipitating components at a pH of 3.5. The partial polarization curves were compared with the curves of deposition of the pure metals. It was shown that entry of a metal into an alloy is accompanied by considerable displacement of the separation potential in relation to its separation potential when pure.

2. The values of depolarization of iron and of over-polarization of cobalt depend on the composition of the cathodic deposit.

3. In all of the cases the partial polarization curves become straight lines when plotted in semilogarithmic coordinates. The values of coefficients α change with the temperature within the limits demanded by the theory of retarded discharge of ions.

LITERATURE CITED

- [1] V. M. Kochegarov, A. L. Rotinyan, and N. P. Fedot'ev, Trudy Leningrad. Tekh. Inst. im. Lensovetu 40, 112 (1957).
- [2] B. S. Krasikov and V. V. Sysoeva, Doklady Akad. Nauk SSSR 114, 826 (1957). *
- [3] B. S. Krasikov and L. S. Akulova, Vestnik Leningrad. Gosudarst. Univ. Ser. Fiz. i Khim. 16 (3), 112 (1958).
- [4] M. G. Smirnov, V. A. Smirnov and L. I. Antropov, Trudy Novocherkasskogo Politekh. Inst. 34/48 (1956).
- [5] V. A. Smirnov and L. I. Antropov, Trudy Novocherkasskogo Politekh. Inst. 34/48 (1956).
- [6] N. V. Kozovin, Zhurnal Neorgan. Khim. 2, 2259 (1957).

*Original Russian pagination. See C. B. Translation.

- [7] M. Hansen, The Structure of Binary Alloys (Russian translation) (1941).
- [8] N. S. Fedorova, Zhur. Fiz. Khim. 32, 1211 (1958).
- [9] Yu. M. Polukarov and K. M. Gorbunova, Zhur. Fiz. Khim. 30, 515, 871, 878 (1956).

Received April 2, 1959

DETERMINATION OF THE EXCHANGE CURRENT OF SILVER AND COBALT ON A SOLID METALLIC SURFACE WITH THE HELP OF RADIOACTIVE INDICATORS

S. E. Vaisburd, N. M. Kozhevnikova, and V. L. Kheifets

Gipronikel' Project and Scientific Research Institute, Leningrad

It was previously shown [1] that by using radioactive indicators one can directly determine the magnitude of the exchange current at a solid surface. Partial solutions were given of the over-all kinetic equation for the case of a solid electrode. In the present work we submit experimental data obtained by the method in question.

Technique of Measurements

Experiments were run in the vessel sketched in Fig. 1. In experiments with cobalt the rotating electrode (copper disk with a surface of 1.77 cm^2) was previously coated with cobalt from a CoSO_4 solution in an atmosphere of purified hydrogen in order to avoid formation of an oxide film.

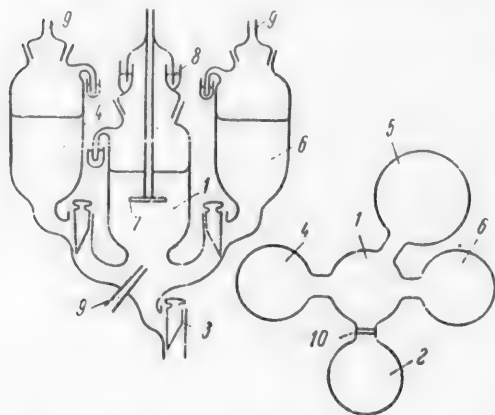


Fig. 1. Vessel for exchange experiments. 1) Exchange compartment; 2) anode chamber; 3) tap for draining solutions from compartment 1; 4) compartment for active solution; 5) compartment for double-distilled water; 6) compartment for inactive solution; 7) rotating disk electrode; 8) mercury seal; 9) hydrogen inlet tube; 10) diaphragm.

For this operation compartment 1 was filled with CoSO_4 solution which had been saturated with hydrogen for 20 minutes before the start of electrolysis; the hydrogen stream was not interrupted during the electrolysis.

Electrolytically prepared hydrogen was purified in concentrated sulfuric acid and potassium permanganate solution and then saturated with water vapor in a vessel containing double-distilled water. This measure ensured that the concentration of the working solution would not be changed due to absorption of water vapor by the hydrogen.

The anodic compartment 2 was isolated by a diaphragm. At the conclusion of electrolysis, the CoSO_4 solution was removed under a blanket of hydrogen through tap 3. Thereupon compartment 1 was twice washed out with double-distilled water which had been saturated with hydrogen beforehand. After this, the working solution (labeled with isotope Co^{60}) was transferred in a hydrogen stream from compartment 4 into compartment 1. The instant of contact of the rotating disk electrode with the solution was recorded by a stopwatch. The rate of rotation of the disk electrode during an experiment and the preliminary electrolysis was 250-300 rev./min. At the

completion of an experiment (the disk remained in the solution for 1 to 20 hours) the working solution was taken off through tap 3. The disk was twice washed with double-distilled water and dried with acetone. The activity of the disk was measured by determination of the γ -radiation with a Geiger-Müller counter. By careful adherence

to the conditions of measurement, it was possible to utilize the data of relative measurements. The statistical error of counting was 3%.

Since the accuracy of determination of the period of immersion of the disk in the solution had a marked effect on the error of determination of the exchange current, the apertures of the taps were 1 cm in diameter. This enabled the operations of removal of the radioactive working solution from compartment 1 and the washing of the electrode to be completed in 8-10 sec. Consequently, the error in the determination of the cobalt exposure period did not exceed 0.3%. The total relative error in determination of the cobalt exchange current was $\pm 10\%$.

When working with silver, the oxide film was removed from the silver disk by dissolution in 0.1 N nitric acid in a hydrogen atmosphere. The disk was thereupon washed twice with double-distilled water. In the experiments with silver the CoSO_4 solution for the cathodic deposition of cobalt in compartment 2 was replaced by HNO_3 solution, and the active solution of $\text{Co}(\text{NO}_3)_2$ or CoCl_2 in compartment 4 was replaced by active AgNO_3 solution. Very dilute solutions were used — down to 10^{-5} N AgNO_3 . The effect of the diffusion potential jump on the magnitude of the exchange current was eliminated by addition to the solutions of a strong electrolyte (KNO_3 in quantity equivalent to a concentration of 1 N).

Since the exchange current of silver is considerably higher than that of cobalt, the period of exposure of the silver disk in the active solution was 5 to 60 min; this increased the error in the recording of the exposure period to 3%.

The activity of the disk was measured with a Geiger-Müller counter from the intensity of the β -radiation of the isotope Ag^{110} . The statistical counting error was 1%. The total relative error in the determination of the exchange current of silver was $\pm 10\%$.

The electrode activities found by the above method were used for calculation of the exchange current i_0 from the equations [1]

$$i_0 = -\frac{S_p \cdot z \cdot F}{N_0 \cdot t} \cdot 2.3 \lg \left(1 - \frac{C_{p1}}{C_{p\infty}} \right), \quad (1)$$

$$i_0 = -\frac{S_p \cdot z \cdot F}{N_0 \cdot t} \cdot 2.3 \lg \left(\frac{C_{p2}}{C_{p1}} - 1 \right) \quad (2)$$

or

$$i_0 = \frac{S_p \cdot z \cdot F}{N_0 \cdot t} \cdot 2.3 \lg \frac{C_{p2} - C_{p1}}{C_{p3} - C_{p4}}, \quad (3)$$

where S_p is the number of atoms of metal per 1 cm^2 of electrode surface; z is the ionic charge; F is the Faraday number; N_0 is the Avogadro number; t is time; C_p is the number of radioactive atoms per 1 cm^2 of electrode surface; subscripts 1, 2, and 3 denote that the magnitude of C_p corresponds to contact times of electrode with solution of, respectively, t , $2t$, and $3t$.

Number of layers of solid metal participating in the exchange. The values of i_0 obtained by the above method are the exchange current in its true electrochemical sense only when only one atomic layer of the solid metal participates in the exchange. The extremely small diffusion velocities of metals at low temperature indicate that actually one atomic layer participates in the exchange. But since conflicting data have been published in the literature (see the literature survey in the preceding paper [1]), it was desirable to make a further experimental check of this fact. This can take the form of comparison of the concentration of labeled atoms at the surface of the metal and in the solution after isotopic equilibrium has been established.

Knowing the absolute activity of the isotope a introduced into the solution, we can calculate the total quantity of radioactive ions in solution. We obtain the following expression if the half-life period T is expressed in seconds and the activity in millicuries:

$$N_1 = 5.35 \cdot 10^7 \cdot a \cdot T,$$

where N_1 is the number of radioactive ions in solution; the total number of metallic ions in solution P is equal to $6.02 \cdot 10^{23} \cdot C$, where C is the normality of the solution.

The sought-for concentration of labeled atoms in solution is

$$m = \frac{N_1}{P}.$$

The number of labeled atoms per unit of visible surface of metal N_2 is determined by measurements of the activity of the plate in comparison with a standard. The total number of atoms per unit surface can be calculated, on the assumption that the metal has a cubic lattice, from the atomic weight A and the density of the metal \underline{d} :

$$S_P = \sqrt[3]{\left(\frac{6.02 \cdot 10^{23} \cdot d}{A}\right)^2}.$$

The concentration of labeled atoms at the surface is

$$x = \frac{N_2}{S_P}.$$

In the equilibrium state $x = m$. But if the exchange extends over several layers, $x > m$ according to the above discussion, since the surface concentration relates to a monoatomic layer. Here, we must remember that since the true surface of a "smooth" metal is approximately 10 times larger than the geometrical surface, exchange solely with a monoatomic layer of metal can still lead to values of \underline{x} such that $x/m \approx 10$.

In Table 1 we present values of \underline{m} and \underline{x} for silver and cobalt which we determined after attainment of isotopic equilibrium in solutions of various concentrations. The experimental conditions were the same as in the determination of current exchange. We see from Table 1 that only one ionic layer of metal participates in the exchange.

TABLE 1
Comparison of Concentrations of Labeled Atoms in Solution and on Metal
at Equilibrium Distribution

Metal	Solution	\underline{m}	\underline{x}
Co	2 n CoCl_2	$1.1 \cdot 10^{-6}$	$2.1 \cdot 10^{-6}$
Co	0.1 n CoCl_2	$1.1 \cdot 10^{-6}$	$2.5 \cdot 10^{-6}$
Ag	10^{-3} n AgNO_3	$3.2 \cdot 10^{-6}$	$1.5 \cdot 10^{-5}$
Ag	10^{-4} n AgNO_3	$1.4 \cdot 10^{-6}$	$1.1 \cdot 10^{-5}$

Exchange current of silver. Results of measurements in AgNO_3 solutions of various concentrations are presented in Table 2. The experimental data of each experiment were used for plotting of a curve of counting rate of the metal plate versus period of its immersion in solution. The curve was evaluated by Eqs. (2) and (3), as well as by Eq. (1) if saturation had been attained, and the exchange current values calculated in each experiment were averaged. The resulting values of i_0 are set forth in the third column of Table 2. The error in their determination was $\pm 10\%$. In the fourth column are presented the mean values of the exchange current of silver in solutions of identical AgNO_3 concentration. We see that the error in determination of i_0 is $\pm 10-15\%$.

According to theory [2] the magnitude of the exchange current in each case is determined by the equation

$$i_0 = K (a_{\text{Ag}^+})^\beta \cdot e^{\frac{-\alpha F \psi_0}{RT}}, \quad (4)$$

where K is the velocity constant of the electrode process, a_{Ag^+} is the activity of the silver ions in solution, φ_0 is the standard potential of the silver electrode, α and β are fractional coefficients.

TABLE 2
Exchange Current of Silver in AgNO_3 Solutions of Various Concentrations

Solu- tion No.	AgNO_3 con- centration (nor- mality)	$i_0 \cdot 10^7$ (in a/cm^2)	Mean value of $i_0 \cdot 10^7$ (in a/cm^2)	Solu- tion No.	AgNO_3 con- centration (nor- mality)	$i_0 \cdot 10^7$ (in a/cm^2)	Mean value of $i_0 \cdot 10^7$ (in a/cm^2)
I	$1.9 \cdot 10^{-5}$	2.2 1.7 2.1	(2.0 ± 0.2)	IV	$1.9 \cdot 10^{-4}$	2.9 2.8 3.6	(3.1 ± 0.4)
II	$3.5 \cdot 10^{-5}$	1.8 2.3 2.1 2.2	(2.1 ± 0.2)	V	$3.0 \cdot 10^{-3}$	5.3 6.0 6.8	(6.1 ± 0.5)
III	$1.5 \cdot 10^{-4}$	2.7 3.8 3.3 2.8	(3.1 ± 0.5)	VI	$1.0 \cdot 10^{-2}$	11.4 10.1 13.9	(11.8 ± 1.4)
				VII	$5.0 \cdot 10^{-2}$	37.0	(37.0 ± 4.5)

We see from Table 2 that the exchange conforms to theory in increasing with increasing silver concentration in solution.

It follows from Eq. (4) that

$$\frac{i'_0}{i''_0} = \left(\frac{a'}{a''} \right)^\beta \quad (5)$$

The data set forth in Table 2 are presented graphically in Fig. 2 as plots of $\log i'_0/i''_0$ versus $\log a'/a''$.

The solution with a concentration of $5 \cdot 10^{-2}$ N AgNO_3 did not contain other salts; all of the remaining solutions, as noted above, contained KNO_3 in 1 N concentration. The activity coefficient of silver in solution [3] was therefore taken into consideration for calculation of the ratio of a' to a'' . Due to the lack of data for potassium nitrate and in view of the similar activity coefficients of series of potassium and sodium salts, the

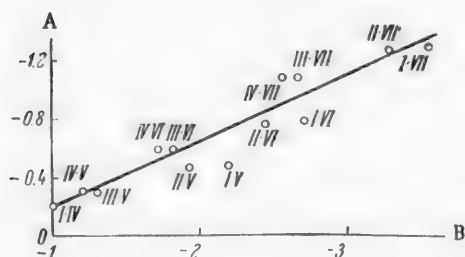


Fig. 2. Dependence of $\log i'_0/i''_0$ on $\log a'/a''$. A) Value of $\log i'_0/i''_0$; B) value of $\log a'/a''$. [Data for calculation of coefficient β from Eq. (5)]. The Roman numbers on the graph relate to pairs of solutions and correspond to the numbers in the first column of Table 2.

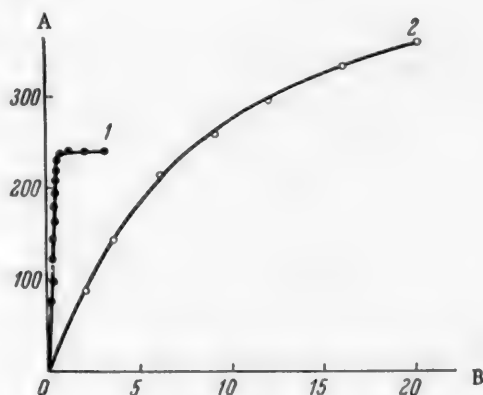


Fig. 3. Activity of the metal as a function of the period of its immersion in solution. A) Activity (in pulses/min); B) Period (hour). 1) Silver, 0.01 N concentration of AgNO_3 ; 2) cobalt, 0.1 N concentration of $\text{Co}(\text{NO}_3)_2$.

activity coefficients of 1 N KNO_3 solutions was assumed to be the same as the coefficient of 1 N NaNO_3 . The tangent of the angle of slope of the straight line of Fig. 2 gives a value of 0.47 for β . This is close to the value of $\beta = 0.5$ often found for reactions of this type.

The standard exchange current i_0 in AgNO_3 solution with an activity of unity can be calculated from Eq. (5). Assuming the value of $\beta = 0.5$, we obtain $i_0 = 3.2 \cdot 10^{-5}$ A/cm². This value is comparable with that of the exchange current of copper [4] which, like silver, is a poorly polarizing metal.

We also determined the exchange current of silver in solutions containing heptyl and octyl alcohols as surface-active additives. Results of these measurements coincide (allowing for experimental errors) with results for solutions free of surface-active agents. This result is fully consistent with literature reports [5] of the absence of an influence of surface-active additives on the polarization potential of silver.

Exchange current of cobalt. Results of measurements of the exchange current of cobalt in $\text{Co}(\text{NO}_3)_2$ and CoCl_2 solutions at two different concentrations are set forth in Table 3.

TABLE 3
Exchange Current of Cobalt in Solutions of $\text{Co}(\text{NO}_3)_2$ and CoCl_2

Solution	Concentration (normality)	i_0 (in a/cm ²)	Mean value of i_0 (in a/cm ²)
$\text{Co}(\text{NO}_3)_2$.	2 {	$5.0 \cdot 10^{-8}$	$(6.3 \pm 0.8) \cdot 10^{-8}$
		$6.3 \cdot 10^{-8}$	
		$7.5 \cdot 10^{-8}$	
$\text{Co}(\text{NO}_3)_2$.	0.1 {	$2.6 \cdot 10^{-8}$	$2.6 \cdot 10^{-8}$
		$2.5 \cdot 10^{-8}$	
		$2.6 \cdot 10^{-8}$	
CoCl_2 . . .	2 {	$1.8 \cdot 10^{-7}$	$(2.0 \pm 0.1) \cdot 10^{-7}$
		$2.6 \cdot 10^{-7}$	
		$2.0 \cdot 10^{-7}$	
CoCl_2 . . .	0.1 {	$2.0 \cdot 10^{-7}$	$2.0 \cdot 10^{-7}$
		$2.2 \cdot 10^{-7}$	
		$1.9 \cdot 10^{-7}$	

The values in the third and fourth columns were obtained by the same procedure as for silver. The error in the mean values of exchange current is ± 10 -15%.

We see from Table 3 that with cobalt, just as with silver, the exchange current increases with the concentration of metal in solution.

The experimental curves for cobalt and silver in solutions of their nitrates are compared in Fig. 3. Whereas equilibrium in distribution of radioactive isotope is established for silver after twenty minutes, equilibrium is not established for cobalt even after the metal has been kept for 20 hours in the solution even though the $\text{Co}(\text{NO}_3)_2$ concentration is 10 times higher than that of AgNO_3 . This fact is accounted for by the extremely low exchange current of cobalt which is characteristic of a strongly polarizable metal. We see from Table 3 that the exchange current of cobalt is considerably lower than that of silver.

The value of coefficient β was calculated, with the help of the activity coefficients for $\text{Co}(\text{NO}_3)_2$ [6], from Eq. (5) from two values of i_0 ; the value obtained was 0.27.

Calculation with Eq. (5), using the value of $\beta = 0.27$, leads to a standard value of the exchange current of cobalt in nitrate solution of $i_0 = 6.3 \cdot 10^{-8}$ A/cm². This is close to that calculated from oscillographic measurements for nickel [4] and iron [7] which, like cobalt, are strongly polarizable metals.

The exchange current value found for cobalt may prove smaller than the true value due to the setting up of a compromise potential, and not of an equilibrium potential when metallic cobalt is immersed in a solution containing cobalt ions. This is caused by the hydrogen reaction. The consequence is a retardation of the rise in activity of the metal plate with time, giving rise to lowered values of exchange current.

Table 3 also contains data for the exchange current of cobalt in CoCl_2 solutions. The values obtained were 5 times greater on the average than in solutions of $\text{Co}(\text{NO}_3)_2$.

SUMMARY

1. The method previously proposed for direct determination of the exchange current at a solid metallic surface with the aid of radioactive isotopes was applied to determination of the exchange currents on silver and cobalt in solutions of the nitrates and chlorides.
2. It was shown that the monoatomic surface layer of metal participates in exchange at the solid surface.
3. The exchange current of a strongly polarizing metal (cobalt) is considerably smaller than that of a substantially nonpolarizing metal (silver). The exchange current of silver is unaffected by additions of surfactants.
4. The value of the fractional coefficient β for silver is close to 0.5. In nitrate solutions, the value for cobalt was close to 0.3.

LITERATURE CITED

- [1] V. L. Kheifets and S. E. Vaisburd, *Zhur. Priklad. Khim.* 32 (8), 1181 (1959). *
- [2] V. L. Kheifets and N. E. Polyakova, *Zhur. Priklad. Khim.* 22, 81 (1949).
- [3] S. Glasstone, *Introduction to Electrochemistry* (Russian translation) (Foreign Lit. Press, Moscow, 1951).
- [4] V. A. Yuza and L. D. Kopyl, *Zhur. Fiz. Khim.* 14, 1074 (1940).
- [5] M. A. Loshkarev and A. D. Kryukova, *Zhur. Fiz. Khim.* 23, 209 (1949).
- [6] R. A. Robinson and R. H. Stokes, *Trans. Faraday Soc.* 45, 612 (1949).
- [7] V. A. Roiter, V. A. Yuza, and E. S. Poluyan, *Zhur. Fiz. Khim.* 13, 605 (1939).

Received September 18, 1958

*Original Russian pagination. See C. B. Translation.

SPECTROPHOTOMETRIC METHOD OF DETERMINATION OF THE CONTENT OF PRIMARY AND SECONDARY HIGHER ALCOHOLS

Ya. É. Shmulyakovskii

Determination of the content of primary and secondary alcohols in their mixtures is extremely difficult.

The known method of determination of primary alcohols, based on their oxidation with chromic acid [1], is fairly lengthy and insufficiently accurate.

In 1958 a method was described for the determination of alcohols on the basis of selective dehydration of secondary alcohols and measurement of the water evolved [2]. Primary alcohols are found by difference in this procedure after determination of the hydroxyl value. The analysis is time-consuming because the duration of the dehydration reaction alone is 9 hours. Another disadvantage is that the quantity of alcohol necessary for analysis is several grams.

In a paper by Tarte [3] on infrared spectroscopy of alcohols, it was concluded that at the present time the reliability of identification of alcohols (primary, secondary or tertiary) decreases with increasing degree of complexity of the carbon chain.

We previously developed a spectrophotometric method of determination of primary, secondary and tertiary butyl alcohols [4]. It was found possible to extend this method to alcohols higher than C_4 . The method is based on examination of the absorption spectra of the nitrites of the alcohols. The spectra possess characteristic bands in the ultraviolet region due to electronic transitions in the $O-N=O$ group of the molecules of alkyl nitrites. The position of this group in the hydrocarbon radical is reflected in the spectra.

Absorption curves of nitrites prepared from primary and secondary alcohols were plotted with the help of the SF-11 spectrophotometer. The spectra of the two types of alcohols were different. We had the following normal alcohols at our disposal: hexyl, octyl, decyl, dodecyl, hexadecyl and octadecyl; also the following secondary alcohols: pentyl and octyl (two isomeric structures).

Table 1 contains the molar absorption coefficients for the absorption maxima of the nitrites. The diagram shows the absorption curves.

All of the nitrites prepared from primary alcohols have absorption maxima at 344, 357, 370 and 384 $m\mu$, whereas nitrites prepared from secondary alcohols have their maxima at 346, 358, 371 and 385 $m\mu$. Although there is little difference between the absorption maxima of primary and secondary alcohols, there is a considerable difference between their molar absorption coefficients.

The fairly similar values of molar absorption coefficients of primary alcohols on one hand and those of secondary alcohols on the other was the basis of development of a method of their separate determination in mixtures.

The nitrite prepared from cyclohexanol has the same molar absorption coefficients as secondary paraffinic alcohol nitrites, but the maxima are displaced by 2 μ in the direction of longer waves.

Alcohols were converted to the nitrites in the following manner [4, 5]. Ten to twenty mg of the alcohol (weighed exactly) was dissolved in 10 ml heptane in a small flask. The solution was then poured into a 100 ml separating funnel. Addition was then made of 10 ml water, 0.5 ml 5 N HCl and 0.5 ml 25% $NaNO_2$ solution. The funnel was shaken for 5 minutes. Reaction took place according to the equations:

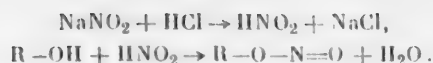
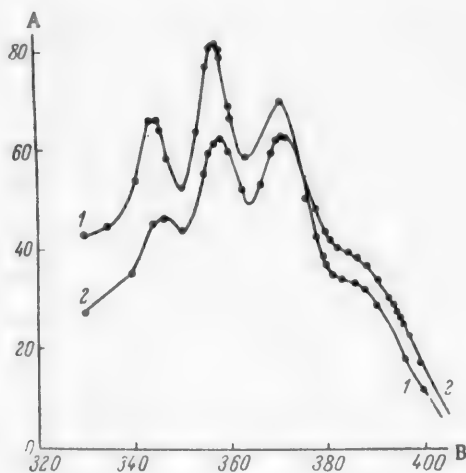


TABLE 1
Wavelengths (I) and Molar Absorption Coefficients (II)

Alcohols	Wavelengths of maxima (in mμ) and molar absorption coefficients							
	I	II	I	II	I	II	I	II
Primary :								
C ₆	344	65.4	357	81.2	370	69.2	384	32.9
C ₈	344	67.1	357	83.1	370	70.6	384	33.5
C ₁₀	344	66.2	357	82.9	370	71.9	384	33.8
C ₁₂	344	68.5	357	84.8	370	72.8	384	34.8
C ₁₆	344	68.4	357	84.1	370	72.7	384	34.9
C ₁₈	344	67.2	357	82.8	370	71.1	384	34.2
Secondary :								
C ₅	346	47.7	358	62.9	371	63.6	385	39.6
C ₈	346	46.8	358	63.2	371	63.7	385	38.7
C ₈	346	47.5	358	63.5	371	63.7	385	38.7

After the shaking operation and subsequent settling the aqueous portion was run off. Excess nitrous acid in the separating funnel was neutralized by addition of 10 ml 0.5 N (NH₄)₂CO₃ solution (alkyl nitrites are stable in an alkaline medium [6]). The separating funnel was again shaken for 5 minutes. After settlement, the aqueous

layer was again poured off. The alkyl nitrite remained in the funnel and was extracted with heptane.* This solution was poured into the cylindrical cells (d = 1 cm) of the spectrophotometer and measurements of the optical density were carried out at various wavelengths. Heptane was tested in a comparison cell. The optical density of the reagents used was zero (in the working portion of the spectrum). The standards and the analyzed samples received standardized chemical treatments.



Absorption curves of alkyl nitrites prepared from primary and secondary aliphatic alcohols. A) Molar absorption coefficient ϵ ; B) wavelength (in mμ). Octyl nitrite: 1) primary, 2) secondary.

Conformity to the Bouguer-Beer Law ($D = \log \frac{I_0}{I} \epsilon cd$)

was verified for several concentrations of the alcohols. It was thus possible, using mean values of the molar coefficients to derive a system of equations of the form of $D = d \sum \epsilon_i C_i$.

With the help of the method of least squares, the following formulas were obtained for determination of primary and secondary alcohols (in moles/liter):

$$C_{\text{prim}} = 0.0352 D_{357} + 0.0206 D_{358} - 0.0059 D_{370} - 0.0124 D_{371} - 0.0418 D_{375}, \quad (1)$$

$$C_{\text{sec}} = -0.0381 D_{357} - 0.0209 D_{358} + 0.0103 D_{370} + 0.0179 D_{371} + 0.0520 D_{375}.$$

* The heptane may be replaced as a solvent for alkyl nitrites by a purified gasoline fraction which has been checked in the spectrophotometer.

We chose as analytical wavelengths 357, 358, 370, 371 and 375 m μ (in addition 344 and 385 m μ can also be used). At 375 m μ , the absorption curves of primary and secondary alcohols intersect and therefore the total content of alcohols can also be determined by measurement of the absorption at one point.

We then have:

$$C_{\text{prim}} + C_{\text{sec}} = \frac{D_{375}}{55.4} = 0.018 D_{375} \quad (2)$$

The method was tested by analysis of prepared mixtures of primary and secondary alcohols in heptane.

The results shown in Table 2 indicate the satisfactory accuracy of the method.

TABLE 2
Results of Determination of the Quantity of Alcohols in the Mixtures

Mixtures	Alcohols introduced (in M/liter)							Alcohols determined (M/liter)			% of primary alcohols		Relative error in determination of total alcohols
	primary			secondary			Mixtures	primary	secondary	Over-all total	introduced	determined	
	C ₁	C ₂	Total	C ₃	C ₄	Over-all total							
1 (15)	0.98	0.81	1.79	1.17	1.19	2.36	4.15	1.89	2.22	4.11	43.2	45.8	-1.0
2 (18)	4.90	2.43	7.33	1.17	1.19	2.36	9.69	7.37	2.36	9.73	75.6	75.7	+0.4
3 (19)	1.96	1.62	3.58	1.17	1.19	2.36	5.94	3.49	2.45	5.94	60.3	58.8	0
4 (20)	0.98	0.81	1.79	3.51	3.57	7.08	8.87	1.81	6.65	8.46	20.2	21.4	-4.6
5 (21)	1.96	1.62	3.58	2.34	2.38	4.72	8.30	3.31	4.70	8.01	43.2	41.3	-3.5
6 (22)	0.98	2.43	3.41	1.17	2.38	3.55	6.96	3.16	3.57	6.73	49.0	47.0	-3.3
7 (C ₁₂ prim)	-	9.94	9.94	-	-	-	9.94	10.11	0.37	10.49	100	96.3	+5.5
8 (C ₈ sec)	-	-	-	13.88	-	13.88	13.88	-	13.97	13.97	0	0	+0.6

The alcohols were isolated from the analytical samples in order to exclude a possible effect of oxygen-containing compounds on the accuracy of determination of the alcohols. In view of the high sensitivity of the method, the concentrates of alcohols for analysis were diluted with heptane to give final concentrations of alcohols of 0.005 to 0.01 mole/liter. The molar proportions of primary and secondary alcohols in 1 g of product for analysis were determined from the weight of the sample. In a number of cases it was sufficient to know only the ratio between the concentrations of primary and secondary alcohols.

On the basis of the similarity between the spectra of nitrites prepared from normal butyl and isobutyl alcohols (both of which are primary [4]) we can postulate that branched structure of the molecules of higher primary and secondary alcohols does not interfere with determinations by this method.

The time required for analysis of a sample is 40-45 minutes.

Primary and secondary alcohols in the products of the hydrocarbon oxidation laboratory of VNIINEFTEKhimA* are being determined by the present method.

SUMMARY

A spectrophotometric method was developed for determination of primary and secondary alcohols on the basis of the characteristic absorption of their nitrites in the ultraviolet.

The small quantities of alcohols (≈ 10 mg) needed for determination, the comparative speed of analysis, and the satisfactory accuracy permit its application for identification of alcohols obtained in various synthetic and petrochemical processes.

* M. F. Shnitko participated in the work.

LITERATURE CITED

- [1] A. N. Bashkirov, V. V. Kamzolkin, K. M. Sokolova, and T. P. Andreeva, *Khím. Tekh. Topliv i Masel* 4, 7 (1957).
- [2] A. N. Bashkirov, S. A. Lodzik, and V. V. Kamzolkin, *Trudy Inst. Nefti* 12, 297 (1958).
- [3] P. Tarte, *Bl. Soc. Roy. Sci. Liége* 26, 1, 40 (1957).
- [4] Ya. É. Shmulyakovskii, *Khím. i Tekh. Topliv i Masel* 12 (1959).
- [5] S. A. Shchukarev, S. N. Andreev and N. A. Ostrovskaya, *Zhur. Anal. Khím.* 9, 1, 354 (1954)*
- [6] I. V. Patsevich, A. V. Topchiev, and V. Ya. Shtern, *Zhur. Anal. Khím.* 13, 5, 608 (1958).*

Received April 4, 1959

*Original Russian pagination. See C. B. Translation.

THE EBULLIOSTATIC METHOD OF DETERMINATION OF REDUCING SUGARS

V. K. Nizovkin and I. Z. Emel'yanova

Reducing sugars can be quantitatively determined in pure aqueous solutions and in industrial liquors by a large number of methods based on various properties of these sugars [1].

The basis of the ebulliosstatic method is the oxidation of sugars with an alkaline solution of a copper salt. Chemists have made use of this reaction for more than 100 years [2-4] for the quantitative determination of reducing sugars. Many gravimetric, volumetric and colorimetric variants have been developed [5-8] as well as methods of direct titration of the copper solution with sugar solution in presence of various indicators [9-18]. The very large number of such methods testify to the specific value of alkaline copper solution as a sugar oxidant [19]. At the same time, they indicate that serious difficulties arise in obtaining sufficiently accurate results.

The oxidation of sugars with alkaline copper solution consists not in a single specific reaction but in several hundred simultaneous reactions. The bearers of the reducing properties of sugars are the products of transformation and breakdown of the sugars in alkaline copper solution. Glucose alone can yield 113 compounds, some of which react with copper oxide [20].

The quantity of copper reduced by a given quantity of a sugar depends on the temperature and duration of heating of the reacting liquid, on the possibility of access of atmospheric oxygen to the reaction products, on the composition and concentration of the components of the alkaline copper solution, on the concentration of the sugar in the sample, on the autoreduction of the copper solution during the reaction, etc. All of the methods for calculation of the results of analysis must therefore make use of empirical tables of the quantitative ratio between oxidized sugar and reduced copper. Special tables are required for each method [6, 21-26].

In the ebulliosstatic method, the reaction takes place in a special apparatus (an ebulliosstat) enabling exclusion of atmospheric oxygen from the reaction sphere, uniform heating, good stirring, and avoidance of local overheating of the reacting liquid. The alkaline copper solution employed has such a composition that no precipitates of compounds of reduced copper are formed during the reaction to interfere with observation of the end point in the case of direct titration [9-11]. Concentrations of components of the copper solution are so selected that a sugar can be determined in a colored solution. The indicator is methylene blue. This fixes the end point exactly since the instant of its color change coincides with the instant of the jump in the oxidation-reduction potential during potentiometric titration of the alkaline copper solution with sugar solution [27].

EXPERIMENTAL

The ebulliosstat (Fig. 1) comprises an outer vessel 1 and an inner vessel 2. Vessel 1 is a 0.8-1 liter conical flask in which steam is generated. Vessel 2 is the reaction vessel in which titration is performed in a current of steam. It is a cylinder narrowed at the top. Sealed to its interior is a tube for admission of steam from vessel 1. Steam is taken off from vessel 2 during a titration through a side opening. The excess of steam from vessel 1 goes off through tube 3. The quantity of steam entering the reaction vessel is regulated by a screw clip 4.

The first solution contains 10 g of $\text{CuSO}_4 \cdot 5\text{H}_2\text{O}$ and 0.04 g methylene in one liter. The second solution contains 50 g Selgnette salt, 75 g sodium hydroxide and 5 g potassium ferrocyanide in one liter. Solutions I and II are measured out with the help of the proportionators sketched in Fig. 2.

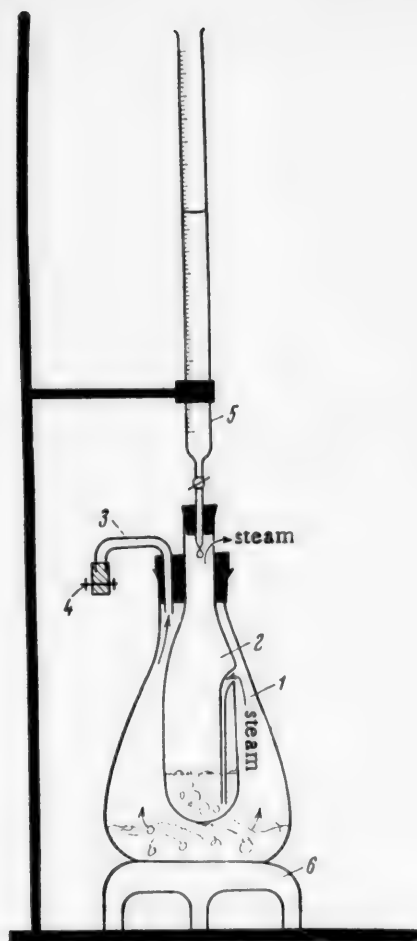


Fig. 1. Determination of reducing sugars by the ebulliostatic method. 1) Steam generator; 2) reaction vessel; 3) excess steam lead-off tube; 4) screw clip; 5) buret containing sugar solution for analysis; 6) electric hot plate.

Solution I is measured out with apparatus 1 (Fig. 2) in the following manner. While tap 2 is open, bulb 3 is filled to the upper mark on the capillary tube. Tap 2 is then closed, tap 4 is opened — at first only a little in order that the displaced liquid should not stick to the walls of the capillary from which it is displaced. When liquid starts to flow out of the bulb, tap 4 can be opened fully. After the bulb has been freed of liquid, tap 4 is again closed and the last portions of liquid discharged slowly in order to ensure that tap 4 is closed when the level of the solution has reached the lower mark on the capillary.

Solution II is measured with proportionator 5; this is a pipet to whose upper end is attached a three-way tap. Tap 6 is turned to position a, bulb 7 is squeezed, the lower end is lowered into the vessel containing solution II, the bulb is released, the solution is drawn up to the

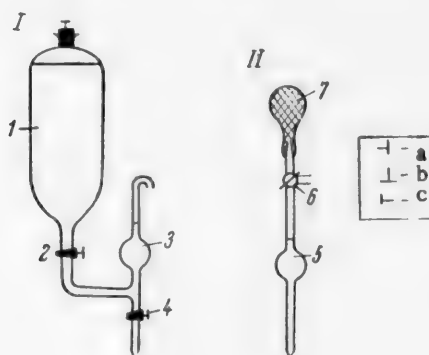


Fig. 2. Proportionators. I) Proportionator for measuring solution I; II) proportionator for measuring solution II. a, b, c) positions of three-way tap during measuring-out of liquid.

mark and the tap is turned to position b. The vessel with solution II is then removed and the ebulliostat put in its place. Tap 6 is turned to position c, whereupon the liquid runs from the proportionator into the positioned ebulliostat.

The titer of the alkaline copper solution in this method is arbitrarily taken to be the number of milligrams of sugar required for reduction of 10 ml of alkaline copper solution. Different sugars differ in their reducing power, so that the titer of the copper solution must be established with the sugar which is being analyzed.

The titer for copper solution for any given sugar is adjusted by taking 2 to 3 weighed samples of the anhydrous and absolutely dry sugar in the form of 0.1% solutions and then carrying out 3 to 4 titrations of each solution by the procedure detailed below.

The titer is calculated from the formula

$$T = a \cdot C,$$

where a is the number of milliliters of sugar solution used in the titration, and C is the concentration (in mg/ml) of sugar in solution (from the weighed amount).

The mean of the results is taken.

Direct titration is practiced when the sugar concentration of the analyzed solution is 0.13-0.05%. Strongly colored solutions or solutions with concentrations of sugar below 0.05 are analyzed by back titration. Large series of solutions are likewise analyzed by back titration.

Titration of clear solutions containing 0.13-0.05% sugar (direct titration). Samples containing over 0.13% of sugar must be diluted beforehand.

Conductivity water is run into vessel 1 (Fig. 1). Beads are introduced to ensure smooth boiling. The apparatus is placed on the heater. When the water begins to boil, 5 ml each of solutions I and II are admitted into the cold reaction vessel 2 from the proportionators; vessel 2 is slowly immersed in vessel 1 (rapid lowering into the steam with simultaneous closing of the vessel by a stopper leads to reduction in pressure in vessel 1 which is accompanied by spurting of copper solution through its internal tube into the steam generator). The top opening of vessel 2 is then closed with a stopper attached to the tip of the buret containing the solution for analysis. Commencement of passage of steam through the alkaline copper solution is then awaited. Heating of 10 ml of alkaline copper solution to the temperature of boiling water requires 0.5 to 0.7 minute. The quantity of steam passing through the reaction vessel is regulated with screw clip 4.

As soon as steam commences to pass in a vigorous stream through vessel 2, the tap of the buret is opened and 90% of the quantity of sugar solution used up in the titration is run in (this quantity is established beforehand in a trial analysis). After a wait of 2 minutes (using a sand glass) the titration is completed by addition of sugar solution from the buret at the rate of one drop per 6-7 seconds. Completion of analysis is indicated by change of the violet color of the reacting liquid to yellow on addition of one drop of sugar solution.

The percentage concentration of sugar K in the sample is calculated from the formula

$$K = \frac{T \cdot n \cdot 100}{a \cdot 100},$$

where T is the arbitrary titer of the alkaline copper solution (in mg sugar); n is the dilution; a is the number of milliliters of sugar solution consumed for the titration.

Titration of strongly colored solutions and solutions whose sugar concentration is below 0.05% (back titration). A 0.1% solution of the glucose or other sugar is made up. Its concentration is found by direct titration and it is used in the analysis as a comparison solution.

Into the reaction vessel are run 5 ml each of solutions I and II from the proportionators. The vessel is then immersed in the steam generator; then the sugar solution (measured by the pipet) is run into the alkaline copper solution.

The quantity of sugar solution taken for analysis is found by preliminary titration. It must not exceed 5 ml when the sugar solutions are very weak. In the case of dark solutions it should be about 1 ml.

The upper opening of the reaction vessel is closed with the stopper on the tip of the buret which is filled with sugar solution of known concentration. The sugar solution is run into the reaction vessel from the buret in an initial analysis step until a violet color appears. In the final stage of the analysis, about 0.5 ml of solution is added in addition. After a waiting period of two minutes, the final titration is continued by addition of sugar solution from the buret at the rate of one drop per 7 seconds until the violet color changes to yellow.

The sugar concentration K in the analyzed solution (in percent) is calculated from the formula

$$K = \frac{(T - Ca) \cdot 100}{b \cdot 100},$$

where T is the arbitrary titer of the alkaline copper solution (in mg sugar); C is the sugar concentration in the comparison solution (in mg/ml); a is the volume of the comparison solution consumed for analysis (in ml); b is the volume of the sample of sugar solution taken for analysis (in ml).

The accuracy of the method is characterized by the magnitude of the deviation of the analytical result from the true content of the substance and by the reproducibility of the determinations. The ebulliostatic method

was tested on pure solutions of glucose and galactose and on solutions of glucose in wood hydrolyzates and sulfite liquors which were taken as specimens of colored liquids. Before the colored solutions of glucose were prepared, the content of reducing solutions in the hydrolyzate and sulfite liquor was determined; a known quantity of glucose was then added to them.

Results of the analyses are set forth in Table 1.

TABLE 1
Analysis of Sugar Solutions by the Ebulliostatic Method

Substance determined	Sugar concentration (%)					Maximum deviation from mean (in %)	Error of analysis (in % of original value)
	taken	determination					
		I	II	III	mean		
Aqueous solution of glucose	0.100	0.099	0.100	0.100	0.0997	1	—0.3
Aqueous solution of galactose . . .	0.110	0.109	0.110	0.110	0.1097	1	—0.3
Hydrolyzate	3.25	3.28	3.22	3.24	3.25	1	0
Hydrolyzate + glucose	3.25+1.10	4.33	4.30	4.37	4.33	1	—0.5
Sulfite liquor	1.50	1.50	1.51	1.50	1.50	0.7	—
Sulfite liquor + glucose	1.50+1.55	3.03	3.10	3.10	3.08	1	+0.8

We see from Table 1 that determinations by the ebulliostatic method are accurate to within $\pm 1\%$. The maximum deviation of the analytical results from the mean value does not exceed 1%.

By means of the above method of analysis the reducing power of glucose, galactose, fructose, xylose and arabinose was determined at various concentrations. The concentrations of the sugar solutions ranged from 0.44-0.070% to 0.135-0.220%. Chemically pure preparations of the sugars were taken for analysis. Each solution was titrated three times. The arithmetical means from the three determinations are set forth in Table 2.

TABLE 2
Reducing Power of Sugars at Various Concentrations

Glucose	Consumed for analysis (in mg)	Galactose		Fructose		Xylose		Arabinose	
		Concentration (in mg)	Consumed for analysis (in mg)	Concentration (in mg)	Consumed for analysis (in mg)	Concentration (in mg)	Consumed for analysis (in mg)	Concentration (in mg)	Consumed for analysis (in mg)
0.1356	5.70	0.1385	6.18	0.2000	6.18	0.1506	5.70	0.2200	5.38
0.1240	5.69	0.1205	6.18	0.1600	6.17	0.1069	5.67	0.1100	5.39
0.1145	5.72	0.1160	6.17	0.1514	6.17	0.0846	5.68	0.0800	5.40
0.0984	5.69	0.1040	6.17	0.1000	6.15	0.0753	5.68	0.0650	5.42
0.0977	5.72	0.0897	6.16	0.0800	6.18	0.0527	5.66	0.0500	5.40
0.0904	5.70	0.0767	6.16	0.0700	6.17	0.0440	5.67	0.0450	5.41
Mean	5.70	—	6.17	—	6.17	—	5.68	—	5.40

The data of Table 2 show that in the range of concentrations investigated the quantity of sugar consumed for titration is a constant which is independent of the sugar concentration in solution. Reduction of 10 ml of alkaline copper solution, prepared exactly as described above, requires 5.70 mg glucose, 6.17 mg fructose, 6.17 mg galactose, 5.68 mg xylose and 5.40 mg arabinose.

The ratios between copper and the different sugars are set forth in Table 3.

TABLE 3
Reducing Power of Sugars for Copper

Sugar	Amount of copper oxidized by 1 mg of sugar (in mg)	Amount of sugar reduced by 1 mg of copper (in mg)	Number of oxygen atoms consumed in oxidation of one molecule of sugar
Glucose	2.24	0.445	3.16
Galactose	2.07	4.482	2.92
Fructose	2.07	4.482	2.92
Xylose	2.25	0.444	3.17
Arabinose	2.36	0.423	3.33

The analysis of sugar solutions by the ebulliostatic method consequently does not call for empirical tables of the dependence of the reduced copper on the sugar concentration. Calculation of the concentration of a sugar solution requires knowledge only of the titer of the alkaline copper solution in relation to the sugar being determined.

The ebulliostatic method has been adopted as a standard method of determination of reducing sugars in intermediate products of wood hydrolysis and sulfite alcohol factories.

SUMMARY

1. An ebulliostatic method is proposed for determination of reducing sugars. It is based on the titration of alkaline copper solution with sugar solution. Analysis is performed in a special apparatus — an ebulliostat — which excludes the effect of atmospheric oxygen on the oxidation of sugars, and ensures constant temperature and good stirring of the mixture of reactants.
2. The quantity of copper reduced does not depend on the concentration of sugar in the solution being analyzed. Empirical tables are therefore unnecessary. The method is accurate to $\pm 1\%$.
3. The method has been adopted as standard in the wood hydrolysis and sulfite alcohol industries.

LITERATURE CITED

- [1] Z. Dische, *Microchemie* 1, 1 (1929).
- [2] M. Barreswil, *J. Pharm.* 3, 6, 301 (1844).
- [3] H. Fehling, *Ann.* 72, 106 (1849); 106, 75 (1858).
- [4] W. Braun and B. Bleyer, *Z. Analyt. Chem.* 76, 1 (1929).
- [5] J. Bertrand, *Bull.* 3, 35, 1293 (1906).
- [6] J. Kjeldahl, *Compt. rend. trav. Laboratoire Carlsberg*, 1, 4 (1895).
- [7] N. Ya. Dem'yanov and V. N. Pryanishnikov, *General Methods of Analysis of Vegetable Materials* [In Russian] (Moscow, 1938).
- [8] P. M. Silin, *Chemical Control in the Beet-Sugar Industry* [In Russian] (Food Industries Press, 1949).
- [9] F. Soxhlet, *J. pr. Chem.* 2, 21, 227 (1878).
- [10] L. Eynon and J. H. Lane, *J. Soc. Chem. Ind.* 42, 32T (1923).
- [11] S. R. Benedict, *J. Amer. Med. Assoc.* 57, 1193 (1910).

- [12] S. Haddon, *La Revue Agrical.* 59, 131 (1931).
- [13] W. L. Daggett, A. W. Campbell, and J. L. Whitman, *J. Amer. Chem. Soc.* 45, 1045 (1923).
- [14] J. Niederl and R. Miller, *J. Amer. Chem. Soc.* 51, 5, 1292 (1929).
- [15] B. O. Lyubin and K. A. Kazakevich, *Trans. Leningrad Sci.-Res. Inst. of the Food Ind.* (1937).
- [16] P. S. Bukharov and B. B. Evstigneev, *Electrometric Determination of Invert Sugar [In Russian]* (1933).
- [17] V. K. Nizovkin, O. I. Okhrimenko and M. K. Suzi, *Trans. All-Union Sci. Res. Inst. Hydrolysis and Sulfite Alcohol Ind.* 2, 257 (1947).
- [18] V. K. Nizovkin and I. Z. Emel'yanova, *Trans. All-Union Sci. Res. Inst. Hydrolysis and Sulfite Alcohol Ind.* 2, 277 (1947).
- [19] V. I. Sharkov and O. D. Kamaldina, *Zhur. Lesokhim. Prom.* 5 (1933).
- [20] J. U. Nef, *Ann. Chem.* 335, 323 (1904); 357, 214 (1907); 376, 1 (1910).
- [21] H. T. Brown, J. H. Morris and J. H. Miller, *J. Chem. Soc.* 71, 95 and 281 (1897).
- [22] S. Adler, *Biochem. J.* 190, 433 (1927).
- [23] F. A. Quisumbing and A. W. Thomas, *J. Amer. Chem. Soc.* 43, 1503 (1921).
- [24] Ph. A. Shaffer and M. Somogyi, *J. Biol. Chem.* 100, 695 (1933).
- [25] V. J. Harding and C. E. Downs, *J. Biol. Chem.* 101, 487 (1933).
- [26] A. Heiduschka and W. Biethan, *J. pr. Chem.* 2, 133, 273 (1932).
- [27] I. Z. Emel'yanova, *Candidate's Dissertation* (1954).

Received March 1, 1959

THE DISTRIBUTION OF C_1 - C_3 ACIDS IN THE SYSTEM DIISOPROPYL ETHER - WATER

V. P. Sumarokov and Z. M. Volodutsкая

The literature contains very scanty data about the distribution of formic, acetic and propionic acids in the system diisopropyl ether - water.

Brik [1] studied various solvents for extraction of acetic acid from weak solutions and determined the coefficients of distribution of acetic acid between diisopropyl ether and liquor containing various percentages of acetic acid (8-12%). According to his results the coefficient of distribution is variable and decreases with increasing concentration of acid in the liquor.

Werkman [2] submitted data for the distribution of acetic, propionic and butyric acids between diisopropyl ether and water and made use of his results in the determination of those acids in their mixtures. We were unable to find any literature data for the distribution of formic acid in the system in question.

Diisopropyl ether has an advantage over diethyl ether as an extractant for low-molecular fatty acids in that it is nearly insoluble in water: water dissolves in diisopropyl ether at 23° to the extent of 0.4 wt. %, as against a solubility of diethyl ether of 1.3 wt. % (at 25°). Diisopropyl ether dissolves in water (at 23°) to the extent of 2.7 wt. %, as against a solubility of diethyl ether (at 25°) of 6.02 wt. %. Diisopropyl ether boils at 67.5° (760 mm); diethyl ether boils at 34.6°.

Due to the low solubility of water in diisopropyl ether, nearly anhydrous acid at once remains behind after the ether has been distilled off from the extract. The separation of formic and acetic acids by rectification is therefore facilitated. There are reports of the utilization in the U.S.A. of diisopropyl ether as an additive to ethyl acetate for lowering of the solubility of water in the solvent during extraction of acids from aqueous solutions. Diisopropyl ether has a big potential raw material basis in Russia in connection with the development of the petrochemical industry since it can be easily obtained from oil cracking products.

In this work we investigated the distribution of formic, acetic and propionic acids in the system $C_3H_7OC_3H_7-H_2O$ with acid concentrations of 0.25 to 1.5 mole/liter in the original aqueous solutions. These concentrations are typical of industrial conditions.

EXPERIMENTAL

Starting materials. 1) Diisopropyl ether ($C_3H_7OC_3H_7$), "pure" grade to specification TU 741/52, produced by the Kharkov Chemical Reagent Works. The ether had specific gravity (γ_{20}^{20}) 0.7240. 2) Acetic acid, pure grade (98.48 %). It was treated with permanganate and rectified before use. The fraction used came over at 117-118° and contained 99.90% acid; it had specific gravity (20°) 1.0528, refractive index (n_D^{20}) 1.3720; oxidizability with 0.1 N $KMnO_4$ solution in the cold: pink color with one drop. 3) Formic acid (product of the Kharkov Chemical Reagent Works) had specific gravity (20°) 1.195 and acid content of 85.01%. 4) Propionic acid (product of Kharkov Chemical Reagent Works) had specific gravity (20°) 0.9899, acid content (by titration) 100.5%, refractive index (n_D^{20}) 1.3860. It formed a transparent solution (1:1) in water; in the Engler distillation it distilled completely between 135 and 144°.

TABLE 1

Distribution of Formic Acid in the System Diisopropyl Ether - Water

in starting solution		HCOOH concentration		in aqueous layer at equilibrium		Partition coefficient $\frac{C_e}{C_w}$
		in ether layer at equilibrium				
g/liter	M/liter	in wt. -%	C_e (g/liter)	in wt. -%	C_w (g/liter)	
11.5	0.25	0.325		0.959		
		0.331		0.978		
		0.335		0.985		
		0.333		0.980		
	Mean value	0.331	2.40	0.975	9.68	0.248
23.0	0.50	0.608		1.779		
		0.610		1.775		
		0.608		1.775		
		0.611		1.757		
	Mean value	0.609	4.43	1.772	17.63	0.251
46.0	1.00	1.182		3.399		
		1.180		3.373		
		1.181		3.390		
		1.186		3.380		
	Mean value	1.182	8.63	3.385	33.81	0.255
69.0	1.50	1.916		5.406		
		1.929		5.367		
		1.951		5.410		
		1.909		5.380		
	Mean value	1.926	14.13	5.391	54.09	0.261

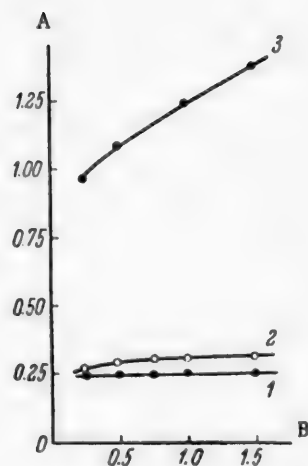


Fig. 1. Effect of concentration of original solution C_0 on the value of the partition coefficient C_e/C_w of C_1 - C_3 acids in the system $C_6H_{14}O$ - H_2O . A) Partition coefficient C_e/C_w ; B) concentration of original solution C_0 (in mole/liter). Acid: 1) $HCOOH$, 2) CH_3COOH , 3) C_2H_5COOH .

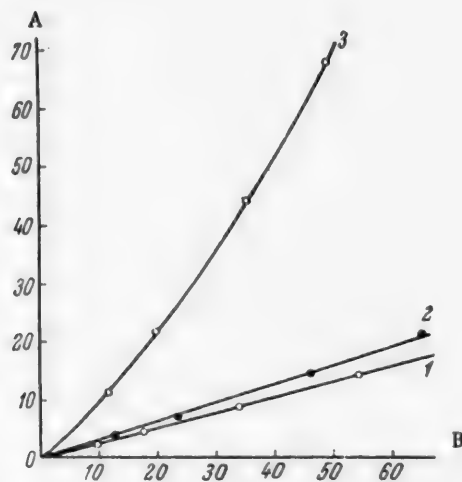


Fig. 2. Equilibrium concentrations of C_1 - C_3 acids in the system diisopropyl ether - water at 20° . A) Acid concentration in ether layer (in g/liter); B) acid concentration in aqueous layer (in g/liter). Acid: 1) $HCOOH$, 2) CH_3COOH , 3) C_2H_5COOH .

Experimental procedure. 20 ml of the acid and 20 ml of diisopropyl ether were pipeted into a separating funnel; the latter was then shaken for 5 minutes and placed in a water thermostat at 20° for 30 minutes. At the expiration of this period, the funnel was removed from the thermostat. The aqueous and ethereal layers were separated and the concentration of acid in the two layers was determined by titration with 0.1 N NaOH solution in presence of phenolphthalein. The concentration was expressed as percentages by weight and as grams per liter. The partition coefficient was expressed as the ratio C_e/C_w , where C_e is the acid concentration (in g/liter) in the ether layer and C_w is the concentration in the aqueous layer.

Partition of C_1-C_3 acids between diisopropyl ether and water. Solutions of formic, acetic and propionic acids were made up in concentrations of 0.25, 0.50, 1.00 and 1.50 mole/liter. Equilibrium concentrations were determined by the method described above. Between 4 and 6 determinations were carried out with each solution of acid.

Results of the determinations are set forth in Tables 1-3. Mean results were used for construction of graphs (Figs. 1 and 2).

TABLE 2

Distribution of Acetic Acid in the System Diisopropyl Ether - Water

CH ₃ COOH concentration						Partition co- efficient $\frac{C_e}{C_w}$
in starting solution		in ether layer at equili- brium		in aqueous layer at equilibrium		
g/liter	M/liter	in wt. -%	C _e (g/liter)	in wt. -%	C _w (g/liter)	
15.0	0.25	0.483		1.281		
		0.486		1.279		
		0.486		1.306		
		0.477		1.302		
	Mean value	0.483	3.50	1.292	12.81	0.273
30.0	0.50	0.965		2.336		
		0.949		2.360		
		0.974		2.392		
		0.970		2.401		
	Mean value	0.965	7.02	2.372	23.53	0.298
60.0	1.00	1.964		4.632		
		1.965		4.632		
		1.955		4.679		
		1.947		4.668		
		1.984		4.614		
		1.993		4.667		
	Mean value	1.968	14.30	4.649	46.18	0.310
90.0	1.50	2.846		6.556		
		2.861		6.557		
		2.876		6.583		
		2.923		6.601		
	Mean value	2.877	21.10	6.574	65.37	0.323

Figure 1 shows the partition coefficients C_e/C_w as a function of the concentration of the original solution; Fig. 2 shows the equilibrium concentrations of C_e and C_w . The graphs enable us to make the following generalizations about the distribution of C_1-C_3 acids in the system in question.

1. The concentration of the original solution hardly influences the ratio of distribution of HCOOH in the system (the plot of C_e/C_w is nearly rectilinear and parallel to the axis of the abscissas), has little influence on the ratio of distribution of CH₃COOH (the C_e/C_w plot is nearly rectilinear with a slight inclination to the axis of the abscissas), and has a strong influence on the distribution of CH₃CH₂COOH (the C_e/C_w plot has a marked curvature with a large angle of inclination to the axis of the abscissas).

The very weak effect of the concentration on the distribution of acetic acid sharply differentiates the system diisopropyl ether - water from the systems ethyl acetate - water, butyl acetate - water and diethyl ether - water [3].

TABLE 3
Distribution of Propionic Acid in the System Diisopropyl Ether—Water

C ₂ H ₅ COOH concentration						Partition co- efficient $\frac{C_e}{C_w}$
in starting solution		in ether layer at equilibrium		in aqueous layer at equilibrium		
g/liter	M/liter	in wt. -%	C _e (g/liter)	in wt. -%	C _w (g/liter)	
18.5	0.25	1.546		1.173		
		1.553		1.162		
		1.531		1.186		
		1.531		1.174		
	Mean value	1.540	11.23	1.174	11.63	0.965
37.0	0.50	2.975		2.031		
		2.898		1.984		
		2.992		2.004		
		2.995		2.024		
	Mean value	2.965	21.73	2.011	19.92	1.091
74.0	1.00	5.952		3.590		
		5.951		3.564		
		5.950		3.578		
		5.957		3.595		
	Mean value	5.952	44.10	3.582	35.48	1.243
111.0	1.50	9.092		5.022		
		9.043		5.072		
		9.108		4.883		
		9.093		4.903		
	Mean value	9.084	68.06	4.970	49.22	1.383

2. The equilibrium concentrations of HCOOH and CH₃COOH are represented as nearly straight lines in the plot of C_e versus C_w. These plots are close to one another and have a small angle of slope to the axis of the abscissas. On the other hand, the equilibrium concentration plot of CH₃CH₂COOH is slightly curved and rises steeply with increasing C_w. This indicates the extremely favorable possibilities for use of diisopropyl ether for extraction of this acid (and higher homologs) from aqueous solutions. The number of theoretical stages for this purpose will be small in comparison with the requirements in apparatus for extraction of acetic acid from aqueous solutions and can be calculated by known methods on the basis of the results obtained.

SUMMARY

1. Of the three acids — HCOOH, CH₃COOH, C₂H₅COOH — the first two are extracted relatively weakly by diisopropyl ether from aqueous solutions and more weakly than by diethyl ether. Propionic acid is extracted very efficiently by diisopropyl ether.

2. Unlike the systems known in technology (diethyl ether—water, ethyl acetate—water, butyl acetate—water) the concentration of the original aqueous solution in the system diisopropyl ether—water has no influence on the partition coefficient of CH₃COOH and HCOOH. The concentration of original solution markedly influences the partition coefficient during extraction of propionic acid.

3. The equilibrium concentration plots of acetic and formic acids in this system are represented by straight lines slightly inclined towards the axis of the abscissas. On the other hand the propionic acid plot has a slight curvature and a large angle of slope. This indicates the possibility of extraction of propionic acid from aqueous solutions in an extractor with a small number of theoretical stages.

LITERATURE CITED

- [1] A. N. Brik, Trudy Tsentral. nauch.- issled. lesokhim. inst. 1, 129 (1933).
- [2] C. H. Werkman, Ind. Eng. Chem. Anal. Edit. 2, 302 (1930).
- [3] V. P. Sumarokov and E. V. Klinskikh, Zhur. Priklad. Khim. 23, 641 (1950).

Received February 28, 1959

HETEROGENEOUS EQUILIBRIA IN THE SYSTEM METHYL ACETATE - CHLOROFORM - WATER

N. V. Lutugina and V. M. Kalyuzhnyi

Leningrad State University

Molodenko and Bushmakina [2] followed up the work of Reinders [1] on the possibility of predicting the behavior of three-component system during free evaporation. They constructed isobar-isotherms and distillation lines from the boiling points of the pure components and from the compositions and boiling points of the binary azeotropes. Utilizing their experimental data and a few results of other authors [3, 4], they also suggested the possibility of extending this method to stratifying systems, although in this case the pattern of the isobar-isotherm and distillation plots is badly distorted in relation to systems not possessing a stratification region.

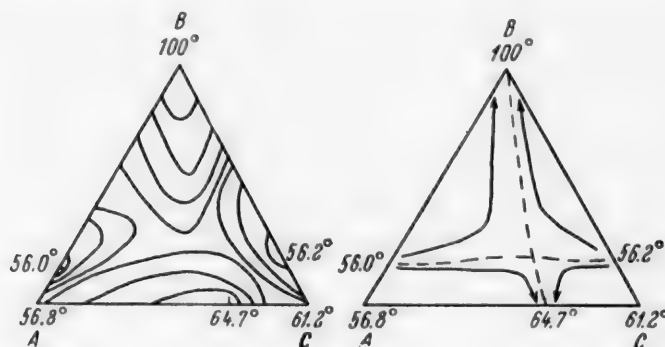


Fig. 1. Proposed arrangements of the isobar-isotherms and distillation lines in the system methyl acetate - chloroform - water. A) Methyl acetate; B) water; C) chloroform.

Their statement calls for further experimental confirmation in particular for complex systems in which there are several singular points of various types.

As an example of such a system, we chose methyl acetate - chloroform - water in which two pair of components (chloroform - water and methyl acetate - water) possess incomplete reciprocal solubility. According to [5] this system contains two binary homogeneous azeotropes (a maximum in the system chloroform - methyl acetate and a minimum in the system methyl acetate - water) and a binary azeotrope of chloroform - water. Data for compositions and boiling points of binary azeotropes and of pure components, ignoring possible stratification indicate the possibility of only one arrangement of isobar-isotherm and distillation plots on the triangle of compositions (Fig. 1). This diagram indicates that we should expect in this system a ternary azeotrope (or a heteroazeotrope) of the saddle-point type. The experimental objective of the present work was to establish whether agreement exists between the proposed pattern of the plots and the true pattern of the isobar-isotherms and distillation lines. Bushmakina and Kish [6] carefully verified the compositions of co-existing liquids and vapors and also the boiling points in the system methyl acetate - chloroform. Further confirmation was therefore not

attempted. Our own experiments were in connection with the position of the stratification curve in the ternary system, the disposition of the liquid-liquid intersections on the triangle of compositions and the isobar-isotherms of the homogeneous liquids, the course of the distillation lines and the position of the vapor line in the three-phase equilibrium region.

Substances. Methyl acetate was prepared by the usual method [7] from methanol (n_D^{20} 1.3289) and glacial acetic acid. It was purified by washing with sodium carbonate solution and water; after drying over CaCl_2 it was rectified three times in a 20-plate column (column efficiency evaluated with C_6H_6 - CCl_4 mixture). Commercial chloroform was distilled three times in a 20-plate column. The purities of our products and of the products used by Bushmakín and Kish [6] are set forth in Table 1. Distilled water was generally employed.

TABLE 1
Characteristics of Substances Used in the Work

Data of	Methyl acetate		Chloroform	
	n_D^{20}	b. p. (in ° C)	n_D^{20}	b. p. (in ° C)
Authors	1.3614	56.8	1.4461	61.2
Bushmakín and Kish [6]	1.3614	56.8	1.4461	61.22

Analysis of three-component solutions. During the work it was necessary to determine both the compositions of the homogeneous ternary solutions and the over-all compositions of the stratifying liquids. In both cases, preliminary determinations were made of the position of the reciprocal solubility curve by the previously described method. Determinations were also made of the refractive index of solutions corresponding to points lying on this binodal system. The data were employed for construction of calibration curves of n_D^{20} versus weight % of one of the components (methyl acetate) in saturated solutions.

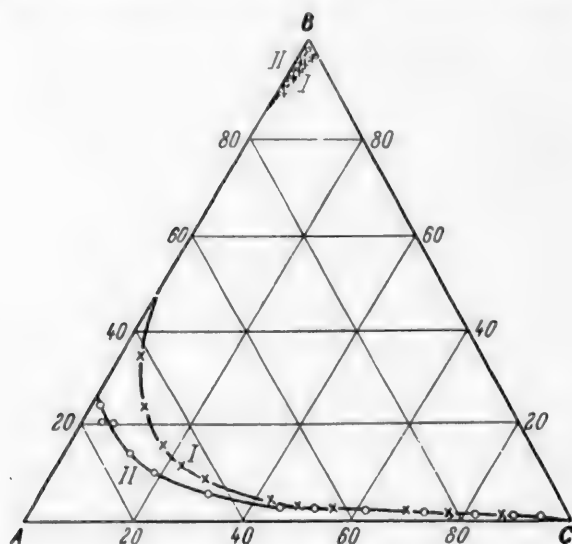


Fig. 2. Curves of reciprocal solubility of components in the system methyl acetate-chloroform-water at $p = 760$ mm Hg. A) Methyl acetate; B) water; C) chloroform. I) At the boiling point of the solution; II) at 20° . (Concentrations of components are expressed as molar percentages).

Over-all compositions of the heterogeneous liquids were determined by the following procedure: after complete stratification of the sample, the two layers were separated in a separating funnel. Each layer was then weighed and its percentage content of one component (methyl acetate) was found from the refractive index calibration curve; the percentage of the remaining two components was found from the binodal curve plotted on the triangle of compositions. The over-all composition by weight and then the over-all molar composition of the investigated heterogeneous liquid was then calculated.

Compositions of homogeneous solutions were determined in the following manner. A previously weighed quantity of the solution was titrated with one of the components of the system (water) until a faint permanent cloudiness had developed. The solution was then weighed again and its refractive index was measured. The concentrations and weight percentages of each component were then read off from the calibration curves. The original weights of each component were then obtained by subtracting from the total quantity of water in the new solution the quantity of water added during titration. The composition of the solution taken for analysis was thus calculated.

A large number of preliminary blank experiments showed that the absolute error in determination of the gross composition of heterogeneous liquids is ± 0.2 mole %, while the error in analysis of homogeneous solutions is ± 0.3 mole %.

Position of the solubility curve. Clarification of the behavior of systems possessing incomplete miscibility of the components under conditions of free evaporation necessitates knowledge of the position of the solubility curve at the boiling points of the stratified solutions (at 760 mm Hg). Analyses require knowledge of the position of the solubility curve at 20° (room temperature*).

In both cases, the position of the intersection was determined by titration of the two-component homogeneous solutions (prepared by preliminary weighing) with the third component until the mixture turned cloudy.

TABLE 2
Data for Construction of Solubility
Curve at 20° and $p = 760$ mm Hg

Compositions of saturated solutions (in mole-%)

methyl acetate	chloroform	water
6.5	93.0	0.5
9.5	89.6	0.9
12.7	86.3	1.0
26.3	72.1	1.6
37.3	60.6	2.1
48.9	48.2	2.9
60.3	34.9	4.8
70.4	22.1	7.5
71.6	18.5	9.9
77.0	10.0	13.0
77.8	7.3	14.9
77.0	6.6	16.4
76.4	5.5	18.1
77.0	2.8	20.2
74.2	2.9	22.9
74.8	0.7	24.5
75.25	0	24.75
0	0.17	99.83
0.45	0.09	99.46
1.49	0.09	98.42
2.45	0.07	97.48
3.28	0.06	96.66
3.97	0.05	95.98
4.75	0.04	95.21
5.38	0.03	94.59
7.31	0	92.69

TABLE 3
Data for Plotting Solubility Curve at
the Boiling Point of the Stratified
Solutions, $p = 760$ mm Hg

Compositions of saturated solutions (in mole-%)

methyl acetate	chloroform	water
11.1	88.6	0.3
21.0	78.7	0.3
29.4	70.0	0.6
42.2	56.7	1.1
51.2	47.7	1.1
56.1	40.4	3.5
62.2	33.9	3.9
64.7	26.9	8.4
65.8	19.5	15.5
66.9	10.0	23.1
67.0	4.9	28.1
54.4	—	45.6
—	0.2	99.8
1.9	0.1	98.0
2.5	0.1	97.4
2.8	0.1	97.1
3.5	0.1	96.4
4.4	0.1	95.5
10.4	—	89.6

Titration at room temperature was performed in flasks with a long and narrow neck (for convenience in agitation of the mixture), and at the boil in a cylindrical vessel to whose neck was sealed a refluxed condenser.

In the latter case the solution to be titrated was prepared

by weighing of the original substances directly into the apparatus. The solution was agitated by vigorous boiling. Data for the composition of saturated solutions at 20° and at boiling point of the mixture are plotted in Fig. 2 and set forth in Tables 2 and 3.

Boiling points of the binary and ternary systems. The dependence of the boiling points on the concentrations of solutions in the binary system methyl acetate — water and in the ternary system, also the boiling points of the chloroform — water heteroazeotrope, were determined in a Swientoslawski apparatus [8] as modified in our laboratory.

* Since the temperature coefficient of solubility of the components in one another is insignificant, room temperature fluctuations are substantially without influence on the position of the intersection point on the triangle of compositions. Consequently, the experiments were run without a thermostat.

The apparatus was connected to a manostat and its pressure was held at 760 mm Hg. Solutions were prepared by advance weighing. The error in the composition of the solutions was 0.01%. Boiling points were read to an accuracy of 0.05°. The accuracy of the data was checked by several repetitions of the experiments. In these the difference in the boiling points did not exceed 0.1°. According to our data the stratified mixture of chloroform and water boils at 56.2°; according to Lecat [9] and Wade and Finnemore [10] it boils at 56.1°. Data for the boiling points in the system methyl acetate - water are presented in Fig. 3. According to our data the system methyl acetate - water has a homogeneous azeotrope boiling at 56.0°, and the stratified mixture of methyl acetate and water boils at 56.8°.

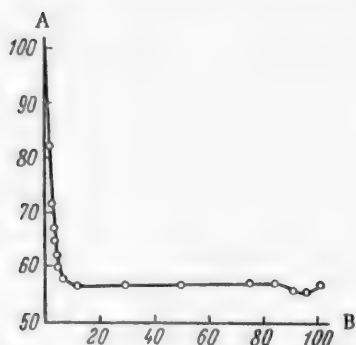


Fig. 3. Boiling point in the system methyl acetate - water as a function of composition. A) Boiling point (in °C); B) methyl acetate concentration (mole %).

We made a more accurate determination of the boiling point of the azeotrope by taking the distillate obtained from a column. It coincided with the temperature found from Fig. 3. The azeotropic composition was also determined in the column. It contained 90.4 mole % methyl acetate. According to Fuchs [11] and Lecat [9], the azeotrope in this system boils at 56.5° and contains 86.7 mole % methyl acetate. The boiling points of the ternary system were determined on solutions whose concentrations lay on the binodal curve plotted at the boiling point of the stratifying solutions. This method of determination of the boiling points enabled simultaneous determination of the composition of the liquid phases co-existing at the boiling point of the stratifying solutions. The correctness of our data and the convenience of construction of the liquid - liquid nodes were also confirmed by investigation of the boiling points of the heterogeneous liquids along two sections of the triangle with a constant water content (50 and 70 mole %). The liquid - liquid nodes obtained from the boiling points of stratifying solutions are plotted as fine lines in Fig. 4.

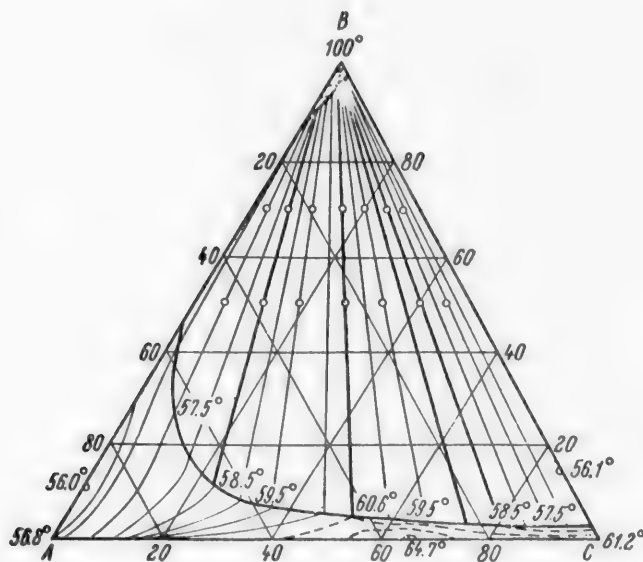


Fig. 4. Liquid - liquid nodes and isobar-isotherms of homogeneous solutions in the system methyl acetate - chloroform - water (concentrations of components in mole %). A) Methyl acetate; B) water; C) chloroform.

A further check on the data was provided by determinations of several compositions of layers co-existing at their boiling point in the apparatus described in detail by Bushmakín and Lutugina [3]. A stirrer was fitted in our work to afford better agitation of the mixture. The liquid-liquid nodes obtained by direct determination of the composition of co-existing phases are plotted in Fig. 4 as dense lines. They are seen to coincide satisfactorily with the nodes obtained from data for the boiling points of saturated solutions. We determined the boiling points of homogeneous solutions only in the region of the triangle of compositions situated close to the peak of pure methyl acetate along three sections with constant methyl acetate contents of 74, 83, and 92 mole %. The isothermal isobars plotted on the basis of these data are shown in Fig. 4 as very dense lines.

In the remaining parts of the triangle of compositions, the binodal plot hugs the sides so closely that determination of the boiling point of the homogeneous solution is impracticable. In these regions of the triangle we noted the course of the isobar-isotherms from the boiling points of solutions whose compositions lie on the binodal plot, and from the boiling points of the binary solutions (these isobar-isotherms are drawn as dashed lines in Fig. 4).

We can conclude from Fig. 4 that the boiling points of solutions lying on the binodal plot pass through a maximum corresponding to a temperature of 60.6° (Fig. 4).

We established by direct experiments and from the boiling points of stratifying solutions that the "extreme" node connects liquids containing (in mole %): Methyl acetate 1.9, chloroform 0.1, water 98.0 and methyl acetate 43.2, chloroform 54.4, water 2.4.

Position of the vapor line in the heterogeneous liquid region. The starting points of the vapor line in the stratification region in our system correspond to compositions of vapors co-existing with the two-phase liquids methyl acetate-water and chloroform-water. The apparatus described in detail by Bushmakín and Lutugina [3] was used for determination of the composition of the vapors in the binary and ternary systems. A stirrer was provided in order to obtain better agitation of the mixture.

The composition of the vapor co-existing with the two liquid phases in the system methyl acetate-water, according to our data, corresponds to 81.0 mole % methyl acetate; the vapor of the chloroform-water heteroazeotrope contains 85.2 mole % chloroform. The figure reported by Horsley [5] is 85.5 mole %.

Liquids with various initial gross compositions were taken for investigation of three-component solutions in order to obtain uniform distribution of the vapor composition points. Results of our experiments are represented graphically in Fig. 5 as the thickened plot. Our experimental values are marked by small triangles.

In our system the vapor curve intersects the "extreme" node; hence at the intersection point the vapor composition is equal to one of the gross compositions of the liquid. It is easily seen from the course of the isobar-isotherms of the homogeneous liquids (Fig. 4) that we have here a heteroazeotrope of the saddle type. The coordinates of the point of intersection enable us to determine the composition of the saddle azeotrope. According to our data, this is 36.0 mole % methyl acetate, 44.0 mole % chloroform, 20.0 mole % water.

Distillation lines. These were investigated by the method described by Bushmakín and Lutugina [3] and Molodénko and Bushmakín [2]. The only modification was the fitting of a stirrer.

We were able to investigate only two sets of distillation lines. The starting point of one of these is the chloroform-water heteroazeotrope, the other is the minimum methyl acetate-chloroform azeotrope. Both of the sets of distillation lines terminate at the "water" peak. The boundary between them is the line joining the water apex with a point on the saddle heteroazeotrope. In the region of two-phase liquids, it coincides with the saddle node. One line of each of these sets is shown in Fig. 5. We see that the vapor composition points lie on tangents to the distillation lines drawn through the points of corresponding gross compositions of liquid (the tangents are shown as broken lines). Line I differs from line II in starting in the homogeneous liquid region, so that its start corresponds to the individual vapor line passing through the homogeneous liquid region (line Ia in Fig. 5).

It is impossible to experimentally investigate the course of the two other sets of distillation lines starting at the same points as lines I and II and terminating at the methyl acetate-chloroform azeotrope maximum. This is because, due to the specific position of the vapor curve, the distillation lines of those sets pass very close to the side of the triangle corresponding to the system methyl acetate-chloroform.

We see from Figs. 4 and 5 that the chloroform-water heteroazeotrope, which is surrounded by lines constituting two sections of the isobar-isotherms and the liquid-liquid node, is the starting point of the distillation lines. The same applies to the methyl acetate-water homogeneous azeotrope which is surrounded by isobar-isotherms. The distillation lines pass by the heteroazeotrope of the saddle type, but the liquid-liquid saddle node serves as a separating line between the sets of distillation lines.

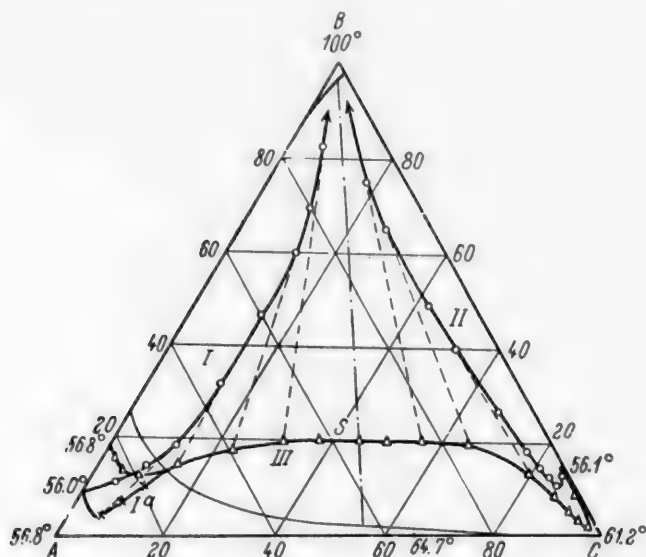


Fig. 5. Vapor line and distillation lines in the system methyl acetate-chloroform-water. A) Methyl acetate; B) water; C) chloroform. I and II) distillation lines; III) line of vapor co-existing with stratifying solutions; Ia) line of vapor co-existing with homogeneous solutions lying on the distillation line I; S) saddle azeotropic point. Concentrations of components are expressed as mole %.

Comparison of the experimental data (Figs. 4 and 5) and the proposed behavior of the system methyl acetate-chloroform-water during free evaporation (Fig. 1) clearly reveals their full agreement in spite of the fact that the positioning of the isothermal isobars and of the distillation lines is sharply distorted by the occurrence of layering in the system.

LITERATURE CITED

- [1] W. Reinders, and C. H. de Minjer, *Rev. trav. chim.* 59, 207, 369, 392 (1940).
- [2] P. Ya. Molodenko and I. N. Bushmakina, *Vestnik Leningrad, Gosudarst. Univ.* 10, 68 (1957).
- [3] I. N. Bushmakina and N. V. Lutugina, *Vestnik Leningrad, Gosudarst. Univ.* 10, 75 (1958).
- [4] W. Reinders and C. H. de Minjer, *Rev. trav. chim.* 66, 552 (1947).
- [5] L. Horsley, *Tables of Azeotropic Mixtures* (Russian translation) (Foreign Lit. Press, Moscow, 1951).
- [6] I. N. Bushmakina and I. N. Kish, *Zhur. Priklad. Khim.* 30, 200 (1957). *
- [7] F. Ullmann, *Enzyklopädie der technischen Chemie*, IV, Berlin-Vienna 683 (1930).
- [8] W. Swientoslawski, *Ebulliometric measurements* 6 (1945).

*Original Russian pagination. See C. B. Translation.

- [9] M. Lecat, *L'Azeotropisme*, Lamertin, Brussels (1948).
- [10] J. Wade and O. Finnemore, *J. Chem. Soc.* 85, 938 (1904).
- [11] O. Fuchs, *Chem. Ztg.* 51, 402 (1927).

Received January 5, 1958

A CHROMATOGRAPHIC STUDY OF ARABOGALACTAN AND OTHER WATER-EXTRACTED SUBSTANCES OF LARIX DAHURICA

I. P. Tsvetaeva and M. K. Yur'eva

The predominant species in the forests of the Eastern USSR is the larch. The enormous reserves of wood of the different larch varieties are of great practical importance and can be efficiently exploited in the national economy by both mechanical and chemical methods. Today, the problems of complete utilization of larch wood and the necessarily detailed study of this species are becoming ever more important.

The wood of *Larix dahurica* (like that of other varieties of larch) is known to contain considerable amounts of a water-soluble polysaccharide — arabogalactan. This substance is of great interest not only chemically but also from the practical aspect due to its adhesive properties and fermentability. Recent work on *Larix dahurica* has covered the chemical composition of its wood [1], the problem of distribution of arabogalactan in the wood [2], the fermentation of arabogalactan to alcohol [3], and the sulfate [4] and sulfite [5] digestion of larch wood.

In the present paper we consider the composition of the arabogalactan of the heartwood and the sapwood of *Larix dahurica*. Samples of young and mature wood were investigated.

There is a fairly extensive literature on the arabogalactan (gum) of different varieties of larch, but the composition and structure of this polysaccharide have not yet been conclusively elucidated [6]. Some interesting publications of recent years indicate the presence of 3- β -L-arabopyranosyl-L-arabinose [7], of 6- β -D-galactopyranosyl-D-galactose [8], and of other di- and trisaccharides based on galactose [9] in the products of mild hydrolysis of larch arabogalactan. Although it has not yet been settled whether this polysaccharide is a homogeneous substance or a mixture of galactan and arabogalactan, it is usually represented as a substance with a highly branched framework with β -galactopyranose units linked in the 1,3'- and 1,6'-positions. They are linked to arabinose, galactose and disaccharides of these sugars. Galactose and arabinose are present in larch arabogalactan in the approximate molar ratio of 6:1 [6]. This is not, however, the only possible ratio. Recently, polysaccharides composed of galactose and arabinose have also been found in other conifers [10] (admittedly in smaller quantity than in larch). The galactose/arabinose ratio in the arabogalactan of Jeffrey pine, for example, is 5:4 [11].

The preceding investigations [6, 1] established that the average arabogalactan content of *Larix dahurica* is 10-12% of the weight of the wood (reaching in isolated cases 20% and higher), and that the main mass of the arabogalactan is contained in the heartwood whereas the sapwood only contains 0.6-1.4%.

EXPERIMENTAL

Arabogalactan was isolated from larch wood by the earlier method [6] of water extraction of the degummed wood (sawdust with particle size of 0.25-1.00 mm) in a Soxhlet apparatus for 14 hours. The extract was filtered, evaporated to a volume of 25 ml and poured into the sixfold volume of ethyl alcohol. The arabogalactan came down and was filtered off and dried to constant weight.

Paper chromatography was employed for determination of the composition of the arabogalactan. The sugars were separated by descending chromatography by the technique of Emel'yanova and Batrakova [12]. The solvent was a 5:1:5 mixture of ethyl acetate, pyridine and water and the developer was aniline phthalate. The paper was the No. 2 grade of the Leningrad Paperworks produced in 1956. The sugars of the chromatogram were quantitatively determined at first by the method of potentiometric ebulliostatic titration [12], but later determinations were carried out colorimetrically with the FÉK-M photoelectric colorimeter. The aniline phthalate

method was used in the latter [13]. We do not consider the colorimetric method to be more accurate than the method of potentiometric titration, but we changed over to it because of its greater simplicity and convenience.

At the start of the investigation we determined the composition of the arabogalactan of *Larix dahurica* (without separation of the heartwood from the sapwood). The isolated arabogalactan was hydrolyzed with 2.5% sulfuric acid for 6 hours on a boiling water bath (modulus 1:50) under a reflux condenser. A drop of hydrolyzate with a volume of 0.03 ml was placed on the paper strip for chromatography. Duration of operation 48 hours.

Two sugars were found in the hydrolyzate: 1.652% of galactose and 0.220% of arabinose. On the basis of these results the hydrolyzed arabogalactan contains 88.20% of galactose and 11.75% of arabinose — a result in agreement with that of other investigators [6].

We may mention that all the values here presented are means of 3-5 parallel determinations. The accuracy of our determinations was $\pm 5\%$ on the average, rising to 1-2% when the sugar content of the drop was 200-600 μg . and falling to 8% when the sugar content was μg .

In the next part of the investigation, the arabogalactan of the heartwood and the sapwood were studied separately. It should be noted that these two substances differ slightly in appearance. The heartwood arabogalactan is a cream-colored powder which comes down immediately from aqueous solution when alcohol is added. Sapwood arabogalactan is a light-gray product which separates gradually as flocks when alcohol is added to the aqueous solution. It tends to become horny on drying.

We had at our disposal, a small quantity of heartwood arabogalactan consisting of a mixture of polysaccharides obtained from two specimens of *Larix dahurica*. The sapwood arabogalactan was a mixture of specimens isolated from three trees. We carried out the first exploratory experiments with this material.

Qualitative chromatography immediately revealed a sharp difference in the compositions of the arabogalactan of the heartwood and sapwood. The heartwood polysaccharide contained only arabinose and galactose, whereas the product obtained from the sapwood contained galactose, mannose, arabinose and xylose. Numerous repeats of the chromatograms of these mixtures (and of individual components of these mixtures) gave identical results.

Results of quantitative determinations are presented in Tables 1 and 2.

TABLE 1
Content of Sugars in Hydrolyzed Arabogalactan from *Larix dahurica* Heartwood

Sugar analyzed	Quantity of sugar found by titration (in ml of standard solution)	Quantity of sugar found in hydrolyzate (in wt. %)		Content of sugars in hydrolyzed arabogalactan (in rel. %)
		individual determinations	mean value	
Galactose	1.09	1.555	1.548	87.9
	1.08	1.540		
	1.08	1.540		
	1.09	1.555		
Arabinose	0.33	0.208	0.213	12.1
	0.34	0.215		
	0.34	0.215		
Total			1.761	100.0

Determinations were made, in parallel with the chromatographic analysis, of the total content of sugars (reducing substances) in the hydrolyzates of the heartwood arabogalactan and of the water-extracted substances of the sapwood by the ebulliosstatic macromethod [14]. 1.70% of RS* was found in the hydrolyzate of heartwood

* RS = reducing substances. This result is in good agreement with the data of chromatographic analysis (Table 1).

arabogalactan and not more than 0.95% in that of sapwood. A 2% (approximately) RS content was to be expected in the hydrolyzate when operating with a hydromodulus of 1:50, and this amount was found for the heartwood polysaccharide. These data justify the assumption that the water-extracted substances of *Larix dahurica* heartwood differ markedly from the water-extracted substances of its sapwood. The latter possibly contain also nonsugars.

TABLE 2
Content of Sugars in Hydrolyzed Product of the Aqueous Extract
of *Larix dahurica* Sapwood

Sugar	Sugar content of hydrolyzate (in weight %)	Sugar contents of hydrolyzate (in relative %)
Xylose	0.149	14.7
Galactose	0.439	43.3
Mannose	0.243	24.0
Arabinose	0.119	11.7
Glucose	0.064	6.3
Total	1.014	100.0

Subsequent work was in two directions: study of the water-extracted substances of the young wood and of the water-extracted substances of the heartwood and sapwood of matured wood.

According to [15] the heartwood of the larch forms only after 10-12 years; in the younger trees, it is not yet differentiated. We were interested in the composition of the water-extracted substances of the young wood. Investigations were carried out on the wood of *Larix dahurica* taken from a nursery. Specimens were prepared in October 1956 from one 40-year old tree. The following specimens were selected: a) Shoots about 4 months old; b) 1-, 2- and 3-year shoots; c) branches 5 and 10 years old in which heartwood was not present; d) 16- and 21-year branches with 4-8 annual rings in the heart. The shoots were cleaned and preserved in 96% ethyl alcohol.

A slightly different method of extraction was applied to these specimens as a precaution. The water-soluble substances were extracted from degummed sawdust by two procedures: at first at 70° (48 hours with change of liquid each 14 hours), then at 100° in a Soxhlet (42 hours with two changes of liquid); modulus 1:20. The extracted substances were precipitated from the aqueous solutions with alcohol. The product was hydrolyzed and chromatographed.

Analytical results appear in Table 3.

We see from Table 3 that also here the water-extracted substances are different. In the shoots the only substance extracted is xylose, but the 5-10 year old wood and the sapwood contain four sugars - galactose, arabinose, xylose and mannose. The aqueous extract of the heart of the young wood contains (as in the case of mature wood) only galactose and arabinose. The quantity of these sugars increases sharply when the heart is formed. Shoots (as well as the young wood of branches) are noteworthy for their high content of uronic acids, probably due to the high content of pectic substances.

Our investigations were then continued with 3- to 5-year old Siberian larches taken from the nursery of the Leningrad S. M. Kirov Academy of Forestry. We had no supply of *Larix dahurica* of the same age. Since the woods of *Larix sibirica* and *Larix dahurica* are similar in properties and chemical composition, we felt justified in using *Larix sibirica* for this section of our work. Specimens were collected in June, 1957. They differed in respect to the intensity of illumination to which they had been exposed (this factor greatly influences the growth of the larch). In Table 4 the saplings which had been well illuminated are arbitrarily graded as saplings with good conditions of growth. Among the selected specimens were "diseased" saplings with a yellowed top. We were interested in the composition of the sugars in the water-soluble substances of 3- to 5-year saplings (still lacking separate heartwood and sapwood). In this case, we determined the quantity of sugars not only in the product precipitated by alcohol from the aqueous extract but also the sugars in the hydrolyzed aqueous extract

itself (before precipitation).^{*} Hydrolysis was performed under the usual conditions (see above).

TABLE 3

Composition of Sugars Present in the Water-extracted Substances of Young Wood of *Larix dahurica*

Specimen of wood	Quantity of water-extracted substances brought down by alcohol (in weight -%)			Content of uronic acids in precipitated product (in %)	Sugars found in precipitated product
	70°	100°	acero		
Shoots:					
4-month	1.03	3.32	4.35	30.90—27.95	} Xylose
one-year	2.59	1.48	4.07	50.91—41.60	
2- and 3-year	1.48	1.69	3.17	—	
Branches:					
5-10-year	1.05	0.56	1.61	13—14	Galactose, arabinose, mannose, xylose
16-year (heart)	16.16	0.55	16.71	3.77	Galactose, arabinose, xylose
sapwoods (outer layer)	0.41	0.22	0.63	—	} Galactose, arabinose, mannose, xylose
sapwoods (inner layer)	0.52	0.25	0.77	—	
21-year (heart)	22.70	0.30	23.00	5.87	
sapwoods (outer layer)	0.42	0.70	1.12	—	} Galactose, arabinose, mannose, xylose
Sapwoods (inner layer)	0.60	0.45	1.05	—	

Composition of Hydrolyzed Aqueous Extract of Young Wood of Siberian Larch

Specimen No.	Age of specimen (years)	Conditions of growth	% of sugars in aqueous extract					Ratio of galactose to arabinose (molar)
			galactose	arabinose	glucose	mannose	xylose	
1	3	Poor	13.51	5.40	62.16	18.91	Traces	2.06
2	3	Good	23.76	18.81	32.67	18.81	6.0	1.04
3	3	Diseased wood	39.75	8.37	42.16	9.63	Traces	3.94
4	5	Good	50.00	6.90	13.79	17.24	12.07	6.01
5	6	Diseased wood	Not determined					

The results enable us to suggest that the investigated aqueous extract can contain various oligosaccharides of the wood and not the arabogalactan that we find in the heartwood of *Larix dahurica*. The aqueous extracts of all of the investigated specimens contain the same sugars but in all cases the quantitative ratios are different. There are no correlations between the composition of these substances and the conditions of growth of the trees. The galactose/arabinose ratio for specimen No. 4 (6.01) corresponds to the characteristic ratio for arabogalactan.

^{*} Hydrolysis of the aqueous extract is necessary because experiment showed that monosaccharides cannot be detected in unhydrolyzed extract (except for a small amount of arabinose).

Even if we assume that the galactose and arabinose found in the extract represent hydrolyzed arabogalactan, the latter differs from the arabogalactan of the heartwood of *Larix dahurica* because it does not occur alone in the extract. Such a composition of sugars is characteristic of the sapwood of mature wood in which 4 or 5 sugars are found.

The results inevitably prompt the question whether the mixture of sugars found in extracts of sapwood and of young wood is simply a mixture of the various hemicelluloses of the wood which undergo hydrolysis or whether the mixture consists of arabogalactan and other substances. Serious experimental difficulties arise in attempting to solve this problem and we have not yet been able to solve it. Simple precipitation of the substances from solution by alcohol evidently does not afford the possibility of isolation of arabogalactan (if present in the extract) from the other components.

From the aqueous extracts of the investigated specimens a product was precipitated by alcohol which after hydrolysis was also subjected to chromatographic analysis.* We may mention incidentally that the quantity of substances precipitated by alcohol was 0.71-1.52% of the weight of the wood, i.e., within the same range as in the sapwood of the mature wood. Analytical results are set forth in Table 5 (same specimen numbers).

TABLE 5
Composition of Product Brought Down by Alcohol from the Aqueous Extract of the Young Wood of Siberian Larch

Specimen No.	% of sugars in precipitated product					Galactose/arabinose ratio (molar)
	galactose	arabinose	glucose	mannose	xylose	
2	42.42	10.91	22.31	18.94	5.23	3.22
4	52.17	12.90	4.03	16.30	14.50	3.37
6	18.75	35.41	20.82	10.41	14.56	0.44

Here we find in each specimen the same five sugars, but in different ratios, although, as before, the ratios are very variable. The individual sugars are evidently incompletely precipitated by alcohol.

The product precipitated by alcohol from the extract of diseased wood is notable for its high content of arabinose. There are still insufficient data to account for this increase.

The very great variations in quantitative composition of the sugars present in aqueous extracts of young wood may be a consequence of the vital activity of the part of the tree in question. There is a constant interplay of accumulation and breakdown of certain substances. The specimens of wood were collected in June, which is the period of intensive growth of the tree, when the physiological individualities of each tree are most conspicuous, and the composition of the carbohydrates of the wood may be changing.

We explored the possibility of changing the composition of the carbohydrate complex, brought down from the aqueous extract of the sapwood of the mature wood of *Larix dahurica*, by repeated reprecipitation. In other words, we had in mind the possibility of purifying arabogalactan (if it was present) from the accompanying sugars. We carried out six reprecipitations with alcohol. The alcoholic filtrates from the reprecipitated products were combined; the alcohol was distilled off, the residue was hydrolyzed, and the hydrolyzate was analyzed for its content of sugars. Results are set forth in Table 6.

Judging by Table 6, the product after the sixth reprecipitation scarcely differs in composition from the starting material, and the filtrate contains the same four sugars. It was consequently impossible to obtain by this method any clue as to whether the sapwood contains arabogalactan.

* The data of Tables 4-6 were obtained with the FÉK-M photoelectrocolorimeter with a blue light filter, $\lambda = 415 \mu$.

The following specimens of *Larix dahurica* were taken from the Yakutsk Leskhoz (Markhinsk forestry) in order to make a closer study of the water-extracted substances of the heartwood and sapwood of the mature wood.

TABLE 6

Composition of the Carbohydrate Complex Precipitated from the Aqueous Extract of Sapwood of *Larix dahurica* after Reprecipitation

Product investigated	Composition of product (in %)			
	galac- tose	arabi- nose	mannose	xylose
Starting product precipitated from aqueous extract	61.16	8.73	20.38	9.70
Starting product after reprecipitation	62.72	5.90	23.66	7.69
1st	63.15	6.31	20.00	10.52
2nd	64.51	8.06	19.35	8.06
3rd	61.56	10.23	20.48	7.83
4th	62.34	11.47	20.00	5.88
6th	15.11	63.95	9.88	11.04
Filtrate from sixth reprecipitation				

1. Specimen 24-1. Age 180 years, height 19.3 m; sample taken halfway up; diameter 168 mm; number of annual rings 133 (working specimen No. 12).
2. Root of model tree No. 2. Age 48 years, diameter 107 mm (working Nos. 80, 81).
3. Stump (ground level) of the same model tree No. 2. Age 71 years, diameter 236 mm (working Nos. 84 and 85).
4. Dead tree I felled for burning in 1948. Age 64 years, diameter 159 mm (working Nos. 94 and 95).
5. Dead tree II felled at same time as I. Age 65 years, diameter 142 mm (working Nos. 96 and 97).

The water-soluble substances were isolated separately from sawdust of the heartwood and sapwood of these specimens by the usual procedure. They were precipitated with alcohol, hydrolyzed and subjected to chromatographic analysis. Results are collected in Tables 7 and 8.

TABLE 7

Composition of the Water-Extracted Substances of *Larix dahurica* Heartwood

Working specimen number	Wt.-% of sugars in hydrolyzate		total content of sugars of hydrolyzate	% composition of arabogalactan of heartwood		Source of specimen	Galactose/arabinose ratio (molar)
	galac- tose	arabin- nose		galac- tose	arabin- nose		
12	2.248	0.379	2.627	85.6	14.4	Trunk	4.95
80	1.725	0.354	2.079	83.0	17.0	Root	4.07
84	2.083	0.314	2.397	86.9	13.1	Stump	5.53
94	1.702	0.328	2.030	83.8	16.2	Trunk of dead tree	4.32
96	1.760	0.325	2.085	84.4	15.6		4.50

As before, only two sugars (galactose and arabinose) were found in all of the specimens. The variations in composition of the different specimens are not very pronounced although the range of galactose/arabinose ratios is fairly wide (from 4.07 to 5.53). A value of 6 for this ratio was not found in a single specimen. Nevertheless, we assume that the water-extracted substances of *Larix dahurica* heartwood constitute arabogalactan consisting of galactose and arabinose.

During our study of the water-extracted substances of the sapwood of the same specimens,* we were struck by the great variability of their composition (this was already noticeable on the qualitative chromatograms), as shown in Table 8. This fact clearly demonstrates the difference between the water-extracted substances of the heartwood and sapwood.

TABLE 8
Composition of Water-Extracted Substances of *Larix dahurica* Sapwood

Working specimen number	Wt. -% of sugars in hydrolyzate						3% composition of sugars of hydrolyzate					Source of specimen	Galactose-arabinose ratio (molar)
	galactose	glucose	mannose	arabinose	xylose	in all (total)	galactose	glucose	mannose	arabinose	xylose		
12	3.788	no	0.160	0.384	0.200	4.532	83.6	—	3.5	8.5	4.4	Trunk	8.3
81	0.658	0.071	0.131	0.210	0.096	1.166	56.4	6.1	11.2	18.0	8.3	Root	2.6
85	5.200	no	0.193	0.974	0.493	6.860	75.8	—	2.8	14.2	7.2	Stump	4.4
95	0.834	no	trace	0.286	0.242	1.362	61.2	—	—	21.0	17.8	Dead trunk	2.4
97	0.393	0.120	0.423	0.092	0.252	1.280	30.7	9.4	33.0	7.2	19.7	Dead trunk	3.5

The water-extracted substances of the sapwood of the investigated specimens consequently differ in their qualitative and quantitative composition. The galactose/arabinose ratio varies between 2.4 and 8.3. It is impossible to establish any regularities in the composition of these substances. The content of individual sugars was subject to very great fluctuations. The composition of the water-extracted substances of the sapwood is clearly variable and differs markedly from the composition of the water-extracted substances of the heartwood of *Larix dahurica*. Further investigations are needed to decide whether arabogalactan is present in the water-extracted substances.

SUMMARY

1. The water-extracted substances of the heartwood differ markedly from the water-extracted substances of the sapwood of the larch.
2. The water-soluble product from the heartwood of *Larix dahurica* is clearly arabogalactan. It is made up from galactose and arabinose but the galactose content varies between 83 and 86.9% and the arabinose content between 17 and 13.1%. The galactose/arabinose ratio correspondingly varies between 4.07 and 5.53.
3. The water-extracted product from the sapwood of *Larix dahurica* apparently contains polysaccharides constituted from various sugars since glucose, galactose, mannose, arabinose and xylose are found in various proportions in the hydrolyzate of this product. Aqueous extracts of the sapwood vary in composition. The galactose/arabinose ratio varies between 2.4 and 8.3. The nature of the water-extracted polysaccharides of larch sapwood makes them not readily amenable to accurate determination.
4. Only xylose is found in the aqueous extract of *Larix dahurica* shoots (4 months, 1, 2, and 3 years). The water-extracted substances of the wood of 5-10 year branches and the sapwood of 16-21 year branches contain galactose, arabinose, mannose, and xylose, whereas the heartwood of 16-21 year branches contains only galactose and arabinose.
5. The hydrolyzed aqueous extract, also the product precipitated from the aqueous extract of young larch-wood, in which the heart has not yet formed, contain glucose, galactose, mannose, arabinose and xylose in various amounts. The composition of the aqueous extracts is variable. In this respect, the young wood resembles the sapwood.

* Hydrolyzates of specimens Nos. 12 and 85 were prepared in advance of the others; the solutions evidently thickened on standing (they had a small volume), and therefore the concentration of sugars increased.

6. After six reprecipitations, the composition of the product precipitated by alcohol from the aqueous extract of Larix dahurica sapwood remained almost unchanged.

LITERATURE CITED

- [1] I. P. Tsvetaeva, M. K. Yur'eva, and N. I. Nikitin, Trudy Inst. Lesa Akad. Nauk SSSR 45, 22 (1958).
- [2] M. M. Chochieva, I. P. Tsvetaeva, M. K. Yur'eva, A. F. Zaitseva, G. A. Petropavlovskii, and N. I. Nikitin, *ibid.* 31 (1958).
- [3] N. I. Nikitin, A. F. Zaitseva, and I. P. Fedorishcheva, *ibid.* 85 (1958).
- [4] A. F. Zaitseva, I. P. Fedorishcheva, S. D. Antonovskii and N. I. Nikitin, *ibid.* 70 (1958).
- [5] N. K. Yur'eva and N. I. Nikitin, *ibid.* 103 (1958).
- [6] I. P. Tsvetaeva, M. K. Mukovnikova, and N. I. Nikitin, Zhur. Priklad Khim. 25, 174 (1952).*
- [7] J. K. N. Jones, J. Chem. Soc. 1672 (1953).
- [8] H. Bouveng and B. Lindberg, Acta Chem. Scand. 10, 1515 (1956).
- [9] G. O. Aspinall, E. L. Hirst, and E. Ramstad, J. Chem. Soc. 593 (1958).
- [10] R. L. Whistler and C. L. Smart, Polysaccharide chemistry (New York, 1953), 203.
- [11] W. H. Wadman, A. B. Anderson, and W. Z. Hassid, J. Amer. Chem. Soc. 76, 4097 (1954).
- [12] N. Z. Emel'yanova and T. A. Batrakova, Zhur. Anal. Khim. 13, 142 (1958).*
- [13] G. N. Zaitseva and T. P. Afanas'eva, Biokhimiya 22, 1035 (1957).*
- [14] L. M. Ageev and I. I. Korol'kov, Chemical Technological Control and Account of the Wood Hydrolysis and Sulfite Alcohol Industry [In Russian] (1953), 52.
- [15] S. I. Vanin, Wood Science [In Russian] (1949).

Received December 15, 1958

*Original Russian pagination. See C. B. Translation.

INVESTIGATION OF THE FORMATION OF CATALYST SYSTEMS AND OF ALKYLALUMINUMS IN CONNECTION WITH THE POLYMERIZATION OF ETHYLENE AT ATMOSPHERIC PRESSURE*

A. Shimon, L. Kovach, D. Dezheni and D. Lekhotski

A catalyst for low-pressure polymerization of ethylene [1] is a complex of an organometallic and a transition-metal compound. The most effective and characteristic representative of this type of catalyst is the system comprising titanium tetrachloride and triethylaluminum.

The reaction of titanium tetrachloride with triethylaluminum has already been the subject of many investigations, but the process is still not fully understood.

The authors previously studied the oxidation-reduction processes taking place during formation of the catalyst. They also studied the factors governing the rate of polymerization [2].

In the present work, we present the results of investigation of the reaction of titanium tetrachloride with triethylaluminum by two methods: in solution and without dilution. We determined the composition of the active precipitate formed from the two components in solution. In experiments without a diluent, this could not be done due to the violence of the reaction and the difficulty of weighing the product.

However, the reaction of concentrated components simplifies measurement of the gas released on mixing since allowance must otherwise be made for the partial pressure of the vapor of the solvent and for dissolution of the gaseous products.

EXPERIMENTAL

Analysis of catalyst prepared from TiCl_4 and AlEt_3 . The triethylaluminum/titanium tetrachloride molar ratio was varied between 0.5 and 5.75. The components were dissolved separately in pure gasoline; 5% TiCl_4 solution and 20% alkylaluminum solution were mixed at room temperature. The maximum rise of reaction temperature of the mixture did not exceed 40-45°. For ten minutes the components were stirred with a magnetic stirrer, after which the mixture was centrifuged and the supernatant liquid was decanted. All operations were performed in an atmosphere of purified nitrogen. The precipitate was washed six times with gasoline by the centrifuging method. The first portion of gasoline contained a colloidal precipitate. Later portions of gasoline has a light-brown color, and the last portions were perfectly colorless. Analysis revealed only traces of titanium and aluminum. This indicates that the precipitate is soluble in gasoline only to a very small extent. Prior to the last two washings, the vessel containing the precipitate was filled with light ligroin (b. p. 50°); after final decantation the solid was dried in vacuo at 40°. The ligroin came off quickly and the solid was converted to a fine powder. Depending on the $\text{AlEt}_3/\text{TiCl}_4$ molar ratio, the color of the powder varied from yellow to dark-brown. The product burned spontaneously in the air.

* Communication II.

The dried precipitate was analyzed in the apparatus proposed by Krause and Grosse [3]. A weighed sample of 0.2-0.3 g was dissolved in methanol. This operation led to considerable evolution of gas. It is very important that the precipitate be freshly prepared. After standing for 24 hours, the solid is no longer soluble without a residue under the specified conditions. After the solid had been dissolved in 5 ml of methanol, 20 ml of distilled water was added and the mixture boiled until the methanol had been completely removed. 5 ml of 20% sodium hydroxide solution was added during the boiling. This resulted in separation of a blue-black solid. Boiling for 10 minutes was followed by addition of 20 ml of 10% nitric acid. The solution was then boiled until the precipitate had completely dissolved (approximately 1-2 minutes). Titanium and aluminum were brought down from the hot solution with ammonia. The precipitate, calcined to constant weight, gives the total of the oxides. The oxides were then determined by fusion with pyrosulfate. Titanium was determined in a Jones reductor by reduction to Ti^{3+} with 0.1 N $KMnO_4$ solution [4]. Aluminum was determined by difference. Chlorine in the ammoniacal filtrate was determined by the Volhard method. Analytical results are plotted in Figs. 1 and 2.

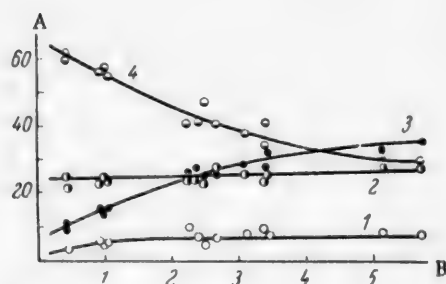


Fig. 1. Composition of precipitate obtained from $AlEt_3-TiCl_4$ as a function of the molar ratio of the components. A) Content of components (in mole %); B) $AlEt_3/TiCl_4$ molar ratio. Components: 1) Al, 2) Ti, 3) Et, 4) Cl.

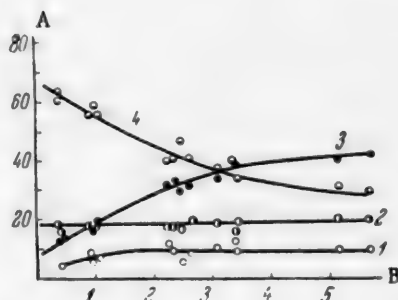


Fig. 2. Composition of precipitate obtained from $AlEt_3-TiCl_4$ as a function of the molar ratio of the components. A) Content of components (in mole-%); B) $AlEt_3/TiCl_4$ molar ratio. Components: 1) Al, 2) Ti, 3) Et, 4) Cl.

Measurement of the gas evolved on interaction of concentrated $TiCl_4-AlEt_3$. Vigorous evolution of gas is observed when the two components of the catalyst interact.

The authors developed a method of determination of the volume of gas formed.

The separate components were weighed in small glass bulbs by a modification of the technique of Krause and Grosse [3]: nitrogen was passed through a 10-15 ml cylinder with a side tube (Fig. 3). The vessel was half-filled with alkylaluminum or titanium tetrachloride; the top opening was closed with a soft rubber sheet through which two small openings were drilled into which were inserted the bends of the two bulbs. The bend of one of the bulbs did not extend as far as the surface of the liquid (the bulbs were thin-walled with a diameter of 4-6 mm and with drawn out capillaries bent at an angle of 90°). Nitrogen was passed through the bulbs for a few minutes. Then the upper, straight capillary of the bulb was sealed off as close to the bulb as possible, the bulb was heated with a small flame, and the capillary was lowered into the liquid in order that the required quantity of substance should be drawn into the bulb. The other capillary was then sealed. Since the weight of the bulb is known, the weight of liquid can be determined.

After a sufficient number of bulbs had been prepared in this manner, the appropriate molar ratios could be selected with satisfactory accuracy.

The method of measurement of the gas volume was similar in principle to Tserevitinov's method. The reaction vessel was a glass tube with a diameter of 15 mm fitted with a ground-glass stopper and a tap with side tube (Fig. 4). The tube contained an iron ball which could be raised or lowered by means of a magnet coiled round the tube. The bulbs were carefully placed in the tube, followed by the iron ball. The side tube of the reaction vessel was connected to the three-way tap of a gas buret which was filled to the top with mercury.

A vigorous stream of nitrogen was admitted through the tap of the reaction vessel. The gas purged the system and was discharged through the three-way tap. After 5 minutes, the level was adjusted to zero and measurement was started. The ball crushed the bulbs. Raising and lowering of the ball was continued for several minutes in order to effect good mixing. The reaction vessel was then put into a thermostat and the quantity of gas formed was determined.

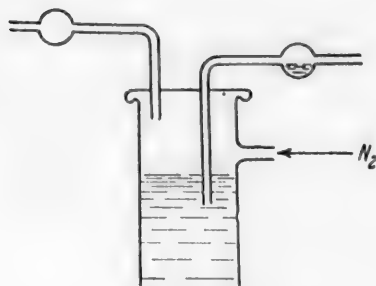


Fig. 3. Beaker with ampoules for weighed sample of alkyl compound.

Glass wool should be inserted in the side tube of the reaction vessel in order to prevent the fume from fouling the buret.

An apparatus with thicker walls (Fig. 5) was used in place of the above set-up for measurements of the gas volume 10 or 30 minutes after crushing of the bulbs. In this arrangement, the bulbs were crushed in a closed test tube.

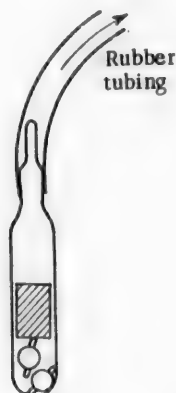


Fig. 5. Sealed test tube containing ampoules with sample.

After 10-30 minutes, the end of the test tube (connected to rubber tubing) was broken and the gas volume was measured (individual determinations varied by 5%).

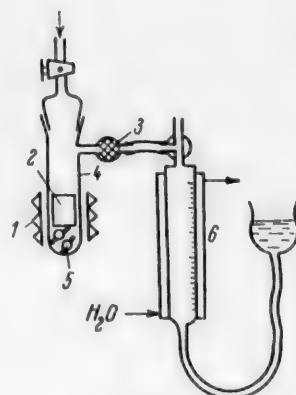


Fig. 4. Modified Tserevitinov apparatus for measurement of gas volume. 1) Magnet; 2) iron ball; 3) glass wool; 4) reaction vessel; 5) bulbs; 6) buret.

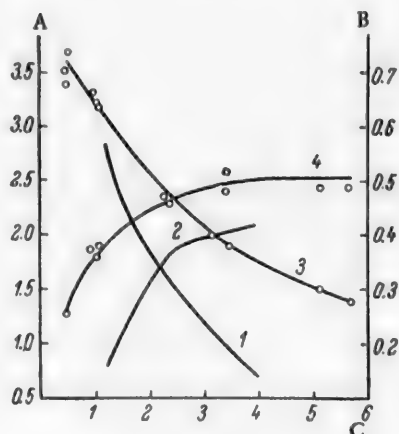


Fig. 6. Composition of precipitate obtained from $AlEt_3-TiCl_4$ as a function of the molar ratio of components. A) Cl/Ti molar ratios (in g-atom); B) Al/Ti molar ratios (in g-atom); C) $AlEt_3/TiCl_4$ molar ratios. 1, 3) Cl:Ti; 2, 4) Al:Ti. Data 1, 2) by Natta and co-workers; 3, 4) by present authors.

Figure 6 shows the relation between the quantity of gas formed and the molar ratio of the catalyst components. The relation between the gas volume to the amount of TiCl_4 is such that x_1 moles of gas formed can be taken as 100% in the case of x_1 moles of TiCl_4 .

DISCUSSION OF RESULTS

Figure 1 showed the change of the original components in dependence on the molar ratio. We see that the content of titanium and aluminum in the range of molar ratios that we investigated was practically constant. The chlorine content varied between 70 and 30%, and the residue (apparently the organic component) varied between 10 and 35%. Reckoning on the basis of the ethyl group and adding together the number of moles of all of the components, we obtain practically an identical value for all initial molar ratios. Although this does not prove the presence of ethyl groups, the satisfactory results justify the plotting of the components in molar percentages (Fig. 2).

It was thus established that each atom of aluminum requires two atoms of titanium at Al/Ti molar ratios of 1.5 to 5; even at values below 1.5 the amount of aluminum only falls slowly.

The following empirical formula can be written on the basis of the data of Fig. 2 for Al/Ti ratios of 1.5 to 5:



The proposed formula is valid only if the tetravalence of titanium is maintained. Experiment shows, however, that under these conditions titanium is reduced to a large extent to the ter- or bivalent state [2]. Further investigations must be made for establishment of the actual (probably complex) structure.

The reactions listed in Table 1 can lead to the above empirical formula.

TABLE 1

Reaction	Molar ratios	
	Al/Ti	Gas volume/Ti
$3\text{AlEt}_3 + 2\text{TiCl}_4 \rightarrow \text{AlTi}_2\text{Cl}_5\text{Et}_2 + \text{AlEt}_2\text{Cl} + \text{AlEtCl}_2 + 4\text{Et} \dots$	1.5	2
$4\text{AlEt}_3 + 2\text{TiCl}_4 \rightarrow \text{AlTi}_2\text{Cl}_5\text{Et}_2 + 3\text{AlEt}_2\text{Cl} + 4\text{Et} \dots$	2.0	2
$3\text{AlEt}_3 + 2\text{TiCl}_4 \rightarrow \text{AlTi}_2\text{Cl}_4\text{Et}_3 + 2\text{AlEtCl}_2 + 4\text{Et} \dots$	1.5	2
$4\text{AlEt}_3 + 2\text{TiCl}_4 \rightarrow \text{AlTi}_2\text{Cl}_4\text{Et}_3 + \text{AlEtCl}_2 + 2\text{AlEt}_2\text{Cl} + 4\text{Et} \dots$	2.0	2
$5\text{AlEt}_3 + 2\text{TiCl}_4 \rightarrow \text{AlTi}_2\text{Cl}_4\text{Et}_3 + 4\text{AlEt}_2\text{Cl} + 4\text{Et} \dots$	2.5	2
$4\text{AlEt}_3 + 2\text{TiCl}_4 \rightarrow \text{AlTi}_2\text{Cl}_3\text{Et}_4 + 2\text{AlEtCl}_2 + \text{AlEt}_2\text{Cl} + 4\text{Et} \dots$	2.0	2
$5\text{AlEt}_3 + 2\text{TiCl}_4 \rightarrow \text{AlTi}_2\text{Cl}_3\text{Et}_4 + \text{AlEtCl}_2 + 3\text{AlEt}_2\text{Cl} + 4\text{Et} \dots$	2.5	2
$6\text{AlEt}_3 + 2\text{TiCl}_4 \rightarrow \text{AlTi}_2\text{Cl}_3\text{Et}_4 + 5\text{AlEt}_2\text{Cl} + 4\text{Et} \dots$	3.0	2

With molar ratios of less than 1.5, when the aluminum content is considerably reduced, the picture becomes complicated. Thus, with a molar ratio of 0.5 the reactions listed in Table 2 can lead to the corresponding formula ($\text{AlTi}_4\text{Cl}_2\text{Et}_2$).

The equations are in good agreement with experiment, especially at low molar ratios.

The composition can be determined in dependence on the molar ratios.

On the basis of the foregoing results, and plotting (as suggested by Natta [5]) the Cl/Ti or Al/Ti molar ratios as functions of the molar ratios of the reactants, the authors obtained a relation similar to that of Natta (Fig. 6) although Natta and co-workers carried out all of their measurements after reaction for 2 minutes at 60° whereas we carried them out after reaction for 10 minutes at 20°.

The volume of gas evolved during the TiCl_4 - AlEt_3 interaction increases with the Al/Ti ratio. Here the difference in activity is manifested by a different degree of substitution of the alkylaluminums (Fig. 7). Gas formation decreases in the order of trialkylaluminum, sesquichloride, dialkylaluminum chloride. It is interesting that the quantity of gas formed by the dialkyl compound is similar to the quantity formed by the sesquichloride although the latter has fewer ethyl groups per mole.

TABLE 2

Reaction	Molar ratios	
	$\frac{\text{Al}}{\text{Ti}}$	$\frac{\text{gas volume}}{\text{Ti}}$
$3\text{AlEt}_3 + 4\text{TiCl}_4 \rightarrow \text{AlTi}_4\text{Cl}_{12}\text{Et}_2 + 2\text{AlCl}_2\text{Et} + 5\text{Et} \dots \dots \dots$	0.75	1.25
$4\text{AlEt}_3 + 4\text{TiCl}_4 \rightarrow \text{AlTi}_4\text{Cl}_{12}\text{Et}_2 + 2\text{AlEt}_2\text{Cl} + \text{AlEtCl}_2 + 5\text{Et} \dots \dots \dots$	1.0	1.25
$5\text{AlEt}_3 + 4\text{TiCl}_4 \rightarrow \text{AlTi}_4\text{Cl}_{12}\text{Et}_2 + 4\text{AlEt}_2\text{Cl} + 5\text{Et} \dots \dots \dots$	1.25	1.25

Gas is formed according to the equations listed above. Its quantity, as calculated according to these equations, is greater than the experimental value, although both experiment and calculation on the basis of lower Al/Ti ratios give a smaller volume of gas. Quantitative agreement cannot be expected due to disproportionation and di- and trimerization of the gas [5]. Therefore, the volume varies considerably. A full quantitative and qualitative gas analysis is needed for clarification of these supplementary reactions. Under the given conditions such an analysis is a difficult problem.

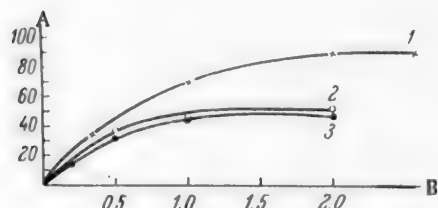


Fig. 7. Quantity of gas evolved during the AlEt_3 - TiCl_4 interaction as a function of the molar ratio of reactants. A) Volume of gas ($\frac{\text{moles gas}}{\text{moles TiCl}_4} \cdot 100$); B) $\text{AlEt}_3/\text{TiCl}_4$ molar ratio. 1) Trialkylaluminum; 2) aluminum sesquichloride; 3) dialkylaluminum chloride.

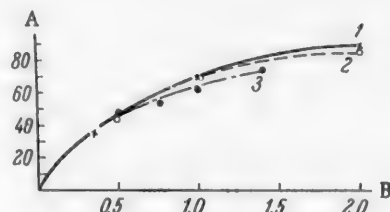


Fig. 8. Quantity of gas evolved during the AlEt_3 - TiCl_4 reaction as a function of the reaction period. A: volume of gas (moles gas / moles Ti) 100; B: $\text{AlEt}_3/\text{TiCl}_4$ molar ratio. Period (in min): 1) 0, 2) 10, 3) 30.

The presence of unsaturated hydrocarbons in the gas mixture is indicated by the following observation: Maintenance of the gases in a relatively small space for 10 or 30 minutes results in contraction, which is associated with polymerization of olefins. Figure 8 contains plots of the quantity of gas released in the reaction with trialkylaluminum versus the $\text{AlEt}_3/\text{TiCl}_4$ molar ratio during different reaction periods. The change in reaction period does not alter the gas volume at low Al/Ti ratios, presumably due to the low sensitivity of the method. A small quantity of paraffin waxes in the precipitate is also evidence of the polymerization of part of the gases.

SUMMARY

A method was developed for quantitative analysis during the AlEt_3 - TiCl_4 reaction with variation of the $\text{AlEt}_3/\text{TiCl}_4$ molar ratios between 0.5 and 5. The quantities of Al and Ti are approximately equal in the region of measurements. Equations appropriate to the process can be formulated from data obtained in analysis of trial equations. Methods are also described for measurement of the quantity of gas formed during preparation of catalyst. Results of measurements in the case of $\text{AlEt}_3/\text{TiCl}_4$ molar ratios of 0 to 3 are also presented. The measured

quantity of gas differs from the value calculated from the proposed reaction equations due to supplementary reactions of the gas. This process is confirmed by the gradual fall in quantity of gas.

LITERATURE CITED

- [1] K. Ziegler and H. Martin, *Makromol. Chem.* 18/19, 186 (1956).
- [2] L. Kovács, A. Simon, Gy. Ghymes, and L. Kollar, *Magyar Kémikusok Lapja* 13, 5/6, 181 (1958).
- [3] E. Krause and A. U. Grosse, *Chemistry of Organometallic Compounds* [In German] (Berlin, Brontraeger, 1937), p. 806.
- [4] J. Barksdale, *Titanium* (New York, 1949).
- [5] G. Natta, P. Pino, G. Marsanti, and P. Longi, *Gazetta Chimica Italiana* 87, 549 (1957).

Received November 15, 1958

BIOLOGICAL AGING OF CABLE RUBBER

G. I. Dubrovin

In previous research [1], migration processes in the basic construction of cable and their effect on the aging of cable rubbers have been studied. Furthermore, a method of calculation has been introduced that permits determining the approximate length of service of cable rubbers, and also a method for the determination of the resistance to electrical breakdown in relation to the time of wetting of insulating rubber through a hose casing.

In the present work some methods of protecting cable rubbers from the action of microorganisms are examined.

Wires and cables with rubber coverings for use under tropical climatic conditions with high humidity and temperature require protection of the rubber from destruction by molds. Therefore, antiseptics (fungicides), as well as vulcanization accelerators and aging inhibitors, are added to the rubber mixtures intended for these cable products. Inasmuch as cable products are used at temperatures up to 65°, it is important that the fungicides not lose their antiseptic properties on prolonged heating.

As antiseptics, organic compounds of mercury and copper, the chlorinated phenol derivatives tetrachlorophenol and pentachlorophenol, and the anilide of salicylic acid have been proposed and described [2-5].

The domestic cable industry employs albichthol from Syzran' schists and salicylanilide as antiseptics, and Thiuram (tetramethylthiuram disulfide) as a second component to increase the thermal stability of these antiseptics. At the time of vulcanization, when there is prolonged heating of the rubber, chemical reactions apparently take place between the fungicides and the Thiuram, with the oxygen of the air participating, and in the case of sulfur-containing rubbers, also the sulfur, with the formation of new compounds that are more heat-stable than the starting antiseptics.

The antiseptics are added to the rubber mixtures for cable products in the amount of 0.9 to 5.0 parts by weight to 100 parts of rubber. Horner et al. [3] recommend the following amounts of antiseptic: copper naphthenate 3-5%, mercury compounds 1.0%, chlorine-substituted phenols 10%, and salicylanilide 7.0 to 8.0%.

Practice has shown that each of the antiseptics mentioned has its deficiencies that limit its range of use. Albichthol, for example, has a sharp, unpleasant odor. Salicylanilide lowers the electrical characteristics of the insulating rubber. The use of Thiuram in small amounts is not very effective, and in large amounts it causes disintegration of the rubber. Chlorinated derivatives of phenol do not withstand prolonged heating of the cable at 65°. Mercury compounds are heat resistant but toxic; therefore, their use involves additional expense for protection of the workers and for safety techniques.

Along with other preparations, azomethine derivatives of the thiophene series were tested. The tests showed that organic compounds of this class are among the better antiseptics for cable rubbers.

EXPERIMENTAL

It had been observed that azomethine derivatives of the thiophene series and nickel and antimony salts of salicylanilide are not only antiseptics, but accelerators for the vulcanization of rubber, and consequently these preparations were tested as fungicides and as vulcanization accelerators. The tests were carried out on ordinary cable mixtures that had approximately the following basic composition.

1. Insulating rubber (TSSh-35 SK-50) and (TS-35 SK-50) prepared from natural rubber (NK) and sodium butadiene rubber (SKB) in 1:1 ratio; tetramethylthiuram disulfide was used as the vulcanizing agent and phenyl- β -naphthylamine (Neozon D) and mercaptobenzothiazole (Kaptaks) as inhibitors of aging; the mixture was filled with chalk and talc; the total rubber content was 35%.

2. Weather-resistant hose rubber (ShN-40) was prepared from polychloroprene rubber (Nairit); zinc and magnesium oxides were used as vulcanizing agents; the mixture was filled with lamp black and chalk and plasticized with dibutyl phthalate (DBF); the total rubber content of the mixture was 40%.

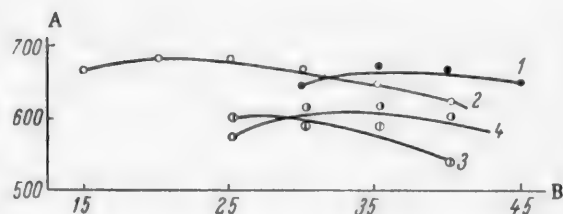


Fig. 1. Relation of relative elongation on tearing of insulating rubber containing various organic materials in place of Kaptaks to time of vulcanization at 203°. A) Relative elongation (in %); B) time of vulcanization (in sec). Organic materials: 1) 0.7 part by weight 5-methyl-2-thenylidene-p-aminophenol, 2) 0.9 part by weight 5-methyl-2-thenylidenaminoethanol, 3) 1.0 part by weight 2-thenylidenoaminophenol, 4) 1.0 part by weight 5-methyl-2-thenylidene-o-aminophenol.

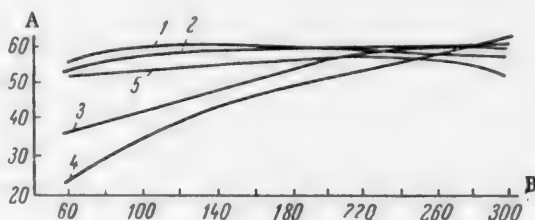


Fig. 2. Relation of yield strength of hose rubber ShBM-40 (sulfur) containing various accelerators instead of Kaptaks (1.0 part by weight to 100 parts of rubber) to time of vulcanization at 203°.

A) Yield strength on tearing (in kg/cm²); B) time of vulcanization (in sec). Accelerators: 1) control mixture of ShBM-40 with Kaptaks, 2) 5-methyl-2-thenylidene-p-aminophenol, 3) hydrozone-di (5-methyl-2-thenylidene), 4) hydrozone-di (thenylidene), 5) di(2-thenylidene)-m-phenylenediamine.

3. Frostproof hose rubber (ShBM-40) was prepared from butadiene-styrene rubber (Buna-S) and frostproof rubber (SKBM); sulfur and Kaptaks were used as vulcanizing agents and Neozon D as an inhibitor of aging; the mixture was filled with lamp black or furnace gas black and kaolin; paraffin petrolatum and granulated bitumen were introduced into the mixture as plasticizers; the total rubber content of the mixture was 40%.

Eighteen azomethine derivatives of the thiophene series of different chemical compositions were tested.

Insulating and hose rubber mixtures were prepared on laboratory rollers and the preparations tested were employed in the mixtures in concentrations of 0.5 to 1.5 parts by weight to 100 parts of rubber instead of Kaptaks and an antiseptic.

The prepared samples of rubber with antiseptic were placed in petri dishes on nutrient medium infected with fungus cultures and were kept in them at 30° for 30 days.

The heat stability of the fungicides was tested by prolonged heating of the rubber at 65° and subsequent testing in fungus cultures. Absence of fungus growth on the rubber samples served as an indication of a positive fungicidal action.

The effect of the preparations studied as vulcanization accelerators was tested by comparison of the optimum mechanical indices of the rubbers prepared from them with rubbers containing a classical vulcanization accelerator, Kaptaks. The inhibitory role of the antiseptics in the aging process of the rubbers was tested by prolonged aging of the test rubbers in parallel with control samples.

It appeared that in mixtures containing Thiuram many azomethine derivatives of thiophene were excellent fungicides and accelerated the vulcanization of the rubber; they withstood heating at 65° for 240 days and subsequent testing in fungus cultures for 30 days. Furthermore, rubber ShBM-40 (sulfur) containing 1.0 part by weight of 5-methyl-2-thenylidene-p-aminophenol to 100 parts of rubber withstood testing in fungus cultures after 90 days aging at 65°, while rubbers vulcanized with sulfur and containing other classes of chemical compounds as antiseptics were overgrown by the fungus considerably more quickly.

The best accelerators of the vulcanization process among the azomethine derivatives were 5-methyl-2-thenylidene-p-aminophenol, 5-methyl-2-thenylidenaminoethanol, and 2-thenylidene-m-nitroaniline.

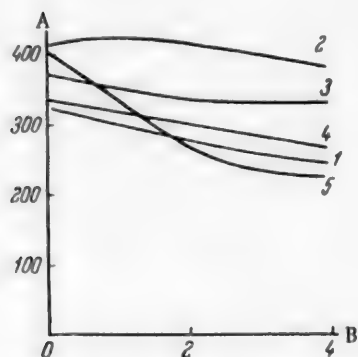


Fig. 3. Relation of relative elongation to time of aging at 70° of rubber ShBM-40 (sulfur) containing antiseptic-accelerators instead of Kaptaks. A) Relative elongation (in %); B) time of aging (in days). Antiseptic-accelerators: 1) 1.0 part by weight Kaptaks (control mixture); 2) 1.5 parts by weight salicylanilide; 3) 1.5 parts by weight Zn salt of salicylanilide; 4) 1.5 parts by weight Ni salt of salicylanilide; 5) 1.5 parts by weight Sb salt of salicylanilide.

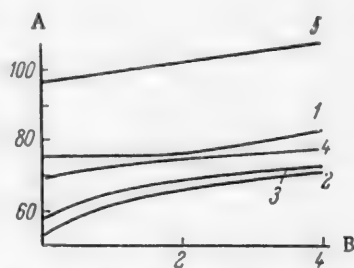


Fig. 4. Relation of yield strength on tearing to time of aging at 70° of rubber ShBM-40 containing antiseptic-accelerators. A) Yield strength on tearing (in kg/cm²); B) time of aging (in days). Designations on curves same as in Fig. 3.

The most active vulcanization accelerator was 5-methyl-2-thenylidene-p-aminoethanol (Fig. 1, curve 2).

From Fig. 2 it can be seen that rubbers containing 5-methyl-2-thenylidene-p-aminophenol and di(2-thenylidene)-m-phenylenediamine (curves 2 and 5) behave in the vulcanization of rubber ShBM-40 (sulfur) approximately the same as rubber containing Kaptaks (curve 1).

The zinc, nickel, and antimony salts of salicylanilide proved to be good antiseptics and vulcanization accelerators for cable rubber. The nickel salt of salicylanilide accelerated the vulcanization of the polychloroprene rubber. The antimony salt of salicylanilide accelerated the vulcanization of the rubber prepared from SKB and Buna-S.

The antimony salt of salicylanilide was very active in promoting the building of rubbers vulcanized with sulfur (Figs. 3 and 4).

In Fig. 5, the role of salicylanilide as an active inhibitor of aging of insulating rubber at 120° is shown.

When insulating rubber containing 1.5 parts by weight of salicylanilide to 100 parts of rubber was wet for long periods, a lowering of the electrical resistance

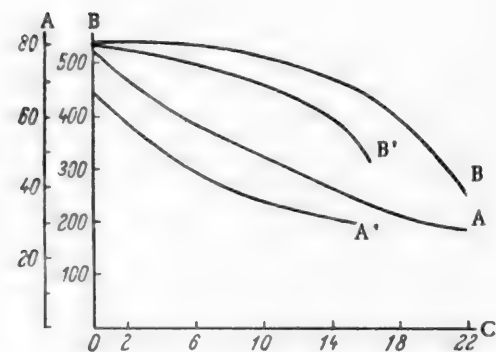


Fig. 5. Relation of mechanical indices of rubber TS-35 SK-50 containing 5.0 parts by weight salicylanilide to time of aging at 120°. A) Yield strength on tearing (in kg/cm²); B) relative elongation (in %); C) time of aging (in days). A' and B') Control samples without salicylanilide.

of the insulation by one order was noted, while rubber containing 0.9 part by weight of 5-methyl-2-thenylidene-p-aminophenol had indices similar to the control samples of rubber insulation.

SUMMARY

1. Azomethine derivatives of the thiophene series are heat-resistant universal fungicides for cable rubber.

2. Some azomethine derivatives of thiophene and salts of salicylanilide have antiseptic properties and accelerate the vulcanization of rubber.

The research on antiseptics for cable rubber was carried out in cooperation with the Ya. V. Samoilov Scientific Institute for Fertilizers and Insectofungicides.

I wish to thank Ya. I. Gol'dfarb and B. P. Fedorov, who kindly gave me the materials necessary for the investigation and actively cooperated in introducing them into the cable industry.

LITERATURE CITED

- [1] G. I. Dubrovin, *Zhur. Fiz. Khim.* 32, 10, 2261 (1959).
- [2] R. Proskauer, *Electronics* 17, 6, 92 (1944).
- [3] Horner, F. Wiltred, F. Koppa, and Russel, *Electronic Ind.* 4, 7, 106 (1945).
- [4] R. Proskauer and H. E. Smith, *Electronics* 18, 5, 119 (1945).
- [5] *Electrical Insulating Problems Under Tropical Conditions (Collection of References)* [In Russian] (ONTI, NIIP, 1955).

Received May 29, 1959

NITRATION OF ETHYLBENZENE*

O. S. Vladychik, L. L. Bessalova, P. M. Kochergin,
V. A. Zasosov, and A. M. Tsyganova

S. Ordzhonikidze All-Union Scientific Research Chemicopharmaceutical Institute

Mononitroethylbenzenes are used as intermediates in the synthesis of medicinal preparations and dyes.

Several communications have been published in the literature in which various directions are given for the nitration of ethylbenzene to obtain nitroethylbenzene (abbreviated name for a mixture of o-, m-, and p-nitroethylbenzenes). Nitric acid [1, 2], ethyl nitrate [3], and a mixture of nitric and sulfuric acids [4-8] have been used as nitrating agents. The methods described for the nitration of ethylbenzene suffer from deficiencies that are especially apparent in working under industrial conditions. Among these are the long period of time required for carrying out the process (3-7 hours), high (up to 135°) or low (down to -2°) temperature of the reaction, high percentage of unreacted ethylbenzene, comparatively low yields of the mixture of mononitroethylbenzenes, and formation of considerable amounts of dinitroethylbenzenes [5, 7] and tarry products. It also should be noted that in the published references on the nitration of ethylbenzene to nitroethylbenzene there are no experimentally based data on the rate of mononitration of the ethylbenzene, the optimum nitration activity factor (F) of the nitro mixture, the necessary excess of nitric acid, the optimum temperature, or other parameters of the process.

The present investigation was undertaken to study the mononitration of ethylbenzene for the purpose of selecting the optimum conditions for carrying it out not only in laboratories, but also on a commercial scale.

First, taking advantage of the instructions of Brown and Bonner [8], we checked the nitration of ethylbenzene with a mixture of nitric and sulfuric acids by the method described by Nelson and Brown [9] for the nitration of tertiary butylbenzene. The yield of nitroethylbenzene was 95-96% of theoretical, considering the nitroproduct as a mixture of mononitroethylbenzenes. Ethylbenzene (3.5-7%), 2,4-dinitroethylbenzene, and tarry products were present in the nitroethylbenzene as contaminants. As has already been reported [10], the 2,4-dinitroethylbenzene was separated by fractionation of the nitroethylbenzene, which previously had been steam-distilled.

On the basis of the results of these experiments, we concluded that such a nitro mixture (F = 78-80%) is too strong and causes the formation of dinitroethylbenzene even at a comparatively low temperature (25-40°), but the use of nitric acid in the amount of 100% of the theoretical calculated for the ethylbenzene does not permit the nitration reaction to go to completion.

To further study the various factors influencing the mononitration of ethylbenzene, we employed the following general method. A weighed sample of ethylbenzene was placed in a glass nitrator equipped with a stirrer, reflux condenser, dropping funnel, and thermometer. With the stirrer operating, and at the given temperature, with the nitrator cooled by tap water, a nitrating mixture of fixed composition was run into the ethylbenzene. When the addition of the nitro mixture was completed, there was a delay during which the duration

* Batch process.

TABLE 1

Effect of Activity Factor of Nitrating Mixtures and Amount of Nitric Acid on Yield and Quality of Nitroethylbenzene

Expt. No.	Charge (in g)		Composition of Nitro Mixture (in %)		Activity Factor of Nitro Mixture (in %)	Amt. of HNO ₃ (in % of theor.)	Duration of Temperature Rise on Holding Nitro (in min)	Duration of Separation of Nitroethylbenzene from Spent Acid (in sec)	Obtained (in g)		Quality of Nitroethylbenzene				Yield of Total Mononitroethylbenzenes (in % of Theor. Calc.)	Composition of Spent Acid (in %)			
	Ethylbenzene	Nitro	H ₂ SO ₄	HNO ₃					Spent Acid	Nitroethylbenzene	Spec. Gr.	Acidity (in %)	Ethylbenzene Content (in %)	Dinitroethylbenzene Content (in %)		H ₂ SO ₄	HNO ₃	N ₂ O ₅	Nitro Compounds
1	99.9	216	55.6	27.8	69.4	101	12	5)	470.9	140.3	1.107	1.10	6.04	None	91.46	68.98	0.72	0.49	0.93
2	250	685	61.0	21.9	72.4	101	15	96)	570.9	356.1	1.123	0.09	0.41	None	99.29	72.07	0.26	0.22	0.09
3	250	798	63.0	21.2	74.5	101	59	270	690.0	350.5	1.117	0.98	0.44	Traces	98.16	74.21	0.23	0.07	0.92
4	250	687	65.1	21.8	77.1	101	43	9)	571.6	355.9	1.122	0.85	0.39	Traces	98.71	76.89	0.29	0.06	0.92
5	250	640.3	61.0	21.9	72.4	95	20	330	541.9	340.0	1.113	0.10	4.07	None	91.63	71.73	Her	0.17	0.95
6	250	680	61.0	21.9	72.4	100.5	15	195	570.0	355.6	1.124	0.07	1.02	None	98.78	72.04	0.20	0.29	0.07
7	250	685	61.0	21.9	72.4	101	6	789	574.0	356.7	1.123	0.08	0.61	None	99.37	71.88	0.32	0.14	0.02
8	250	691	61.0	21.9	72.4	102	17	1219	578.5	356.1	1.122	0.16	0.22	None	99.58	72.07	0.14	0.24	0.04
9	301	842	61.45	21.79	72.7	103	15	129	706.4	425.6	1.121	0.12	0.21	None	99.29	72.93	Her	0.26	0.06
10	350	1001	61.45	21.79	72.7	105	20	18)	840.0	497.5	1.122	0.11	Her	None	99.7	72.95	0.16	0.40	0.04

of the temperature rise in the reaction mixture was recorded. Then the nitro product was separated from the spent acid, and the time duration of the separation was noted. The weight, specific gravity, and acidity of the technical nitroethylbenzene were determined, and also the weight and composition of the spent acid. The ethylbenzene and dinitroethylbenzene content were determined in the nitroethylbenzene, which had been washed with water to a neutral reaction. On the basis of the results obtained, the yield of total mononitroethylbenzene was calculated for the ethylbenzene taken for the reaction.

Contrary to some of the data in [4], we showed that the nitration of ethylbenzene proceeds very rapidly at 25-50°. This was established on the basis of the duration of the spontaneous temperature rise when the reaction mass was held (immediately after the conclusion of addition of the nitro mixture), which amounted to 15-20 minutes (Table 1, experiments 1-10). From the experiments (Table 2) it follows that at a temperature of 45-50°, 81-93% of the ethylbenzene taken for the reaction is nitrated during the time of addition of the nitro mixture, which takes about 15-20 minutes. For full completion of the process (when a nitro mixture is used with 5% excess nitric acid, Table 2, Experiment No. 3) another 25-30 minutes are required.

From the data obtained it follows that the addition of the nitro mixture to the ethylbenzene can be carried out with the maximum permissible speed (15-20 minutes, on the average) with tap water as the cooling agent, maintaining the temperature of the reaction mass not higher than 50°. Keeping the reaction mass at a temperature of 50-55° for 30 minutes is sufficient for completion of the nitration of the ethylbenzene.

It is known that when organic compounds are nitrated with a mixture of nitric and sulfuric acids, the activity factor of the nitro mixture used is very important [11]. According to data in [4-8], nitro mixtures with a nitrating activity factor of 69-80% have been used for the nitration of ethylbenzene.

In the present work, we investigated the nitration of ethylbenzene with nitrating mixtures with a composition of 55.6-65.1% sulfuric acid and 21.2-27.8% nitric acid, and with a nitrating activity factor (in %) of 69.4, 72.4, 72.7,

73.2, 74.5, and 77.1. Evaluation of the activity of the nitro mixtures, and of the other parameters of the process, was accomplished by the yield of nitroethylbenzene, the percent of ethylbenzene and dinitroethylbenzene in it, and the composition of the spent acid. For this purpose, a series of experiments was carried out (Table 1, experiments 1-4) in which only the composition of the nitro mixture was changed, while the rest of the factors were kept constant, namely: 1% excess of nitric acid above the amount theoretically necessary, 20 minutes time for the addition of 100 g of nitro mixture, 30 minutes holding of the nitro mass, temperature of the reaction mixture during addition of the nitro mixture 25-30°, and temperature during holding of the nitro mass 50-55°. The results of the experiments showed that the optimum nitro mixture had a nitrating activity factor of 72.4%, a sulfuric acid content of 61%, and a nitric acid content of 21.9%, and gave the highest yield of total mono-nitroethylbenzene (99.3%). When the nitrating activity factor was decreased to 69.4%, dinitroethylbenzene was formed. To investigate the effect of the amount of nitric acid and the temperature while holding the nitro mass, a series of experiments was carried out on the nitration of ethylbenzene (Table 1, Experiments 5-10) with the other conditions kept constant: nitrating activity factor of nitro mixture 72.4-72.7%, time of addition of 100 g of nitro mixture 20 minutes, temperature while adding nitro mixture 35-40°, time of holding 30 minutes, temperature of reaction mass during holding 50-55°. On the basis of the results obtained, it follows that the optimum amount of nitric acid is 105% of that theoretically calculated from the ethylbenzene, since under these conditions nitroethylbenzene is obtained in almost theoretical yield (99.7%) without contamination by ethylbenzene and dinitroethylbenzene. From these experiments, it also was concluded that the optimum temperature during holding of the nitro mass is 50-55°. In experiments where the nitro mass was held for 30 minutes, but at a higher temperature (75°), nitration of ethylbenzene with the same nitro mixture ($F = 72.7\%$)

TABLE 2

Effect of Duration of Holding Period and Excess of Nitric Acid on Composition of Nitroethylbenzene and Spent Acid

Expt. No.	Charge (in g)		Composition of Nitro Mixture (in %)		Activity Factor of Nitro Mixture (in %)	Excess Nitric Acid Above Theoretical (in %)	Duration of Holding (in min)	Ethylbenzene Content on Nitroethylbenzene (in %)	Dinitroethylbenzene Content of Nitroethylbenzene	Composition of Spent Acid (in %)		
	Ethylbenzene	Nitro Mixture	H ₂ SO ₄	HNO ₃						H ₂ SO ₄	HNO ₃	N ₂ O ₅
1	168	462	61.83	21.89	73.2	1.0	0.5	20.8	None	70.89	3.55	0.19
							15	3.4	"	—	None	—
							30	3.2	"	—	—	—
							45	3.1	"	—	—	—
							60	3.0	"	—	—	—
							75	2.7	"	—	—	—
							90	2.6	"	72.26	—	0.23
											None	
							0.5	15.76	"	72.04	2.32	0.26
2	300	842	61.45	21.79	72.7	3.0	15	1.78	"	72.95	0.14	0.23
							30	0.67	"	72.88	—	0.27
							45	0.48	"	72.68	—	0.27
							60	0.32	"	72.80	None	0.20
							75	0.28	"	72.88	—	0.23
							90	0.21	"	72.93	—	0.26
							0.5	7.54	"	73.88	1.71	0.24
							15	0.48	"	72.50	0.25	0.19
3	360	1000	61.45	21.79	72.7	5.0	30	—	"	73.33	0.17	0.33
							40	—	"	72.69	0.26	0.31
							60	—	"	73.05	0.21	0.31
							75	—	"	72.90	0.19	0.31
							90	—	"	72.95	0.16	0.40

was accompanied by intense oxidation, which was characterized by the evolution of oxides of nitrogen, which was not observed when the nitro mass was held at 50-55°. The nitroethylbenzene obtained contained a small amount of dinitroethylbenzene. During the holding period, the spent acid darkened greatly.

Under industrial conditions the time consumed in separating the nitro product from the spent acid is very important. As can be seen from Table 1, the separation of the nitroethylbenzene from the spent acid takes place very quickly. On the average, the time of separation is 2-3 minutes. This is explained by the considerable difference in the specific gravities of nitroethylbenzene (1.11-1.12) and the spent acid (about 1.75). To more precisely determine the temperature during the addition of the nitro mixture, the optimum holding period, and the excess of nitric acid, another series of experiments was carried out (Table 2) on the nitration of ethylbenzene. Addition of the nitro mixture to the ethylbenzene was carried out with the reaction mass at a temperature of 45-50° with the maximum permissible speed, while the reaction vessel was cooled with ice. A portion of the nitro mass was withdrawn immediately after completion of the addition and then after 15, 30, 45, 60, 75, and 90 minutes holding at 50-55°. After separation, the spent acid was analyzed, and the nitroethylbenzene that was separated out was washed with water until it was neutral, and the ethylbenzene and dinitroethylbenzene in it were determined.

Analysis of the data obtained indicates that a 1% excess of nitric acid above that theoretically necessary for the ethylbenzene is insufficient, since part of the nitric acid probably is consumed in oxidizing processes. After 15 minutes holding, no nitric acid remained in the spent acid, while the amount of ethylbenzene in the sample of nitroethylbenzene withdrawn was 3.4%. With a 3% excess of nitric acid, after 30 minutes holding of the nitro mass the nitroethylbenzene still contained some ethylbenzene (0.67%), and no nitric acid remained in the spent acid. When 105% of the theoretically calculated nitric acid was used, the ethylbenzene was completely nitrated in 25-30 minutes, and there was only 0.2-0.3% of nitric acid left in the spent acid.

On the basis of the experiments carried out, the following optimum conditions were established for the nitration of ethylbenzene to mononitroethylbenzene: activity factor of nitrating mixture 72-73%, composition of nitrating mixture 61-62% sulfuric acid and 21-22% nitric acid, amount of nitric acid 105% of that theoretically calculated for the ethylbenzene, temperature of addition of nitro mixture to ethylbenzene 45-50°, duration of addition of nitro mixture 20 minutes, temperature during holding of reaction mass 50-55°, holding period 30 minutes.

These conclusions were confirmed by numerous experiments on the nitration of ethylbenzene under the indicated conditions for the purpose of obtaining nitroethylbenzene in considerable quantity. The nitroethylbenzene obtained did not contain ethylbenzene. Dinitroethylbenzene was always absent, which made it possible to eliminate from the technological process the steam distillation of the nitroethylbenzene, which is recommended by several authors [2, 5] to free it of dinitroethylbenzene and tarry products. The spent acid was a clear, slightly yellowish liquid with the composition: 72-73% sulfuric acid, 0.1-0.5% nitric acid, 0.2-0.3% oxides of nitrogen (calculated as nitrogen trioxide), 0.02-0.10% nitro compounds. It could be regenerated by denitration and subsequent concentration by known methods.

EXPERIMENTAL

In carrying out the experiments, ethylbenzene meeting the requirements of VTU MKhP No. 3925-54 was used. The nitration mixtures were prepared from standard acids, melanzha,* and oil of vitriol, with the addition of the calculated amount of water.

Nitration of ethylbenzene. In a glass nitrator with a volume of 1.5 liters, equipped with a stirrer, reflux condenser, dropping funnel, and thermometer, was placed 350 g of ethylbenzene. With the stirrer operating and with the reaction vessel cooled by tap water, 1000 g of the following nitro mixture was added to the ethylbenzene: 61.45% sulfuric acid and 21.79% nitric acid ($F = 72.7\%$). The time for the addition of the nitro mixture was 15-20 minutes; the temperature of the reaction mass during the addition was maintained within the limits 45-50°. At the end of the addition, warming of the reaction mass to 50-55° was effected and the mass was held for 30 minutes, with stirring. Then the reaction mass was cooled to room temperature and transferred to a 2-liter separatory funnel. The nitro product that separated out (time for separation 2-3 minutes) was removed from the spent acid. 497.5 g of nitroethylbenzene was obtained with a specific gravity of 1.122 and 0.11% acidity, containing no ethylbenzene or dinitroethylbenzene. With a correction for acidity, the yield of total mononitroethylbenzenes was 497 g or 99.7% of the theoretically calculated amount based on ethylbenzene. The weight of the spent acid was 840 g. Its composition was 72.95% sulfuric acid, 0.16% nitric acid, 0.40% oxides of nitrogen (calculated as nitrogen trioxide), and 0.04% nitro compounds.

* Transliteration of Russian meaning mixed acids.

SUMMARY

1. In a study of the nitration of ethylbenzene with nitrating mixtures of nitric and sulfuric acids, the optimum conditions were found for the nitration of the ethylbenzene to mononitroethylbenzene.
2. An improved batch process is proposed for the nitration of ethylbenzene, which permits obtaining a mixture of mononitroethylbenzenes that does not contain ethylbenzene nor dinitroethylbenzene, in almost theoretical yield based on the ethylbenzene.

LITERATURE CITED

- [1] F. Beilstein and A. Kuhlberg, *Lieb. Ann.* 156, 206 (1870).
- [2] E. Schreiner, *J. pr. Chem.* (2), 81, 558 (1910).
- [3] G. Vavon and V. M. Mitchovitch, *Bl. Soc. Chim. France* (4), 45, 962 (1929).
- [4] G. Schultz and J. Flachsländer, *J. pr. Chem.* (2), 66, 160 (1902).
- [5] E. L. Cline and E. E. Reid, *J. Amer. Chem. Soc.* 49, 3150 (1927).
- [6] H. Kondo and S. Uyeo, *Ber.* 70, 1091 (1937).
- [7] A. H. Ford-Moore and H. N. Rydon, *J. Chem. Soc.* 679 (1946).
- [8] H. C. Brown and W. H. Bonner, *J. Amer. Chem. Soc.* 76, 605 (1954).
- [9] K. S. R. Nelson and H. C. Brown, *J. Amer. Chem. Soc.* 73, 5605 (1951).
- [10] O. S. Vladychik, P. M. Kochergin, K. E. Novikova, L. L. Bespalova, R. M. Titkova, A. M. Tsyganova, G. D. Krasnozhen, and A. M. Grigorovskii, *Zhur. Fiz. Khim.* 32, 8, 1830 (1959).
- [11] A. G. Gorst, *Chemistry and Technology of Nitro Compounds* [In Russian] (Oborongiz, Moscow 1940), p. 84.

Received March 9, 1959

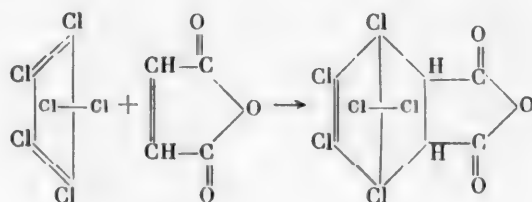
THE BASES OF CHLORENDIC ANHYDRIDE TECHNOLOGY

L. M. Kogan and N. P. Ignatova

Scientific Institute for Fertilizers and Insectofungicides

The anhydride of 1,4,5,6,7,7-hexachlorobicyclo-[2,2,1]-5-heptene-2,3-dicarboxylic acid, or the anhydride of 1,2,3,6-tetrahydro-3,6-endomethylene-3,4,5,6,7,7-hexachlorophthalic acid, so-called "chlorendic anhydride", has recently acquired practical importance for the preparation of fireproof and thermostable polymers [1]. Plastics prepared from chlorendic anhydride burn with great difficulty or not at all and retain high physicomechanical characteristics after prolonged heating at an elevated temperature.

Chlorendic anhydride was first prepared by Prill in 1947 [2] by a diene synthesis reacting hexachlorocyclopentadiene and maleic anhydride:



This was a solid, white compound, with m. p. 232-237° [2, 3]. It was soluble in benzene, toluene, xylene, acetone, and ethanol; it crystallized from chloroform.

Equimolecular quantities of the starting materials were used by Prill for the reaction. The process was carried out at 100° for 14 hours in the presence of a small amount of toluene. However, it was not possible to isolate the chlorendic anhydride by steam-distilling off the unreacted hexachlorocyclopentadiene, since the anhydride apparently was partially converted to the corresponding acid. The yield of the product was 83%. Rimschneider and Kühn [3] repeated the work of Prill. In patents [4-8] it has been indicated that an equimolecular mixture of the starting materials and a small amount of toluene, xylene, or other high-boiling solvent are used for the process. The reaction is carried out at 145-200°. The necessity of introducing a solvent is apparently connected with the fact that the reaction product is a high-melting compound, which in the absence of a solvent is converted into a monolith that is very difficult to remove from the reactor. Recovery of the reaction product is effected by distilling off the solvent or crystallizing the chlorendic anhydride by the addition of hexane or heptane.

The deficiencies of this method of preparing chlorendic anhydride are the complication of the technological process because of the participation of two supplementary materials that present a fire hazard, and also the necessity of carrying out a special operation to separate three compounds, the unreacted hexachlorocyclopentadiene and the two solvents, the conditions for which are not indicated. The problem of the present investigation was to study the characteristics of the reaction for the purpose of proposing a technological process without the indicated deficiencies.

Results of Experiments and Discussion

In the reaction between hexachlorocyclopentadiene and maleic anhydride, we may expect, besides the formation of chlorendic anhydride, the occurrence of side processes with the production of a dimer and polymer of hexachlorocyclopentadiene, a condensation product of chlorendic anhydride with hexachlorocyclopentadiene, and other compounds. Obviously, these reactions will be favored by carrying out the process with an excess of one of the reagents, and by an elevated temperature and much prolonged heating. By carrying out appropriate experiments, it was shown that chlorendic anhydride is practically the sole reaction product. Setting up the experiments with preliminary introduction of chlorendic anhydride into the starting mixture did not alter the results.

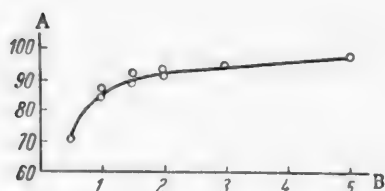


Fig. 1. Effect of duration of heating of a mixture of hexachlorocyclopentadiene and maleic anhydride on yield of chlorendic anhydride: A) yield (in %); B) time (in hrs); 5% excess maleic anhydride; duration of dropwise addition 1 hour; temperature 150°.

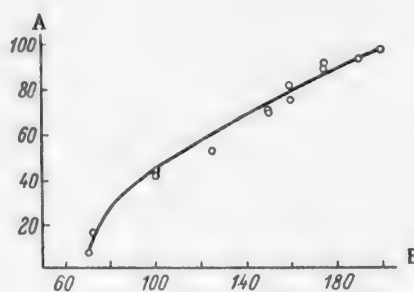


Fig. 2. Effect of temperature on yield of chlorendic anhydride from reaction of hexachlorocyclopentadiene (HCCPD) with maleic anhydride; A) yield (in %); B) temperature (in °C); 5% excess maleic anhydride; duration of dropwise addition 1 hour; duration of standing 30 minutes.

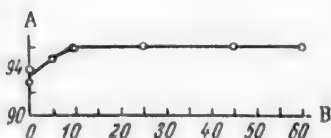


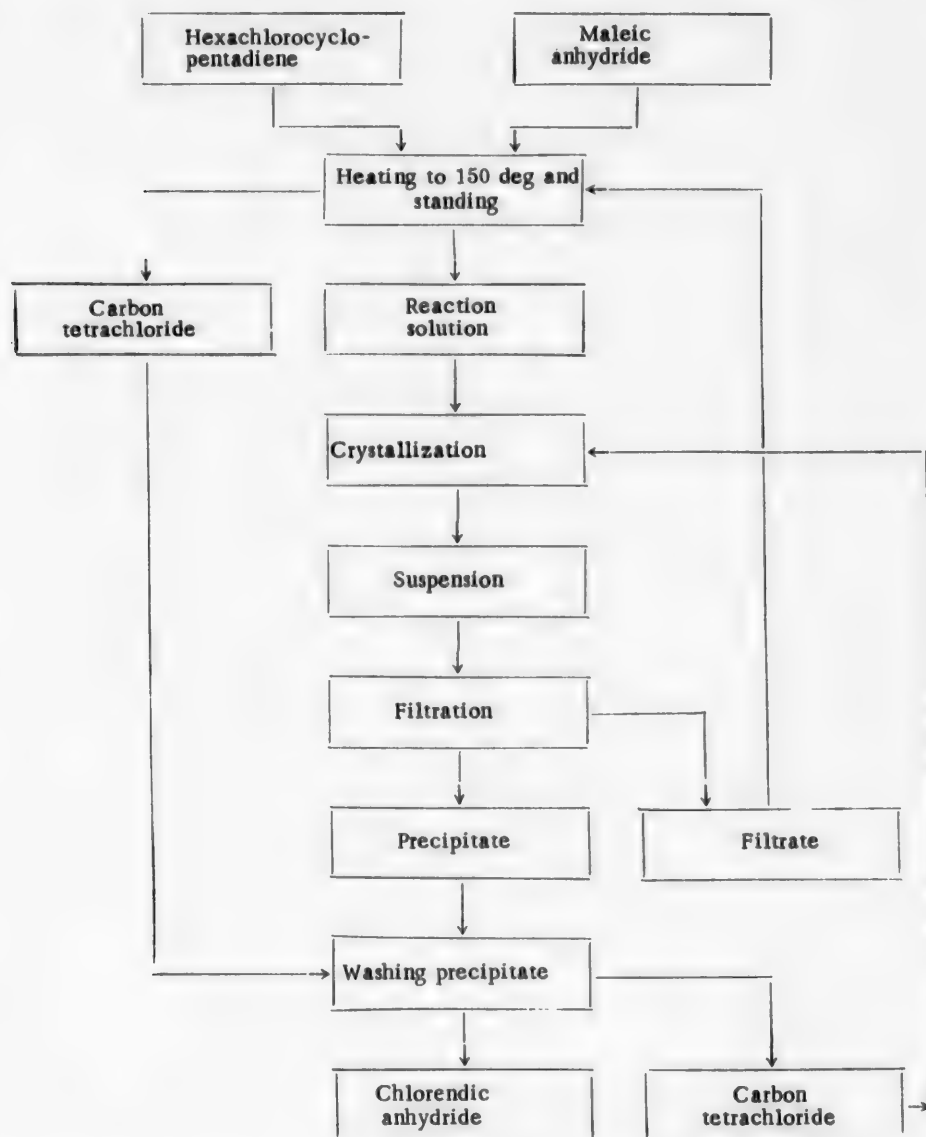
Fig. 3. Effect of amount of excess maleic anhydride on yield of chlorendic anhydride: A) yield (in %); B) excess of maleic anhydride (in %); Duration of heating 2 hours 45 minutes; temperature 160°.

The effect of the temperature, the duration of heating, and the amount of excess maleic anhydride on the yield of chlorendic anhydride was studied (Figs. 1-3). From Fig. 1 and 2 it follows that lowering the temperature can compensate for an increase in the duration of the process, and vice versa. It was established by the experiments that the reaction studied follows a rather simple course with high yield, but the reaction mixture contains some of the starting materials. The reaction product after cooling was a monolithic fused mass, the removal of which from the apparatus, as well as its further treatment, were complicated operations.

Contamination with maleic anhydride does not decrease the technical value of the chlorendic anhydride and apparently is a positive factor, since it lowers the melting point of the product. This facilitates subsequent treatment. Furthermore, the maleic anhydride participates along with the chlorendic anhydride in the subsequent processes of polymer formation. Contamination with hexachlorocyclopentadiene is not permissible because of its high toxicity and pungent odor. Attempts to wash out the hexachlorocyclopentadiene from fragments of the solidified melt proved unsuccessful and showed that solution of this material can be effected only under conditions where the fused product is first pulverized. However, carrying out this operation under plant conditions is very complicated and is not permissible from a sanitary point of view.

This discussion shows that in spite of the simplicity of the synthesis and production of a high yield of chlorendic anhydride, the conditions found for the process cannot be recommended as technologically admissible.

In order to establish a process without the indicated shortcomings, it seemed to us expedient to carry out the reaction in hexachlorocyclopentadiene medium. Experiments that were set up showed that in this case the reaction mixture was a mobile liquid, which was readily transported for the subsequent operations. We carried out the precipitation of the chlorendic anhydride from this solvent with carbon tetrachloride. When this was done, a finely crystalline precipitate settled out, which was easily separated on a filter. The product was washed with carbon tetrachloride, which was then used for the precipitation of chlorendic anhydride in a following experiment. Equimolecular amounts of the starting materials were added to the filtrate, which was a solution of hexachlorocyclopentadiene in carbon tetrachloride. The mixture was further heated to the reaction temperature (150-160°). In this process the carbon tetrachloride distilled off and was then used for washing the precipitate on the filter. After the synthesis was carried out, all the steps were repeated.



In this case, only one material participates in the process besides the crude and the finished product. Compounds that present an explosion hazard are not present in the process, and no waste products are discharged into the atmosphere or water reservoirs. The main scheme of the process for the preparation of chlorendic anhydride is shown on this page.

The experiments carried out established that the yield of chlorendic anhydride exceeds 90% when the hexachlorocyclopentadiene is repeatedly circulated.

EXPERIMENTAL

Starting materials. The hexachlorocyclopentadiene was prepared by catalytic chlorination of polychlorocyclopentanes by a method previously described [10]. The constants of the hexachlorocyclopentadiene were: b. p. 94-95° at 5 mm Hg, d_4^{20} 1.7088, n_D^{20} 1.5650. The maleic anhydride conformed to GOST 5851-51.

Description of apparatus and experimental method. The reaction was carried out in a 500 ml four-necked flask equipped with a thermometer, dropping funnel, reflux condenser, and stirrer. Heating was carried out with Woods metal. The starting materials were loaded into the flask, after which gradual heating was started until the reaction began, and then the desired temperature was maintained. In separate experiments the hexachlorocyclopentadiene was dropped in at the reaction temperature.

Analysis of reaction mixture. The unreacted hexachlorocyclopentadiene was determined by splitting out the two labile chlorine atoms with an alcoholic solution of potassium hydroxide and subsequently determining chlorine by the Volhard method. It was established by special experiments that the chlorendic anhydride molecule remains inert under the conditions of this analysis. The yield of total material was judged by the amounts of unreacted hexachlorocyclopentadiene and by the chlorendic anhydride formed, which was identified by analysis and melting point.

Presented below are the results for two experiments on the preparation of chlorendic anhydride by the proposed scheme.

Experiment No. 1. For the reaction, 109.2 g (0.4 mole) of hexachlorocyclopentadiene and 9.8 g (0.1 mole) of maleic anhydride were used. The mixture was heated for 3 hours at 150°. After the reaction mixture had cooled, and it had been diluted with carbon tetrachloride and filtered, 36.6 g of precipitate was obtained with a 99% chlorendic anhydride content. Then 27.3 g (0.1 mole) of hexachlorocyclopentadiene and 9.8 g (0.1 mole) of maleic anhydride were added to the mother liquor. After the carbon tetrachloride had been distilled off, the temperature was raised to 150° and all the processes were further carried out as described above. As a result of this operation, another 33.6 g of precipitate was obtained with a 99.4% chlorendic anhydride content. The operation described was carried out 4 times more and each time the chlorendic anhydride was isolated. The mother liquor from the last operation was distilled. From this distillation 74.5 g of hexachlorocyclopentadiene was obtained. In all, $109.2 + 27.3 \cdot 5 = 245.7$ g of hexachlorocyclopentadiene and $9.8 \cdot 6 = 58.8$ g of maleic anhydride were used in the process. 210.9 g of precipitate containing 99.4% chlorendic anhydride with m. p. 230-234° was obtained. The yield for each operation was 95-98%; on the whole, taking into account the losses of hexachlorocyclopentadiene in recirculation and the mechanical losses, the yield was 91%.

Experiment No. 2. For the reaction, 109.2 g (0.4 mole) of hexachlorocyclopentadiene and 9.8 g (0.1 mole) of maleic anhydride were used. The mixture was heated for 3 hours at 160°. The further operations did not differ from those indicated in experiment No. 1 except that the reaction was carried out at 160°. Six cycles of the process were carried out in all. The amounts of material taken for the process were $109.2 + 27.3 \cdot 6 = 273.0$ g of hexachlorocyclopentadiene and $9.8 \cdot 7 = 68.6$ g of maleic anhydride. By distillation of the mother liquor 75.9 g of hexachlorocyclopentadiene was obtained. In all, 268.0 g of precipitate containing 98.2% chlorendic anhydride was obtained, corresponding to a yield of more than 95%.

SUMMARY

1. The yield of chlorendic anhydride produced by the reaction of hexachlorocyclopentadiene and maleic anhydride increases with an increase in the temperature and in the duration of the process. The maximum yield was 96-98% at 100-200°.

2. Technological complications in carrying out the process are connected with the fact that the reaction mixture is obtained in the form of a monolithic fused mass that contains hexachlorocyclopentadiene, which is difficult to extract and gives the product an unpleasant odor and toxicity.

3. A process has been proposed for the preparation of chlorendic anhydride in hexachlorocyclopentadiene solution, which provides a mobile reaction liquid. Isolation of the desired product is accomplished by crystallization with the aid of carbon tetrachloride to yield a finely crystalline material without harmful contaminants. The technological process has a closed cycle.

LITERATURE CITED

- [1] L. M. Kogan, Zhur. Khim. Prom. 5, 458 (1959).
- [2] A. Prill, J. Amer. Chem. Soc. 69, 62 (1947).
- [3] R. Rimschneider and A. Kühnl, Mit physiol. Chem. Inst. R 11, 8 (1947); Chem. Abstr. 49, 8216 (1955).
- [4] British Patent 709,582 (1954); Chem. Abstr. 49, 10363 (1955).
- [5] S. H. Herzfeld, R. E. Lidov, and H. Bluestone, U. S. Patent 2,606,910 (1952); Chem. Abstr. 47, 8775 (1953).
- [6] M. Kleiman, U. S. Patent 2,598,562 (1952).
- [7] M. Kleiman, Australian Patent 158,972 (1954); Manufacturing Chemist 24, 51 (1953).
- [8] British Patent 614,931 (1948); Chem. Abstr. 43, 4693 (1949).
- [9] M. Kleiman, U. S. Patent 2,781,360 (1957).
- [10] L. M. Kogan and N. M. Burmakín, Zhur. Priklad. Khim. 31, 1585 (1958). •

Received February 9, 1959

•Original Russian pagination. See C. B. Translation.

THERMAL ISOMERIZATION OF ROSIN

I. I. Bardyshev, A. G. Sokolov and O. T. Tkachenko

The manufacturing process for the production of rosin from soft resin is accompanied by heating of the resin acids to 170-180°, and the conversion of rosin to various esters, resinates, driers, and cable materials is carried out at a higher temperature, reaching 300°.

Consequently, the investigation of the chemical transformations of resin acids and, in particular, of rosin, which take place upon thermal treatment, is of definite practical interest.

The thermal isomerization of levo-pimaric acid has been studied comparatively well [1-3]. It is known that this acid very readily undergoes isomerization transformations, and at 200° it is completely converted in a half hour to a mixture of abietic (52%), palustric (34%), and neoabietic (14%) acids [2]. For this reason, the levo-pimaric acid content of commercial samples of rosin is comparatively small and varies within the limits 0.5-6% [4].

Neoabietic acid is isomerized on heating to a mixture of abietic and palustric acids [5, 6]. After it had been heated at 200° for 0.5 hour and 72 hours, the mixture contained, in addition to neoabietic acid, 11 and 82% of abietic acid and 5 and 13% of palustric acid, respectively.

Palustric acid is in turn isomerized upon thermal treatment to abietic and neoabietic acids [2]. Abietic acid is the most stable toward the action of heat, but it also undergoes complex transformations to some extent at high temperatures (above 200°). In this process, dehydro-, dihydro-, and tetrahydroabietic acids, higher cyclic unsaturated hydrocarbons (resulting from decarboxylation of the abietic acid), and other products are formed [1, 7, 8]. The amount of dehydro-, dihydro-, and tetrahydroabietic acids in rosin depends on the composition of the starting resin and is, for the most part, dependent on the temperature conditions of the resin treatment. According to our investigations [4], the amount of these acids in samples of rosin from domestic wood chemical factories varies from 2 to 17%. The content of disproportionated resin acids should increase on further heating of the rosin, and the higher the temperature, the faster this content should increase.

The effect of temperature and time of heating on the properties of rosin colophony (rosin) has been studied by Stinson and Lawrence [9]. These authors subjected the rosin to thermal treatment at 155° for 195 hours and at 225, 250, 275, and 290° for 8 hours, studying in this process the acid number, saponification number, softening point, tendency to crystallization, and color of the products obtained. The question of the chemical composition of the samples of thermally treated rosin, which is important from the theoretical and practical points of view, was not investigated in this work.

Our investigations make it possible to judge to a certain extent the chemical transformations of the resin acids of rosin obtained from ordinary pine (*Pinus silvestris*) resin at temperatures of 225, 250, 275, and 300° for 8 hours.

EXPERIMENTAL

Thermal treatment of rosin. Samples of rosin (300 g) were heated in an atmosphere of nitrogen in a round-bottomed flask equipped with a stirrer, a thermometer, and a trap for the collection of volatile products, and connected to a reflux condenser. Heating was carried out on a Woods-metal bath. Elevation of the temperature

to the given level was accomplished in all the experiments in a 20 minute interval and its variation thereafter was held within $\pm 1^\circ$. Each experiment lasted 8 hours. Samples of the thermally treated rosin were taken with a pipet, cooled in a desiccator filled with carbon dioxide, and then analyzed. The acid number and the optical rotation (which always was determined for 2% solutions of the rosin in rectified ethyl alcohol) were determined for these samples by the usual methods, as well as the mixed dehydro-, dihydro-, and tetrahydroabietic acid content of the acid fraction.

Isolation of acid fraction from thermally treated rosin. For the recovery of the acid fraction, 5 g of the product was dissolved in methyl alcohol and treated with 0.5 N alcoholic potassium hydroxide solution. After removal of the neutral materials from the solution by repeated extraction with diethyl ether, the salts of the resin acids were decomposed with boric acid and extracted with diethyl ether. The extract of resin acids was washed with distilled water and dried over calcined sodium sulfate.

Determination of mixed dehydro-, dihydro-, and tetrahydroabietic acid content. In order to establish the amount of dehydro-, dihydro-, and tetrahydroabietic acids in the acid fraction of the thermally treated rosin, we first determined by bromometric titration the total of resin acids having two double bonds in the molecule.

The method of bromometric titration of the resin acids [10] is based on the fact that the resin acids with two double bonds add one molecule of bromine comparatively quickly. Dehydro- and tetrahydroabietic acids do not add bromine under the conditions used, and dihydroabietic acid reacts with it slowly. It is therefore possible to determine by difference the amount of these acids in the mixtures under investigation.

We used the following method for the quantitative determination of the total resin acids containing two double bonds. Part of the ether solution of the resin acids that were isolated from the thermally treated rosin was diluted with ether and two identical 10-20 ml samples were withdrawn with a pipet. One of these was titrated from a semimicro buret with 0.5 N alcoholic potassium hydroxide with phenolphthalein as indicator. The ether was distilled off from the other sample in an atmosphere of nitrogen. The residue was dissolved in 20 ml of methanol and after cooling with ice it was rapidly titrated with 0.2 N methanol solution of bromine [11] in the presence of methyl orange. The titration was stopped when there was a momentary change of color of the whole titrated solution. Two parallel analyses were carried out for each sample. The percent of resin acids with two double bonds in the molecule was calculated by the formula

$$X = \frac{0.3512 \cdot T_1 (V_1 - 0.356) \cdot 100}{1.005 \cdot V_2 \cdot T_2},$$

where V_1 is the volume of 0.2 N methanol solution of bromine entering into the titration, V_2 is the volume of 0.5 N alcoholic potassium hydroxide solution entering into the titration of the total resin acids, T_1 is the titer of the methanol solution of bromine, T_2 is the titer of the alcoholic potassium hydroxide solution, 0.3512 is the ratio of the molecular weights of potassium hydroxide and bromine, 0.356 and 1.005 are correction factors found experimentally on artificial mixtures of resin acids.

This method was checked by us on artificial mixtures of resin acids, for the preparation of which we used abietic acid (m. p. 174-175.5° and $[\alpha]_D - 110^\circ$) and a mixture of dehydro-, dihydro-, and tetrahydroabietic acids (m. p. 171°, $[\alpha]_D + 56.2^\circ$) obtained by heating abietic acid with paladinized carbon at 245° and subsequent crystallization from ethyl alcohol [12]. The mean square error of a single analysis (σ) was determined to be $\pm 1.2\%$. It should be noted that use of the method described requires experience in establishing the end-point of the titration with the methanol solution of bromine.

Change in dehydro-, dihydro-, and tetrahydroabietic acid content of mixture. In Fig. 1 are shown curves demonstrating the change in dehydro-, dihydro-, and tetrahydroabietic acid content of the acid fraction of rosin in relation to the temperature and time of thermal treatment. The starting rosin contained 9.3% of dehydro-, dihydro-, and tetrahydroabietic acids, and in all other physicochemical properties it conformed fully with the requirements of GOST 797-55 for the highest grade. As can be seen from the figure, disproportionation of hydrogen in the abietic acid molecules takes place even at 225°. However, at this temperature, it occurs mainly in the first stage of the process, since in 1 hour the amount of dehydro-, dihydro-, and tetrahydroabietic acids increases to 20%, and on subsequent heating for 7 hours it increases only by 3%. When the temperature of the

reaction is increased to 250°, the disproportionation of hydrogen proceeds more rapidly. Thus, after 7 hours heating the dehydro-, dihydro-, and tetrahydroabietic acid content rises to 28.3%. In the acid fraction of the rosin subjected to heat treatment at 275° for 8 hours there were 52.1% of disproportionated resin acids. Approximately the same results (54.5%) were obtained at 300° in 2 hours, and in 8 hours the amount of these acids was 82.6%. It may be assumed that in this time almost complete disproportionation of the abietic acid was achieved, since the dextro- and isodextro-pimaric acid content (according to the data in the literature these compounds do not undergo change under these conditions) in the acid fraction of the oleoresin amounted to 18% [13].

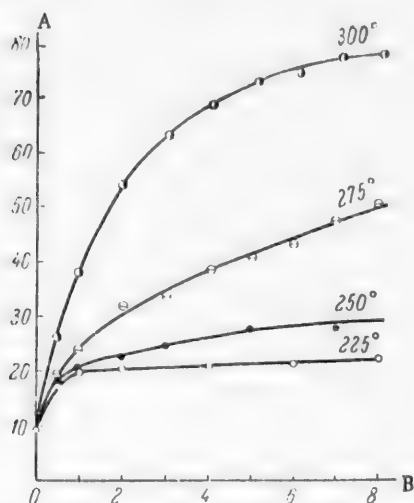


Fig. 1. Dehydro-, dihydro-, and tetrahydroabietic acid content of acid fraction of rosin in relation to temperature and time of thermal treatment of the latter. A) Dehydro-, dihydro-, and tetrahydroabietic acid content (in%); B) time (in hours).

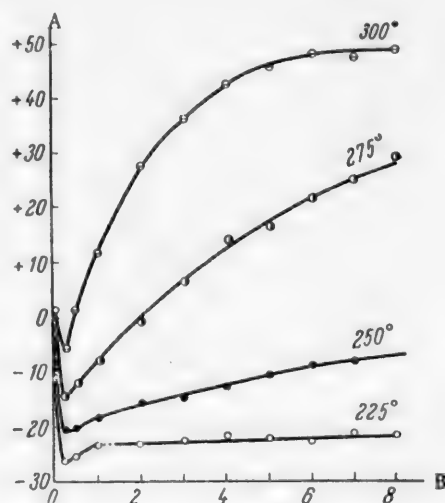


Fig. 2. Specific rotation of rosin in relation to temperature and time of thermal treatment. A) Specific rotation of rosin $[\alpha]_D$; B) time (in hours).

Change in specific optical rotation $[\alpha]_D$ of thermally treated rosin. The change in the optical rotation of the rosin in relation to the temperature and

time of its thermal treatment is shown in Fig. 2. It can be seen from this figure that in the initial stage of heating in all of the experiments there was a change in specific rotation from +1.2° in the negative direction, which reached its maximum value in approximately 15 minutes after establishment of the assigned temperature in all cases. This phenomenon can be explained by the fact that the palustric acid ($[\alpha]_D + 71.4^\circ$) and neoabietic acid ($[\alpha]_D + 175^\circ$) present in the rosin are isomerized to abietic acid. The rate of isomerization of these acids increases with a rise in temperature. In addition to the isomerization of the resin acids there occurs a disproportionation of hydrogen in the molecules of abietic acid, as a result of which the mixed dehydro-, dihydro- and tetrahydroabietic acid content ($[\alpha]_D = 56.2^\circ$) of the acid fraction of the rosin increases. The amount of these acids increases especially sharply at high temperatures. Thus, while the maximum negative specific rotation of rosin thermally treated at 225° was -26.2° , at 300° it was -5.9° .

The comparatively small amount of disproportionated resin acids in the rosin that had been subjected to thermal treatment at 225° and 250° for 8 hours is indicated by the maintenance of the negative specific rotation of the product, which was -21.7° and -8.2° , respectively.

Upon thermal treatment of the rosin at 275° and 300°, the specific rotation again shifted in the positive direction. While such a shift took place at 275° in 2 hours after the start of the reaction, at 300° a similar result was observed in 30 minutes. After 8 hours heating the specific rotation of the rosin was $+30.6^\circ$ and $+50.1^\circ$, respectively.

In the latter case, it was close to the specific rotation of the mixture of dehydro-, dihydro-, and tetrahydroabietic acids, which also indicates almost complete disproportionation of the abietic acid. It is interesting to note the similar character of the curves shown in Figs. 1 and 2. This shows the close connection existing between the dehydro-, dihydro-, and tetrahydroabietic acid content of the rosin and the increase in its specific rotation.

Thus, when rosin is heated the isomerization and disproportionation processes proceed simultaneously. But at 225-250° the isomerization of the palustric and neoabietic acids to abietic acid predominates, while at 275-300° the disproportionation of abietic acid to a mixture of dehydro-, dihydro-, and tetrahydroabietic acids predominates.

Change in acid number of thermally treated rosin. In Fig. 3 are shown the curves for the change in acid numbers in relation to the temperature and time of heating rosin. In Fig. 4 are shown the curves for the change in resin acid content in the rosin in relation to the same factors. At 225° the acid number of the rosin gradually decreased in 8 hours from 168 to 161. At 250°, in turn, in the same time the acid number of the rosin decreased to 150, and at 300° the acid number decreased in 15 minutes to 151, and at the end of the experiment, it was 116. In addition to the other causes, the lowering of the acid number of thermally treated rosin is also dependent on the decarboxylation of the resin acids, the rate of which increases with a rise in temperature.

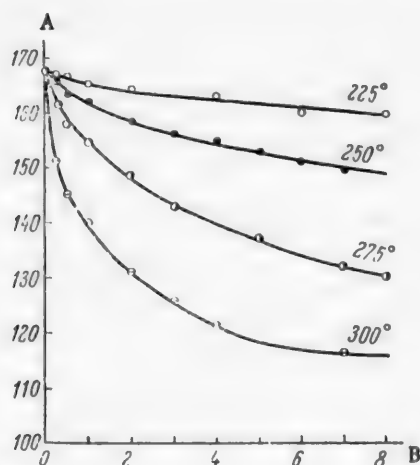


Fig. 3. Acid number of rosin in relation to temperature and time of thermal treatment. A) Acid number of rosin; B) time (in hours).

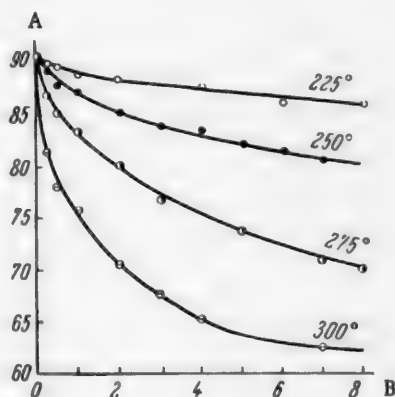


Fig. 4. Resin acid content of rosin in relation to temperature and time of thermal treatment. A) Resin acid content (in %); B) time (in hours).

However, the decrease in the acid number of the rosin slows down as its content of dehydro-, dihydro-, and tetrahydroabietic acids, which are stable to the action of heat, increases. The results obtained by us are in full agreement with the data of Dupont [14], who heated rosin in a current of nitrogen at 250°. The starting rosin had an acid number of 175 and $[\alpha]_D^{25} = -25^\circ$. These physical constants changed in 9, 17, 32, and 80 hours to 171, 170, 158, 145 and -6° , $+10^\circ$, $+32^\circ$, $+57^\circ$, respectively. For the neutral oils $[\alpha]_D^{25}$ was $+72^\circ$. Such a change in the physical constants of thermally treated rosin is explained by Dupont by the fact that all the resin acids with the exception of dextro- and isodextro-pimaric acids are gradually converted into a mixture of dehydro- and dihydroabietic acids.

Spectrophotometric investigation of processes occurring during thermal treatment of rosin and abietic acid. In Fig. 5 the ultraviolet absorption spectra are presented for the starting rosin and the resin acids of the rosin after 6 hours heating at 300°. Judging by the UV absorption maxima at 241, 250, and 266 m μ , the starting rosin contained considerable abietic acid and also neoabietic and palustric acids. In the acid fraction of the thermally treated rosin the amount of abietic acid had decreased to approximately one-third and the neoabietic and palustric acid content had decreased to a still greater extent. Simultaneously, there was a considerable increase in the amount of dehydro-, dihydro-, and tetrahydroabietic acids, which have a weak absorption in the ultraviolet part of the spectrum (Fig. 5, curve 2).

This process is observed particularly clearly upon thermal treatment of pure abietic acid. Thus, after 7 hours heating at 300°, the amount of it in the reaction products is decreased to approximately 15% (Fig. 6). At the same time, the amount of dehydroabietic acid increases greatly, as is clearly shown by the UV absorption maxima at 268 and 276 mμ. There also is an increase in the content of dihydro- and tetrahydroabietic acids, which have no characteristic UV absorption in this region.

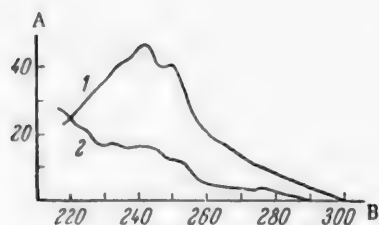


Fig. 5. Ultraviolet absorption spectra. A) Coefficient of specific rotation; B) wavelength of light (mμ). 1 and 2) Absorption spectra of rosin and of acid fraction of rosin after 6 hours heating at 300°, respectively.

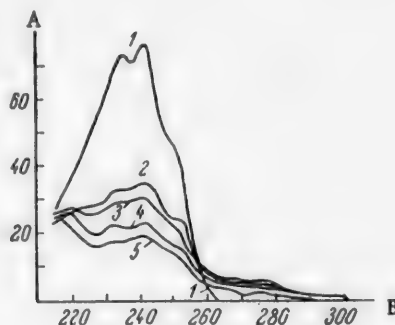


Fig. 6. Ultraviolet absorption spectra. A) Coefficient of specific rotation; B) wavelength of light (mμ). Absorption spectra of abietic acid after heating at 300° for indicated time (in hours): 1) without heating; 2) 2; 3) 3; 4) 6; 5) 7.

The characteristics of UV curve 2 (Fig. 5) and curve 5 (Fig. 6) are almost identical, since dextro- and isodextro-pimaric acids, which are present in the rosin, also have no characteristic UV absorption bands in this wavelength region.

SUMMARY

1. The dehydro-, dihydro-, and tetrahydroabietic acid content of the acid fraction of rosin has been determined in relation to the time of heating at 225-300°.

It has been shown that heating rosin at 225-250° basically causes the isomerization of palustic and neoabietic acids to abietic acid, while heating to 275-300° causes the disproportionation of abietic acid to a mixture of dehydro-, dihydro-, and tetrahydroabietic acids.

2. The isomerization and disproportionation processes in rosin are accompanied by decarboxylation of the resin acids, which causes a decrease in the acid number of the product obtained. The decrease in the acid number is slowed down as the dehydro-, dihydro-, and tetrahydroabietic acid content of the product increases.

LITERATURE CITED

- [1] L. Fieser and M. Fieser, *Chemistry of Natural Compounds of the Phenanthrene Series* (Russian translation) (State Chem. Press, Moscow-Leningrad, 1953).
- [2] V. M. Loeblich, D. E. Baldwin, R. T. O'Connor, and R. V. Lawrence, *J. Amer. Chem. Soc.* 77, 6311 (1955).
- [3] B. V. Erofeev and S. F. Naumova, *Coll. Sci. Works Inst. Chem. Acad. Sci. Belorusskaya SSR* 5 (1955).
- [4] A. G. Sokolov and I. I. Bardyshev, *Gidroliz, 1 Lesokhim. Prom.* 2, 5 (1958).

- [5] G. C. Harris and T. F. Sanderson, J. Amer. Chem. Soc. 70, 334 (1948).
- [6] V. M. Loeblich and R. V. Lawrence, J. Amer. Chem. Soc. 79, 1497 (1957).
- [7] V. N. Krestinskiĭ, N. I. Persiantseva, and A. A. Novak, Zhur. Priklad. Khim. 12, 9, 1407 (1939).
- [8] E. E. Fleck and S. Palkin, J. Amer. Chem. Soc. 61, 247 (1939).
- [9] J. S. Stinson and R. V. Lawrence, Ind. Eng. Chem. 46, 784 (1954).
- [10] P. O. Jalava, Paperi ja Puu 3, 69 (1954).
- [11] K. Bauer, Analysis of Organic Compounds (Russian translation), (IL, Moscow, 1953).
- [12] E. E. Fleck and S. Palkin, J. Amer. Chem. Soc. 59, 1593 (1937).
- [13] N. F. Komshilov, Composition of Rosin and Structure of Resin Acids of Pine and Fir [In Russian] Izd. AN SSSR (Moscow-Leningrad, 1955).
- [14] G. Dupont, Bull. Soc. Chim. France 1 (1958).

Received March 19, 1959

PREPARATION OF DIVINYLBENZENE BY CATALYTIC DEHYDROGENATION OF DIETHYLBENZENE*

A. A. Balandin, N. I. Shuikin, G. M. Marukyan, I. I. Brusov,
R. G. Seimovich, T. K. Lavrovskaya, and V. K. Mikhailovskii

Divinylbenzene, like styrene, is capable of polymerization and copolymerization reactions and has great possibilities for technical use. At the present time divinylbenzene is required in considerable quantities for the ion-exchange resin industry and for other purposes.

It has been shown by the research of Losev et al. [1] and Trostyanskaya [2] that divinylbenzene with styrene yields high-quality cationic and anionic materials of the type of SDV-1, SDV-2, SDV, KMD, and others. In the literature, it is pointed out [3] that resins having different degrees of swelling and porosity can be obtained by changing the divinylbenzene content of the copolymer, for which technical divinylbenzene is used containing 40-45% isomers of divinylbenzene (mainly *m*-divinylbenzene) and the remainder ethylstyrene and diethylbenzenes. If we take into consideration that the ion-exchange materials are finding greater and greater use in industrial practice, it is clear that the development of a method of producing divinylbenzene has important industrial significance. Diethylbenzene, which is obtained in the USSR in a number of plants in large quantities as a by-product in the alkylation of benzene, is not yet widely used.

Divinylbenzene can be used not only in the production of resinous sulfocation exchange sorbents, but also in the production of organic glass, in the plastics industry, in the cable industry, and in others. There is an indication that the use of 25-30% divinylbenzene with styrene decreases the fragility of articles formed from polystyrene resins. Divinylbenzene polymer is a high-frequency dielectric, as shown by Hippel and Wesson [5]. A mixture of divinylbenzene isomers is already used on an industrial scale for the preparation of plastics [4]. Goggin and Boyer [6] also have pointed out the properties of a polymer of the three isomers of divinylbenzene as a good dielectric. Divinylbenzene also gives a heat-stable polymer. There is an indication that divinylbenzene is finding increasing use in various industrial processes and is produced by the dehydrogenation of diethylbenzene [7].

The data presented constitute an additional argument for the practical value of the divinylbenzenes. In the literature there are very few data on the catalytic dehydrogenation of diethylbenzene to divinylbenzene. Hopff and Ohlinger [8] prepared divinylbenzene from diethylbenzene at 600-610° on the catalyst of the composition 50% ZnO, 40% Al(OH)₃, and 10% CaO, with a 40% total yield of unsaturated material. On checking, these data proved not to be reproducible. Catalytic dehydrogenation of diethylbenzene to divinylbenzene with a yield of up to 45% total unsaturation was accomplished by several authors of the present communication [9] on a copper-chromium catalyst in the presence of carbon dioxide as a diluent. In later work [10, 11] it was shown that divinylbenzene and ethylstyrene are obtained by catalytic dehydrogenation of diethylbenzene.

We have prepared and investigated catalysts that have proved to be very active for the dehydrogenation of diethylbenzene. The activity of these catalysts was tested in laboratory ovens and in a specially built large apparatus for dehydrogenation in a circulating system. From the divinylbenzene produced in our apparatus, various organizations have synthesized ion-exchange resins SDV, KMD, SDV-2, SDV-3, and others, which were of high quality.

* The authors express their thanks to I. I. Levitskii, who participated in the first part of the work.

A technological system was worked out, and catalysts and a process for the preparation of divinylbenzene were proposed for the catalytic synthesis of divinylbenzene on an industrial scale. Two semiindustrial set-ups have already been constructed from our data for the synthesis of divinylbenzene, which have been operating since 1957 and yielding 30% or more divinylbenzene in the catalyzate.

EXPERIMENTAL

As the starting material for the preparation of divinylbenzene, a broad fraction of diethylbenzene was used, which boiled in the range 178-185° and had the constants n_D^{20} 1.4960 and d_4^{20} 0.8668. The boiling points of the isomeric diethylbenzenes are very close together and their separation on an ordinary laboratory column is difficult; therefore, we used for the dehydrogenation the indicated broad fraction with the idea that in the catalyzate we would obtain a mixture of the three isomeric divinylbenzenes. To determine the quantitative ratio of the isomeric diethylbenzenes, the 178-185° fraction was oxidized with an alkaline solution of permanganate under the conditions described by Moldavskii [12] and Maslyanskii [13]. The results of the oxidation showed that the fraction of diethylbenzene boiling in the range 178-185° consists of a mixture of all three isomeric diethylbenzenes of the following composition: 1,2-diethylbenzene 11.1%, 1,3-diethylbenzene 48.5%, and 1,4-diethylbenzene 40.4%. Thus, 1,3-diethylbenzene appeared to the greatest extent in this fraction; obviously in the catalyzate we should have mostly 1,3-divinylbenzene. As regards 1,2-divinylbenzene, it is indicated in the literature that it dehydrocyclizes to naphthalene [8].

The dehydrogenation was carried out in the usual contact laboratory electric furnaces of the circulating type, such as had been previously used [14, 15], in the presence of water vapor. The ratio of dilution (diethylbenzene : water) was from 1:2 to 1:4. The concentration of unsaturated compounds in the catalyzate was determined bromometrically by the method of Rosenmund [15], by the nitrosite method [7], and by the curve for the index of refraction [8]. The composition of the exit gas was determined chromatographically [16]. For

TABLE 1

Results of Tests of Catalyst A in Laboratory Apparatus. Volume of catalyst 400 ml, ratio of diethylbenzene : water 1:4, rate of introduction of diethylbenzene 0.2-0.25 hour⁻¹.

Expt. No.	Temperature (in deg C)	Duration of Expt. (in hrs)	n_D^{20} of Catalyzate	Yield of Catalyzate (in wt-%)	Unsaturated Content of Catalyzate (in wt-%)			Yield Based on Diethylbenzene Passed Through (in wt-%)			Yield of Total Unsaturation Based on Diethylbenzene Broken Down (in wt-%)
					Divinylbenzene	Ethylstyrene	Total Unsaturation	Divinylbenzene	Ethylstyrene	Total Unsaturation	
1	605-610	10	1.5270	89.6	18.0	42.0	60.0	16.4	38.0	54.4	84.4
2	600-615	5	1.5345	88.5	22.5	49.0	71.5	20.5	44.2	64.7	81.4
3	603-610	16	1.5305	89.0	19.0	42.0	61.0	17.4	37.6	55.0	89.0
4	608-610	4	1.5255	88.8	17.0	40.0	57.0	—	—	50.8	81.5
5*	595-610	4	1.5328	80.0	25.5	41.0	66.5	21.5	33.0	54.5	79.6
6	600-610	13	1.5330	88.0	25.5	41.0	66.5	23.1	36.3	59.4	84.2
7	610-620	9	1.5365	95.1	28.0	44.0	72.0	27.4	42.2	69.6	94.9
8	607-610	4	1.5368	89.6	28.0	42.0	70.0	25.8	38.0	63.8	87.1
9	610-620	19	1.5365	91.0	25.5	41.0	66.5	22.8	36.1	58.9	82.8
10	600-617	5	1.5278	91.2	17.0	46.0	63.0	15.9	42.6	58.5	88.2
11	620-628	4	1.5215	90.5	12.5	43.0	55.5	11.8	40.6	52.4	88.1
12*	605-610	5	1.5358	77.5	25.0	48.0	73.0	20.0	37.8	59.0	72.7
13	610-620	12	1.5340	82.2	25.0	40.0	65.0	21.4	33.0	54.4	76.7
14	602-612	4	1.5288	—	18.0	41.0	59.0	—	—	—	—
15*	600-620	5	1.5333	—	25.0	40.0	65.0	—	—	—	—
16	603-617	13	1.5345	90.6	25.0	42.0	67.0	22.2	36.7	58.9	82.0
17	614-624	10	1.5385	99.7	28.0	45.0	73.0	26.1	41.4	67.5	89.2

* After regeneration.

the dehydrogenation of the diethylbenzene, we used catalysts A and B. The experiments were carried out at temperatures of 600-630°. Regeneration by air oxidation completely restored the former activity of the catalyst. The rate of introduction of the diethylbenzene was 0.20-0.25 hour⁻¹. The yields of catalyzates were 88-90% and higher with a total unsaturate content on the average of 65-75% and higher. In the catalyzate, there was up to 28% divinylbenzene and up to 58% ethylstyrene (Tables 1 and 2). The catalyzate was clear, with a slight yellowish color.

TABLE 2

Results of Tests of Catalyst B in Laboratory Apparatus. Volume of catalyst 400 ml, ratio of diethylbenzene : water 1:4

Expt. No.	Temperature (in deg C)	Duration of Expt. (in hrs)	Rate of Introduction of Diethylbenzene (hr ⁻¹)	n _D of Catalyzate	Unsaturated Content of Catalyzate (in wt-%)		
					Divinylbenzene	Ethylstyrene	Total Unsaturation
1	620-630	3	0.20	1.5435	28.0	58.0	86.0
2	620-630	9	0.20	1.5405	26.0	45.0	75.0
3	625-630	3	0.15	1.5373	23.8	48.2	72.0
4	630	4	0.20	1.5340	25.5	39.0	64.5
5	625-630	4	0.15	1.5310	19.0	44.0	63.0
6	620-630	4	0.15	1.5322	23.2	38.2	61.4
7	617-622	4	0.15	1.5343	25.5	45.0	70.5
8	612-620	7	0.15	1.5323	23.0	40.0	63.0
9	620-630	5	0.15	1.5280	17.0	40.0	57.0
10*	625-630	4	0.15	1.5425	28.0	56.0	84.0
11	625-630	3	0.16	1.5409	26.0	55.0	81.0
12	620-627	3	0.15	1.5402	26.0	52.0	78.0
13	625-630	4	0.15	1.5430	28.0	54.0	82.0
14	625-630	8	0.20	1.5338	24.5	45.0	69.5
15	625-630	7	0.20	1.5337	24.0	42.0	66.0
16	620-627	5	0.15	1.5418	26.0	58.0	84.0
17	625-630	8	0.20	1.5351	24.5	45.0	69.5
18	624-626	8	0.16	1.5330	23.0	42.0	65.0

* After regeneration.

The data in Table 1 show that catalyst A gave high yields of divinylbenzene at 600-620°. In Table 1, only part of the experiments are presented. The catalyst operated for more than a year without losing its activity. The ratio of diethylbenzene and water was 1:4, since the power of the pump that was available did not permit decreasing this ratio. When laboratory furnaces were used, the ratio of diethylbenzene to water was 1:2.

TABLE 3

Analysis of Gaseous Products of Dehydrogenation of Diethylbenzene at Different Temperatures

Temperature (in deg C)	Content in Gas (in %)					
	H ₂	CO ₂	CH ₄	C ₂ H ₆	C ₂ H ₄	C ₃ H ₆
580	82.8	12.7	3.0	0.6	0.9	—
600	80.0	12.2	4.7	0.9	2.2	—
620	80.0	13.0	3.3	0.8	2.3	0.8

The data in Table 2 show that catalyst B was highly active. It gave good yields of divinylbenzene at 620-630° with a rate of feed of the diethylbenzene of 0.15-0.20 hour⁻¹. The total unsaturation of the catalyzate was also very high.

The catalysts were mechanically durable and after operating for a year they preserved their former activity and form (pellets). The catalysts developed, which were tested in the laboratory furnaces, were checked in a special dehydrogenation set-up. The diethylbenzene and water were fed simultaneously at the given rate by means of pumps from a buret into the vaporizer, where the temperature was maintained at approximately 300°, then from the vaporizer

into the superheater at a temperature of 600-630° and into the reactor with the catalyst, heated to the temperature of the experiment. From there, the catalyzate, after cooling in a condenser, entered the receiver, and the exit

gas entered the gas outlet. The temperature of the reactor, vaporizer, and superheater was measured with a thermocouple and regulated by an electronic thermoregulator. The catalyst was not activated before the experiment. The temperature in the reactor was raised to the necessary level in 1-1.5 hours, after which the mixture of diethylbenzene and water was introduced. Testing of catalysts A and B in the large apparatus gave good results (Tables 1 and 2). The content of unsaturated and saturated materials in the gas is shown in Table 3. The data in Table 3 show the relationship of the rupture of the side chain to the temperature of the experiment. The catalyzate of diethylbenzene (without isolation of the divinylbenzene) was used for the preparation of ion-exchange resins, membranes, and for other purposes.

SUMMARY

1. Highly active, easily regenerated catalysts have been developed for the catalytic dehydrogenation of diethylbenzene to divinylbenzene.

2. A large laboratory apparatus has been constructed for the dehydrogenation of diethylbenzene and the optimum conditions have been established for the dehydrogenation temperature 600-630°, rate of introduction of diethylbenzene 0.20-0.25 hour⁻¹. The ratio of diethylbenzene to water was 1:2 and 1:4. Under these conditions the concentration of divinylbenzene in the catalyzate varied within the limits 20-28% with a total unsaturation content of 65-80%.

LITERATURE CITED

- [1] P. Losev, A. S. Tevlina, and E. B. Trostyanskaya, Coll., Theory and Practice of the Use of Ion-Exchange Sorbents, Izd. Akad. Nauk SSSR 35 (1955).
- [2] E. B. Trostyanskaya, Trudy Komissii Anal. Khim. 6, 216 (1955).
- [3] Chemistry and Technology of Polymers, Sb. Per. Inostr. Lit. 3, 106 (1957).
- [4] Rev. der mat. plast. 15, 12, 333 (1939).
- [5] A. Hippel and L. G. Wesson, Ind. Eng. Chem. 38, 1121 (1946).
- [6] W. S. Goggin and R. F. Boyer, Ind. Eng. Chem. 38, 1090 (1946).
- [7] R. P. Marquardt and E. Luce, Anal. Chem. 23, 4, 629 (1951).
- [8] H. Hopff and H. Ohlinger, Ber. 76, 1250 (1943).
- [9] A. A. Balandin and G. M. Marukin, Doklady Akad. Nauk SSSR 55, 3, 219 (1947).
- [10] R. P. Marquardt and E. N. Luce, Anal. Chem. 20, 751 (1948).
- [11] Boundy-Boyer, Styrene, Its Polymers, Copolymers and Derivatives (Reinhold Publishing Corp., New York, 1952).
- [12] B. L. Moldavskii, G. D. Kamusher, and M. B. Kobylskaya, Zhur. Obshchei Khim., 7, 169 (1937).
- [13] G. N. Maslyanskii and T. S. Berlin, Zhur. Obshchei Khim. 16, 1643 (1943).
- [14] A. A. Balandin, N. D. Zelinskii, G. M. Marukyan, and O. K. Bogdanova, Zhur. Priklad. Khim. 14, 161 (1941).
- [15] R. W. Rosenmund and W. Kuhnenn, Z. Untersuchung der Nahrung u. Genussmittel 46, 154 (1923).
- [16] H. Hrapia and H. G. Kōnnecke, J. pr. Chem. (4), 3, 106 (1956).

Received December 16, 1958

BRIEF COMMUNICATIONS

GROWTH OF GERMANIUM MONOCRYSTALS FROM UNDER MELTS OF SALTS AND OXIDES

V. N. Maslov, Yu. V. Granovskii, and V. D. Samygin

In recent years there have been descriptions in the literature of attempts to use salt melts for protecting molten germanium from contamination and for the purification of prepared monocrystals. Encouraging results were obtained in the extraction of copper from germanium with molten potassium cyanide. Treatment of monocrystalline plates, $20 \times 10 \times 2$ mm, for two hours increased their specific resistance from $2-3 \Omega \cdot \text{cm}$ to 3 to $5 \Omega \cdot \text{cm}$ [1]. It has also been stated that melts of some salts can prevent contamination of the metal with impurities from the atmosphere and the material of the crucible [2, 3]. Borates, phosphates, and cyanides of chemically pure grade have been recommended for this purpose as salts which do not react with molten germanium and have a comparatively low melting point. Indirect evidence of the possibility of introducing impurities into the metal from the salt melts used is provided by data on the electrochemical preparation of germanium [4]. The purest germanium (99.8%) is obtained from an electrolyte bath based on sodium digermanate and fluoride, while electrolysis of germanium oxide with borates added makes it possible to reach 89.5-99.6% purity. It is not clear, however, to what extent the contamination of the metal is caused by physicochemical interaction with the components of the salt melt as compared with the cathode process, leading to simultaneous reduction of the impurities.

The purpose of our experiments was to establish the possibility of growing germanium monocrystals from under molten salts and oxides and also to investigate the properties of prepared monocrystalline plates of germanium, treated with various melts.

Monocrystalline plates, $10 \times 4 \times 1.5$ mm, were treated in vacuum in a quartz tube placed in a muffle furnace. Samples, first pickled in 30% $\text{M H}_2\text{O}_2$ solution and washed with doubly distilled water, were placed in graphite crucibles together with a portion of chemically pure grade salt. Two to three samples were treated in parallel. In addition, in order to determine the role of thermal treatment, we simultaneously fired germanium plates at the same temperatures and under the same conditions. These control samples were sealed in quartz ampoules. The duration of the thermal treatment in the salts was the same in each case, namely, 2 hours. Table 1 gives data on the change in electrophysical properties of germanium plates.

Many salts interact with germanium. Treatment with MnSO_4 at 900° and with a mixture of 50% MgCl_2 + 50% MgSO_4 at 750° led to almost complete corrosion of the plate investigated. Boric oxide, B_2O_3 , also reacted appreciably with germanium at temperatures above 700° , liberating gaseous products. At 800° K_2WO_4 became blue at places in contact with germanium and CuO was partially reduced at 700° . A comparison of the data in Table 1 with the results of thermal treatment indicated that all the salt systems tested, with the exception of a $\text{CuCl} + \text{KCl}$ mixture, regardless of the treatment temperature, reduced the specific resistance ρ . As regards changes in the diffusion length of minority current carriers L , it was not possible to distinguish clearly between the effect of thermal treatment and of the salts themselves.

Monocrystals were drawn from under salt melts in a P-17 furnace from graphite crucibles. The crucibles had double walls to avoid spattering of the salts; the salt was fused before the metal was added. KCl , H_3BO_3 , and mixtures of them were used for the work. During repeated fusions of one portion of metal under a layer of B_2O_3 without the ends of the monocrystals obtained being cut off, there was a change in the type of conductivity from \bar{p} to \bar{n} , beginning from the lower end of the bars. Compensation occurred quite vigorously and led to a rise in specific resistance to $15-20 \Omega \cdot \text{cm}$ with an initial value equal to $0.1-0.3 \Omega \cdot \text{cm}$ if the salt melt covered

the metal surface completely. Otherwise, there was reversion to the p-type and the formation of a metal of a mixed type of conductivity. The diffusion length of minority current carriers was kept at the level of 0.1-0.5 mm with starting material of the same quality and fell to this value with higher starting parameters.

TABLE 1

Change in the Electrophysical Properties of Germanium Plates* Treated with Molten Salts

Expt. No.	Specific resistance ($\Omega \cdot \text{cm}$)	Diffusion Length L (in mm)	Type of Conductivity	Composition of melt (in mol. %)	Melting point of melt (in $^{\circ}\text{C}$)	Treatment temperature (in $^{\circ}\text{C}$)	Remarks
1 {	15(a) 20(b)	1.3 0.7	p { p {	CuCl — 67.5 KCl — 32.5	136	270	Copper deposited on germanium
2 {	26(a) 0.8(b)	1.3 0.3	p { p {	B_2O_3	580	600	Sample disintegrated on cooling
3 {	20(a) 13.3(b)	1.4 —	p { p {	MgSO_4 — 44 Na_2SO_4 — 56	670	750	Germanium reacted partially
4 {	22.0(a) 0.72(b)	2.0 0.15	p { n {	MgCl_2	718	800	
5 {	18.1(a) 0.33(b)	2.4 —	p { n {	KCl	790	800	
6 {	19.0(a) 0.8(b)	1.1 —	p { n {	BaCl_2	976	990	Germanium melted and formed polycrystals on cooling

* (a) — before experiment, (b) — after experiment.

TABLE 2

Change in Specific Resistance of p-Type Seed Crystals in the Drawing of Germanium Monocrystals from Under a B_2O_3 Melt

Seed No.	Original specific resistance ρ_{orig} ($\Omega \cdot \text{cm}$) along crystal	Specific resistance after experiment ρ_{exp} ($\Omega \cdot \text{cm}$) along crystal	Remarks
1 {	28 36 41 43 40	10.6 0.5 2.2 1.6 —	p-type of the seed was unchanged. Part of the seed with $\rho_{\text{exp}} = 10.6 \Omega \cdot \text{cm}$ was hidden in the holder
2 {	44 44 35 29	8.5 7.6 2.7 2.5	p-type of the seed was unchanged. Part of the seed with $\rho_{\text{exp}} = 7.6$ and $8.5 \Omega \cdot \text{cm}$ was hidden in the holder

It was confirmed that there is transfer of p-type impurities from the vapor phase into the metal by the change in the specific resistance of the seed crystals. The results of the measurements are given in Table 2.

Investigation of monocrystals obtained from under B_2O_3 and differing in the type of conductivity showed that the n-type region was always inside the bar, while the p-type sections were mainly at the surface. Figure 1 shows a photograph of a longitudinal section of such a monocrystal, etched electrolytically to show the regions with different conductivities.



Fig. 1. Etched surface of a longitudinal section of a germanium monocrystal. Light sections — n-type, dark sections — p-type

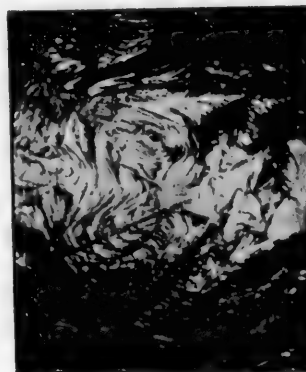


Fig. 2. Section of the end surface of a monocrystal after spontaneous cleaving.

Monocrystals obtained from under KCl or a mixture of 50% B_2O_3 + 50% KCl had a tendency to change to n-type with starting material of p-type. With the use of material of n-type with $\rho = 10^{-3} \Omega \cdot \text{cm}$ and a diffusion length of minority current carriers that could not be measured, it was possible to obtain from under KCl monocrystals of the same type of conductivity with $\rho = 0.01-0.1 \Omega \cdot \text{cm}$ and a diffusion length of 0.1 mm.

In work with a mixture of B_2O_3 + KCl and a high ohmic starting material, there was a considerably lower fall in L than when B_2O_3 was used under the same conditions. The presence of KCl in other mixtures also had a positive effect. The discrepancy between data on the growth of monocrystals and the results of treating prepared plates is apparently explained by the difference in the thermal conditions and the possibility of redistribution of impurities along the bar during its drawing.

Vacuum drawing without salts of monocrystals obtained from under a mixture of 50% KCl + 50% NaCl sometimes led to exceptionally good results. Thus, the first draw of an n-type metal for which L was not measured and $\rho = 0.1 \Omega \cdot \text{cm}$ gave monocrystals of the same type of conductivity with $L = 0.5-0.8 \text{ mm}$ and $\rho = 25$ to $40 \Omega \cdot \text{cm}$. It is possible that by exchange the salts were able to change the nature of the impurities in the germanium and thus influence the efficiency of the subsequent crystallophysical purification.

The seeding on monocrystals from under salt melts did not usually present particular difficulties, though the salt layer was not completely clear. The moment of seeding could be determined from the increase in brightness of the light emitted by the seed.

The molten salt phase enveloped and collected slag and graphite particles floating on the metal surface. The germanium mirror was found to be free from possible crystallization nuclei and polycrystals could only be obtained by considerable disruption of the thermal conditions of drawing.

With strong supercooling of the melt it was possible to observe the growth of single nuclei under the B_2O_3 layer, leading to the formation of right tetragonal and rhombic crystals 1-2 cm in size.

The salt film on the molten metal in the growing monocrystal was capable of protecting the metal from oxidation to an appreciable extent. Monocrystals obtained in a vacuum of 0.1 mm Hg did not show even traces of oxide films. It should be noted that B_2O_3 and some mixtures based on it wetted germanium readily and during crystallization, produced deformation and disruption of the adjoining surface layer of the germanium. This indicates that the forces acting were sufficient to produce interesting structural changes in the monocrystal. The end section after spontaneous cleavage shown in Fig. 2 is reminiscent of hoarfrost figures.

SUMMARY

1. The possibility of growing germanium monocrystals with a specific resistance of up to $10-15 \Omega \cdot \text{cm}$ and a minority carrier diffusion length up to 0.5 mm from under salt melts based on B_2O_3 and KCl of chemically pure and analytical grades was demonstrated.

2. It was established that a molten salt phase may suppress the action of foreign crystallization nuclei and partly protect the molten germanium and also the growing crystal from oxidation.

LITERATURE CITED

- [1] Pei Wang, J. Phys. Chem. 60, 1, 45-48 (1956).
- [2] P. L. Günther, Fed. German Rep. Patent 905,069, 25 II (1954).
- [3] G. Rosenberger, Fed. German Rep. Patent 826,775, 3, VI (1952).
- [4] J. four. electr. et inds. electrochim. 65, 4, 131 (1956); Referat. Zhur. Khim. 7, 23859 (1957).

Received August 6, 1958

DETERMINATION OF COPPER AND IRON IMPURITIES IN ARSENIC BY MEANS OF ION EXCHANGE

L. N. Rozanova and G. A. Kataev

V. V. Kulbyshev State University, Tomsk

The determination of impurities in metallic arsenic has acquired great practical interest in connection with the fact that arsenic is a suitable substance for the preparation (and alloying) of a number of semiconductor materials, for which there are rigid requirements as regards purity. Moreover, the literature contains no analysis methods for microimpurities in metallic arsenic.

The principle of the method proposed in the present work for the determination of copper and iron in arsenic consists of the following. Arsenic (As^{5+}), present in solution as arsenic acid after the sample has been dissolved, is separated from the other impurity ions by filtration through a cation-exchange resin. The copper and iron are washed out of the column with an eluent and determined in solution polarographically. Copper (Cu^{2+}) and iron (Fe^{3+}) may be determined in each other's presence in a base electrolyte of a 0.5 M solution of potassium

sodium tartrate and 0.5 M ammonia solution. In this base electrolyte copper (Cu^{2+}) gives two waves with half-wave potentials $\varphi_{1/2} = -0.38$ v and $\varphi_{1/2} = -0.54$ v (relative to a saturated calomel electrode). Iron also gives two waves with $\varphi_{1/2} = -1.44$ v and $\varphi_{1/2} = -1.62$ v (relative to a saturated calomel electrode). The value of $\varphi_{1/2}$ of the first iron wave depends on the amount of gelatin added and may be displaced to $\varphi_{1/2}$ of the second wave. Thus, with a sufficient amount of gelatin (in the absence of chloride ion) the iron ion (Fe^{3+}) gives only one wave with $\varphi_{1/2} = -1.62$ v, equal to the sum of the two waves (formed with insufficient gelatin).

The copper wave decreases with the addition of gelatin. One drop of phenolphthalein added to the solution improves the copper wave, making it sharper and more reproducible. The base electrolyte was prepared by first adding a measured volume of potassium sodium tartrate solution to a flask with the solution investigated, then adding ammonia solution, and diluting the solution to the mark. When a mixture of potassium sodium tartrate and ammonia solutions was added to the solution investigated directly, the iron partially precipitated as the hydroxide and could not be determined.

After the solution has been prepared, it was poured into a beaker for polarography and the two copper waves plotted (from -0.2 to -0.8 v), then 5 drops of a 0.5% gelatin solution added (to 25 ml of solution) and the iron determined (from -1.2 to -1.8 v). The copper was best determined from the second wave and the iron as indicated above. The wave height was directly proportional to concentration. A calibration curve was used for the calculation.

We previously found conditions for separating arsenic from impurities by means of a KU-2 cationite in the hydrogen form. They were used here for analysis purposes.

For quantitative determination of copper and iron, present in arsenic in microamounts (thousandths of a percent), it was necessary to choose an eluent which could simultaneously serve as the base electrolyte for polarography. The eluent we used was a solution of potassium sodium tartrate (1 M) to which ammonia solution (2 M) was added. To check the possibility of a complete separation of copper and iron from arsenic and their quantitative elution with this eluent, we carried out the experiments whose results are given in Table 1.

TABLE 1

Data on the Determination of Microamounts of Copper and Iron in Arsenic

Copper (in mg)		Iron (in mg)	
intro- duced	detected	intro- duced	detected
0.22	0.21	0.66	0.66
0.37	0.36	0.99	1.00
0.74	0.72	1.32	1.50
1.62	1.60		
2.07	2.08	2.11	2.32
2.21	2.28	2.38	2.36

TABLE 2

Results of Analyzing Arsenic for Copper and Iron

Expt. No.	Detected (in mg)		Content in arsenic (in %)	
	copper	iron	copper	iron
1	0.20	1.50	0.0088	0.092
2 a	0.79	6.44	0.0080	0.109
2 b	0.46	5.26	0.0087	0.099

Note: A PV-5 polarograph was used for the work.

Into an arsenic acid solution, which did not contain copper or iron (analysis), were introduced definite amounts of copper and iron. The pH of the solution was then adjusted to 1.5 and the solution passed through a column of KU-2 cationite in the hydrogen form (column diameter, 1 cm, bed height, 6-7 cm). The impurities were eluted with potassium sodium tartrate solution (12.5 ml, 1 M), to which was added 1 ml of 2 M ammonia solution to prevent precipitation of tartaric acid in the column, then the column was washed with a further 6 ml of 2 M ammonia solution and finally with water. All the wash solutions were collected in a 25 ml graduated flask to which was added one drop of phenolphthalein. The solution was diluted to the mark, mixed, and polarographed as described above.

As follows from Table 1, the completeness of the separation of copper and iron from arsenic (V) on the cationite was satisfactory.

The method developed was applied to the determination of impurities in technological arsenic.

A sample of arsenic (2-5 g) was dissolved in hot, concentrated nitric acid (sp. g. 1.4), the solution evaporated, and hydrochloric acid added until the residue dissolved. The solution was evaporated to as small a volume as possible and diluted with water to pH = 1.5 (until methyl violet added to the solution had a blue color).

The solution obtained was passed through a column at a rate of 0.5 - 1.0 ml/min. The column was washed with 50 ml of water to remove residual acid. The adsorbed impurities were first eluted with potassium sodium tartrate solution and then ammonia, as described above, into a 25 ml graduated flask. The copper in the solution obtained was determined polarographically with a sensitivity of 1/200 and the iron with a sensitivity of 1/500 by means of calibration curves.

Table 2 gives data on the analysis of arsenic for copper and iron.

In Experiment No. 1, 40 ml of solution prepared from 2.2906 g of metallic arsenic was passed through the column.

In Experiment No. 2, 100 ml of solution was prepared from 10.589 g of arsenic and was divided into two equal portions of 50 ml each. To one beaker (Experiment No. 2a) was added 0.369 mg of copper and 0.66 mg of iron (in the form of salt solutions).

The solution in the other beaker was passed through the column without any additions (Experiment No. 2b). As the data in Table 2 show, the reproducibility and accuracy of the analysis was satisfactory.

The method makes it possible to determine copper and iron in arsenic in thousandths of a percent with a galvanometer sensitivity of 1/200 on a sample of 2-5 g of arsenic.

SUMMARY

1. It was shown that iron may be determined polarographically in a base electrolyte of potassium sodium tartrate and ammonia.

2. A method was developed for determining copper and iron impurities in arsenic with the aid of a chromatographic separation.

NEW METHOD OF PREPARING MAGNESIUM SULFATE

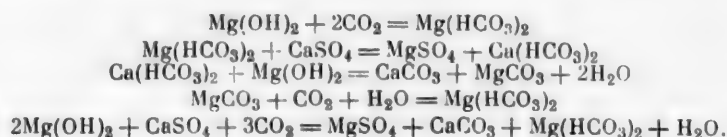
L. G. Berg, S. G. Ganelina, and É. F. Gubanov

In an investigation of solubility in the system of calcium and magnesium carbonates and sulfates, it was established that reactions forming calcium carbonate proceed quite readily, especially the reaction of magnesium carbonate trihydrate, $\text{MgCO}_3 \cdot 3\text{H}_2\text{O}$, with gypsum:



It seemed of definite interest to study the course of this reaction not with magnesium carbonate trihydrate, but with a more soluble salt such as the bicarbonate.

Since magnesium bicarbonate is a very unstable compound, its reaction with calcium sulfate was carried out at the moment of formation of the bicarbonate: carbon dioxide was passed into an aqueous suspension of crude, milled gypsum and magnesium hydroxide. The magnesium hydroxide was carbonated to magnesium bicarbonate, which reacted with calcium sulfate to form magnesium sulfate. The course of this process may be represented by the following equations:



It should be noted that there were no special investigations of the kinetics of this quite complex reaction, and the scheme presented may not cover certain details of the process.

Results of Experiments to Determine the Rate of MgSO_4 Formation

Ratio of MgO and CaSO_4	MgSO ₄ content of solution (in %)					
	after 1 hr		after 2 hrs		after 5 hrs	after 8 hrs
	25°	70°	25°	70°	25°	25°
1 : 1	4	—	4.5	—	5	11
1 : 2	3	—	4	—	4.5	6
2 : 1	4	4	5	4.5	6	15

* The passage of carbon dioxide for more than 8 hours led to an insignificant increase in the magnesium sulfate concentration in the solution.

The reaction vessel was a cylinder with a porous bottom (glass filter No. 1), through which carbon dioxide was bubbled. This design of reaction vessel seemed very advantageous to us as it produced the most vigorous mixing of the reagents and increased the contact surface of the gas with the solid phase, i.e., increased the reaction rate. After the carbon dioxide had been bubbled through, the filtrate was separated from the precipitate directly through the porous bottom. When bubbling was carried out in this way, the rate of magnesium sulfate formation increased when an excess pressure of carbon dioxide was established above the liquid.

In connection with the fact that an efficient method of firing dolomite to caustic dolomite has been developed in the Physical Chemistry Laboratory of the Kazakh Branch of the Academy of Sciences of the USSR for the production of dolomite cement [1], the production of a mixer for caustic dolomite (magnesium sulfate) is of great practical value.

Instead of magnesium oxide, caustic dolomite ($\text{MgO} \cdot \text{CaCO}_3$) can be used successfully for the production of magnesium sulfate. The use of dolomite lime ($\text{MgO} \cdot \text{CaO}$) is possible but undesirable since in this case the formation of magnesium sulfate is considerably retarded due to carbonation of the calcium hydroxide (simultaneously with the carbonation of magnesium hydroxide).

Gypsum, caustic dolomite, and water were taken in the following proportions (in weight %): gypsum 12, caustic dolomite 19, and water 69.

The reaction rate was determined as the rate of increase in the concentration of magnesium sulfate in the solution. It depended to a considerable extent on the weight ratio of the reaction components and the temperature (table).

The table shows that the optimal component ratio was $\text{MgO} : \text{CaSO}_4 = 2 : 1$. This is understandable since an increase in the hydroxide content of the mixture led to further solution of magnesium as magnesium bicarbonate, while an increase in the gypsum content did not change its concentration in solution due to its comparatively low solubility.

A reaction temperature of no higher than 30° was desirable as an increase in temperature reduced the solubility of carbon dioxide, i.e., decreased the reaction rate. Under these conditions, bubbling in carbon dioxide for not more than 8 hours led to a 15-16% solution of magnesium sulfate.

Experiments were also carried out in which the mixer used was not magnesium sulfate solution, but the unseparated final product of the reaction we described. The latter was a very liquid paste, consisting of a magnesium sulfate solution, unreacted magnesium hydroxide, and calcium carbonate obtained as a result of the reaction. Samples mixed with this paste had a compression strength of 60-70 kg/cm².

Investigation of the properties of dolomite cement carried out in our laboratory when the mixer used was 15-16% magnesium sulfate solution showed that the mechanical quality of this cement was as good as that of Portland cement of 200-300 grade.

Dolomite and gypsum are found in most regions of our country. It is evident that dolomite cement should find very wide application as a high-grade domestic building material.

Until now magnesium sulfate has been obtained either by solution of natural magnesite in sulfuric acid or from the natural brine of salt lakes, rich in magnesium sulfate. In the first case, the product obtained contains some impurities in the form of salts of calcium and other heavy metals (for example, iron), not to mention the fact that the sulfuric acid method of producing magnesium sulfate is quite dear. In the second case, the separation from alkali metal salts presents considerable difficulty; a second recrystallization is required in this case.

The method proposed for the preparation of magnesium sulfate is free from these two essential drawbacks of the old methods (cost and low purity of the product obtained); with a comparatively low expenditure it is possible to obtain a very pure product. In addition to magnesium sulfate, the filtrate was found to contain only magnesium bicarbonate and a small amount of gypsum (not more than tenths of a percent). The magnesium bicarbonate was removed simply by heating the solution and then filtering it free from the precipitated carbonate, while with excess magnesium hydroxide (as we recommend) gypsum did not remain in the solution at all. Evaporation of the filtrate yielded pure crystalline magnesium sulfate.

For the production of magnesium sulfate by the method proposed, instead of carbon dioxide it is possible to use gases containing it, for example, furnace gases containing up to 15% of carbon dioxide. If we consider that in the firing of dolomite to caustic dolomite, the emergent furnace gases contain up to 20% of CO₂, it would obviously be economical to combine the production of caustic dolomite and its mixer (magnesium sulfate) by the method proposed.

LITERATURE CITED

- [1] L. G. Berg and S. G. Ganelina, Caustic Dolomite [In Russian] (Tatar Book Press, 1957).

Received February 2, 1959

SPECTRAL ABSORPTION OF ALUMINOBOROSILICATE GLASSES COLORED WITH COBALT COMPOUNDS

A. A. Appen and Kan Fu-hsi

We previously investigated the alumino boron anomaly of some properties of silicate glasses [1]. The present work was designed to determine how the alumino-boron anomaly is reflected in the spectral absorption curves of glasses colored with cobalt.

As is known, melting and thermal treatment conditions have little effect on the coloring of glasses by cobalt, though the chemical composition of the glass is of great importance [2]. It may be considered that cobalt in the glass is an indicator which reflects a change in the glass structure. Therefore, a study of the spectral absorption of glasses colored with cobalt makes possible a better elucidation of the nature of the alumino-boron anomaly of the properties. The coloring of glass by cobalt compounds depends mainly on the coordination number of the Co^{2+} ion. It is considered that $[\text{CoO}_4]$ tetrahedra give glass a blue color. The coloring center $[\text{CoO}_4]$ forms a characteristic complex absorption maximum in the visible region of the spectrum over the range 580-680 $\text{m}\mu$. The glasses' pink color is caused by the formation of $[\text{CoO}_6]$ octahedra and is characterized by an absorption maximum in the range 540-560 $\text{m}\mu$ [3]. The intensity of the blue color centers is much stronger than that of the pink ones.

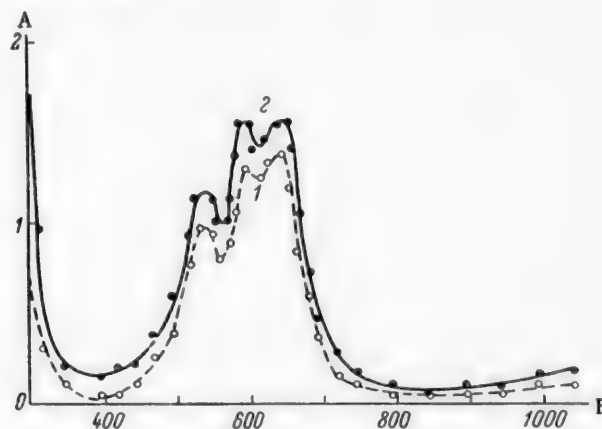


Fig. 1. Spectral curves of glasses with the composition $32\text{Na}_2\text{O} \cdot x\text{Al}_2\text{O}_3 \cdot (68-x)\text{SiO}_2$. A) Optical density D; B) wavelength (in $\text{m}\mu$). 1) $x=0$, 2) $x=8$.

The spectral absorption of borate and borosilicate glasses was investigated by Kefeli [4] and Moore [5]. It was found that the ratio $\text{Me}_2\text{O}/\text{B}_2\text{O}_3$ had a strong effect on the character of the spectral absorption of glasses; when the ratio $\text{Me}_2\text{O}/\text{B}_2\text{O}_3 < 1/3$, the glasses had a pink color, while with a ratio $\text{Me}_2\text{O}/\text{B}_2\text{O}_3 > 1/3$, the glasses had a blue color. The effect of Al_2O_3 on the spectral absorption curves of glasses has not been studied previously.

We prepared 3 series of glasses corresponding to the following molecular formulas:

Series No.	Composition (in mol. %)	Al_2O_3 content x , (in mol. %)	$\text{Na}_2\text{O}/\text{B}_2\text{O}_3$
1	$32\text{Na}_2\text{O} \cdot x\text{Al}_2\text{O}_3 \cdot (68-x)\text{SiO}_2$	0,8	∞
2	$16\text{Na}_2\text{O} \cdot 16\text{B}_2\text{O}_3 \cdot x\text{Al}_2\text{O}_3 \cdot (68-x)\text{SiO}_2$	0,8,12	1
3	$10\text{Na}_2\text{O}_3 \cdot 30\text{B}_2\text{O}_3 \cdot x\text{Al}_2\text{O}_3 \cdot (60-x)\text{SiO}_2$	0,10,20	1/3

The glasses were melted in quartz crucibles. The melts were stirred. The spectral absorption curves of the glasses were plotted on an SF-4 spectrophotometer. The results of the experiments are shown in Figs. 1-3. The spectral absorption for the different wavelengths is expressed as the optical density at a plate thickness of 5 mm and a Co_2O_3 concentration of 0.05%.

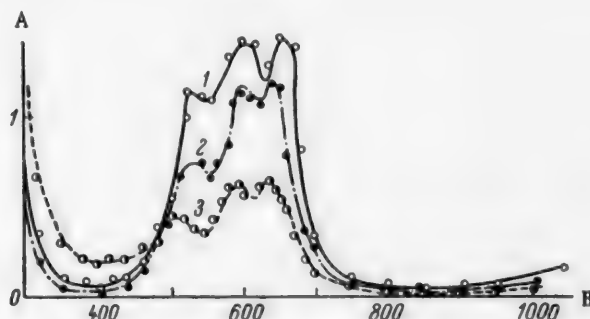


Fig. 2. Spectral curves of glasses with the composition $16\text{Na}_2\text{O} \cdot 16\text{B}_2\text{O}_3 \cdot x\text{Al}_2\text{O}_3 \cdot (68 - x)\text{SiO}_2$. A) Optical density D; B) wavelength (in $\text{m}\mu$). 1) $x = 0$, 2) $x = 8$, 3) $x = 12$.

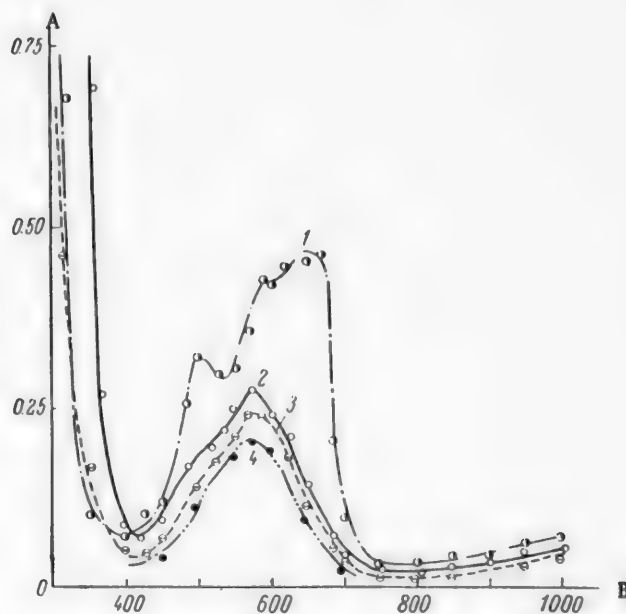


Fig. 3. Spectral curves of glasses with the composition $10\text{Na}_2\text{O} \cdot 30\text{B}_2\text{O}_3 \cdot x\text{Al}_2\text{O}_3 \cdot (60 - x)\text{SiO}_2$. A) Optical density D; B) wavelength (in $\text{m}\mu$). 1) $x = 0$, 2) $x = 10$, 3) $x = 20$, 4) $\text{Na}_2\text{O} \cdot 10\text{B}_2\text{O}_3$.

As Fig. 1 shows, the replacement of SiO_2 by Al_2O_3 in silicate glasses did not change the character of the spectral absorption of the glasses and only an increase in absorption intensity was observed.

The change in spectral absorption was different with the replacement of silica by alumina in borosilicate glasses. Firstly, the absorption intensity did not increase, but decreased in this case. Secondly, the character of the spectral absorption changed essentially. The maximum in the region of 580-680 $\text{m}\mu$ gradually became

indefinite and moved toward shorter wavelengths (Fig. 2). The spectral absorption of borosilicate glasses changed to the same extent and in the same direction with a decrease in the ratio $\text{Na}_2\text{O}/\text{B}_2\text{O}_3$. This has been reported in the literature and we also confirmed it (Figs. 1-3, curves 1).

If in the original borosilicate glass of series 3 $\left(\frac{\text{Na}_2\text{O}}{\text{B}_2\text{O}_3} = \frac{1}{3}\right)$, 10% or more of SiO_2 was replaced by Al_2O_3 , the spectral absorption became the same qualitatively as for glassy boric oxide. As Fig. 3 shows, the positions of the maxima on curves 2-4 almost completely coincided and only their sizes were different.

DISCUSSION OF RESULTS

The experimental data we obtained showed that the alumino-boron anomaly of the properties is expressed clearly on the spectral absorption curves of glasses. We explain the existence of the alumino-boron anomaly by the change in structure of the glass, which was discussed in detail in our other articles [1]. When there is a deficiency of alkali $\left(\frac{\text{Na}_2\text{O}}{\text{B}_2\text{O}_3} \lesssim 2\right)$ and silica is replaced by alumina, $[\text{AlO}_4]$ tetrahedra are incorporated into the glass lattice instead of $[\text{BO}_4]$ tetrahedra, and boron is displaced from the lattice and changes to ternary coordination. This interpretation is confirmed by the present investigation.

In actual fact, the main result of our experiments may be reduced to the fact that replacement of SiO_2 by Al_2O_3 in borosilicate glasses changes the spectral absorption of the glass in the same way qualitatively as raising the B_2O_3 concentration. In both cases the blue color has a tendency to change gradually to pink. The maximum on the absorption curves in the region of 580-680 m μ weakens and becomes indefinite and a new maximum appears in the region of 540-560 m μ . With an insufficiency of alkali, an increase in the B_2O_3 concentration in silicate glasses inevitably leads to the decomposition of $[\text{BO}_4]$ tetrahedra and the formation of $[\text{BO}_3]$ triangles (this is not quite true for borate glasses [6]; as regards borosilicate glasses, this rule is based on the sum total of knowledge of the composition dependence of the properties of borosilicate glasses). Consequently, the same process occurs in borosilicate glasses when Al_2O_3 is introduced instead of SiO_2 . Judging by the spectral curve, the decomposition of $[\text{BO}_4]$ tetrahedra is expressed even more strongly in this case. When all the $[\text{BO}_4]$ tetrahedra have decomposed, further introduction of Al_2O_3 has no further effect on the position of the maximum of the pink cobalt color centers formed.

According to contemporary ideas, the presence of pink color centers indicates that the Co^{2+} ion is in the hexa-coordinate state and the boric oxide remains in the form of $[\text{BO}_3]$ triangles.

SUMMARY

1. It was established that the alumino-boron anomaly is clearly reflected on the spectral curves of glasses.
2. It was shown that the introduction of Al_2O_3 into borosilicate glasses, colored with cobalt, effects the change in color in the same way qualitatively as increasing the B_2O_3 concentration, but in the first case the effect is expressed more strongly.

LITERATURE CITED

- [1] A. A. Appen and Kan Fu-hsi, Zhur. Priklad. Khim. 32, 5, 983, 991 (1959); * 6, 1206 (1959)*
- [2] V. V. Vargin, Production of Colored Glass [In Russian] (State Light Industry Press, 1940).
- [3] W. A. Weyl, Colored Glass, Sheffield (1951).
- [4] A. A. Kefeli, Doklady Akad. Nauk SSSR 57, 61 (1947); 58, 1051 (1947).
- [5] H. Moore and M. A. Aglan, J. Soc. Glass. Techn. 39, 191 (1955).
- [6] K. Grjotheim and I. Krogh-Moe, Kgl. Norske Videnskab. Forh. 27, 1 (1954); 29, 24 (1956).

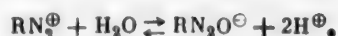
*Original Russian pagination. See C. B. Translation.

Received March 11, 1959

CALCULATION OF THE HYDROLYSIS CONSTANTS OF A DIAZO CATION*

B. V. Passet and B. A. Porai-Koshits

As we reported previously [1], the equilibrium state of aqueous solutions of aromatic diazo compounds may be characterized by the approximate equation



The constant of this equilibrium (hydrolysis constant of the diazo cation) may be defined as the ratio:

$$K = \frac{[\text{RN}_2\text{O}^{\ominus}][\text{H}^{\oplus}]^2}{[\text{RN}_2^{\oplus}]}.$$

The fact that this value, determined for various concentrations of diazo cation and diazo anion at different pH values, was found to be constant confirms the accuracy of the theoretical premises [1] and makes it possible to calculate a number of other physicochemical constants, characterizing the acid-base properties of diazo compounds [2].

Below we give a description of experiments which allowed us to calculate the hydrolysis constants of the p-nitrobenzene diazo cation.

1. An accurately weighed sample (223 mg, 0.001 mole) of the chemically pure potassium salt of p-nitrodiazobenzene was dissolved in 100 ml of doubly distilled water. To the solution was added from 1 to 8 ml of 0.2 N hydrochloric acid. The solution was kept until a constant pH value had been established and then a solution of 350 mg of silver nitrate in 5 ml of distilled water was added with vigorous stirring.

To prevent displacement of the equilibrium due to transition of the diazo cation into diazo anion under the action of silver nitrate, the suspension was rapidly filtered into a solution of 300 mg of β -naphthol in 100 ml of a saturated alcohol solution of para red. The diazo anion remained on the filter in the form of the water-insoluble silver derivative and the diazo cation underwent azo coupling with β -naphthol almost instantaneously. After 2 hours the precipitated dye was collected by filtration, washed thoroughly with a saturated solution of para red in ethyl alcohol and dried to constant weight at 60-70°. The experimental data are given in the table.

pH value	Weight of dye (in g)	pK value	pH value	Weight of dye (in g)	pK value
7.49	0.1647	15.09	7.22	0.2324	15.02
7.80	0.0876	15.23	7.15	0.2525	15.10
7.81	0.1016	15.36	7.52	0.1461	15.04
7.62	0.1190	15.07	7.25	0.2240	15.00
7.53	0.1386	15.01	7.80	0.0825	15.19
7.65	0.0890	14.94	7.83	0.0800	15.23
7.87	0.0608	15.16	8.00	0.0300	15.05
7.89	0.0605	15.19	—	—	—

The hydrolysis constant was calculated from the formula

$$\text{pK} = 2\text{pH} - \frac{293 - a}{a},$$

where 293 is the molecular weight of para red and a is the weight of dye obtained (in mg). Hence $\text{pK}_{\text{av}} = 15.11$ and $K = 7.95 \cdot 10^{-16}$.

* Communication XV in a series of papers on the structure and conversions of diazo compounds.

However, considering that there could be an error due to displacement of the equilibrium under the action of the reagents introduced into the solution, we did not limit ourselves to determining the concentrations of diazo cation and diazo anion by a gravimetric method, but developed a special method, making it possible to use the much more accurate spectral method for determining the value of K .

2. One ml of a 0.01 M solution of chemically pure potassium salt of p-nitrodiazobenzene in distilled water was mixed with 99 ml of various buffer solutions with pH values from 7.1 to 7.98.

An SF-4 spectrophotometer was used to record the change in optical density of each solution with a solution layer thickness of 10 mm and at wavelengths of 250, 260, 270, 320, 330, and 340 mμ.

From three to five experiments were carried out for each pH value of the solution. The discrepancies between the results of different experiments were within the limits of error of the apparatus. By means of Firordt's method [3], the average values of the optical densities of the solutions for each wavelength were used to determine the concentrations of diazo cation and diazo anion, whose total was always found to equal the total concentration of diazo compound in the solution.

From the equilibrium concentrations of diazo cation and diazo anion we calculated the values of the hydrolysis constant by the formula

$$pK = 2pH - \lg \frac{[O_2N-\text{C}_6\text{H}_4-N_2O^\ominus]}{[O_2N-\text{C}_6\text{H}_4-N_2^\oplus]}.$$

Under conditions when the equilibrium state of the system could not be reached due to decomposition of the diazo compound (which occurred at pH = 7.1), the equilibrium concentrations of diazo cation and diazo anion were obtained by graphical extrapolation.

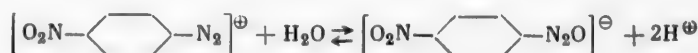
As it is not possible to give the results of all the experiments in the present article, we will limit ourselves to giving only the final results, each of which was the average of calculations from 3-5 experiments with six wavelengths used in each experiment.

pH value of buffer solution	7.98	7.80	7.67	7.38	7.10
Equilibrium concentration of diazo anion (in % of the total diazo compound content of the solution)	84.4	70.4	57.7	26.7	10.7
Equilibrium concentration of diazo cation (in % of the total diazo compound content of the solution)	15.6	28.8	42.3	73.3	89.7
Calculated pK value	15.2	15.2	15.2	15.2	15.1

From the data presented it follows that $K = 10^{-15.2} = 6.3 \cdot 10^{-16}$.

SUMMARY

1. The equilibrium state of dilute aqueous solutions of p-nitrodiazobenzene may be characterized by the equation



2. From quantitative analysis data on aqueous solutions of p-nitrodiazobenzene, obtained both gravimetrically and by spectroscopy, it may be taken that the hydrolysis constant of the p-nitrobenzenediazo cation $K = 6.3 \cdot 10^{-16}$.

LITERATURE CITED

- [1] B. V. Passet and B. A. Porai-Koshits, *Trudy LTI im. Lensova* 46, 133 (1958).
 [2] B. A. Porai-Koshits and B. V. Passet, *Zhur. Obshchei Khim.* 29, 1407 (1959).
 [3] A. Gillam and E. Stern, *Electronic Absorption Spectra of Organic Compounds* [Russian translation], (Foreign Lit. Press, Moscow, 1957), p. 259.

Received April 16, 1959

LIQUID - VAPOR PHASE EQUILIBRIA IN THE SYSTEM ISOPROPYL
 ALCOHOL - WATER - CALCIUM CHLORIDE

L. L. Dobroserdov

This investigation is connected with the study of the separation of azeotropic mixtures by salt rectification [1-7].

The isopropyl alcohol had the following characteristics: specific gravity 0.7870, refractive index 1.3777, boiling point 81.9°; the calcium chloride was "chemically pure" grade (GOST 4141-48). After purification, recrystallization, and drying to a completely anhydrous state, the calcium chloride contained 99.64 weight % of CaCl_2 .

The phase equilibrium of the system without salt was first studied. The experimental data obtained** are given in Table 1.

TABLE 1

Boiling point at atmos- pheric pres- sure (in °C)	Composition of liquid phase (in mol. % of al- cohol)	Composition of vapor phase (in mol. % of al- cohol)	Evaporation coefficient	Relative volatility coefficient
93.2	0.92	26.16	28.4	38.0
86.2	3.54	40.84	11.5	18.7
84.1	7.01	46.26	6.6	11.4
82.7	10.85	50.20	4.6	8.2
81.6	22.75	52.0	2.3	3.7
81.4	31.26	53.66	1.7	2.5
80.8	44.18	57.14	1.06	1.4
80.3	57.70	62.28	1.07	1.2
80.27	58.84	62.66	1.06	1.13
80.22	65.25	66.19	1.014	1.04
80.16	66.45	66.45	1.00	1.00
80.19	68.09	67.44	0.99	0.99
80.2	71.75	69.0	0.96	0.87
80.46	80.25	75.38	0.94	0.75
80.55	85.35	77.66	0.91	0.6

*Original Russian pagination. See C. B. Translation.

**V. P. Il'ina participated in the experimental work.

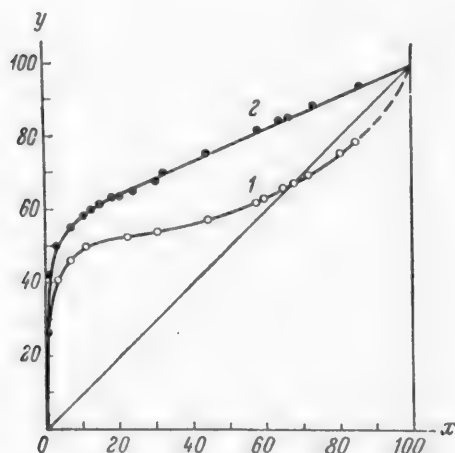
TABLE 2

Boiling point at atmos- pheric pres- sure (in °C)	Composition of liquid phase (in Mol % of alcohol)	Composition of vapor phase (in Mol % of alcohol)	Evaporation coefficient	Relative volatility coefficient
89.75	1.29	42.14	32.6	57.4
83.1	3.63	50.28	13.8	26.6
81.2	7.88	55.5	7.04	14.6
81.1	10.24	58.2	5.7	12.2
80.9	12.28	59.74	4.8	10.4
80.6	15.8	61.1	3.9	8.4
80.42	18.41	62.2	3.3	8.0
80.22	21.13	63.1	2.9	6.2
80.3	24.91	64.9	2.6	5.5
80.2	30.43	67.5	2.2	4.7
80.2	33.60	70.1	2.1	4.7
80.23	44.20	75.22	1.7	3.8
80.82	58.52	82.10	1.4	3.2
81.12	63.40	83.40	1.3	2.9
81.26	65.85	85.10	1.3	3.15
81.36	73.8	89.25	1.2	2.92
82.15	86.00	93.14	1.19	2.4

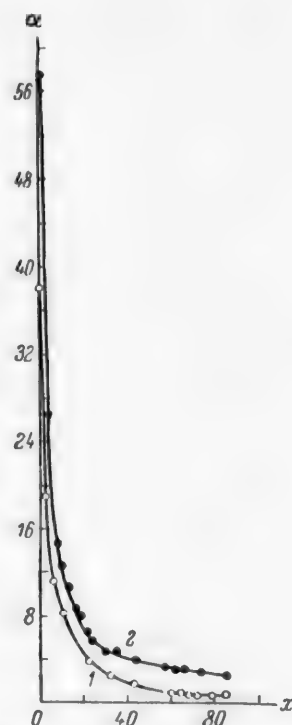
The evaporation coefficient $K = \frac{y_1}{x_1}$ and the relative volatility coefficient $\alpha = \frac{y_1 x_2}{x_1 y_2}$, where y_1 is the content of the volatile component (alcohol) in the vapor phase, y_2 is the content of the second component (water) in the vapor phase, x_1 is the content of the volatile component (alcohol) in the liquid phase, and x_2 is the content of the second component (water) in the liquid phase.

Table 1 shows that the azeotropic mixture isopropyl alcohol - water corresponds to the composition 66.45 mol. % of alcohol, which is equivalent to 86.9 weight %.

Our data differ from data presented in the literature, which also differ amongst each other. In Horsley's tables of azeotropic mixtures [8], the composition of the isopropyl alcohol - water azeotrope corresponds to 87.9 wt. %

Fig. 1. Equilibrium curves of $y = f(x)$.

1) $C_3H_7OH - H_2O$, 2) $C_3H_7OH - H_2O - CaCl_2$.

Fig. 2. Relation between the relative volatility coefficient and the composition of the liquid phase, $\alpha = f(x)$.

1) $C_3H_7OH - H_2O$, 2) $C_3H_7OH - H_2O - CaCl_2$.

of alcohol. In the tables of Kogan and Fridman [9], the composition of the same azeotrope is given as 68.13 mol. % of alcohol.

The boiling points of the azeotrope given also differ. In Horsley's tables the boiling point is given as 80.38°, while we obtained 80.16°, which agrees with the value given by Kogan and Fridman.

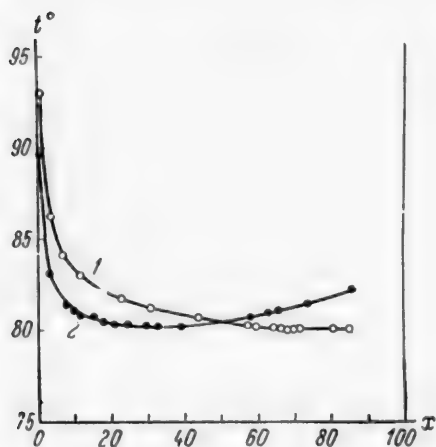


Fig. 3. Relation between boiling point and the liquid phase composition $t = f(x)$.
1) $C_3H_7OH - H_2O$, 2) $C_3H_7OH - H_2O - CaCl_2$.

Figure 3 shows curves of the relation between the boiling point and the liquid composition. Here, as in the other systems we investigated, we observed two regions where the boiling points were changed by the salt. The region where the system with the salt had a lower boiling point in comparison with the system without salt was in the zone of alcohol concentrations in the liquid up to 50 mol. %. The region of higher boiling points was beyond the limit of 50% alcohol concentration. Thus, this system also obeyed the laws we observed for other systems.

SUMMARY

1. The azeotropic mixture was completely broken when an isopropyl alcohol - water mixture was distilled in the presence of calcium chloride.
2. Enrichment of the vapor phase in the volatile component was greater at all liquid phase compositions than for the binary mixture.
3. Absolute isopropyl alcohol may be obtained by rectification of a mixture of isopropyl alcohol and water in the presence of calcium chloride.

LITERATURE CITED

- [1] L. L. Dobroserdov and V. P. Il'ina, Trudy Leningrad Tekhnol. Inst. Pishchevoi Prom. 13 (1956).
- [2] L. L. Dobroserdov and V. P. Il'ina, Trudy Leningrad Tekhnol. Inst. Pishchevoi Prom. 14 (1958).
- [3] L. L. Dobroserdov and V. P. Il'ina, Trudy Leningrad Tekhnol. Inst. Pishchevoi Prom. 14 (1958).
- [4] L. L. Dobroserdov and V. P. Il'ina, Trudy Leningrad Tekhnol. Inst. Pishchevoi Prom. 14 (1958).
- [5] L. L. Dobroserdov and V. P. Il'ina, Trudy Leningrad Tekhnol. Inst. Pishchevoi Prom. 14, (1958).
- [6] L. L. Dobroserdov, Trudy Leningrad Tekhnol. Inst. Pishchevoi Prom. 15 (1958).

- [7] L. L. Dobroserdov, *Trudy Leningrad Tekhnol. Inst. Pishchevoi Prom.* 15 (1958).
- [8] L. Horsley, *Tables of Azeotropic Mixtures* [Russian translation] (Foreign Lit. Press, 1951).
- [9] V. B. Kogan and V. M. Fridman, *Handbook of Equilibrium between Liquid and Vapor in Binary and Polycomponent Systems* [In Russian], (State Chem. Press, Leningrad, 1957).

Received December 10, 1958

THERMAL STABILITY OF THE SYSTEM UREA - AMMONIUM NITRATE

B. Yu. Rozman and L. I. Borodkina

The thermal decomposition of urea has been studied mainly from the point of view of elucidating the chemical reactions occurring when urea is heated and resulting in its conversion into certain other compounds (cyanuric acid, biuret, ammeline, melamine, etc.). In general, very little attention has been paid to the decomposition kinetics in these investigations. As far as we know from the literature, the thermal decomposition of the system urea - ammonium nitrate has not been studied at all.

As a result of an investigation of the thermal stability of ammonium nitrate [1, 2], it was established that urea is a very effective inhibitor of thermal decomposition of the nitrate. In addition, the very interesting phenomenon of mutual stabilization was observed. Urea, being an inhibitor of ammonium nitrate decomposition, stabilized the latter and, on the other hand, ammonium nitrate stabilized urea. Therefore, it seemed profitable to study the thermal stability of the system urea - ammonium nitrate by investigating the kinetics of the thermal decomposition of urea and this system and this is the subject of the present communication.

Three different methods were used to investigate the thermal decomposition kinetics: 1) thermogravimetric, 2) manometric, and 3) a method based on determination of the amount of ammonia liberated. Experiments were carried out over the temperature range 150-200°.

In all experiments with mixtures of urea and ammonium nitrate, the weight of urea used remained constant (5 g with the gravimetric method and 0.5 g with the others). Sufficient ammonium nitrate was added to the urea to give mixtures of the given composition.

The results of some experiments by the gravimetric method, characterizing the relation between the weight loss and the decomposition time, are given in Fig. 1 (at 200°).

Kinetic curves of time against pressure at 150 and 175°, obtained by the manometric method, are given in Fig. 2. The manometric experiments were carried out without preliminary evacuation. To eliminate the effect of the thermal expansion of air on the reading of the manometer, the latter was connected only after the samples had been heated for the first 5 minutes.

In the third method a slow stream of air was passed through the heated samples and this carried away the ammonia liberated during the decomposition. Ammonia entrained with the air was absorbed with 0.1 N sulfuric acid and the excess of this was titrated with 0.1 N alkali. The results of some experiments in this series (at 175°) are given in Fig. 3.

The kinetic curves obtained by the different methods differed little in form. Analysis of them indicated progressive retardation of decomposition.

In all cases the addition of ammonium nitrate to urea produced a very considerable increase in the thermal stability of urea. The higher the nitrate content of the mixture (for a constant weight of urea), the greater was the absolute stabilization effect. On the other hand, the relative stabilization effect fell, in general, as the nitrate content of the mixture increased.

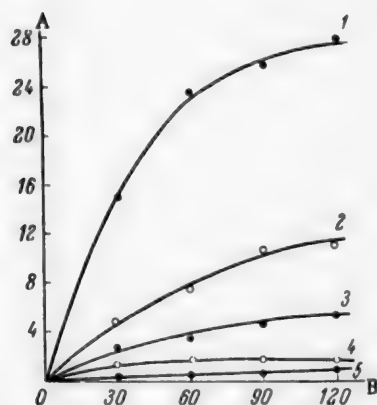


Fig. 1. Relation between weight loss and decomposition time at 200°. A) Weight loss (in %), B) time (in min). 1) Urea, 2) 75% urea in the mixture, 3) 50%, 4) 25%, 5) ammonium nitrate.

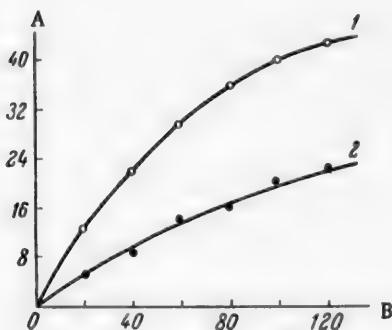


Fig. 3. Relation between the amount of ammonia liberated during decomposition and decomposition time at 175°. A) Amount of NH_3 (in mg-equiv. $\times 10$), B) time (in min). 1) Urea, 2) 50% urea in the mixture.

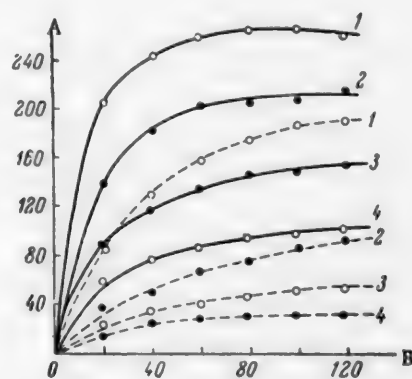


Fig. 2. Relation between decomposition pressure and decomposition time at 150° and 175°. A) Decomposition pressure (in mm Hg), B) time (in min). Solid lines) at 175°, broken lines) at 150°. 1) Urea, 2) 75% urea in the mixture, 3) 50%, 4) 25%.

Mathematical treatment of the experimental results showed that the experimental data we obtained was satisfactorily described by the following empirical equation, which is similar in principle to the Langmuir adsorption isotherm equation:

$$x = a \frac{bt}{1 + bt}$$

where x is the weight loss in the thermogravimetric method, the decomposition pressure in the manometric method, or the amount of ammonia liberated during decomposition, t is the decomposition time and a and b are constants at a given temperature and a given mixture composition for a given investigation method.

The error of determinations by this equation did not exceed 6%.

It should be noted that with the thermogravimetric method, it could be assumed that b depended only on temperature and not on the mixture composition: at 175° $b = 0.010$ and at 200° $b = 0.014$.

As a result of studying the thermal stability of the system urea — ammonium nitrate it was established that the addition of ammonium nitrate to urea leads to very considerable stabilization of the latter, which is greater, the greater the nitrate content of the mixture.

LITERATURE CITED

- [1] B. Yu. Rozman, Thermal Stability of Ammonium Nitrate [In Russian] LIIVT (1957).
- [2] B. Yu. Rozman and L. I. Borodkina, Zhur. Priklad. Khim. 32, 2 (1959) •

Received January 16, 1959

CHANGE IN THE REACTIVITY OF PULVERIZED CELLULOSE IN DIFFERENT MEDIA

V. I. Sharkov, I. I. Korol'kov, and E. N. Garmanova

In previous work [1, 2] we showed that during the pulverization of dry cotton or wood cellulose in a mill of the percussion type, the cellulose changed into the so-called "amorphous state," characterized by the disappearance of the x-ray pattern typical of natural cellulose, a considerable decrease in density, and an increase in reactivity under ethanolysis conditions. When amorphous cellulose preparations were moistened with water they underwent a series of changes which appeared as an increase in the specific gravity of the material, the appearance of interferences on x-ray patterns, typical of normal cellulose, and a sharp fall in reactivity with respect to ethanolysis. This change in the properties of pulverized cellulose is usually regarded as due to its contraction or recrystallization.

It was also established that the contraction of pulverized cellulose did not occur when it was treated with anhydrous alcohols in the cold or with heating to 100°.

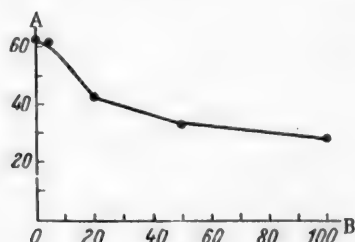


Fig. 1. Change in reactivity of pulverized cellulose when treated with aqueous solutions of ethanol of various concentrations. A) Amount of cellulose dissolved (in %), B) water content of mixture (in %).

These observations made it possible for us to use ethanolysis for quantitative characterization of different cellulose preparations. The amount of the fraction readily undergoing alcoholysis gave a measure of the changes in structure of the cellulose produced by different methods of treating it.

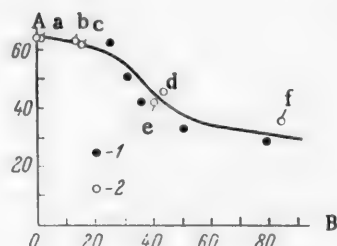


Fig. 2. Change in reactivity of pulverized cellulose when treated with organic liquids of different dielectric constants and also with mixtures of water and ethanol. A) Amount of cellulose dissolved (in %), B) dielectric constant. 1) Water-ethanol mixtures, 2) organic liquids: benzene a, benzyl alcohol b, isoamyl alcohol c, glycerol d, glycol e, and formamide f.

•Original Russian pagination. See C. B. Translation.

In this work ethanolysis was used to observe the contraction of pulverized cellulose under the action of sorbed moisture and various organic liquids.

For the investigation we used absolutely dry, bleached spruce sulfite cellulose (viscose grade), pulverized on a vibration ball mill of VNIIGSa design. The "amorphous" cellulose obtained in this way contained 65.0% of a fraction which readily underwent ethanolysis. To simplify the method, the amount of the latter was determined from the loss in weight of the sample after it had been heated in copper autoclaves for 3 hours at 100° in anhydrous ethanol, containing 10% sulfuric acid monohydrate, and the insoluble cellulose residue had been washed with cold water and then ethanol. This method was found to be convenient and quite reliable for comparing different cellulose preparations.

For investigation of the changes occurring in pulverized cellulose under the action of sorbed water, samples of absolutely dry pulverized cellulose were kept for 100 hours in desiccators over sulfuric acid of various concentrations in a thermostat at 20°. The amount of water in the moistened preparations was determined by drying them to constant weight at 105°. The amount of cellulose in the moistened preparations which dissolved on ethanolysis by the above method was then determined.

The results obtained are given below.

Moisture content (in %)	Cellulose dissolved (in %)
0.0	65.0
5.4	63.9
14.2	62.8
18.0	59.5
20.0	41.4
24.0	38.2

The data presented show that when pulverized cellulose absorbed up to 14% of moisture, the reactivity of the preparations in ethanolysis changed very little. With a further increase in the moisture content up to 20%, the reactivity of the cellulose decreased rapidly. The water apparently penetrated between the cellulose macromolecules, separated them, and increased the mobility of the macromolecules, thus facilitating their closer packing.

As was stated above, absolute ethanol hardly changed the reactivity of pulverized cellulose. On the other hand, water was found to have a strong contracting action on pulverized cellulose. Hence, it could be surmised that mixtures of ethanol and water would have a greater effect on the cellulose, the greater their water content.

Effect of Treating Pulverized Cellulose with Organic Liquids
on Its Reactivity

Nature of liquid medium	Dielectric constant of liquid medium	Cellulose dissolved (in %)
Benzene	2.3	64.1
Benzyl alcohol	13.0	63.1
Isoamyl alcohol	15.0	62.2
Ethyl alcohol	25.6	61.7
Glycol	41.2	41.5
Glycerol	43.0	45.8
Formamide	84.0	35.5
Water	80.0	29.0

To test this hypothesis, pulverized cellulose was heated for 30 minutes at 100° in autoclaves in aqueous alcohol mixtures of various compositions. Then after being washed with alcohol and dried at 100°, the cellulose preparations obtained were assayed for the reactive fraction content by the method described above.

The results obtained are presented in Fig. 1. The curve illustrated in Fig. 1 shows that no fall in cellulose reactivity was observed when the ethanol contained up to 4% of water. With a further increase in the water content of the mixture, the effect of the latter rapidly increased.

A similar method was used to investigate the action of various organic liquids. After the pulverized anhydrous cellulose had been treated with them for 30 minutes at 100°, it was washed with absolute ethanol and dried at 100°. The results of examining these cellulose samples are given in the table.

The data presented (table) show that a fall in the reactivity of pulverized cellulose can be produced not only by water but also by a series of organic liquids with a high polarity and the capacity to produce swelling of cellulose and other polysaccharides.

This conclusion can be illustrated by Fig. 2 where the dielectric constants of the liquids examined are plotted along the abscissa and the solubility of cellulose during ethanolysis, along the ordinate. The same diagram shows analogous data for water - alcohol mixtures.

This diagram shows that there is a definite relation between the dielectric constant or the polarity of different liquids and their action on pulverized cellulose. The greater the dielectric constant or polarity of the liquid, the more the reactivity of pulverized cellulose falls due to its contraction (recrystallization).

SUMMARY

1. It was established that natural cellulose, which has been pulverized in a dry state, changes under the action of sorbed moisture and loses its reactivity in ethanolysis. With a moisture content of less than 14% the fall in reactivity is small. With a further increase in the moisture content up to 20%, the reactivity of the cellulose rapidly falls.
2. Water - alcohol mixtures reduce the reactivity of cellulose the more strongly, the greater their water content.
3. Organic liquids with a high dielectric constant (glycol, glycerol, and formamide) act on pulverized cellulose similarly to water.

LITERATURE CITED

- [1] I. I. Korol'kov, V. I. Sharkov, and E. N. Garmanova, *Zhur. Priklad. Khim.* 30, 586 (1957). *
- [2] I. I. Korol'kov, V. I. Sharkov, and A. V. Krupova, *Zhur. Priklad. Khim.* 31, 1560 (1958). *

Received September 29, 1958

*Original Russian pagination. See C. B. Translation.

APPLICATION OF PRECIPITATION CHROMATOGRAPHY TO THE QUANTITATIVE DETERMINATION OF NICKEL SOAPS

V. P. Golendeev

Gor'kii Polytechnic Institute

The chromatographic separation of ions in the form of difficultly soluble salts, which has been called precipitation chromatography, was proposed by E. N. Gapon, T. B. Gapon, and Belen'kaya [1, 2]. A case where the substance chromatographed and the precipitant form a difficultly soluble compound on the carrier is precipitation chromatography of nonelectrolytes, and this has not been developed at all [2]. The purpose of the present work was to use the principles of precipitation chromatography of nonelectrolytes for developing a method of quantitatively determining small amounts of nickel soaps in fatty products (oil and hydrogenated fat).

EXPERIMENTAL*

The problem of determining nickel soaps in hydrogenated fatty materials has become particularly important since it was shown that in the hydrogenation of fats with copper-nickel carbonate catalysts, which are now widely used in industry, nickel soaps are formed in a number of cases [3, 4].

Nickel soaps are undesirable side products of fat hydrogenation. They accumulate in the hydrogenated fat, hinder its filtration and pass through the filters, causing high nickel losses with the filtered hydrogenated fat as compared with standard norms. In addition, nickel soaps, present in the fat solution in a colloidal state, are readily adsorbed on the surface of finely dispersed copper-nickel catalyst, lowering its catalytic activity and hampering its repeated use.

Up to now there have been no methods, either for quantitative determination, or for qualitative detection of nickel soaps in fatty products. The development of such a method therefore became an urgent problem which was vital to industrial practice. It was required for control and the choice of correct technological conditions for filtering hydrogenated fat and for assessing the quality of a spent catalyst for reuse.

As a basis for searching for such a method we used the principle of precipitation chromatography where the substance chromatographed was the nickel soap, the precipitant dimethylglyoxime, and the carrier silica gel with a particle size of 0.12 to 0.088 mm and an adsorption activity of 2.5 ml for benzene, determined by the standard method described by Kazanskii and Mikhailov [5]. It was found that if the fatty product (hydrogenated fat or oil) containing nickel soaps was passed through a glass tube filled with silica gel which was then moistened with a solution of dimethylglyoxime in *n*-butyl alcohol, that is also a solvent for nickel soaps, then the latter was selectively adsorbed on the silica gel and after removal of the fat with solvents (chloroform and ether), reacted with the dimethylglyoxime to form an insoluble, colored precipitate of nickel dimethylglyoxime in the form of a chromatogram. The amount of substance chromatographed was determined by comparing the intensity of the precipitate color and the length of the colored zone with standard chromatograms where the nickel content, bound in the form of nickel soap, was known.

The method of determining nickel soaps quantitatively, developed from this principle, was found to be simple as regards procedure and design of apparatus and made it possible to determine thousandths of a percent of nickel, bound as a nickel soap.

Application of this method to the analysis of hydrogenated fat and oil samples into which had been introduced known amounts of nickel soaps, prepared in the laboratory, showed that it was quite accurate and that repeated determinations were readily reproducible.

* T. M. Frolova participated in the experimental work.

Description of method. The analysis was performed in an apparatus consisting of a glass adsorption tube drawn out at one end, 100 mm long and 7 mm in diameter (the length of the drawn-out end was 50 mm and the internal diameter 1-1.5 mm), connected to a Bunsen flask, which was evacuated with a water pump.

The adsorption tube was filled with silica gel (over a small layer of cotton wool) to a bed height of 25 mm, which was compressed slightly. The whole apparatus was placed in a drying cupboard with an electrical heater, and the temperature kept constant (90-100°) with a rheostat.

The analysis was carried out simultaneously in two adsorption tubes, connected to one vacuum pump. Before the analysis, the adsorbent in the adsorption tube was moistened with a 1% solution of dimethylglyoxime in butanol and the solvent sucked out.

For the analysis, a 1 g sample of the hydrogenated fat or oil, in which the nickel soap was to be determined, was weighed into a small beaker on technical balances (with an accuracy of up to one hundredth of a gram) and dissolved with heating in 1 ml of *n*-butyl alcohol. For solution of the hydrogenated fat, in contrast to the oil, in addition to butanol 1 ml of vegetable oil (sunflower or cottonseed) was added to reduce the viscosity of the solution. Then at 90-100° the dissolved fat sample was slowly sucked through the adsorption tube at 2-3 drops per minute.

The fat remaining in the adsorption tube was completely removed from the adsorbent by careful washing with solvents (chloroform and ethyl ether) since the formation of nickel dimethylglyoxime did not occur in the presence of fat. For this purpose, the adsorption tubes were cooled to about 50° by passing air through them and washed under suction, first with chloroform and then with ether. We used 3 ml of chloroform for an oil sample and 4 ml for a hydrogenated fat sample and this was introduced into the tube as equal portions of 1 ml each. Traces of chloroform were removed from the tube by washing with 1 ml of ether.

As the formation of nickel dimethylglyoxime was strongly retarded in the presence of ethyl ether, the residual ether was removed by sucking 0.5 ml of ethyl alcohol through the tube.

After the ethyl alcohol had filtered through, into the adsorption tube was poured 1 ml of a 1% butanol solution of dimethylglyoxime and slowly passed through the adsorbent without sucking. When nickel soaps were present in the fat analyzed, a colored precipitate of nickel dimethylglyoxime was formed in the adsorbent in the form of a chromatogram. By comparing the intensity of the color and the depth of the colored zone of the adsorbent (i.e., the chromatogram obtained) with standard chromatograms where the nickel soap content was known, we determined the amount of nickel bound in the form of nickel soap in milligrams per kg of fat analyzed.

Our experiments showed that the length of the colored zone of adsorbent was affected by the melting point of the fat. It was therefore necessary to prepare separate standard chromatograms for oil and for hydrogenated fat under conditions analogous to those for determining the nickel soaps in the fatty product.

Standard chromatograms were prepared containing 10, 20, 30, 40, 50, 60, 70, 80, etc. mg of nickel, bound as nickel soap, in 1 kg of fat (the normal nickel content of technical hydrogenated fat).

Preparation of standard chromatograms. For the preparation of standard samples, 1 ml of a 1% butanol solution of dimethylglyoxime was first introduced into an adsorption tube with silica gel and the solvent sucked through. After this a solution of 1 g of oil in 1 ml of a standard butanol solution of nickel soap, containing 10, 20, 30, 40, etc. mg of metallic nickel per liter, was slowly passed through the adsorbent at 2-3 drops per minute and 90-100°. The standards for technical hydrogenated fat were prepared under the same conditions but 1 ml of oil was also added to 1 g of hydrogenated fat as a solvent.

The technical hydrogenated fat for the standards was first carefully freed from nickel by treatment with hot 10% sulfuric acid, washed free from acid, and dried.

Thus, standard chromatograms were prepared under the same conditions as determinations of nickel soap in fat. After removal of the fat from the adsorption tube by washing with chloroform, ether, and alcohol, 1 ml of a 1% butanol solution of dimethylglyoxime was added to form nickel dimethylglyoxime. The butanol was then slowly sucked from the tube to almost complete dryness and the standards stored with protection from light.

In our experiments, repeated preparations of standards with the same nickel content, bound as nickel soap, gave good reproducibility and identical chromatograms were obtained.

Nickel soap for the preparation of standards was obtained by an exchange reaction of nickel acetate with sodium soap in an aqueous alcohol solution. For this purpose, to a hot 2-3% aqueous alcohol solution (1:1) of sodium soap was added an equivalent amount of a 5% aqueous solution of nickel acetate with careful stirring. The precipitate of nickel soap was carefully washed with hot alcohol to a negative reaction for sodium soap with phenolphthalein and dried in a vacuum desiccator over calcium chloride.

The results of analyzing the nickel soap samples obtained (by Chugaev's method) showed that the nickel contents were close to the theoretical values of from 9.0 to 9.7%, depending on the average molecular weight of the fatty acids in the soap sample.

TABLE 1
Effect of Adsorption Activity of Silica Gel on the Stability of the Chromatograms

Silica gel sample No.	Color of silica gel	Adsorption activity found (in ml)	Stability of chromatograms
1	White	0.0	Nickel dimethylglyoxime precipitate diffused along tube
2		2.0	Precipitate partly diffused along tube
3		2.5	Precipitate held in upper layer of adsorbent, chromatograms stable
4	Gray	3.3	Color masked, chromatograms unclear
5		5.5	
6	White	6.5	Silica gel darkened by dimethylglyoxime, chromatograms distorted

The nickel soaps were emerald-green, crystalline substances. They were insoluble in the usual solvents, but dissolved readily in fats and oils and also in butyl alcohol, especially on heating.

When stored in air the nickel soaps were partially oxidized and their solubility in butanol sharply decreased. This property of nickel soaps evidently made solutions of them in butyl alcohol unstable during storage. Therefore the most interesting solvent for the preparation of standard solutions of nickel soaps was hydrogenated fat, freed from nickel, with which the nickel soaps gave stable solutions.

Choice of adsorbent sample. Several samples of silica gel found in the laboratory, whose grades could not be established, were tested as a carrier-adsorbent. In the determination of nickel soaps, we studied the effect of various factors on the stability of the chromatograms: adsorption activity of the silica gel sample, the particle size, and the color of the silica gel.

The experimental results showed that the most stable and clearest chromatograms were obtained with a silica gel adsorption activity of 2.5 ml (with respect to benzene), and a particle (white in color) size of from 0.12 mm to 0.088 mm. When silica gel samples with particle sizes greater than 0.12-0.088 mm were used, the precipitate was partly displaced and the chromatograms were distorted. When the particle size was less than 0.12-0.088 mm, there was a strong increase in resistance in the adsorption tube and an increase in the analysis time. The adsorption activity of the silica gel hardly changed with a change in grain size from 0.12 to 0.07 mm.

The results of this series of experiments are presented in Table 1.

Table 1 shows that the stability and clearness of the chromatograms were affected by the adsorption activity and the color of the silica gel (original and that obtained when a butanol solution of dimethylglyoxime was poured through). The best sample was white silica gel with an adsorption activity of 2.5 ml.

Quantitative determination of nickel soaps in oil and hydrogenated fat. Samples of fatty products (oil and hydrogenated fat), containing definite amounts of nickel, bound as nickel soap, were prepared for the determination of nickel soaps. Nickel was introduced in amounts usually encountered in technical hydrogenated fats (from 20 to 100 mg/kg). The experimental results are given in Table 2.

TABLE 2
Nickel Soap Content Found Chromatographically.
Fat Sample 1 g

Expt. No.	Fat	Melting point of fat (in °C)	Nickel soap introduced, calculated on metallic nickel (in mg/kg)	Nickel found chromatographically (in mg/kg)
1	Refined cotton-seed oil	—	20	20
2			30	30
3			40	40
4			50	50
5			60	60
6	Technical hydrogenated fat	45	20	20
7		45	30	30
8		48	40	40
9		48	50	50
10		48	60	60
11		48	70	70
12		47	90	90
13		47	180	180
14		47	200	200

Thus, Table 2 shows that in all cases the amount of nickel found chromatographically corresponded completely with the actual nickel content of the fat samples analyzed.

SUMMARY

1. A method based on precipitation chromatography was developed for the quantitative determination of nickel soaps in fatty products (oil and hydrogenated fat), which made it possible to determine thousandths of a percent of nickel.
2. The quantitative chromatographic determination of nickel soaps is quite accurate and requires simple apparatus and the procedure is not complicated.
3. It is of interest in the fat hydrogenation industry for the technological control of hydrogenated fat filtration, in the hydrogenation of fats and for a qualitative assessment of a spent catalyst.

LITERATURE CITED

- [1] E. N. Gapon and I. M. Belen'kaya. Collection: Investigation of Chromatography [In Russian] (Acad. Sci. USSR Press, 1952), p. 35.
- [2] F. M. Shemyakin, É. S. Mitselovskii, and D. V. Romanov, Chromatographic Analysis [In Russian] (State Chem. Press, 1955), p. 55.

[3] V. P. Golendeev, *Maslobolno-Zhirovaya Prom.* 4, 17 (1958).

[4] V. P. Golendeev, K. G. Bogareva, E. I. Bobkova, and O. N. Dobrynina, *Maslobolno-Zhirovaya Prom.* 9, 18 (1958).

[5] E. A. Mikhailov and B. A. Kazanskii, *Collection: Investigation of Chromatography* [In Russian] (Acad. Sci. USSR Press, 1952), pp. 155 and 162.

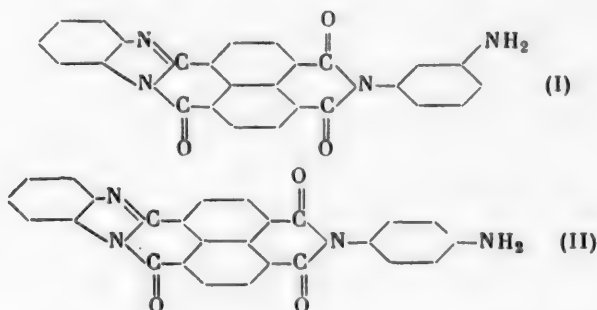
Received November 5, 1958

AMINOPHENYLIMIDES OF 1,8-NAPHTHOYLENE-1',2'-BENZIMIDAZOLE-4,5-DICARBOXYLIC ACIDS

B. M. Krasovitskii, E. E. Khotinskaya, and V. L. Plakidin

We previously [1] proposed a method of preparing aminophenylimides of naphthalic acid by heating naphthalic anhydride with nitroanilines in an aqueous alcohol medium in the presence of sodium hydrosulfite ($\text{Na}_2\text{S}_2\text{O}_4$). We later prepared aminophenylimides of 4-bromonaphthalic [2], naphthalene-1,4,5,8-tetracarboxylic, and perylene-3,4,9,10-tetracarboxylic [3] acids in a similar way.

The present communication is devoted to the preparation of m- and p-aminophenylimides of 1,8-naphthoylene-1',2'-benzimidazole-4,5-dicarboxylic acid, (I) and (II).



These amines were obtained by the method mentioned above. Their synthesis again confirmed our previous conclusion on the applicability of this method to the preparation of aminophenylimides of various peri-di- and peri-tetracarboxylic acids.

EXPERIMENTAL

p-Aminophenylimide of 1,8-naphthoylene-1',2'-benzimidazole-4,5-dicarboxylic acid. A mixture of 10 g of 1,8-naphthoylene-1',2'-benzimidazole-4,5-dicarboxylic acid and 8 g of p-nitroaniline was added to 300 ml of 50% ethyl alcohol, the contents of the flask heated to boiling under reflux, and, without heating being stopped, 30 g of sodium hydrosulfite introduced in small portions. When all the hydrosulfite had been introduced, heating was continued for a further 2 hours and the precipitate collected and heated first with dilute hydrochloric acid,

and then with 5% sodium carbonate solution to 70-80° to remove unreacted starting materials. The yield was 10.2 g (84%).

Found %: N 13.10, 12.87. $C_{26}H_{14}N_4O_3$. Calculated %: N 13.02.

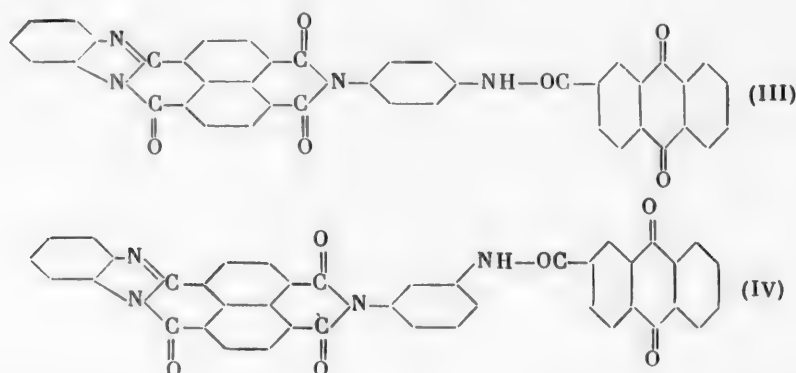
The product obtained was a brown powder which did not melt when heated to 360° and was insoluble in water and dilute hydrochloric acid, but dissolved in concentrated sulfuric acid.

m-Aminophenylimide of 1,8-naphthoylene-1',2'-benzimidazole-4,5-dicarboxylic acid. This substance was prepared similarly from 1,8-naphthoylene-1',2'-benzimidazole-4,5-dicarboxylic acid and m-nitroaniline in an aqueous alcohol medium in the presence of sodium hydrosulfite. The yield from the same amounts of starting materials was 6.8 g (57%).

Found %: N 13.03, 12.73; NH_2^* 3.53. $C_{26}H_{14}N_4O_3$. Calculated %: N 13.02, NH_2 3.72.

The product obtained was a brown powder which did not melt when heated to 360° and was insoluble in water, sparingly soluble in dilute hydrochloric acid, and soluble in concentrated sulfuric acid.

The aminophenylimides of 1,8-naphthoylene-1',2'-benzimidazole-4,5-dicarboxylic acid were used as intermediates in the synthesis of the yellow vat dyes (III) and (IV) [5]:



SUMMARY

The p- and m-aminophenylimides of 1,8-naphthoylene-1',2'-benzimidazole-4,5-dicarboxylic acid were prepared by the method previously proposed by the authors, which consists of heating a peri-di- or peri-tetra-carboxylic acid or its anhydride with the appropriate nitroaniline in an aqueous alcohol medium in the presence of sodium hydrosulfite.

LITERATURE CITED

- [1] B. M. Krasovitskii, R. M. Matskevich, and E. E. Khotinskaya, Doklady Akad. Nauk SSSR 86, 953 (1952).
- [2] B. M. Krasovitskii and E. E. Khotinskaya, Trudy. Khim. Fak. i Inst. Khim. KhGU 14, 145 (1956).
- [3] B. M. Krasovitskii, Trudy Khim. Fak. i Inst. Khim. KhGU 18, 231 (1957).
- [4] L. M. Litvinenko and A. P. Grekov, Zhur. Anal. Khim. 10, 164 (1955).*
- [5] V. L. Plakidin, B. M. Krasovitskii, E. E. Khotinskaya, L. Ya. Tupalova, and L. M. Tolomb, Author's Certificate 114,328 (1958).

Received May 30, 1958

* The amino group was determined by potentiometric titration with sodium nitrite [4].

** Original Russian pagination. See C. B. Translation

DIAZOTIZATION AND AZO COUPLING OF COPOLYMERS BASED ON ACRYLONITRILE AND p-AMINOSTYRENE

G. I. Kudryavtsev, E. A. Vasil'eva-Sokolova, and M. A. Zharkova

All-Union Scientific Research Institute of Artificial Fibers

At the present time, polyacrylonitrile fibers are of great importance in the production of technical articles. The extensive use of fiber from pure polyacrylonitrile is restricted by its low hygroscopicity and very poor dyeing properties.

Despite the fact that for several years there have been intensive investigations in a number of countries aimed at discovering methods of dyeing polyacrylonitrile, until now there has been no satisfactory method of dyeing fibers from this polymer. Some success in this direction has been achieved by copolymerizing acrylonitrile with other vinyl monomers [1, 2]. Copolymers of acrylonitrile with vinylpyridine, acrylamide, methyl methacrylate, and other monomers have better dyeing characteristics than polyacrylonitrile.

In the present work we developed an essentially different method of dyeing articles based on polyacrylonitrile. The essence of this method consisted of preparing a copolymer of acrylonitrile with some other monomer which made it possible to use subsequent chemical conversions to give a product capable of being dyed. As a second component for the copolymerization we chose p-aminostyrene.

The introduction of p-aminostyrene into the macromolecule chains, even in very small amounts, should confer on the copolymer the capacity to be dyed by acidic dyes. In addition to this, the presence of the p-aminostyrene component made it possible to carry out more complex chemical conversions, namely, diazotization of the amino group and subsequent azo coupling to yield intrinsically dyed polymeric compounds.

Work is described in the literature on the preparation of compounds which are actually polymeric dyes. Kern and Schulz [3] obtained colored compounds by coupling hydrazones of polyacrylic acid with various diazo salts. Polymeric azo dyes were synthesized by these authors by the interaction of polyvinyl alcohol with aromatic aldehydes and coupling the condensation product with diazo compounds.

Rogovin, Yashunskaya, and Bogoslovskii [4] have described the coupling of aldehydocellulose with hydroxy-arylamines and subsequent coupling with diazo components.

Diazotization has been applied to some polymeric amino compounds for the preparation of polymers with specific properties [5, 6].

EXPERIMENTAL

Starting materials. The acrylonitrile was purified by treatment with a 2% aqueous solution of NaOH, washed with water, dried over CaCl_2 , and distilled at 25° (18 mm Hg). p-Aminostyrene was synthesized from p-aminophenylethyl alcohol by dehydration [7]. It had b. p. 122-124° (10 mm Hg) and n_D^{20} 1.6078.

Copolymerization of acrylonitrile with p-aminostyrene. The copolymerization of acrylonitrile with p-aminostyrene has not been described in the literature. We copolymerized acrylonitrile with p-aminostyrene in an aqueous emulsion with a monomer phase : water ratio of 1 : 5. The initiator was azoisobutyrodinitrile (0.3% of the weight of monomers).

The emulsifier was potassium mersolate (5% of the weight of monomers). The experiments were carried out in the presence of a molecular-weight controller, namely, lauryl mercaptan (0.2%). Copolymerization was at 60° for 3 hours. In choosing an initiator for the copolymerization of acrylonitrile with p-aminostyrene it was established that copolymerization did not occur in the presence of benzoyl peroxide. This result confirmed literature reports [8] that the decomposition products of benzoyl peroxide could react with an amino group, thus losing their capacity to initiate the polymerization process.

The method described above was used to prepare copolymers of acrylonitrile with p-aminostyrene at monomer ratios from 98:2 to 70:30.

The characteristics of the copolymers obtained at different monomer ratios are given in the table.

Characteristics of Copolymers. Reaction Temperature 60°, Time 180 Minutes

Expt. No.	Initial ratios of monomers				Yield (in %)	Specific viscosity	Composition of copolymer			
	weight %		mol. %				weight %		mol. %	
	acrylonitrile	p-aminostyrene	acrylonitrile	p-aminostyrene			acrylonitrile	p-aminostyrene	acrylonitrile	p-aminostyrene
1	98	2	99	1	40.3	—	93.5	6.5	97.0	3.0
2	95	5	97.6	2.4	24.8	0.46	81.1	18.9	90.5	9.5
3	90	10	95.5	4.5	49.45	1.06	76.0	24.0	87.4	12.6
4	80	20	90	10	40.5	0.625	54.0	46.0	72.8	27.2
5	70	30	84	16	47.6	0.96	42.6	57.4	62.5	37.5

The copolymers of acrylonitrile with p-aminostyrene were white or cream powders, which dissolved readily in dimethylformamide. In contrast to pure polyacrylonitrile, the copolymer of acrylonitrile with p-aminostyrene dissolved in 50% sulfuric acid.

The solubility of the copolymer in 50% sulfuric acid depended on the composition of the copolymer, i.e., on the amino-group content. Copolymers containing less than 20 mol. % of p-aminostyrene were insoluble in 50% sulfuric acid.

The specific viscosity of the copolymers obtained varied from 0.43 to 1.06. Copolymers with a specific viscosity of 1 and above formed viscous solutions and films and fibers could be formed from them.

All the copolymers obtained at different monomer ratios were enriched in the second component, relative to the starting monomer mixture (table).

Application of diazotization and azo coupling to copolymers of acrylonitrile with p-aminostyrene. The amino groups in the copolymer were diazotized by the following method: a sample of the copolymer was dissolved in 50% H_2SO_4 with heating to 70° and stirring. The solution was cooled to 0° and to the reaction mixture was added a 10% aqueous solution of sodium nitrite. At the end of the reaction, the polymeric diazo compound was coupled with an azo component.

As a result of the azo coupling, the polymer formed a colored precipitate. The fact that the polymer became colored under our diazotization and coupling conditions showed that the amino groups of the copolymer were converted into the corresponding diazonium salts.

For determining the degree of diazotization and the corresponding percent of reagent added during azo coupling we used an indirect method based on determination of the increase in weight of the polymer as a result of the reaction. In special experiments, the azo component used was 2-naphthol-3,6-disulfonic acid, a compound with a high molecular weight (304).

Depending on the degree of swelling of the copolymer in the acid, the percent of reacting amino groups varied from 32 to 45%. The degree of conversion reached 75% for acid-soluble copolymers. In all the cases we examined, even for polymers which were diazotized to a small extent due to limited swelling, the polymers were converted into colored compounds. However, from the point of view of color intensity, the amino-group content of the copolymer played the most important role. Copolymers containing 3 mol. % of p-aminostyrene acquired only pale tones as a result of diazotization and azo coupling.

For a complete study of the reaction and to prepare polymers of different color, the diazo polymer was coupled with different azo components.

For this purpose we used: β -naphthol, phenol, 2-naphthol-3,6-disulfonic acid, α -naphthylamine, acetyl-H-acid, and also some specially synthesized intermediates. Thus, a black polymeric dye was obtained in analogy with the known aniline dye, "Naphthol Blue-Black" [9]. This was prepared by azo coupling of the diazo polymer with the product of coupling diazotized p-nitroaniline with H-acid.

In all the dyes synthesized from the copolymer of acrylonitrile with p-aminostyrene, the color of the dye obtained was the same as the dye synthesized from aniline. This shows that the reaction proceeded in the required direction and that the synthesis of such polymeric dyes is achieved quite readily.

The copolymers of acrylonitrile with p-aminostyrene could be diazotized and azo coupled not only in solution, but also under heterogeneous conditions. Films prepared from copolymer solutions were readily dyed bright colors as a result of brief immersion in a solution of sodium nitrite and acid and then in β -naphthol solution.

A p-aminostyrene content of 12.6 mol. % in the copolymer was sufficient for a color to appear when a film was immersed in a β -naphthol solution after being held in a solution of nitrite and acid for 5 minutes. With a higher amino group content in the copolymer, the dyeing began even more rapidly.

The application of diazotization and azo coupling to copolymers of acrylonitrile and p-aminostyrene is of definite practical interest. In this connection, the stability of colored films to the action of various chemical agents was studied. Prolonged treatment (40 minutes) of a colored film with 10% H_2SO_4 , 10% NaOH and 14% NH_4OH solutions at 100° had no effect on the color. The color was resistant to treatment with 20% H_2SO_4 at 70°. Slight darkening of the film occurred only when it was heated to 100° in 20% H_2SO_4 . Organic solvents such as pyridine, dioxane, chloroform, and glacial acetic acid did not change the color of the film and did not become colored themselves.

Thus the color of the polymer obtained as a result of diazotization and coupling was quite stable chemically and had a greater stability than the colors of azo dyes prepared by usual methods. Chemically dyed samples of copolymer had a high thermal stability. The color of the polymer changed at 248-250° when the temperature was gradually raised over a period of 1 hour; there was no change in color when a colored film was heated for 3 hours at 200-210°.

As the results of the work showed, dyeing under heterogeneous conditions was the most effective way of applying diazotization and coupling to copolymers. In connection with this, a cross section of a colored film was examined under a microscope to determine the depth of coloring of the film as a result of the chemical reactions. The cross section of the film from a copolymer containing 25.6 mol. % of p-aminostyrene, held for 5 minutes in a nitrite solution, had been dyed completely through the whole depth of the film. A film from the same copolymer, held in nitrite solution for 3 minutes, had a narrow uncolored band in the middle of the section.

Thus, as a result of simple operations, consisting of holding the copolymer film for 5 minutes in an acid solution of nitrite and immersing it in a β -naphthol solution, it was possible to dye the film throughout its depth. The colored samples had high chemical resistance and thermal stability.

The results on the dyeing of films may be transposed completely to fibers from acrylonitrile - p-aminostyrene copolymer.

SUMMARY

1. A method was developed for preparing copolymers from acrylonitrile and p-aminostyrene with a monomer ratio in the starting mixture from 98:2 to 70:30 and their properties were investigated. It was established that the copolymer was enriched in p-aminostyrene with respect to the original mixture of monomers.
2. The diazotization and azo coupling of copolymers of acrylonitrile and p-aminostyrene were investigated and it was shown that when the copolymer was diazotized in solution, 75-79% of the amino groups of the copolymer underwent conversion.
3. It was shown that diazotization and azo coupling can be used for dyeing manufactured articles from the acrylonitrile - p-aminostyrene copolymer (films and fibers) by carrying out the reaction under heterogeneous conditions. The time required for dyeing a film through its whole thickness did not exceed 5 minutes.

4. The dye formed as a result of the chemical reactions was stable to the action of organic solvents and hot solutions of acids and alkalis (10-20%).

LITERATURE CITED

- [1] G. E. Haml, *Text. Research J.* 24, 604 (1954).
- [2] B. C. Dorset, *Text. Manufacturer* 80, 87 (1954).
- [3] W. Kern and F. Schulz, *Makromol. Chem.* 69, 153-188 (1957).
- [4] Z. A. Rogovin, A. G. Yashunskaya, and B. M. Bogoslovskii, *Zhur. Priklad. Khim.* 23, 631 (1950).
- [5] W. Hahn and A. Fischer, *Makromol. Chem.* 21, 77 (1955).
- [6] J. Nakamura, *J. Chem. Soc. Japan, Ind. Chem. Sec.* 57, 892 (1954).
- [7] P. P. Shorygin and N. V. Shorygina, *Zhur. Obshchei Khim.* 12, 852 (1939).
- [8] W. B. Bond, *J. Pol. Sci.* 22, 181 (1956).
- [9] N. M. Kogan, *Chemistry of Dyes* [In Russian] (State Chem. Tech. Press, 1933), 108.

Received January 21, 1959

COKE FORMATION DURING DESTRUCTIVE CATALYTIC HYDROGENATION OF MAZUT

Ya. R. Katsobashvili, N. P. Volynskii, and T. N. Kuz'mina

Coke formation during the destructive hydrogenation of petroleum residues is a most undesirable process, leading to a reduction in the activity of the catalyst, a fall in the yields and quality of the petroleum products, and complication of the technological scheme of the process.

There are reports in the literature on the possibility of completely stopping coke formation by increasing the hydrogen pressure. According to Sakhanov and Tilicheev [1], in the destructive catalytic hydrogenation of semiasphalt, coke formation practically ceases with an initial hydrogen pressure of 200 atm (working pressure of about 400 atm). A high pressure in the reaction zone increases the partial pressure of hydrogen and displaces the equilibrium toward its addition to unsaturated and aromatic compounds, hindering their condensation, which finally leads to coke formation. Ipat'ev and his co-workers [2] also report that the decrease in coke formation with a rise in pressure depends on the increase in the partial pressure of hydrogen and not on the rise in pressure as such.

Somewhat later, Diner and Nemtsov [3] showed that the statements of Sakhanov and Tilicheev and others on the absence of coke formation in the destructive hydrogenation of petroleum residues can be ignored as the problem of quantitatively determining the coke was not solved satisfactorily. By means of elementary analysis they established that the coke content of the catalyst never fell below 4-5 weight % during the destructive hydrogenation of Groznyl paraffin mazut with an initial hydrogen pressure of 100-150 atm (operating pressure of about 250-375 atm). From three successive experiments with a spent catalyst, Diner and Nemtsov [4] arrived

at the conclusion that during operation a kind of "equilibrium" was established between coke formation and its hydrogenation so that the coke content of the catalyst was stabilized and no further coke formation was observed. Nemtsov [5] considered that this was confirmed by experiments on the hydrogenation of some petroleum products and tars, which he carried out in a flow apparatus in the presence of nickel and molybdenum catalysts at an operating pressure of 150 atm and 430°. However, in all these experiments a considerable amount of pitch (from 4.7 to 27% of the raw material weight) was formed in the reaction chamber, and in our opinion this should be considered as a product of polymerization and condensation finally leading to coke formation; the author said nothing on the coke content of the catalyst.

In the All-Union Scientific Research Institute of Synthetic Liquid Fuel and Gas, Karzhev [6] attempted the liquid-phase hydrogenation of heavy crude oil (d_{40}^{20} 0.956) over a stationary catalyst (WS_2) in a flow apparatus. Despite the low space velocity (0.2 kg/liter · hour) and high operating pressure (300 atm), the catalyst was rapidly covered with an asphalt-like film and lost its activity. From available literature material it follows irrefutably that the destructive catalytic hydrogenation of heavy crude oil is always accompanied by coke formation. Nonetheless, opinions on the possibility of the complete elimination of coke formation by the use of a high hydrogen pressure have been accepted despite the fact that they lack adequate foundations [7-9].

The present work was undertaken to elucidate the character of coke formation during destructive catalytic hydrogenation of mazut at a high hydrogen pressure in an autoclave.

EXPERIMENTAL

The experiments were carried out in a 1 liter rotating autoclave with a rotation rate of 75 rev/min, heated by an electric heater and designed for operation at 500 atm and 500°. The temperature was registered with an automatic recording potentiometer. The raw material used was 50% mazut from a mixture of oils from the Romashkina and Shugurovo deposits (sp. g. 0.961), containing (in weight %): sulfur 2.49, asphaltenes 4.90, coke number 9.1 weight %; 13.9 weight % distilled up to 350°. For all the experiments we used industrial aluminomolybdenum catalyst No. 7360, containing 14% of molybdenum oxide on aluminum oxide. Into the autoclave was loaded a mixture of 100 g of mazut and 100 g of catalyst,* the autoclave flushed with hydrogen, and hydrogen pumped in to a pressure of 110 atm. The time required to heat the autoclave up to the experimental temperature (455°) was about 60 minutes. The autoclave was kept at this temperature for 12-18 minutes and then heating was stopped and the autoclave cooled. After the pressure had been reduced to atmospheric, the contents of the autoclave were transferred to a Wurtz flask, which was heated on an oil bath (oil temperature 170-180°) and part of the volatile fractions distilled; the heavier fractions were distilled under reduced pressure (about 5 mm Hg). The dry catalyst powder was transferred from the Wurtz flask to a Soxhlet extractor, where the heavy petroleum products were extracted with benzene. The benzene was distilled from the extract obtained, at first at atmospheric pressure and finally in vacuum; the heavy fractions of the petroleum product thus isolated were mixed with the light fractions distilled previously. The hydrogenation product thus obtained was distilled to give fractions with boiling points up to 200°, 200-350° and a residue > 350°. The catalyst was dried in air and the residual adsorbed benzene removed by heating the catalyst at 170° for 30 minutes in vacuum. A 0.5 g sample of catalyst was taken for determination of its coke content,** and the rest of the catalyst mixed with a fresh portion of mazut and the next experiment on the destructive hydrogenation of mazut with spent catalyst carried out.

* Katsobashvili and Kurkova [10] established that the optimal ratio of catalyst to raw material in the destructive hydrogenation of mazut in an autoclave equals approximately 1:1 by weight.

** The coke content of the catalyst was determined by elementary analysis (combustion of a catalyst sample in a stream of oxygen in a quartz tube filled with granulated copper oxide). The carbon dioxide was absorbed in potash bulbs in which the second, upper reservoir was replaced by an S-tube with sulfuric acid, making it possible to determine the amount of carbon dioxide absorbed after one weighing. To exclude excessive wetting of the sulfuric acid during storage of the potash bulbs, the latter were fitted with a tap which cut off communication between the S-tube and the potash bulbs.

We carried out 21 successive destructive hydrogenations of mazut on the same portion of alumino-molybdenum catalyst at 455° and a working pressure of 250-270 atm. The catalyst from an experiment was used for the next experiment without regeneration. These experiments showed that despite the high hydrogen pressure, the amount of coke on the catalyst steadily increased from experiment to experiment. In the first experiment, the fresh catalyst adsorbed 1.8% of coke due to its adsorption properties, and the subsequent increase in the coke content of the catalyst was 0.1 to 0.3% in each experiment (table). The coke content of the catalyst reached 6.1% in the last experiment (No. 21). Thus, the widespread opinions [3-5, 7, 9] on the possibility of complete elimination of coke formation by using a high hydrogen pressure (200 - 300 atm) and on the establishment of an "equilibrium" between coke formation and its hydrogenation are not confirmed by our experimental data.

The table shows that the error of the method of determining the carbon on the catalyst did not exceed 0.1-0.15% in most cases, and data were quite reliable. Since these values correspond to the increase in the coke content of the catalyst from experiment to experiment, it was not possible to draw any conclusions on coke formation from 2-3 experiments. This is apparently the reason for the error of Nemtsov et al., who concluded that there is no coke formation in the destructive hydrogenation of mazut on the basis of only three successive experiments.

Coke Formation During Destructive Catalytic Hydrogenation of Mazut in an Autoclave.
Operating Pressure 270 atm, Temperature 455°, Experiment time 12-18 minutes

Expt. No.	Catalyst taken from experiment	Amount of coke in catalyst (in weight%) by determination			Hydrogenation product		Residue above 350°	
		I	II	average	Residue above 350°	Sulfur content (in weight%)	specific gravity (d ₄ ²⁰)	Sulfur content (in weight%)
1	Fresh	1.82	1.88	1.85	0.8555	0.045	0.8899	0.06
2	№ 1	1.98	2.05	2.01	—	—	0.8850	0.09
3	№ 2	2.42	2.45	2.43	0.8509	0.029	0.8803	0.06
4	№ 3	2.85	3.14	3.00	0.8569	0.026	0.8866	0.05
5	№ 4	3.24	3.35	3.30	0.8595	0.035	0.8895	0.07
6	№ 5	3.60	3.70	3.65	0.8546	0.051	0.8873	0.08
7	№ 6	4.07	4.08	4.08	0.8539	0.020	0.8845	0.06
8	№ 7	4.28	4.40	4.34	0.8325	0.010	0.8800	0.05
9	№ 8	4.34	4.47	4.40	0.8480	0.010	0.8895	0.05
10	№ 9	4.60	4.64	4.62	0.8377	0.020	0.8742	0.02
11	№ 10	4.61	4.65	4.63	0.8495	0.030	0.8940	0.02
12	№ 11	4.48	4.74	4.61	0.8484	0.030	0.8820	0.05
13	№ 12	5.03	5.10	5.06	0.8506	0.030	0.8887	0.04
14	№ 13	5.20	5.40	5.30	0.8585	0.060	0.8927	0.08
15	№ 14	5.27	5.30	5.28	0.8612	0.080	0.8900	0.09
16	№ 15	5.27	5.53	5.40	0.8593	0.080	0.8953	0.10
17	№ 16	5.37	5.62	5.50	0.8625	0.040	0.8854	0.10
18	№ 17	5.60	5.62	5.61	0.8525	0.030	0.8928	0.06
19	№ 18	5.58	5.58	5.58	—	—	0.8884	0.09
20	№ 19	5.98	6.00	5.99	0.8496	0.020	0.8851	0.10
21	№ 20	6.02	6.18	6.10	0.8648	0.040	0.8870	0.08

The difference between the coke content of the catalyst after experiment No. 21 and experiment No. 1 was 4.3%, which excludes any effect of the error in determining the carbon content on our conclusions on the existence of coke formation during the destructive hydrogenation of mazut at a pressure of the order of 300 atm. There was no appreciable decrease in the activity of the catalyst after experiment No. 21; the yields of hydrogenation products, fractions up to 350° and residues above 350°, and also specific gravities, sulfur contents and other properties, remained practically the same throughout the experiments (table).

SUMMARY

The use of a high operating hydrogen pressure (250-270 atm) in the destructive catalytic hydrogenation of mazut did not lead to the cessation of coke formation or to "equilibrium" operating conditions of the catalyst, and consequently the need for a catalyst regeneration stage cannot be excluded.

LITERATURE CITED

- [1] A. N. Sakhanov and M. D. Tilicheev, Transactions of the Conference on Cracking and Hydrogenation [In Russian] (State United Sci. Tech. Press, Moscow-Leningrad, 1931), p. 147.
- [2] V. N. Ipat'ev, M. A. Belopol'skii, and M. S. Nemtsov, Transactions of the Conference on Cracking and Hydrogenation [In Russian] (State United Sci. Tech. Press, Moscow-Leningrad, 1931), p. 119.
- [3] I. S. Diner and M. S. Nemtsov, Khim. Tv. Topl., 3, 9-10, 727 (1932).
- [4] I. S. Diner and M. S. Nemtsov, Khim. Tv. Topl., 4, 2, 136 (1933).
- [5] M. S. Nemtsov, Destructive Hydrogenation of Fuels [In Russian] (United Sci. Tech. Press, 1934).
- [6] V. I. Karzhev, Trudy VNIGI 4, 87 (1952).
- [7] V. I. Karzhev and D. I. Orochko, Trudy VNIGI 3, 71 (1951).
- [8] V. I. Karzhev and D. I. Orochko, Neft. Khoz. 9, 38 (1953).
- [9] I. V. Rapoport, Synthetic Liquid Fuels, 1 [In Russian] (State Fuel Tech. Press, Moscow-Leningrad, 1949), p. 131.
- [10] Ya. R. Katsobashvili and N. S. Kurkova, Trudy Inst. Nefti Akad. Nauk SSSR 1, 89 (1954).

Received September 29, 1958

ELECTROSYNTHESIS OF TETRA-(β -CYANOETHYL)STANNANE

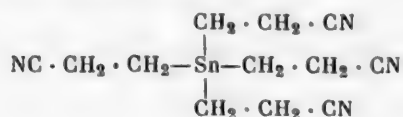
A. P. Tomilov and L. V. Kaabak

In the electrolysis of a mixture of an electrolyte solution and an organic substance, the latter is usually reduced at the cathode, but in some cases a completely different type of cathode process is observed which consists of solution of the cathode metal to form an organometallic compound.

Up to now this type of reaction has been observed in the electroreduction of a series of aldehydes and ketones at lead and mercury cathodes. Thus, electroreduction of acetone on a mercury cathode gave diisopropylmercury [1], and diisobutylmercury was obtained from methyl ethyl ketone [2] and dimethylmercury from menthol [3] by a similar method. Acetone formed a mixture of diisopropyl- and tetraisopropyllead on a lead cathode; methyl ethyl ketone gave tetrabutyllead, and diethyl ketone gave tetraamyllead [4, 5]. Organolead compounds were isolated, but not identified in the electrolysis of some aldehydes [6, 7].

We established that in the electrolysis of an aqueous alkaline solution of acrylonitrile with a tin cathode, a heavy, colorless oil collected at the bottom of the electrolyzer. A study of this substance showed that it was tetra-(β -cyanoethyl)stannane, which has not been described in the literature.

Tetra-(β -cyanoethyl)stannane was a heavy, colorless liquid which



was insoluble in water, benzene and ether; it dissolved in dioxane and chloroform. Recrystallization from chloroform gave colorless crystals which melted at 23-23.5°; d_4^{20} 1.4358, n_D^{20} 1.5339. The substance decomposed when heated above 200° and could not be distilled without decomposition, even in high vacuum (10^{-4} mm Hg).

The yield of organotin compound depended to a considerable extent on the electrolysis conditions. At high current densities (above 2000 A/m²) the tin cathode lost hardly any weight. As the current density was decreased, the yield of organometallic compound increased and at a current density of about 200 A/m² it was 50-60%.

In similar experiments with lead and mercury cathodes, the formation of an organometallic compound was not observed.

It is quite probable that similarly to the electroreduction of ketones [8], the formation of the organotin compound in this case occurred through the intermediate formation of a free radical $-\text{CH}_2-\text{CH}_2\cdot\text{CN}$, the possibility of whose formation has already been discussed in an examination of the reduction mechanism of acrylonitrile with alkali-metal amalgams [9].

EXPERIMENTAL

A 200 ml rectangular glass bath without a diaphragm was used as the electrolyzer. The cathode was cast from pure tin in the form of a rectangular bar, 60 × 80 mm and 6 mm thick. A bent steel tube was placed in the form during casting of the electrode. This tube was used for the electrical connection and at the same time for maintaining the required temperature in the bath; cold water was circulated through the tube to cool the solution. Two perforated nickel plates were the anodes.

The procedure was as follows: 0.5-1.0 N sodium hydroxide solution, saturated with acrylonitrile, was placed in the electrolyzer. The addition of acrylonitrile was begun after the current had been switched on. The electrolysis lasted 4-5 hours.

After electrolysis the solution was poured into a separating funnel. The heavy oil that accumulated was separated, washed several times with water, and then dried in vacuum.

A typical experiment is described below: 200 ml of 0.7 N sodium hydroxide solution, saturated with acrylonitrile was loaded into the electrolyzer and acrylonitrile was added at the rate of 15 ml/hr after a 5 A current had been switched on. The bath temperature was 14-16°. After 5 hours of electrolysis the cathode weight had decreased by 8.00 g. 23.6 g of organotin compound was isolated, which corresponds to a current yield of 36.3%.

The compound obtained was recrystallized twice from chloroform.

Elementary analysis gave: C 43.33, 43.21; H 5.10, 5.28; N 16.67, 16.37; Sn 35.25, 35.11; n_D^{20} 1.5339, d_4^{20} 1.4358; molecular weight (ebullioscopy in chloroform) 361.3, 353.9, molecular refraction 72.736 (the tin was determined by Gilman's method [10]).

Calculated for $(\text{C}_3\text{H}_4\text{N})_4\text{Sn}$: C 43.024, H 4.815, N 16.717, Sn 35.433; molecular weight 335.0, molecular refraction 72.461.

LITERATURE CITED

- [1] J. Haggerty, Trans. Amer. Electrochem. Soc. 56, 421 (1929).
- [2] J. Tafel, Ber. 36, 3626 (1906).
- [3] C. Schall and W. Kirst, Z. Elektrochem. 29, 537 (1923).
- [4] J. Tafel, Ber. 44, 323 (1911).
- [5] G. Renger, Ber. 44, 337 (1911).
- [6] H. Law, J. Chem. Soc. 1016, 1544 (1912).
- [7] W. Schepss, Ber. 46, 2564 (1913).

- [8] W. Waters, Chemistry of Free Radicals [Russian translation], (Foreign Lit. Press, Moscow, 1948), p. 161.
- [9] I. L. Knunyants and N. S. Vyazankin, *Izvest. Akad. Nauk SSSR Otdel. Khim. Nauk* 2, 238 (1957).*
- [10] H. Gilman and B. King, *J. Amer. Chem. Soc.* 51, 1213 (1929).

Received February 9, 1959

SYNTHESIS OF RHODANINE

A. P. Grishchuk and S. N. Baranov

Rhodanine (2-thionthiazolidone-4) is used for the synthesis of various derivatives which are used in inorganic analysis [1] and photography and have lately acquired interest as substances with physiological action [2]. The condensation products of aldehydes and rhodanine are often used to prepare thiopyruvic acids which can be converted readily to hydroxyamino acids, amino acids, nitriles and amines, which often cannot be synthesized by other methods [3]. We also proposed a method for synthesizing a new group of rhodanine derivatives, namely azorhodanines [2].

Rhodanine was first synthesized by Nencki [4] in 1877, who condensed monochloroacetic acid with ammonium thiocyanate in an aqueous solution. In 1935 Julian and Sturgis [5] proposed a method, that was included in the collection "Synthesis of Organic Preparations" [6], which gave a high yield of highly pure rhodanine (72-77% of recrystallized product, calculated on chloroacetic acid).

However, this method of preparing rhodanine is carried out at a low temperature (cooling with ice), requires a poisonous and inflammable material, carbon bisulfide, and an alcohol-ammonia solution, and it takes about 30 hours.

As rhodanine is not produced by the Soviet chemical industry, we decided to study the possibility of increasing its yield, confining ourselves to the Nencki method as the simplest one.

We investigated the condensation of Na, K or NH_4 salts of monochloroacetic acid with various thiocyanates (NH_4 , K, Na) in an aqueous solution followed by acidification with hydrochloric acid. We studied the yields and purity of the rhodanine in relation to the thiocyanates taken, solution concentration, condensation temperature, reagents taken for neutralizing the chloroacetic acid, and hydrochloric acid concentration. We established that any of the three thiocyanates could be used with equal success in the reaction by this method and that the chloroacetic acid was best neutralized with solid potassium carbonate. The primary heating (before acidification) should be for 3-5 minutes at 60-70°; an increase in time and temperature gave a worse result.

Of the different versions for the condensation, the following method gave the best result: 19 g (0.2 mole) of monochloroacetic acid was dissolved in 40 ml of water and neutralized to phenolphthalein with solid potassium carbonate. Then 46 g (0.6 mole) of ammonium thiocyanate or 49 g of NaSCN was added and the solution heated to 60-70° for 2-4 minutes, after which 90 ml of hydrochloric acid (1:1) was added rapidly and the whole solution was again heated to 80°. Voluminous but steady gas evolution began and the temperature rose to 105-110°. The light yellow solution was shaken and heated until foaming ceased (5-10 minutes), after which the solution was left. Rapid crystallization began immediately. The yield of quite coarse, pale-yellow rhodanine crystals was 15-16 g and after the product had been recrystallized from water with charcoal, it was 13.2-13.6 g, i.e., 50% [7].

*Original Russian pagination. See C.B. Translation.

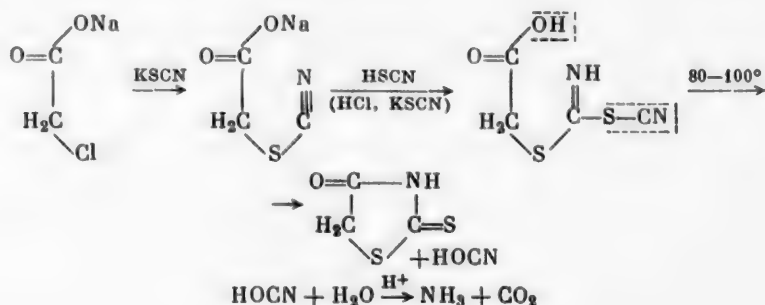
As is known, the details of the Nencki reaction have not been elucidated, but one may consider that thiocyanoacetic acid is the intermediate product. This is confirmed by the experiment of Klason [8] who in 1877 obtained rhodanine by treating thiocyanoacetic acid with HSCN in an ether solution.

The whole course of our experiments indicated that rhodanine is formed in three stages: 1) formation of thiocyanoacetic acid (or its salts), 2) interaction of thiocyanoacetic acid with free HSCN, and 3) cyclization of the compound formed to give rhodanine.

The success of the synthesis depended directly on the amount of free thiocyanic acid in the solution and an insufficient amount is the main reason for low rhodanine yields in the Nencki method. When Nencki introduced chloroacetic acid into the reaction a small amount of HSCN formed immediately and therefore the process of thiocyanoacetic acid decomposition of HSCN volatilization dominated the cyclization to rhodanine.

By neutralizing the monochloroacetic acid, we ensured the formation of the more stable thiocyanoacetate in the absence of free HSCN and then the latter was formed by hydrochloric acid acidification of the reaction mixture containing excess thiocyanate. The addition of HSCN and then cyclization at a comparatively high temperature proceeded in parallel with rapid volatilization of HSCN from the solution and the latter process presumably explains the yield of not more than 51%.

We propose the following scheme for the formation of rhodanine:



SUMMARY

1. New conditions for a simple synthesis of rhodanine were developed by modifying the Nencki method, and this increased the yield from 15-16% to 49-51%, i.e., by a factor of three.
2. A probable scheme for the formation of rhodanine is proposed.

LITERATURE CITED

- [1] V. I. Kuznetsov, Doklady Akad. Nauk SSSR 50, 233 (1949).
- [2] A. P. Grishchuk and S. N. Baranov, Zhur. Obshchei Khim. 28, 896 (1958).
- [3] R. Adams, Organic Reactions [Russian translation] (Foreign Lit. Press, 1948).
- [4] M. Nencki, Ber. 17, 2278 (1884).
- [5] P. Julian and B. Sturgis, J. Amer. Chem. Soc. 57, 1126 (1935).
- [6] Syntheses of Organic Preparations [Russian translation] Coll. 4, (Foreign Lit. Press, Moscow, 1953), p. 436.
- [7] A. P. Grishchuk and S. N. Baranov, Soviet Author's Certificate No. 119,529, June 23, 1958.
- [8] P. Klason, Bih. Sven. Vet.-Acad. 8, 11 (1877).

*Original Russian pagination. See C. B. Translation.

Received June 23, 1959

PREPARATIVE METHOD FOR β -(*o*-CARBOXYMETHYLPHENYL)PROPIONIC ACID

F. N. Stepanov and M. O. Iodko

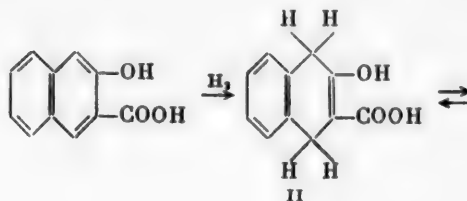
Scientific Research Institute of Organic Intermediates and Dyes

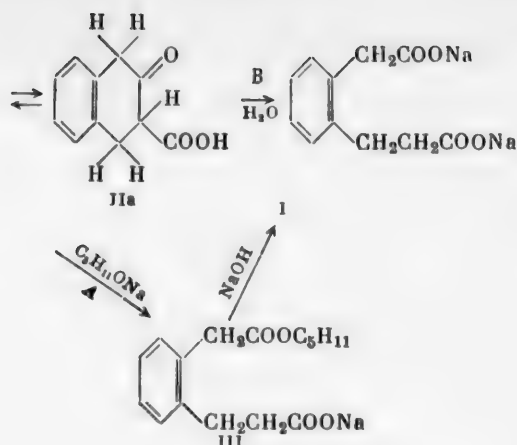
In carrying out an investigation [1] in which β -(*o*-carboxymethylphenyl) propionic acid (I) was used as a starting material, we found that on preparing this substance by the Einhorn and Lumsden method [2] the result depended considerably on the degree of moisture in the reaction mass. We were unable to obtain an appreciable amount of (I) by using anhydrous 3-hydroxy-2-naphthoic acid and dry isoamyl alcohol (0.03% moisture). The introduction of water into the reaction mass had a favorable effect. As the amount of water added was increased to 1.5 mole per mole of 3-hydroxy-2-naphthoic acid, an increase in the yield of (I) was observed, as can be seen from the following.

Amount of water in moles per mole of 3-hydroxy-2-naphthoic acid	Yield of (I) (in % of theoretical)
0.05	3.0—5.2
0.10	11.9—12.7
0.60	31.0—32.0
0.80	34.8—36.2
1.00	36.9—39.0
1.50	46.6—53.2
2.00	44.0
3.00	33.9—40.1

The maximum yield of (I), equal to 53.2% of theoretical, was obtained with a molar ratio of water to 3-hydroxy-2-naphthoic acid of 1.5:1. A further increase in the amount of water had a negative effect.

The results obtained not only made it possible to select the optimal conditions for a preparative method of obtaining (I), but also to draw some conclusions on the mechanism of the reaction. The discoverers of this reaction put forward the hypothesis that the primary product is the dihydro compound (II) whose tautomeric form (IIa) is then cleaved to form (I). As the reaction proceeds in an alcoholic medium, one might think that (IIa) is cleaved by the action of the alcoholate to form (III) and only then by boiling the reaction mass in an aqueous alcohol-alkali medium is (IIa) converted to (I) (Scheme A). Our observations indicate that scheme B is more probable and according to it (IIa) is converted directly to (I) by the action of the water in the reaction medium.





EXPERIMENTAL

In a 1 liter flask 60 g of metallic sodium was melted under a layer of 125 ml of isoamyl alcohol (b. p. 129-130°) and then a solution of 34 g of 3-hydroxy-2-naphthoic acid in 500 ml of isoamyl alcohol, containing the required amount of water, added to the vigorously boiling solution over a period of an hour. Toward the end of the addition of the acid solution the temperature of the mass was raised to 160-170°. The solution was boiled until the sodium had dissolved completely (about 6 hours), cooled to 140-150° and poured carefully into 300 ml of cold water. After the mass had dissolved, the aqueous layer was separated, the alcohol layer washed 3 times with 150 ml portions of hot water, and the aqueous solutions combined. The mixture was acidified with concentrated hydrochloric acid to a weakly acid reaction to congo, the residual isoamyl alcohol steam distilled, and the unreacted 3-hydroxy-2-naphthoic acid removed by filtering the solution cooled to 90°. The filtrate was made strongly acid, cooled, and repeatedly extracted with ether. The combined ether extracts were washed with small portions of water and dried with sodium sulfate and the ether removed. The residue was quite pure β -(o-carboxymethylphenyl)propionic acid with m. p. 139-140° (literature data: m. p. 140° [2]). A water content of 1.5 moles (relative to 3-hydroxy-2-naphthoic acid) resulted in a yield of 17.5-20.0 g.

SUMMARY

It was established that to obtain good yields of β -(o-carboxymethylphenyl)propionic acid by the Einhorn and Lumsden method, it is necessary to add to the reaction mass 1.5 moles of water, relative to the 3-hydroxy-2-naphthoic acid taken.

LITERATURE CITED

- [1] F. N. Stepanov, M. O. Iodko, and N. S. Vul'fson, Ukrain. Khim. Zhur. 23, 489 (1957).
- [2] A. Einhorn and I. S. Lumsden, Lieb. Ann. 286, 257 (1895).

Received December 7, 1958

SYNTHESIS AND PROPERTIES OF SOME POLYESTERS OF SUBSTITUTED PHOSPHORIC ACIDS

I. K. Rubtsov and R. D. Zhilina

Polyesters of substituted phosphoric acids are usually prepared by polycondensing equimolecular amounts of diacid halides of these acids with glycols or dihydric phenols [1-3]. The purpose of our work was to synthesize a series of polyesters of substituted phosphoric acids and to investigate the thermal stability of the resins obtained in relation to the starting materials. The components used for the preparation of the diacid chlorides of substituted phosphoric acids were phenol, p-tert-butylphenol, p-cumylphenol, and o- and p-chlorophenols. The diacid chlorides, prepared by the usual method, were condensed with dihydric phenols (hydroquinone, resorcinol and diphenylolpropane).

EXPERIMENTAL

Preparation of p-tert-butylphenyl phosphorodichloridate. Into a three-necked, round-bottomed flask fitted with a stirrer, thermometer and reflux condenser, were placed 428 g of p-tert-butylphenol, 437 g of phosphorus oxychloride and 12.8 g of potassium chloride (3% of the phenol weight). The reaction mixture was heated to the boiling point with continuous stirring. During the reaction a voluminous amount of hydrogen chloride was evolved. As the diacid chloride formed, and consequently, as the amount of phosphorus oxychloride decreased, the temperature of the reaction mixture rose. When it reached 150° (after approximately 4 hours) the reaction mixture was kept at that temperature for a further hour. After cooling, the diacid chloride obtained was transferred to a Claisen flask and the residual hydrogen chloride removed under reduced pressure.

The substance was vacuum distilled for final purification. The reactions with phenol, p-cumylphenol, and o- and p-chlorophenols were carried out analogously.

The properties of the substances obtained are given in the table.

All the diacid chlorides of the substituted phosphoric acids synthesized were used as starting materials for polycondensation. As an example, we will describe the preparation of a polyester based on the p-tert-butylphenyl phosphorodichloridate and resorcinol. A mixture of 667.5 g of p-tert-butylphenyl phosphorodichloridate (2.5 moles), 275 g of resorcinol (2.5 moles) and 0.6 g of tin (0.1% of the weight of diacid chloride), protected from atmospheric moisture, was heated to 145-150° for 8 hours and then kept at 185° for 20 hours.

Samples were collected during the reaction to determine the acid numbers. After approximately 28 hours the acid number reached 22.5 and further heating of the reaction mixture hardly reduced it. After the reaction the residual hydrogen chloride was removed from the resin at 120-130° in vacuum. The hot resin was poured into molds in which it solidified as a clear, slightly yellow, glassy mass.

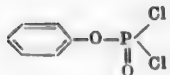
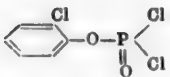
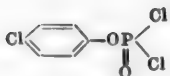
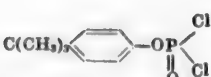
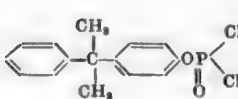
Diphenylolpropane and hydroquinone were reacted similarly.

The polyesters obtained from the diacid chlorides of substituted phosphoric acids synthesized and dihydric phenols were solid and, in most cases, glassy products with very small differences in melting points (over the range 33-86°) depending on the components used in the reaction.

All the resins were soluble in acetone, benzene, toluene, xylene, and dichloroethane; they were insoluble in alcohols (ethyl, methyl, butyl, 2-ethylhexyl, etc.), water, and ether.

The most interesting property of these resins is their complete incapacity for burning or supporting combustion (test with alcohol-burner flame). The addition of not less than 30% of phosphorus-containing resins to phenol-formaldehyde, urea-formaldehyde and polyester resins gave incombustible products. The phosphorus-containing polyesters may be added by the usual methods, namely, rolling, solution, etc.

Properties of Diacid Chlorides of Substituted Phosphoric Acids

Formula of diacid chloride	Boiling point (in °C)	Residual pressure (in mm Hg)	n_D^{20}	d_4^{20}	MR_D		Cl content (in %)		Yield of diacid chloride (in %)
					found	calc.	found	calc.	
	105—108	8	1.5320	1.4207	45.75	45.32	33.1	32.98	86.7
	123—125	7	1.5372	1.5234	50.32	50.35	43.01	43.34	77.1
	127—130	7	1.5380	1.5236	50.36	50.35	43.10	43.34	79.5
	141—143	4	1.5136	1.2472	64.38	64.7	26.41	26.57	87.3
	167—170	2	1.5670	1.2658	84.8	84.1	21.2	21.56	71.5

LITERATURE CITED

- [1] H. Zenftman, Brit. Plast. 25, 347 (1952).
- [2] R. Tunteler, Plastica 6, 156 (1953).
- [3] B. Helferich and H. G. Schmidt, Federal German Republic Patent 905,318; Chem. Zentr. 9169 (1954).

Received February 9, 1959

BOOK REVIEW

Z. V. Pushkareva, *New Synthetic Materials* [In Russian], (Sverdlovsk Book Press, 1959), 10,000 copies.

The publication of popular scientific literature is a difficult but extremely important and laudable task. The author of a popular scientific book must select, check, and organize the factual material especially carefully and make sure that it is presented in a well-edited and widely available form at a modern scientific level. Ignoring this immutable rule always leads to undesirable, but inescapable results: the efforts are fruitless and the published book, a barren product.

That is what happened with the book being reviewed; the importance of the theme did not help the author to produce a valuable work.

The factual material is presented unsystematically, in a summarized form, not clearly enough for the lay reader, and too primitively and incompletely to interest the specialist. It appears that it was not edited by a specialist. The book contains many inaccuracies, confused terms and ideas, crude misrepresentations and mistakes which are inadmissible in print and the more so in a popular edition.

Through a whim of the author, the unequivocal concept of a "molecule", which we learned at school, acquires an "original" multiplicity of meanings (unacceptable scientifically) which are, furthermore, inaccurate. The author writes "chemical molecules" on p. 11, "simple molecules" on pp. 15, 16, and 21, and "radical molecules" on p. 20. The last term is quite absurd from the point of view of classical physical concepts.

Generally accepted scientific terms are often replaced by the author's own expressions which are unclear and incorrect in a majority of cases. Thus, the author mentions "polymeric resins" on pp. 40 and 49 and "polymeric fibers" on p. 48.

The term "multiple center" is changed to "multiple bond" (p. 17). "Ethyl alcohol" is called "ethyl, wine alcohol" (p. 24). On p. 21 two different sciences are confused, namely, radiation chemistry* and radiochemistry.**

With this strange tendency to replace everything, the author distorts even the coefficient "n" (small Latin "n"), which is generally accepted in science, to the Russian capital "H", thus completely bewildering the reader, as with this transcription, the letter coincides with the chemical symbol for hydrogen (pp. 21 and 33).

There are other inaccuracies, contradictions and errors. On some pages they appear in groups. Thus, for example, p. 15 contains an incorrect molecular weight for penicillin*** and the incorrect statement (without any provisos) "that polymers are water insoluble", while a whole series of water-soluble high polymers (for example, glycogen, inulin, etc.) are known. On the same page the term "polymerization" is identified with the unacceptable expression "condensation".

* БЭС (2nd Edition), Vol. 46, p. 177.

** БЭС (2nd Edition), Vol. 35, p. 576.

*** Actually 312 and 334.

On p. 10, in writing of the preparation of urea by the German chemist Wöhler, the author makes an error of exactly one hundred years.

The author incorrectly informs the reader of the use of nitrate silk (p. 46). It is known that the industrial production of this was stopped in the 1930's. *

In speaking of chemicals, which (as an exception) decompose fluoroplastics, (p. 18) the author forgets to mention chlorine trifluoride. ** The book also does not mention that this remarkable plastic not only has greater chemical stability than other plastics, but also has greater thermal stability and better dielectric properties than the majority of them.

On p. 16 there is another error: it is not high-frequency cable itself, but its insulation that is prepared from polyethylene.

A whole series of the author's statements will quite naturally perplex the majority of readers: for example how is a protein fiber prepared from cellulose (p. 45)? How is a molecule of natural cellulose "rebuilt" to give a continuous fiber (ibid)? What is a foam plastic, a name which is only mentioned in the text (p. 32)?

How are fibers made from polystyrene (p. 32)? How is one to understand the capacity of polypropylene to "withstand any impact"? Why is polypropylene welded in an inert gas atmosphere if, as the author states, it has "excellent chemical properties" (chemical stability — I. F., pp. 34 and 35)?

With the best of intentions, it is impossible to find answers to any of these and many other questions in the book as the factual material in it is written in such a summarized, fragmentary and confused form.

Without explaining the meanings of synonyms for high polymers or plastics, the author unreservedly uses for some of these quite varied and sometimes incorrect names, such as phenol-formaldehyde plastic masses (p. 30), phenoplastics and phenol-formaldehyde plastics (p. 28); condensation plastics (p. 30) and polycondensation resins (p. 28). In addition, in the last case the concept of "resin" is erroneously identified with plastics, while polymers (pp. 14, 16, 17, etc.) are identified with high-polymer substances (pp. 15, 67). It is clear that special remarks on this subject are required in a popular book.

The basic conception of plastics (p. 27) is given in outline and simplified; for example, there is no mention of the binder as an important component of these complex compositions. The expedient and convenient (especially for manufacturers and technologists) classification of plastics by the behavior of their main binder on heating (division into thermoplastic and thermosetting resins) is completely ignored. The book also makes no mention of the remarkable property of synthetic fibers of being unaffected by the action of microorganisms which is an advantage over natural materials (especially when used under tropical conditions).

This gives an incomplete list of the serious shortcomings of this publication.

The book reviewed cannot be recommended for popular reading. There can be no talk of reprinting it. There are too many errors in a comparatively short book (74 pages). The publication of such valueless books, and furthermore, the printing of a large number of copies is surprising. This is an outstanding error on the part of the Sverdlovsk Book Press.

I. G. Filatov

* BES, Vol. 9, p. 13.

** D. D. Chegodaev, *Fluoroplastics* [In Russian] (State Chem. Press, 1956), p. 70.

SIGNIFICANCE OF ABBREVIATIONS MOST FREQUENTLY
ENCOUNTERED IN SOVIET PERIODICALS

FIAN	Phys. Inst. Acad. Sci. USSR.
GDI	Water Power Inst.
GITI	State Sci.-Tech. Press
GITTL	State Tech. and Theor. Lit. Press
GONTI	State United Sci.-Tech. Press
Gosenergoizdat	State Power Press
Goskhimizdat	State Chem. Press
GOST	All-Union State Standard
GTTI	State Tech. and Theor. Lit. Press
IL	Foreign Lit. Press
ISN (Izd. Sov. Nauk)	Soviet Science Press
Izd. AN SSSR	Acad. Sci. USSR Press
Izd. MGU	Moscow State Univ. Press
LEIIZhT	Leningrad Power Inst. of Railroad Engineering
LET	Leningrad Elec. Engr. School
LETI	Leningrad Electrotechnical Inst.
LEIIZhT	Leningrad Electrical Engineering Research Inst. of Railroad Engr.
Mashgtz	State Sci.-Tech. Press for Machine Construction Lit.
MEP	Ministry of Electrical Industry
MES	Ministry of Electrical Power Plants
MESEP	Ministry of Electrical Power Plants and the Electrical Industry
MGU	Moscow State Univ.
MKhTI	Moscow Inst. Chem. Tech.
MOPI	Moscow Regional Pedagogical Inst.
MSP	Ministry of Industrial Construction
NII ZVUKSZAPIOI	Scientific Research Inst. of Sound Recording
NIKFI	Sci. Inst. of Modern Motion Picture Photography
ONTI	United Sci.-Tech. Press
OTI	Division of Technical Information
OTN	Div. Tech. Sci.
Stroiizdat	Construction Press
TOE	Association of Power Engineers
TsKTI	Central Research Inst. for Boilers and Turbines
TsNIEL	Central Scientific Research Elec. Engr. Lab.
TsNIEL-MES	Central Scientific Research Elec. Engr. Lab. - Ministry of Electric Power Plants
TsVTI	Central Office of Economic Information
UF	Ural Branch
VIESKh	All-Union Inst. of Rural Elec. Power Stations
VNIIM	All-Union Scientific Research Inst. of Meteorology
VNIIZhDT	All-Union Scientific Research Inst. of Railroad Engineering
VTI	All-Union Thermotech. Inst.
VZEI	All-Union Power Correspondence Inst.

Note: Abbreviations not on this list and not explained in the translation have been transliterated, no further information about their significance being available to us. - Publisher.



RESEARCH BY SOVIET EXPERTS

Translated by Western Scientists

INSTABILITY CONSTANTS OF COMPLEX COMPOUNDS

by K. B. Yatsimirskii and V. P. Vasil'ev

Instability constants quantitatively characterize the equilibrium in solutions of complex compounds and, in this connection, are very widely used by chemists in different fields (analytical chemistry, electrochemistry, technology of nonferrous and rare metals, etc.) for appropriate calculations.

The instability constants of 1381 complex compounds are given. The authors have prefaced the summary of instability constants with an introductory section which examines methods of calculating instability constants from experimental data, the effect of external conditions (temperature and ionic strength) on the stability of complexes and the main factors determining the stability of complex compounds in aqueous solutions.

Cloth

200 pages

\$6.75

SOVIET RESEARCH ON COMPLEXES AND CO-ORDINATION CHEMISTRY

This collection consists of 372 articles by Russian scientists in the general area of the chemistry of complexes. These reports have been compiled from the Consultants Bureau translations of the following Soviet journals:

Journal of General Chemistry
Journal of Analytical Chemistry
Bulletin of the Academy of Sciences
Division of Chemical Sciences
Proceedings of the Academy of Sciences
Journal of Applied Chemistry
Soviet Journal of Atomic Energy

The articles have been grouped into five volumes, each of which may be purchased separately.

I. Inorganic Complexes—103 articles	\$65.00
II. Metal-Organic Complexes—86 articles	\$45.00
III. Thermodynamic and Kinetic Studies—57 articles	\$37.50
IV. Complexes in Analytical Chemistry—57 articles	\$37.50
V. Condensed Inorganic Systems; {		
Miscellaneous {		
—38 articles	..	
—31 articles	..	\$45.00
Complete collection	..	\$200.000

Tables of contents on request

Payment in sterling may be made to Barclays Bank in London, England

CONSULTANTS BUREAU

227 West 17th Street • New York 11, N. Y.

RESEARCH BY SOVIET EXPERTS

Translated by Western Scientists

BORATE GLASSES

by L. Ya. Mazelev

Boron as an element has been known for a long time, but the role of its oxide in glass has been studied little. This book is based mainly on the results of investigating silicate and borosilicate glasses. The purpose of the author's work was a systematic study of the technology of glass melting, the processes and reactions of glass formation, the crystallisation of glasses and the composition of the crystallisation products, the physicochemical properties and their relation to the composition and structure of glass and methods of calculating these properties. This book is important for all those interested in the problems of the structure of glass.

Cloth

176 pages

\$10.00

SILICON AND ITS BINARY SYSTEMS

by A. S. Berezhnoi

Data accumulated on the physical chemistry of silicon and its binary systems are critically reviewed. The properties and descriptions of the crystal structures of silicon and all its binary compounds known at present are given in detail and the most important ways of using these substances in practical applications are indicated. Silicon carbide is treated in detail, as are silicon compounds of the transition metals. All sections have been provided with a historical outline and the basic literature is cited with each problem considered.

Cloth

265 pages

\$8.50

CRYSTAL CHEMISTRY OF SIMPLE COMPOUNDS OF URANIUM, THORIUM, PLUTONIUM AND NEPTUNIUM

by E. S. Makarov

This book represents the first attempt to correlate crystal structure data on the simplest compounds of the most thoroughly studied actinide elements. No books dealing specifically with crystal chemistry of the actinides have been published hitherto either abroad or in the Soviet Union, although separate surveys by Zachariasen have appeared in various collective volumes.

The abundant factual data on crystal structures of actinide compounds are summarised in compact form. This work will enable research workers and engineers to make wider use of crystal structure data which, until now, have been scattered throughout numerous literature sources.

The author considers certain questions of general crystal chemistry, gives full details of the crystalline structures of the polymorphic modifications of the actinides and their simplest compounds, adopts Seaborg's cautious position regarding the parent of the "5f" family of elements, and advances an interesting theory concerning the dual chemical nature of the actinides.

Cloth

146 pages

Illus.

\$5.25

Payment may be made in sterling to Barclay's Bank in London, England.

Tables of contents upon request

CONSULTANTS BUREAU

227 W. 17th ST., NEW YORK 11, N. Y.

